Alterations in the expression of CCSP and SPLUNC1 in the respiratory tract following viral infection of murine models

Thesis submitted in accordance with the requirements of the University of Liverpool for the degree of Doctor in Philosophy

by

Gail Helen Leeming

September 2010

Abstract

Murid herpesvirus 4 (MHV-68) has been widely studied as a model of gammaherpesvirus infection. Infection of *Apodemus sylvaticus*, a natural host for MHV-68, revealed that a virally-encoded chemokine binding protein (M3) influences the composition of the perivascular and peribronchiolar inflammatory infiltration and the formation of BALT in the lung during lytic infection. In addition, host genes were identified which were expressed at higher levels in the presence of MHV-68 M3 at 14 days post infection (dpi), including *Clara cell secretory protein* (*CCSP*), *Short palate lung and nasal epithelium clone 1* (*SPLUNC1*) and *Anterior gradient 3* (*AGR3*). The aim of this work was to further investigate the expression of these genes and their corresponding proteins in relation to respiratory viral infection.

CCSP and *SPLUNC1* have previously been shown to have anti-inflammatory properties in models of virus, bacteria and allergen induced inflammation. *AGR3* is thought to be homologous to *AGR2*, which is associated with the transition of Clara cells to mucous cells in the lung. Following MHV-68 infection in *A. sylvaticus*, levels of both CCSP and SPLUNC1 were reduced in the bronchioles at 7 dpi and increased at 14 dpi, compared to mock-infected controls. In the absence of M3, the level of CCSP was reduced compared to wild type MHV-68 infected animals at both timepoints, whereas no significant difference in the expression of SPLUNC1 in the bronchioles was present. The regulation of both of these genes has previously been associated with interferon γ (IFNγ); infection of 129 wild type and IFNγR$^{-/-}$ mice revealed that CCSP expression was increased and SPLUNC1 expression decreased in the presence of IFNγ. However, this effect was smaller than that due to MHV-68 infection. Expression of *AGR3* in the respiratory tract was increased in response to MHV-68 infection, whereas *AGR2* was decreased. To investigate whether these effects were specific to MHV-68, infection with other respiratory viruses, with different cellular tropisms in the respiratory tract were examined in BALB/c mice. Infection with Human respiratory syncytial virus, Sendai virus and several strains of Influenzavirus A led to a decrease in both CCSP and SPLUNC1 expression during acute infection, when this was associated with a significant inflammatory response in the lung.

The findings of this work showed that CCSP and SPLUNC1 are constitutively expressed in the non-ciliated cells of the respiratory epithelium and support the hypothesis that they have an anti-inflammatory role in the lung. Expression of both proteins is reduced in the event of acute viral infection resulting in significant inflammation. In MHV-68 infection of *A. sylvaticus*, increased expression of CCSP and SPLUNC1 at later timepoints suggests that these proteins are implicated in the resolution of the inflammatory response.

Acknowledgements

Many people have provided me with support, advice, time, reagents and other materials to enable me to complete this PhD, for which I am very grateful. My supervisors, Prof. Anja Kipar and Prof. James Stewart have provided me with guidance, support and encouragement to do this work and I would like to thank them both for their time and the opportunity to do this work, which I appreciate greatly.

Dr. Colin Bingle, University of Sheffield, kindly provided several plasmids and antibodies in addition to many helpful discussions and advice regarding *SPLUNC1* and *CCSP* expression. Thank you also to Dr. Bernadette Dutia, University of Edinburgh for providing the tissues for the analysis of the effect of IFNγ in MHV-68 infection and for the LHΔGFP virus. Two groups from outside the University of Liverpool performed experiments for this work, for which I am very grateful. They are Prof. Ralph Tripp, University of Georgia College of Veterinary Medicine and his group, who performed the Influenza virus infections and Dr. Ultan Power, Centre for Infection and Immunity, Queen's University Belfast and his group, in particular, Ms. Candice Poux, who performed the HRSV and Sendai virus infections, and made me very welcome in Belfast, thank you all. Ms. Alison Bigley, Analytical Morphology Group, AstraZeneca Alderley Park kindly provided her time and expertise for the digital analysis of immunohistology sections, which gave me a fantastic opportunity to begin to learn this technique. I would also like to thank Dr. Stacey Efstathiou, University of Cambridge for supplying the pEH1.4 plasmid and Profs. Samuel Speck and Herbert Virgin of the Emory University School of Medicine, Atlanta and Washington University School of Medicine, St. Louis for the MHV-68 M3.MR and M3.stop viruses.

Numerous people in Liverpool have assisted me with my work, in both the Dept. of Medical Microbiology and Dept. of Veterinary Pathology, all of whose support I greatly appreciate. In particular I would like to thank past and present members of the MHV-68 group; Dave, Helen, Elaine, Bahram, Vicky, Bruno and Rita, the staff of the Veterinary Laboratory Services; Marie, Val, Sean and Mark for all the histology and immunohistology they have performed and Marion Pope for electron microscopy technical expertise. Thanks also to Sue Jopson and John Waters for their assistance in animal husbandry.

I would also like to offer a very big thank you to Mike, again, for his love and support during my seemingly endless student days. I promise I am now going to get a "proper job"! Thank you.

Contents

List of figures

List of tables

List of abbreviations

AB-PAS	Alcian blue – Periodic acid Schiff
ADAR	dsRNA-specific adenosine deaminase
AGR	anterior gradient
ANXA1	annexin A1
APC	antigen presenting cells
BAL	bronchioalveolar lavage
BL	Burkitt's lymphoma
BPI	bactericidal/permeability increasing protein
CCSP	Clara cell secretory protein
$CCSP^{-/-}$	CCSP knock out
DC	dendritic cells
DNA	deoxyribonucleic acid
dpi	day(s) post infection
EBV	Epstein-Barr virus
EGFR	epidermal growth factor receptor
EHV	*Equid herpesvirus*
g	relative centrifugal force (gravity)
GFP	green fluorescent protein
GPCR	G-protein-coupled receptor
H&E	haematoxylin and eosin
HBEC	human bronchial epithelial cells
HHV	*Human herpesvirus*
HNF	hepatocyte nuclear factor
HPAI	high pathogenicity avian influenza
HRSV	*Human respiratory syncytial virus*
HVS	herpesvirus saimiri
ICAM	intercellular adhesion molecule
IFN	interferon
$IFN\gamma^{-/-}$	interferon γ knock out
IFNγR	interferon γ receptor
$IFN\gamma R^{-/-}$	interferon gamma receptor knock out
Ig	immunoglobulin

IL	interleukin
IM	Infectious mononucleosis
IP-10	IFN-inducible protein 10
IRF	interferon regulatory factor
Jak/STAT	janus kinase/signal transducer and activator of transcription
kb	kilobase(s)
kDa	kiloDalton(s)
ko	knock out
KS	Kaposi's sarcoma
KSHV	Kaposi's sarcoma-associated herpesvirus
LMP	latent membrane protein
LPAI	low pathogenicity avian influenza
LPB	lipopolysaccharide binding protein
LPS	lipopolysaccharide
MCD	multicentric Castleman's disease
MCF	malignant catarrhal fever
MCP	monocyte chemoattractant protein
MHC	major histocompatibility complex
MHV	murine herpesvirus
MIG	monokine-induced by IFNγ
MIP	macrophage-inflammatory protein
MuHV	*Murid herpesvirus*
NFL	nasal lavage fluid
NFκB	nuclear factor kappa-light-chain-enhancer of activated B cells
NO	nitric oxide
NPC	nasopharyngeal carcinoma
NSCLC	non-small cell lung cancer
ORF	open reading frame
PEL	primary effusion lymphoma
PFU	plaque forming units
pi	post infection
RANTES	regulated upon activation, normal T cell expressed and secreted

RNA	ribonucleic acid
SCID	severe combined immunodeficiency
SEM	standard error of the mean
SPDEF	SAM-pointed domain-containing Ets-like factor
SPLUNC1	short palate nasal and lung epithelium clone 1
SPLUNC1$^{-/-}$	SPLUNC1 knock out
TEM	transmission electron microscopy
TGF	transforming growth factor
TNF	tumour necrosis factor
TTF	thyroid transcription factor
VCAM	vascular cell adhesion molecule
VEGF	vascular endothelial growth factor
vtRNA	viral transfer RNA
wt	wild type

Chapter 1 Introduction

1.1 *Herpesviridae*

1.2 *Paramyxoviridae*

1.3 *Orthomyxoviridae*

1.4 Interferon γ

1.5 Expression of proteins in the lung in relation to MHV-68 *M3*

1.6 Aim of this thesis

1.1 *Herpesviridae*

1.1.1 Properties of herpesviruses

Membership of the *Herpesviridae* family is based on the architecture of the virion. The core consists of linear double stranded DNA within an icosadeltahedral capsid, 100 to 110 nm in diameter with 162 capsomeres. The capsid is surrounded by an amorphous tegument of variable thickness causing occasional asymmetry, and a lipid bilayer envelope with viral glycoprotein spikes. The genome consists of a single linear segment of 125-290 kb (Davison et al., 2009). The encapsulated virion is 120 – 300 nm in diameter; the variation being due to the variable thickness of the tegument [(Pellett and Roizman, 2007) Figure 1-1].

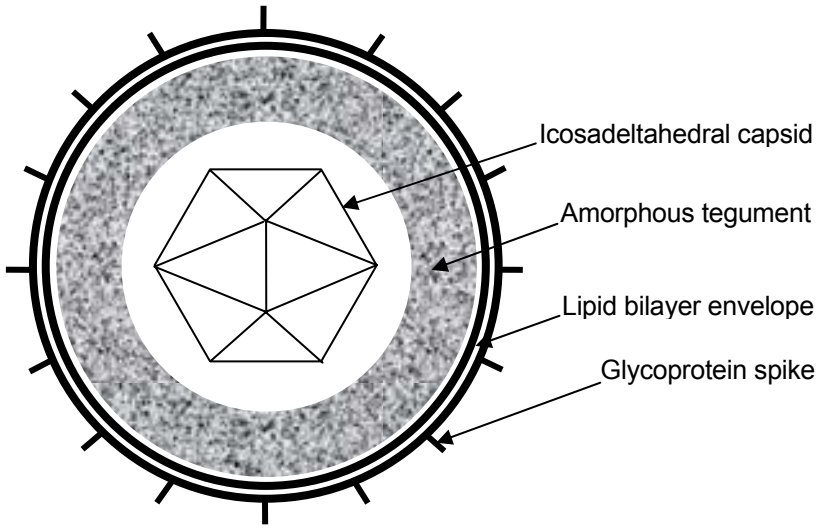

Figure 1-1 Schematic diagram of the structure of a herpesvirus virion.

Herpesviruses are widely disseminated and most species have at least one (usually species specific) herpesvirus; 200 are known to date and this number is likely to increase with further research; it is likely that all vertebrates carry multiple herpesvirus species (Davison et al., 2005; Pellett and Roizman, 2007). Several species of veterinary importance have one or more herpesviruses; host species include mammals, birds, reptiles, fish, amphibians and molluscs and eight herpesviruses are known that have humans as their primary host (Pellett and Roizman, 2007).

In addition to morphological similarities, biological properties common to all herpesviruses are known. Firstly, there are common enzymes present in numerous herpesviruses, which are involved in nucleic acid metabolism, DNA synthesis and the processing of proteins, although the exact combination of enzymes may vary between virus species. Secondly, viral DNA and capsid assembly occurs within the nucleus of an infected cell. The process of viral DNA synthesis and virion assembly (i.e. production of progeny virus) causes destruction of the infected host cell. Lastly, the capacity of the virus to establish a latent infection in the host, maintaining the presence of the virus and the potential for future reactivation and further replication (Pellett and Roizman, 2007). Herpesviruses are generally found within a single host species and are highly host adapted. As a result, severe infection is not the norm and occurs only during infection of the very young, the foetus, immunocompromised hosts, or on the occasions that an alternative host species is infected (Davison et al., 2005).

1.1.2 Classification of herpesviruses

Herpesviruses are in the Order *Herpesvirales*, which is divided into three families; the family *Herpesviridae* contains herpesviruses species which infect mammals, birds and reptiles, *Alloherpesviridae* the herpesviruses of fish and amphibians and *Malacoherpesviridae*, herpesviruses of molluscs (Davison et al., 2009). Within the *Herpesviridae* there are three subfamilies, designated *Alpha-, Beta-* and *Gammaherpesvirinae*. This classification is based on the biological properties of the virus, made by the Herpesvirus Study Group of the International Committee on Taxonomy of Viruses (Davison et al., 2009; Roizman et al., 1981; Roizman et al., 1992) and is supported by the more recent information obtained from DNA sequence analysis (Davison et al., 2005). Phylogenetic analyses of DNA sequences have demonstrated that mammalian herpesviruses come from a clear common evolutionary origin, from which the subfamilies have evolved. Subdivision of the *Herpesviridae* into the three subfamilies occurred 80-60 million years ago, around the time of the extinction of the dinosaurs (McGeoch et al., 1995; McGeoch et al., 2005). Co-evolution with hosts since this time has lead to close host-specificity and the ability to latently infect these hosts, often over their entire lifespan (Davison,

2002). *Alphaherpesvirinae* exhibit a variable host range (including mammalian, avian and reptilian species) and have a short reproductive cycle which efficiently destroys infected cells both *in vivo* and *in vitro* where virus spread is rapid. Unlike other genera in this and other subfamilies (Table 1-1), infection with viruses of the genus *Simplexvirus* is not associated with viraemia, but is localised to the epithelium at the site of infection and the sensory neurones innervating this site (Davison et al., 2005). The establishment of latency within neurones and ganglia, however, is a characteristic of many *Alphaherpesvirinae* (Davison et al., 2005; Pellett and Roizman, 2007). *Betaherpesvirinae* exhibit a more restricted host range, a long reproductive cycle and slow progression of growth in culture. A characteristic of this subfamily is the development of cytomegaly of infected cells and latency within monocytes, found in various tissues, including secretory glands, lymphoreticular cells and the kidney (Davison et al., 2005; Pellett and Roizman, 2007). *Gammaherpesvirinae* are restricted to hosts from the family or order to which the natural host belongs and predominantly replicate in lymphoblastoid cells, although some may also cause lytic infection in epithelioid or fibroblastic cells. Latent infection is usually restricted to lymphocytes (Davison et al., 2005; Pellett and Roizman, 2007). Within each genus, there is a designated “type species” virus, details of which are found in Table 1-1.

1.1.3 *Gammaherpesvirinae*

The subfamily *Gammaherpesvirinae* contains four genera; *Lymphocryptovirus* contains Epstein-Barr virus (HHV4) and other viruses which are restricted to (new world and old world) primate hosts; *Rhadinovirus* contains viruses of new world and old world primates, as well as humans and other mammals including cattle and mice. Two more recently created genera are *Macavirus*, named for Malignant Catarrhal Fever-associated herpesviruses and *Percavirus* named for perissodactyl and carnivore herpesviruses. Further details of individual species are given in Table 1-2 (Davison et al., 2009). Each type species from each of the genera belonging to the *Gammaherpesvirinae* is discussed in greater detail below.

Subfamily	Genus	Type species	Acronym	Common name
Alpha-herpesvirinae	*Simplexvirus*	*Human herpesvirus 1*	HHV1	Herpes simplex virus type 1
	Varicellovirus	*Human herpesvirus 3*	HHV3	Varicella-zoster virus
	Mardivirus	*Gallid herpesvirus 2*	GaHV2	Marek's disease virus type 1
	Iltovirus	*Gallid herpesvirus 1*	GaHV1	Infectious laryngotracheitis virus
Beta-herpesvirinae	*Cytomegalo-virus*	*Human herpesvirus 5*	HHV5	Human cytomegalovirus
	Muromegalo-virus	*Murid herpesvirus 1*	MuHV1	Mouse cytomegalovirus
	Roseolovirus	*Human herpesvirus 6*	HHV6	Human herpesvirus 6
	Proboscivirus	*Elephantid herpesvirus 1*	ElHV1	Elephant endotheliotropic herpesvirus
Gamma-herpesvirinae	*Lymphocrypto-virus*	*Human herpesvirus 5*	HHV4	Epstein-Barr virus
	Rhadinovirus	*Saimiriine herpesvirus 2*	SaHV2	Herpesvirus saimiri
	Macavirus	*Alcelaphine herpesvirus 1*	AlHV1	Malignant catarrhal fever virus
	Percavirus	*Equid herpesvirus 2*	EHV2	Equine herpesvirus 2

Table 1-1 Type species of each genus in the Order *Herpesvirales*, Family *Herpesviridae*.
Assembled after Davison et al., 2009.

Genus	Name	Acronym	Former name	Common name
Lymphocryptovirus	*Callitrichine herpesvirus 3*	CalHV3		Marmoset lymphocryptovirus
	Cercopithecine herpesvirus 14	CeHV14		African green monkey EBV-like virus
	Gorilline herpesvirus 1	GoHV1	*Pongine herpesvirus 3*	Gorilla herpesvirus
	*Human herpesvirus 4**	HHV4		Epstein-Barr virus
	Macacine herpesvirus 4	McHV4	*Cercopithecine herpesvirus 15*	Rhesus lymphocryptovirus
	Panine herpesvirus 1	PnHV1	*Pongine herpesvirus 1*	Herpesvirus pan
	Papiine herpesvirus 1	PaHV1	*Cercopithecine herpesvirus 12*	Herpesvirus papio
	Pongine herpesvirus 2	PoHV2		Orangutan herpesvirus
Rhadinovirus	*Ateline herpesvirus 2*	AtHV2		Herpesvirus ateles strain 810
	Ateline herpesvirus 3	AtHV3		Herpesvirus ateles strain 73
	Bovine herpesvirus 4	BoHV4		Movar virus
	Human herpesvirus 8	HHV8		Kaposi's sarcoma-associated herpesvirus
	Macacine herpesvirus 5	McHV5	*Cercopithine herpesvirus 17*	Rhesus rhadinovirus
	Murid herpesvirus 4	MuHV4		Murine gammaherpesvirus 68
	*Saimiriine herpesvirus 2**	SaHV2		Herpesvirus saimiri
Macavirus	*Alcelaphine herpesvirus 1**	AlHV1		Malignant catarrhal fever virus
	Alcelaphine herpesvirus 2	AlHV2		Hartebeest malignant catarrhal fever virus
	Bovine herpesvirus 6	BoHV6		Bovine lymphotropic herpesvirus
	Caprine herpesvirus 2	CpHV2		Caprine herpesvirus 2
	Hippotragine herpesvirus 1	HiHV1		Roan antelope herpesvirus
	Ovine herpesvirus 2	OvHV2		Sheep-associated malignant catarrhal fever virus
	Suid herpesvirus 3	SuHV3		Porcine lymphotropic herpesvirus 1
	Suid herpesvirus 4	SuHV4		Porcine lymphotropic herpesvirus 2
	Suid herpesvirus 5	SuHV5		Porcine lymphotropic herpesvirus 3
Percavirus	*Equid herpesvirus 2**	EHV2		Equine herpesvirus 2
	Equid herpesvirus 5	EHV5		Equine herpesvirus 5
	Mustelid herpesvirus 1	MusHV1		Badger herpesvirus

Table 1-2 Confirmed species of the genera from the subfamily *Gammaherpesvirinae.*
* type species of the genera. Assembled after Davison et al., 2009.

1.1.3.1 Epstein-Barr virus (*Human herpesvirus 4*)

Epstein-Barr virus (EBV, HHV4) is the type species of the genus *Lymphocryptovirus* (Davison et al., 2009). It is a widely disseminated herpesvirus in humans, with more than 90 % of people having been exposed to and carrying antibodies to the virus (Rickinson and Kieff, 2007). Spread of the virus is via the oral route by close contact with a virus-shedding carrier, and infection during the first three years of life (as is most common in the developing world) appears to be asymptomatic. However, in developed nations up to half of children are seronegative at the age of ten years and acquisition of the virus in adolescence or early adulthood results in the development of infectious mononucleosis (IM) in approximately 25 % of cases; such cases may be underdiagnosed in other parts of the world (Rickinson and Kieff, 2007). IM is characterised clinically by pyrexia, generalised lymphadenopathy, splenomegaly, sore throat and the presence of atypical activated T lymphocytes (mononucleosis cells) in the blood; some patients develop hepatitis, meningoencephalitis and pneumonitis (McAdam and Sharpe, 2005). These clinical symptoms occur 4 to 6 weeks after transmission and coincide with high titres of virus in throat washings and saliva. It is now thought that the target cells for infection are the epithelial cells of the oral cavity, particularly the tongue, with lytic replication having been demonstrated in cases of oral hairy leukoplakia lesions (a condition seen in AIDS patients) and subsequently in the tongue of immunocompetent carriers (Rickinson and Kieff, 2007). Infection of oral epithelial cells may occur via initial binding of EBV to B cells within the lymphoepithelium of the oropharynx, as it has been shown that infection of epithelial cells *in vitro* is 1,000 times more efficient in the presence of resting B cells with surface-bound EBV; binding occurs between viral gp350 and cellular CD21 (Shannon-Lowe et al., 2006).

Infection of B cells via CD21 binding leads to two potential outcomes for the cell; either lytic infection in which further infectious virions are produced, resulting in cell death, or a process which results in latent infection. EBV infection of a naive B cell mimics the physiological process whereby the B cell enters the germinal centre as a result of antigen stimulation. This occurs via hypermutation of immunoglobulin (Ig) light and heavy chains, in which the cells

which produce Ig with the highest affinity for the antigen are rescued from apoptosis and become memory B cells. Memory B cells are longer lived and provide the potential for life-long latent infection of the host (Kutok and Wang, 2006; McAdam and Sharpe, 2005; Rickinson and Kieff, 2007). Maintenance of latent infection is achieved by activation of latency-associated genes causing B cells to proliferate, for example, *LMP-1*, which actives the NF-κB and JAK/STAT pathways and inhibits apoptosis by activation of BCL-2. These pathways for continued B cell proliferation are a critical component in the formation of the B cell lymphomas that are seen in association with EBV infection. However, they also facilitate the development of other neoplastic conditions, usually in the presence of some form of immunosuppression or concomitant infection (Stricker and Kumar, 2010).

Burkitt's Lymphoma (BL) is a neoplasm of B cells which was first described by Denis Burkitt in 1958 as a neoplasm of high incidence in children under the age of 15 years in equatorial Africa, a location with endemic malaria. These lymphomas are unusual in their location (the mandible, orbit, kidney, adrenal gland and ovaries) and have a characteristic "starry sky" histological appearance due to the presence of macrophages within sheets of neoplastic lymphocytes. Culture of BL cells *in vitro* led to the identification of a herpesvirus by Epstein and Barr in the 1960's. EBV is believed to contribute to the development of the neoplasm by increasing the potential of a genetic translocation within the *c-MYC* gene, promoting entry into the cell cycle and activating anti-apoptotic pathways. Subsequently, other forms of BL in other geographical locations have been described; sporadic BL (also a neoplasm of children and adolescents) and AIDS-BL, which accounts for 30 % of lymphoma cases in AIDS patients. The association with EBV in these types of BL is less consistent, although all display the same *c-MYC* mutation (Epstein, 2001; Kutok and Wang, 2006; Rickinson and Kieff, 2007; Stricker and Kumar, 2010; Thorley-Lawson and Allday, 2008).

Several other B cell lymphomas are associated with EBV, in both immunocompromised patients (e.g., AIDS-associated B cell lymphoma, post-transplantation lymphoproliferative disorder, Severe combined

immunodeficiency-associated B cell lymphoma) and immunocompetent patients (e.g. Classical Hodgkin lymphoma), in addition to several neoplasms of other cellular origin, for example, nasopharyngeal carcinoma (Kutok and Wang, 2006).

1.1.3.2 Herpesvirus saimiri (*Saimiriine herpesvirus 2*)

Herpesvirus saimiri (HVS) is the species type rhadinovirus and a natural pathogen of squirrel monkeys (*Saimiri sciureus*), which are found in the rainforests of South America. Squirrel monkeys are naturally infected within the first two years of life via saliva, which leads to lifelong persistent infection. However, there is no evidence that transformation occurs in Squirrel Monkeys and consequently lymphomas are not a feature of infection in this species (Melendez et al., 1968). Experimental infection of other new world primate species leads to T cell lymphoma within two months of infection, including cotton top tamarins (*Saguinus oedipus*), common marmosets (*Callithrix jacchus*) and owl monkeys (*Aotus trivirgatus*) and some old world primates; cynomolgus macaques (*Macaca fascicularis*) and rhesus macaques (*Macaca mulatta*). In these species, lymphoma develops within lymphoid organs such as lymph nodes and the spleen, as well as intestines, kidney, liver, lung pancreas and salivary glands. Malignant cells are lymphoblast-like in appearance and CD3+ and have been described as pleomorphic T-lymphoproliferative disorders, which are similar in appearance to EBV-induced post-transplantation B-lymphproliferative disease (Fickenscher and Fleckenstein, 2001).

1.1.3.3 Kaposi's sarcoma-associated herpesvirus (*Human herpesvirus 8*)

Kaposi's sarcoma-associated virus (KSHV) is the only herpesvirus of humans in the genus *Rhadinovirus*. It was first described in 1994 after the rise in the incidence of Kaposi's sarcoma in AIDS patients led to a search for an associated pathogen. Viral DNA with significant but distant homology to EBV was found within Kaposi's sarcoma (KS) tissue (Chang et al., 1994). KS was first described much earlier, in the late 19th century in Eastern Europe and this classical form of KS is predominantly found in older men, but is benign and non-life threatening (Ganem, 2007). Despite its relatively recent discovery,

sequence analysis has shown that different strains are present in different geographically distinct populations, suggesting that the virus was established within the human population at the time that humans started to migrate from Africa into Europe and Asia. This also suggests that there are strong familial patterns of spread, either from parents to offspring or between siblings in these populations (Ganem, 2007).

Today, the prevalence of KSHV varies widely in different populations of the world. The highest incidence is in Africa where up to 60 % of the population are seropositive. The Mediterranean basin also shows a higher incidence, where 20-25 % of the population have been exposed (Ganem, 2006). In these areas, the prevalence in both men and women and the presence of KSHV in young children is highly suggestive of either vertical or horizontal spread within families via saliva, in which KSHV is most commonly detected. In the United States the incidence in the general population is 1-7 %, however, the familial route of infection is less likely as seroprevalence of KSHV increases with age. The much higher incidence in homosexual men suggests sexual transmission; there is a clear correlation between seroprevalence and the number of sexual partners. However, it is still thought that saliva is the main route of transmission (Ganem, 2007). The higher incidence within the homosexual population became evident in the treatment of AIDS patients, who exhibited a much higher incidence of KS. The overall incidence of KS is 1 case per 10,000 seropositive individuals. The incidence within HIV-positive persons is much higher; it is has been found that men infected with both HIV and KSHV, who are treated for neither, have a 50 % incidence of KS within ten years (Ganem, 2007).

Classical KS, as described by Kaposi, is a tumour of “spindle cells”, the majority of which are latently infected with KSHV. The origin of these cells is not clear as they variably express cell markers indicative of either vascular endothelium, lymphatic endothelium or smooth muscle cells (α-actin); the expression of these markers may vary within a single mass. To complicate matters, it has been shown *in vivo* that viral infection can cause endothelial cells to express lymphatic markers and vice versa. Furthermore, the spindle

cells differ from normal neoplastic cells in that they are polyclonal. In addition to the spindle cells, other histological features are highly characteristic of KS. Neovascular spaces, lined by endothelial cells that are often KSHV negative are present early on in tumour growth. Implantation of KS cells into nude mice does not result in the growth of a tumour, due to involution of the KS cells, but while they are present, new vessels of murine origin grow, suggesting that the neoplastic cells induce angiogenic activity. Similarly, inflammatory cells are a feature of KS, but these cells do not appear in response to necrosis but are present from the earliest stages, suggesting that this too is a result of signalling from the KS spindle cells. Individual KS lesions often arise simultaneously, within the dermis of the skin on the lower abdomen and legs and may either progress slowly to nodular form, or spontaneously regress (Ganem, 2006, 2007).

KS in AIDS patients has a more aggressive form; dermal lesions are more widespread, often disfiguring and in addition, extracutaneous sites are frequently affected, especially the lungs and the gastrointestinal tract. Intravisceral lesions are often accompanied by haemorrhage and oedema, and gastrointestinal bleeding and respiratory failure are serious sequalae. Other more aggressive forms of KS are also seen in young children in endemic areas and in iatrogenically immunosuppressed transplant recipients (Ganem, 2006).

Other than KS, other disorders are associated with KSHV, principally in AIDS patients. Primary effusion lymphoma (PEL) and multicentric Castleman's disease (MCD) are both lymphoproliferative B cell disorders which are associated with KSHV (Cohen et al., 2005). PEL is characterised by proliferation of monoclonal B cells on serosal surfaces (peritoneum, pleura, pericardium) and occasionally invasion of solid organs. It is most frequently seen in patients with end stage AIDS. The B lymphocytes are CD138+, indicative of germinal centre B cell origin, and are most likely of plasmablastic lineage, due to their transcription profile and secretion of IL-6 and IL-10, which is found in other plasmablastic tumours (Jenner et al., 2003). MCD is a more aggressive form of the rare polyclonal lymphoproliferative disease,

Castleman's disease and is characterised by sustained pyrexia, sweating, weight loss, lymphadenopathy and splenomegaly. KSHV-positive cells are limited to the mantle zone surrounding germinal centres and represent 10-50 % of the B cells in this area. Virtually all HIV-positive patients with MCD have KSHV-positive B cells, compared to the very rare cases of MCD in HIV-negative patients in whom only 40-50 % have KSHV-positive B cells; Castleman's disease (in HIV-negative patients) is not associated with KSHV (Ganem, 2007).

1.1.3.4 *Alcelaphine herpesvirus 1*

Alcelaphine herpesvirus 1 is the species type of the genus *Macavirus*, one of several in the genus that is associated with the disease Malignant Catarrhal Fever (MCF). Identification of a herpesvirus as the causative agent of MCF was first reported in 1960 (Plowright et al., 1960). The natural hosts of these viruses are usually asymptomatically infected, so wildebeest (*Connochaetes turinus*), the natural hosts of AlHV1, are unlikely to show clinical symptoms of infection (Russell et al., 2009). The virus is transmitted by cell free virus in either nasal or ocular secretions via direct contact or aerosol. Virus secretion is highest in young animals; up to 61 % of one to two-month old free and captive wildebeest shed virus in ocular fluid, this decreases to less than 2 % in animals over 6 months old (Barnard et al., 1989). Transmission of virus to susceptible species (many ungulate species including domestic cattle, deer, water buffaloes and other free living and captive ruminants) can result in MCF, however, these are dead end hosts and are unlikely to infect other animals, probably due to viral replication being restricted to cell-associated means with no cell-free virus being produced (Russell et al., 2009). The most common clinical form of MCF presents with "head and eye" signs, namely, pyrexia, inappetance, ocular and nasal discharge and haemorrhagic and erosive lesions of the buccal cavity and muzzle. At post mortem examination, petechial haemorrhage is found on the tongue, buccal mucosa, urinary bladder, gastrointestinal and respiratory tracts, and lymph nodes are enlarged and may be haemorrhagic (Russell et al., 2009; Whitaker et al., 2007). In other cases, overlapping lesions may include those centred on the skin, alimentary or neurological organs. Histologically, lymphoid hyperplasia is present in the

paracortical, interfolicular and sinusoidal regions of lymph nodes and the periarteriolar sheaths of the spleen. Vasculitis in numerous major organs is also a predominant feature, with lymphocytic infiltration of one or more layers of arterioles and arteries (Whitaker et al., 2007). Experimental infection of rabbits has shown that these infiltrates are predominantly of CD8+ T cells (Anderson et al., 2007). Recently, it has been shown that viral gene sequences can be detected within many of these infiltrating lymphocytes, suggesting that proliferation of lymphocytes and their localisation at the sites of the lesion may be due to a direct effect of the virus (Russell et al., 2009). In fatal cases of AlHV1-associated MCF in many deer species, death occurs as early as 48 hours after the onset of clinical signs, but up to one week in cattle. However, outbreaks of the disease are sporadic within groups of animals and there is evidence that some animals may survive infection having shown relatively few clinical signs (Russell et al., 2009).

1.1.3.5 *Equid herpesvirus 2*

Equid herpesvirus 2 (EHV2) is the type species of the genus *Percavirus*, which contains gammaherpesviruses from perissodactyls and carnivores, namely (to date) equines and badgers (Davison et al., 2009). EHV2 has an endemic, worldwide distribution, with detection of viral DNA in peripheral blood leukocytes ranging from 51 to 80 % of adult horses and 75 to 100 % foals (Bell et al., 2006; Borchers et al., 1997; Craig et al., 2005; Dunowska et al., 2002; Nordengrahn et al., 2002; Torfason et al., 2008). Foals are infected early in life and infection occurs via horizontal transmission, by ingestion or inhalation of nasal secretions. It is likely that transmission to young foals also occurs via asymptomatic shedding mares. Detection of EHV2 in nasal secretions with concurrent signs of upper respiratory infection is common in foals but less frequent in adult horses (Dunowska et al., 2002; Fortier et al., 2009; Slater, 2007). The pharynx has been thought the likely site for initial replication of EHV2, due to its frequent isolation from this location, followed by localised inflammation and lymphoid activation and dissemination to other organs via peripheral blood leukocytes. The site of latency is not known; B lymphocytes have been suggested by many researchers, but EHV2 has also been isolated from alveolar macrophages, and from peripheral nervous tissue (trigeminal

ganglia), particularly when associated with ocular disease (Borchers et al., 1997; Fortier et al., 2009; Rizvi et al., 1997).

Infection with EHV2 has been associated with keratoconjunctivitis, upper respiratory tract disease and may be involved, along with EHV5 (another equine gammaherpesvirus) with equine multinodular pulmonary fibrosis (Fortier et al., 2009; Kershaw et al., 2001; Williams et al., 2007). Furthermore, it has been suggested as a factor in poor performance syndromes or in immunosuppression, with evidence of EHV2 predisposing to other respiratory infections in foals (Dunowska et al., 2002; Fortier et al., 2009; Nordengrahn et al., 1996) .

1.1.4 Murine herpesvirus strain 68 (*Murid herpesvirus 4*)

1.1.4.1 Natural history of MHV-68

Murid herpesvirus 4 (MuHV4, commonly known as MHV-68, γHV-68) is a gammaherpesvirus in the genus *Rhadinovirus* and was first isolated from bank voles (*Myodes* [was *Clethrionomys*] *glareolus*) and yellow necked mice (*Apodemus flavicolis*) in Slovakia (Blaskovic et al., 1980). Initially several strains were isolated; MHV-60, MHV-68, MHV-72 from *M. glareolus* and MHV-76 and MHV-78 from *A. flavicollis.* It is now thought that these are all related strains of MHV-68 (Stewart et al., 2005). Survey of wild rodents in the UK, Germany and Thailand found that MHV-68 was present in three *Apodemus* spp., namely *A. flavicollis, A. sylvaticus* (wood mouse, or long-tailed field mouse) and *A. agrarius* (striped field mouse), but not bank voles, the species in which MHV-68 was first described (Ehlers et al., 2007). Furthermore, another survey of wood mice and bank voles found that although 13 and 24 % wood mice in England and Northern Ireland, respectively, were positive for MHV-68 antibodies in sera, only 2.7 % of bank voles were seropositive, suggesting that the virus is endemic in wood mice, while bank voles are less susceptible to MHV-68 and are not likely to be a natural host (Blasdell et al., 2003). Bank voles are not found in Northern Ireland, which confirms that they are not required for transmission of the virus between wood mice (Blasdell et al., 2003). More recently, a longitudinal study of MHV-68 seroprevelance showed similar rates of infection in wild populations of wood mice and bank

voles (11 % and 3 %, respectively), but also that MHV-68 was only detected in bank voles on a single occasion, whereas 69 % of wood mice that tested positive and were retested, remained seropositive on at least one subsequent occasion (Telfer et al., 2007).

A survey of wild caught *Mus musculus domesticus* (house mouse; the species of origin of laboratory mice) for common pathogens found 2 out of 43 mice (5 %) seropositive for MHV-68, results which the authors speculated were likely to be false positive results as subsequent PCR based assays failed to confirm the result (Becker et al., 2007). Similarly, Ehlers et al. (2007) did not find MHV-68 in *M. musculus*, but found another, novel gammaherpesvirus which was named MmusRHV1. This virus is phylogenetically separate from MHV-68 and sequence analysis placed it in a separate clade to MHV-68. MmusRHV1 has genetic sequences more akin to members of the *Percaviruses* and *Macaviruses* than the *Rhadinoviruses*, of which MHV-68 is a member (Ehlers et al., 2007; Ehlers et al., 2008).

1.1.4.2 Pathogenesis of MHV-68

MHV-68 has been widely studied in laboratory mice as it is a useful model of gammaherpesvirus infection, due to its similarity to other gammaherpesviruses in other species (e.g. acute EBV infection in humans) and as the host-specificity of gammaherpesviruses prevents study of human gammaherpesviruses in other species (Nash et al., 2001; Sunil-Chandra et al., 1992a). The natural route of infection is not known, but is likely to be via the respiratory tract, as the lung is a frequent site of virus isolation in wild rodents (Nash et al., 1996; Nash et al., 2001). Following intranasal infection of laboratory mice with MHV-68, titres of infectious virus increase in the lung, peak at 3 dpi then decrease to undetectable levels between 10 and 15 dpi (Cardin et al., 1996; Sunil-Chandra et al., 1992a). Alveolar epithelial cells and macrophages are the primary sites of infection, with viral antigen detected in peribronchiolar and perivascular infiltrates by day 3 pi and within alveolar epithelium by day 5 pi. Pulmonary lesions include peribronchiolar, perivascular and interstitial infiltration by lymphoid cells, within which necrosis is observed from 3 dpi, suggesting that this is a site of virus replication (Sunil-Chandra et

al., 1992a). No evidence of lytic replication within lymphocytes has been found (Dutia et al., 1999). Lymphoid infiltrates become more extensive by 5 dpi, when cellular debris is present within the bronchiolar lumen. Bronchial alveolar lavage identified the components of the inflammatory response to be CD11b+ macrophages, which peaked in number at days 3-4 pi and then CD8+ T cells, which peaked at 8-10 dpi (Nash et al., 1996). From 10 dpi inflammation begins to subside, coinciding with viral clearance from the lung, which is mediated by CD8+ T cells (Ehtisham et al., 1993). MHV-68 DNA detected by *in situ* hybridisation in peribronchiolar mononuclear cells at 30 dpi, suggests that the lung may be a site of viral persistence (Nash et al., 1996; Stewart et al., 1998; Sunil-Chandra et al., 1992a). In addition, germinal centre formation in perivascular and peribronchiolar areas is present at 30 dpi. Such lymphoproliferative responses are common features of gammaherpesvirus infections (Stewart et al., 1998; Sunil-Chandra et al., 1994).

Subsequent to the establishment of infection in the lung there is no evidence of viraemia, other than in animals less than 3 weeks of age (Nash et al., 1996), but dissemination of the virus occurs via the local (mediastinal) lymph nodes where dendritic cells, macrophages and B lymphocytes are infected (Nash et al., 2001). The tropism of MHV-68 for B lymphocytes is indicated by the increased efficacy of infection of these cells via the binding of the gp150 viral envelope protein to CD19, present on B lymphocytes. However, this protein is not required for the infection of pulmonary epithelial cells (Stewart et al., 1996; Stewart et al., 2004). From the lymph node, it is thought that the B lymphocyte is the principal cell responsible for dissemination of virus to distant sites, including the spleen where latent virus can be detected from one week pi, peaking at 2-3 weeks pi and is maintained indefinitely (Nash et al., 1996; Sunil-Chandra et al., 1992b; Sunil-Chandra et al., 1992a; Weck et al., 1996). In the absence of B cells, latency is still established but is less efficient and leads to a fatal outcome in B cell deficient mice (Weck et al., 1996). Therefore B lymphocytes have a role in the regulation of both latency and reactivation of infection (Weck et al., 1999a).

The establishment of latency is a characteristic of herpesvirus infection. In MHV-68, latency in the lung is established in epithelial cells and B lymphocytes, subsequent to clearance of acute infection (Flano et al., 2003; Stewart et al., 1998). Latent infection is also detected in the lung in the absence of B cells, confirming that other pulmonary sites are capable of establishing latency (Usherwood et al., 1996b). In the spleen, in addition to B lymphocytes, latent virus can also be detected in macrophages and dendritic cells (Flano et al., 2000; Weck et al., 1999b). Splenomegaly and the associated lymphoproliferation, arises due to the response of CD4+ T cells to infected B lymphocytes (Ehtisham et al., 1993). Latently infected B cells are concentrated within germinal centres and increase in number, giving rise to either memory B cells, which are disseminated to the bone marrow and other lymphoid tissues, or antibody producing plasma cells. This process ensures the maintenance of latent MHV-68 infection (Flano et al., 2003; Willer and Speck, 2003). The increase in the number of latently infected B cells in the spleen also triggers a virus specific CD8+ T cell response, which leads to a decline in the number of infected B cells within the spleen and the resolution of splenomegaly, which is important in the long term control of infection. However, some latently infected B cells escape this cytotoxic T cell response (most likely in a similar fashion to EBV, which is dependent on the latency genes expressed) and maintain the latent infection (Cardin et al., 1996; Ehtisham et al., 1993; Usherwood et al., 1996a; Weck et al., 1996). Alongside the development of splenomegaly, there is a subsequent CD8+ T cell-dominated mononucleosis within the blood, which is mediated by the CD4+ T cell-mediated cytokine response and antigen presentation by MHC class II. This is similar to the infectious mononucleosis response to EBV infection in adolescents (Tripp et al., 1997; Usherwood et al., 1996a).

1.1.4.3 MHV-68 infection in wood mice

Although MHV-68 has been extensively studied in laboratory mice (*Mus musculus*), this species is not a natural host for this virus and so the pathogenesis in the natural host may differ, as other gammaherpesviruses can show greatly altered pathogenesis in species other than their natural hosts (Ackermann, 2006; Ehlers et al., 2007). Various species of the genus

Apodemus have been shown to be hosts of naturally occurring MHV-68 (Blasdell et al., 2003; Ehlers et al., 2007; Telfer et al., 2007), including *Apodemus sylvaticus* (wood mouse), which has been used to investigate the pathogenesis of MHV-68 in a natural host and compared to that seen in BALB/c mice (Hughes et al., 2010). Several differences in the inflammatory response and behaviour of the virus are seen between wood mice and laboratory mice; infectious virus is only detected in the lung at day 7 pi, compared to days 5 to 10 pi in BALB/c mice, the titre of which is 1000-fold lower in wood mouse lung. Viral antigen is detected in alveolar epithelial cells in both species at day 7 pi but persists in the wood mouse to day 14 pi when it is found within macrophages and peribronchiolar and perivascular lymphocytes. Viral tRNA (vtRNA; a marker for latent virus) is also detected in the lung at day 14 pi in wood mice, within lymphocytes, suggesting that despite the lower levels of virus replication in the lung, infection results in the effective establishment of latency in the natural host. This could be due to better evolutionary adaptation in the natural host (Hughes et al., 2010) and is consistent with the finding of viral DNA in the lungs of wild wood mice (Blasdell et al., 2003).

The inflammatory response also differs in the wood mouse. At day 7 pi the diffuse increase in interstitial cellularity observed in BALB/c mice is less pronounced in the wood mouse, and the occurrence of alveolar epithelial cell necrosis is also reduced. Perivascular and peribronchiolar inflammatory infiltrates are a much more significant feature in the wood mouse and are dominated by B lymphocytes, as is the iBALT (present at day 14 pi); a feature peculiar to MHV-68 infection of the wood mouse (Hughes et al., 2010). Moreover, this B lymphocyte population is a significant site of latent infection and the increase in numbers of infected B lymphocytes between days 7 and 14 pi is considered to be due a to a proliferation of this population during primary infection (Hughes et al., 2010).

Differences are also present between the two species in the spleen, following infection with MHV-68. Splenomegaly and leukocytosis are not features of infection in wood mice, in dramatic contrast to that seen in laboratory mice.

Despite this, the peak level of latent infection (at day 14 pi) is significantly higher in wood mice, with latent virus detected within well-defined secondary follicles in germinal centres, in contrast to poorly defined follicles without germinal centres in BALB/c mice. This has been postulated to be a result of stimulation by the higher number of viral antigen positive macrophages in the red pulp of the spleen in wood mice at day 14 pi, in contrast to BALB/c mice, in which viral antigen is not detected at this timepoint, despite the marked increase in red pulp cellularity seen in this species (Hughes et al., 2010).

1.1.4.4 MHV-68 genome

The genome of MHV-68 comprises 118kb of double stranded DNA, with variable numbers of 1.23kb terminal repeats at either end (Efstathiou et al., 1990b). The structure and organisation of the genome together with the homology of MHV-68 protein-coding open reading frames (ORFs) with ORFs of HVS and EBV, suggested that this was a gammaherpesvirus (Efstathiou et al., 1990a). Two strains of MHV-68 have been completely sequenced, the WUMS strain (Virgin et al., 1997) and strain g2.4 (Nash et al., 2001), which revealed 73 ORFs. MHV-68 also contains genes which are unique to this virus, located at the left hand end of the virus genome (Figure 1-2); namely M1-M4 and eight vtRNAs (Bowden et al., 1997; Nash et al., 2001).

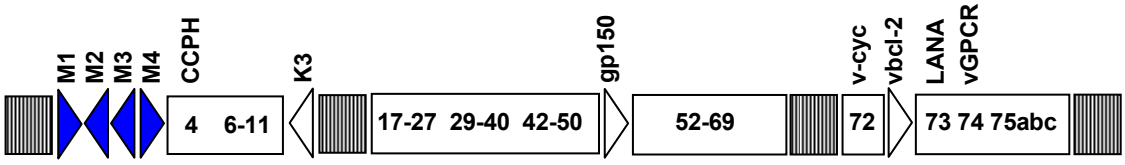

Figure 1-2 The genome of MHV-68.
Open boxes represent homologous herpesvirus genes involved in DNA replication and virus structure. Shaded boxes represent terminal repeat sequences. Blue triangles represent MHV-68 specific genes. Abbreviations: CCPH = complement control protein homologue; v-cyc = viral cyclin D; vbcl-2 = viral Bcl-2; LANA = latent nuclear antigen; vGPCR = viral G-protein coupled receptor (Stewart et al., 2005).

Of the 80 ORFs originally identified, 63 are homologues of genes in HVS (also conserved in KSHV) and were named accordingly (Virgin et al., 1997). One gene (K3) is an additional homologue of a KSHV gene and so was similarly named. Other, unique, genes were named numerically with the “M” prefix (M1-M14).

Several conserved genes have been identified as having significant homology to cellular or viral genes and are potentially involved in the pathogenesis of infection (Virgin et al., 1997). ORF4 has significant homology with multiple complement regulatory proteins which regulate C3 in the complement cascade (Virgin et al., 1997). ORF72 encodes a viral homologue of cyclin-D, critical for reactivation from latency and is oncogenic, promoting cell cycle progression but is non-essential for lytic infection (van Dyk et al., 1999; van Dyk et al., 2000). M11 has weak homology to the *bcl-2* family of genes, which inhibit apoptosis (Virgin et al., 1997). M11 has been shown to protect infected cells from TNFα induced apoptosis *in vitro* (Roy et al., 2000; Wang et al., 1999), and M11 protein or RNA is detected in the lung and spleen during both lytic and persistent infection and contribute to amplification of latently infected cells. M11 mutants are found to result in lower B cell activation, lower viral genome loads and reduced viral tRNA expression (de Lima et al., 2005; Roy et al., 2000). ORF74 is homologous to mammalian G-protein-coupled receptors (GPCRs), a homologue of which is also encoded by KSHV (Wakeling et al., 2001). The predicted structure suggests that this viral protein may signal constitutively and is expressed on the surface of infected cells both during acute and persistent infection, especially in the lungs of mice. This ORF is expressed within transcripts that also contain a viral *bcl-2* and therefore, these genes may function to promote the growth and survival of MHV-68-infected cells (Wakeling et al., 2001).

The functions of M1-M4 viral genes have been studied both independently and using MHV-76, a virus isolated at the same time as MHV-68 from *Apodemus flavicollis* (Blaskovic et al., 1980). MHV-76 is essentially identical to MHV-68 minus the left hand end genes M1 to M4 and the vtRNAs (Macrae et al., 2001). Infection of mice with this virus reveals that although the genes from the

left hand end of the genome are not essential for productive viral replication, these genes may play a key role in the pathogenesis of the virus as suggested by differences observed in the host response. These differences include an increase in pulmonary inflammation which leads to enhanced clearance and reduced persistence of MHV-76 in the lung and diminished splenomegaly compared to MHV-68 infection with lower numbers of infective centres in the spleen. This suggests that the M1-M4 genes and eight vtRNAs play a key role in MHV-68 infection, most likely via evasion of the host immune response (Macrae et al., 2001).

M1 has homology with poxvirus serpin proteins (Virgin et al., 1997) and also with *M3* (Alexander et al., 2002; Nash et al., 2001). Poxvirus serpins are homologous to cellular proteins which have a wide range of functions, including within the inflammatory response, complement activation, coagulation, fibrinolysis and apoptosis (Turner and Moyer, 2002). Deletion of *M1* (and four of the vtRNAs) does not alter the ability of MHV-68 to establish, or reactivate from, latency *in vivo* (Simas et al., 1998). Despite this unaltered establishment of latency, *M1*-deleted viruses show increased reactivation from latency, suggesting that a function of M1 is to suppress reactivation (Clambey et al., 2000). More recently this has been further investigated and appears to occur via induction of CD8+ T cells and subsequent IFNγ secretion, promoting latency (Evans et al., 2008).

The *M2* gene is not essential for effective lytic replication in the lung during acute infection, or for the establishment of latent infection (Macrae et al., 2003). However, M2 appears to be associated with the establishment of latency, as infection with MHV-68 virus with deleted or null M2 results in a decrease in the number of latently infected follicles in the spleen and loss of the transient rise in the number of latently infected cells following intranasal infection (Jacoby et al., 2002; Simas et al., 2004; Usherwood et al., 2000). The protein is expressed in the plasma membrane of latently infected B cells, located within the germinal centres of the spleen and is recognised by CD8+ T cells (Husain et al., 1999; Macrae et al., 2003; Simas et al., 2004). M2 also promotes the activation, proliferation and survival of latently infected B cells,

via the inhibition of apoptosis and also by interference with the STAT pathway, thereby reducing the cellular response to interferons (Liang et al., 2004; Madureira et al., 2005). The majority of cells from which virus is reactivated on explantation of splenic cells are plasma cells; latently infected plasma cells are not a feature of infection with a M2 null MHV-68 virus, suggesting that the differentiation of latently infected cells to plasma cells is driven by M2, and that M2 is required for efficient reactivation (Jacoby et al., 2002; Liang et al., 2009). This plasma cell differentiation has also been shown to be due to IL-10, high serum levels of which are M2 dependent (Siegel et al., 2008).

M4 is an immediate/early gene, expressed during lytic replication (Ebrahimi et al., 2003; Virgin et al., 1999) and encodes a secreted protein (Evans et al., 2006; Geere et al., 2006). Infection of mice with a MHV-76 “knock in” virus which had *M4* inserted, revealed that *M4* was expressed during lytic infection in the lung and also during the establishment of latency in the spleen; the addition of M4 to MHV-76 increased the number of latently infected cells (Townsley et al., 2004). This concurs with the use of a mutant MHV-68 M4.stop virus which showed that M4 was required for the efficient establishment of latency in the spleen (Evans et al., 2006; Geere et al., 2006).

Eight vtRNA genes are present in the left hand end of the MHV-68 genome, interspersed within the M1 – M3 genes. They are expressed soon after infection and are present throughout lytic infection and during latency, when they are abundant in the splenic germinal centres (Bowden et al., 1997; Cliffe et al., 2009). Their function is as yet unknown, but four of the vtRNAs can be deleted without effect on the establishment, or reactivation from, latency (Simas et al., 1998). More recently, up to 14 miRNAs have been identified as being coded within the vtRNA region (Pfeffer et al., 2005) and this region of the MHV-68 gene is responsible for as yet uncharacterised transcripts which are implicated in the pathogenesis of the fibroplastic response to MHV-68 infection in IFNγR$^{-/-}$ mice (Dutia et al., 2004).

1.1.4.5 MHV-68 *M3* gene

Many viruses have evolved mechanisms to interact with the host's immune system in order to promote virus survival within the host. Poxviruses and herpesviruses encode proteins that either mimic cytokines or their receptors as a method of evading or altering the host immune response (Alcami, 2003). Chemokines are chemoattractant cytokines that regulate the movement and function of leukocytes (Weinberg et al., 2002). The *M3* gene of MHV-68 is a viral chemokine binding protein, a class of protein that is secreted from the cell during infection and has the ability to neutralise chemokines in solution (Alcami, 2003). *M3* encodes a 44kDa protein with a signal peptide which is abundantly secreted by infected cells *in vitro* (van Berkel et al., 1999). *M3* is transcribed *in vivo* abundantly during lytic infection in the lung and during early stages of latency; latently infected mice show expression of *M3* in the spleen (Simas et al., 1999; Virgin and Speck, 1999). The M3 protein has no clear homology with known cellular or viral gene products, other than a low level of homology with MHV-68 M1 (van Berkel et al., 1999). As a secreted protein, M3 is a candidate for interaction with the host immune response, and has been found to bind to a wide range of chemokines *in vitro*, including at least one from each of the CC, CXC, C and CX_3C subtypes (Table 1-3). Chemokine binding by M3 is functional as shown by inhibition of chemokine-induced elevation of intracellular calcium levels and the inability of bound chemokines to bind with their receptors due to a higher affinity to M3 than their receptors (Parry et al., 2000; van Berkel et al., 2000). M3 was found not to bind CXCL12 /SDF-1 and evidence of binding of CXCL13/BCA-1 (also known as BLC) was variable between authors, which is of note, as these are both B cell chemokines (Parry et al., 2000; van Berkel et al., 2000). The binding of M3 to CCL2/MCP-1 and CXCL8/IL-8 has been found to be in a similar spatial arrangement to that of the receptors of these chemokines, despite the lack of sequence homology between these proteins (Alexander et al., 2002; Webb et al., 2003).

Intranasal infection of laboratory mice with *M3*-deficient MHV-68 reveals that M3 is non-essential for lytic replication in the lung, nor for spread of the virus to the spleen (Bridgeman et al., 2001; van Berkel et al., 2002). However,

amplification of latently infected B lymphocytes in the spleen fails to occur and leads to a decrease in splenic latent load compared to wild type MHV-68 infected mice, demonstrated by a decrease in vtRNA transcripts and viral DNA load and decreased reactivation of latent virus *ex vivo* (Bridgeman et al., 2001). Depletion of CD8+ T cells abrogates the differences seen in *M3*-null infections, which suggests that chemokine neutralisation by M3 blocks effective CD8+ T cell recruitment into lymphoid tissue during B lymphocyte proliferation (Bridgeman et al., 2001). Intracranial infection of mice with wild type and *M3*-null MHV-68 showed a greater difference when M3 was present; *M3*-null infected mice exhibit considerably lower viral titres in the brain and the intracranial inflammatory response is altered from a neutrophilic to a lymphohistiocytic meningitis (van Berkel et al., 2002).

Systematic name	Alternative name(s)	Responding cell types	Notes	Reference
CCL2	MCP-1	actT cells, MØ, EL, NK cells, BL, immDC	*In vitro*	(van Berkel et al., 2000)
			In vivo (GEM)	(Martin et al., 2006)
CCL3	MIP-1α	actT cells, MØ, EL, NK cells, immDC	*In vitro*	(van Berkel et al., 2000)
CCL5	RANTES	actT cells, MØ, EL, NK cells, immDC	*In vitro*	(Parry et al., 2000; van Berkel et al., 2000)
CCL19	MIP-3β	T cells, actT cells, mDC	*In vitro*	(Jensen et al., 2003)
CCL21	6Ckine	T cells, actT cells, mDC	*In vitro* *In vivo* (GEM)	(Jensen et al., 2003)
CXCL8	IL-8	NL	*In vitro*	(Parry et al., 2000; van Berkel et al., 2000)
CXCL13	BCA-1 BLC	B cells	*In vitro* (weak binding)	(Parry et al., 2000)
			In vivo (GEM)	(Martin et al., 2006)
CX_3CL1	Fractalkine	actT cells, MØ, NK cells	*In vitro*	(Parry et al., 2000; van Berkel et al., 2000)
XCL1	Lymphotactin	T cells	*In vitro*	(van Berkel et al., 2000)

Table 1-3 Evidence for M3-binding of chemokines.
Key: actT cells = activated T cells; MØ = macrophages; EL = eosinophils; NL = neutrophils; BL = basophils; immDC = immature dendritic cells; mDC = mature dendritic cells; GEM = transgenic mice that expressed M3 and the chemokine of interest in the pancreas

Expression of *M3* following intranasal infection of wood mice is highest at days 12 and 14 pi, later than that seen in *Mus musculus* (Hughes, 2006). *M3* transcripts are located in perivascular and peribronchiolar accumulations of B lymphocytes, and macrophages within granulomatous infiltrates at day 7 pi; at day 14 pi *M3* is present in numerous lymphocytes in the iBALT, in addition those in the perivascular and peribronchiolar infiltrates. Extrapulmonary *M3* transcripts are present in the bronchial and submandibular lymph nodes from day 7 pi and within splenic follicles from day 10 pi onwards (Hughes, 2006).

Infection of wood mice with a *M3*-deficient MHV-68 (M3.stop) leads to alterations in the inflammatory response, including mixed T and B lymphocytic infiltrates in the interstitium, perivascular and peribronchiolar areas (opposed to B cell dominated in the wild type MHV-68). A decrease in vtRNA in perivascular lymphocytes occurs, indicating a decrease in latency, which is either secondary to the smaller infiltrates or a lower proportion of B cells and is attributed to the absence of *M3*. Additionally, no iBALT is present in the M3.stop infected lungs, which suggests that iBALT formation is stimulated in the presence of *M3* due to increased viral persistence and the promotion of B cell proliferation (Hughes, 2006). In the spleens of M3.stop-infected wood mice, lymphoid follicles are expanded but lack germinal centres; this is similar to the response seen in MHV-68 infected *Mus musculus*. The number of cells containing vtRNA transcripts is also decreased, and the reduction in latency can be confirmed by a reduction in infective centre assay in the spleen of M3.stop-infected wood mice (Hughes, 2006).

The presence or absence of M3 also alters the presence of chemokines in the lungs of MHV-68-infected wood mice. MIP-1α/CCL3, RANTES/CCL5 and MIP-3β/CCL19 are increased in M3.stop infection, consistent with the *in* vitro binding of M3 to these chemokines. These chemokines are involved in T cell recruitment and depletion of their effects *in vivo* decreases inflammation and increases viral titre following viral infection; therefore binding of M3 to these chemokines may confer a survival advantage (Cook et al., 1995; Culley et al., 2006). Additionally, MIP-1β/CCL9, MIP-3α/CCL20, KC/CXCL1, MIP-2/CXCL2 and MIG/CXCL9, which either have not exhibited binding, or have been shown

not to bind to M3, are also increased in M3.stop infection. Significantly, SDF-1α/CXCL12, BLC/CXCL12 and CD30L are decreased in M3.stop infection, suggesting that the presence of M3 increased the levels of these chemokines, either in relative or absolute terms (Hughes, 2006). SDF-1α and BLC are B cell chemoattractants, so an increase in wild type MHV-68 infection corresponds with the higher numbers of B lymphocytes in the inflammatory response to wild type MHV-68 infection in the wood mouse. CD30L has a role of T and B cell segregation in the spleen and BLC/CXCL12 may be relevant to the formation of iBALT in the lung. The contradictory reports as to whether BLC is bound by M3 may be due to the location and timing of the increased levels of M3 in response to viral infection, or due to subtle differences in the coding of these chemokines between *Mus musculus* and *Apodemus sylvaticus* (Hughes, 2006).

Analysis of gene expression in the lung in response to M3.MR compared to M3.stop infected wood mice also reveals alteration in the expression of other genes. These include members of the Palate, lung and nasal epithelium clone (PLUNC) family of proteins, *SPLUNC1* and *LPLUNC1*, which were expressed at levels 17.6 and 7.3-fold higher, respectively, in M3.MR compared to M3.stop infected wood mice; Clara cell secretory protein (*CCSP*), which showed a 3.3-fold increase in the presence of M3 and Anterior gradient homologue 3 (*AGR3*), which was also increased in the presence of M3 (Hughes, 2006). Further details of these proteins are given below (1.5 Expression of proteins in the lung in relation to MHV-68 *M3*).

1.2 *Paramyxoviridae*

1.2.1 *Paramyxoviridae* family

The family *Paramyxoviridae* (within the order *Mononegavirales*) contains many viruses of great significance to human and veterinary health (Table 1-4). Paramyxoviruses are enveloped negative-strand RNA viruses; the genomic negative sense RNA serves as a template for the synthesis of mRNA and also the antigenomic (+) strand, from which further copies of the negative sense genomic RNA are synthesised. In addition to this, the paramyxoviruses are

defined by the presence of the F (fusion) protein within the virus capsid, which functions to allow virus-cell membrane fusion (Lamb and Parks, 2007).

Subfamily	Genus	Viruses
Paramyxovirinae	*Rubulavirus*	Mumps virus Human parainfluenza virus 2
	Avulavirus	Avian paramyxovirus 1 (Newcastle disease virus)
	Respirovirus	Murine parainfluenza virus 1 (Sendai virus) Human parainfluenza virus 1 and 3 Bovine parainfluenza virus 3
	Henipaviruses	Hendra virus Nipah virus
	Morbillivirus	Measles virus Canine distemper virus Rinderpest virus
Pneumovirinae	*Pneumovirus*	Human respiratory syncytial virus Bovine respiratory syncytial virus Pneumonia virus of mice
	Metapneumovirus	Human metapneumovirus Avian metapneumovirus

Table 1-4 Examples of members of the family *Paramyxoviridae*. (ICTVdb-Management, 2006; Lamb and Parks, 2007).

The family *Paramyxoviridae* is divided into two subfamilies (*Paramyxovirinae* and *Pneumovirinae*), both of which contain more than one genus, distinguished by the size and shape of the nucleocapsid, antigenic cross-reactivity between members of a genus, the presence (or absence) of neuraminindase activity and the differences in the number and nature of encoded proteins. The virions consist of a lipid bilayer derived from the plasma membrane of the host cell, within which are glycoprotein spikes (fusion protein, haemagglutininneuraminidase), are roughly spherical in shape and 150-350 nm in diameter. The nucleocapsid core contains the 15-19 kb single stranded RNA, which combined with the N protein, form the helical structure, to which P and L proteins are attached. Between the nucleocapsid core and the lipid

bilayer there is the matrix protein, which is the most abundant protein in the virion (Lamb and Parks, 2007).

1.2.2 *Murine parainfluenza 1* (Sendai virus)

1.2.2.1 Natural history of Sendai virus

Sendai virus was first isolated from laboratory mice in Sendai, Japan in 1953, which were being inoculated with suspensions of lung from an infant who died from pneumonia. The origin of the virus is unclear however, as it has been isolated from many laboratory species worldwide, including mice, rats, hamsters and guinea pigs and was also reported to be the agent of epizootic outbreaks of influenza-like disease in pigs in Japan in the 1950's (Faísca and Desmecht, 2007; Percy and Barthold, 2007). Sendai virus is rarely found in wild populations of mice, but has been isolated from grey squirrels (*Sciurus carolinensis*) in North Wales (Becker et al., 2007; Greenwood and Sanchez, 2002). Therefore, Sendai virus appears not to have a restricted host-range and could be a zoonotic pathogen, although it is now generally accepted that Sendai virus is a rodent pathogen and humans are not natural hosts (Brownstein, 2007; Percy and Barthold, 2007).

Sendai virus has been studied in mice both as a model for its human parainfluenza counterpart and due to its potential importance as an endemic pathogen in laboratory mice. It is also capable of causing acute epizootic disease outbreaks in colonies, which cause significant illness in most strains and ages, including adult immunocompetent mice (Faísca and Desmecht, 2007; Percy and Barthold, 2007). Infection is spread most effectively via close contact or contaminated fomites, although aerosol transmission has been shown to be possible (Faísca and Desmecht, 2007).

1.2.2.2 Pathogenesis of Sendai virus

Intranasal infection of mice causes a descending respiratory infection in the nose, trachea, bronchi and bronchioles with spread into the alveoli (type II pneumocytes) also seen. The tropism for the respiratory tract is due to the reliance of the virus on a host protease (Tryptase Clara) to cleave the viral fusion (F) protein; in the absence of this protease, other cells may be infected,

but only one round of replication of the virus occurs (Kido et al., 1992; Tashiro et al., 1992). Productive infection occurs within respiratory epithelium and virus is detectable in the lung soon after infection, with titres peaking at 4-8 dpi, depending on the strain, age and immunocompetence of the mouse. Microscopically, the infected epithelium appears focally disorganised, with vacuolation of the cytoplasm and a mild neutrophilic infiltrate. These foci progress to areas of irregular hyperplasia, with loss of cilia and cellular hypertrophy. Eosinophilic intra-cytoplasmic inclusion bodies (accumulated ribonucleoproteins) are occasionally present in the epithelium (Faísca and Desmecht, 2007; Percy et al., 1994). Infiltration of CD4+ and CD8+ T cells leads to cytotoxic T cell-mediated apoptosis of infected cells causing sloughing and accumulation of epithelium, mixed with mucin, neutrophils and lymphocytes within the airway lumina. This inflammatory response coincides with the decline in viral titre in the lung. The inflammatory response and subsequent apoptosis may spread into the alveolar walls at the distal end of the terminal bronchioles; these foci may coalesce to affect large areas of a lobe or several lobes, whereas other areas may be spared (Brownstein et al., 1981; Brownstein, 2007; Faísca and Desmecht, 2007; Itoh et al., 1991; Percy et al., 1994).

Antibodies specific to Sendai virus are detected within the lung as early as 3 dpi; in the local lymph nodes, IgM levels peak at day 7 pi and IgA and IgM at day 10 pi. Levels of these antibodies peak in the spleen at day 14 pi. Circulating IgG titres remain high for a prolonged period (Brownstein, 2007; Faísca and Desmecht, 2007). Conversely, Sendai virus infection has been utilised to study secondary bacterial infection as it induces suppression of antibacterial defences; reported potential mechanisms include abnormalities of macrophage phagocytosis of bacteria, synergism between Sendai virus and bacterial pathogens, destruction of the mucociliary system and beneficial properties of the inflammatory oedema for bacterial growth (Faísca and Desmecht, 2007; Jakab, 1975).

1.2.3 *Human respiratory syncytial virus* (HRSV)

1.2.3.1 Natural history of HRSV

Human respiratory syncytial virus was first isolated from a laboratory chimpanzee, and then soon after from human infants with respiratory illness (Collins and Crowe, 2007). It is now considered one of the most common respiratory viruses, with nearly 70 % of infants infected in their first year and the remainder by the age of three years; reinfection occurs every two to three years throughout life (Glezen and Denny, 1973; Winn and Walker, 1994). Despite this association of HRSV-induced illness in children, the virus is also an important risk factor in the elderly and in immunocompromised patients, especially those with SCID and following haematopoietic stem cell or lung transplants (Graham et al., 2002).

The virion is similar in structure to that described for members of the *Paramyxoviridae* generally (1.2.1 *Paramyxoviridae* family), although in addition to roughly spherical virions of 100 to 350 nm diameter, long filamentous forms are also common, which are 60-200 nm in diameter and up to 10 μm in length (Collins and Crowe, 2007). The nucleocapsid is a symmetrical helix which contains the 15.2 kb negative-sense single strand RNA and is surrounded by matrix protein and a lipid envelope that is derived from the host cell's plasma membrane. Within this membrane there are three types of glycoproteins. The Fusion (F) protein directs the entry of the virus into the host cell via fusion between the virion membrane and the host cell plasma membrane and later in infection can mediate fusion of adjacent cells to form syncytia. The G protein is the major attachment protein, required for the virus to attach to the host cell. The small hydrophobic (SH) protein is the third envelope protein, the function of which is not known, but is not required for efficient viral growth either *in vitro* or *in vivo* (Collins and Crowe, 2007).

1.2.3.2 Pathogenesis of HRSV in humans

HRSV is one of the most infectious viruses that affect humans; it is spread via respiratory secretions in large droplets and close contact with infected individuals or fomite contamination, usually with subsequent self-inoculation (contaminated hands coming into contact with nasal or conjunctival mucosa).

Humans are the only source of infection; there are no other reservoir hosts (Collins and Crowe, 2007; Graham et al., 2002; Winn and Walker, 1994). The virus replicates in the nasopharynx and in susceptible patients is spread to the lower respiratory tract by aspiration of the superficial layer of the respiratory epithelium, in a multifocal pattern; the virus is shed from the apical (and not basolateral) surface of the cell (Peebles and Graham, 2005). The cytoplasm is the site of viral replication and eosinophilic intra-cytoplasmic inclusion bodies are often observed in H&E stained sections, in a paranuclear location in infected cells (Winn and Walker, 1994). Immunohistology reveals viral antigen in small foci (even in fatal cases) in bronchial, bronchiolar and alveolar epithelium as well as some syncytial cells, which are not a prominent feature in all cases (Neilson and Yunis, 1990). The F protein of HRSV has been reported to bind to TLR4, which may alter the recruitment and activation of macrophages and monocytes, as well as neutrophils. There is an increase in the number of dendritic cells (DC) following infection. However, HRSV is associated with plasmacytoid DC-induced reduction of IFNα and myeloid DC-induced reduction of IFNγ secretion from CD4+ T cell (Collins and Crowe, 2007).

Infection of the bronchiolar epithelium with HRSV results in necrosis and loss of cells, along with proliferation of the epithelium and a neutrophilic infiltrate. Lymphocytes, plasma cells and macrophages accumulate in perivascular and peribronchiolar cuffs (Graham et al., 2002; Neilson and Yunis, 1990). In bronchioalveolar lavage fluid, the predominant cell type are neutrophils (76 %) with lymphocytes (9 %), mononuclear cells (10 %) eosinophils (1 %) being much less frequent (Everard et al., 1994; Graham et al., 2002). The predominance of neutrophils not only leads to clearance of the virus, but also, through the destruction of infected cells, contributes to the lesions in the lung (Wang et al., 1998). The presence of the inflammatory response is consistent with the high level of a number of cytokines commonly found in HRSV, e.g. RANTES, MCP-2, MIP-1α, MIP-1β, IL-8 and fractalkine (Peebles and Graham, 2005; Zhang et al., 2001). Pneumonia is associated with the thickening of the alveolar walls due to an infiltration of the interstitium by monocytes (Neilson and Yunis, 1990). Excessive mucus secretion is frequently seen and this is an

important part of the clinical consequences of infection. In children, the narrow diameter of the bronchioles leads to obstruction by mucus, which is admixed with desquamated airway epithelial cells, neutrophils, fibrin and lymphocytes; this leads to wheezing, air trapping and bronchiolitis obliterans as potential outcomes (Peebles and Graham, 2005). It has been shown in mice that this excessive mucus secretion is mediated by IL-13, but there are strain variations in the extent of this effect (Lukacs et al., 2006; Moore et al., 2009).

1.2.3.3 Experimental infection of mice with HRSV

Infection of laboratory animals has been performed in cotton rats, mice, ferrets, guinea pigs, hamsters and marmosets (Collins and Crowe, 2007). Different strains of mice show differences in levels of viral replication, BALB/c mice being one of the more permissive strains, although cotton rats are more so; however, virus replication is still limited (Domachowske et al., 2004; Graham et al., 2002). Using *in situ* hybridisation on sections from lung of cotton rats, only few bronchiolar and alveolar cells showed evidence of virus at the peak of infection [day 4 pi (Murphy et al., 1990)]. This is similar to the pattern of virus infection in children's lungs, as described by Neilson and Yunis (1990).

The main histological lesion seen in infected BALB/c mice is bronchiolitis, which differs to natural cases, most likely as experimental infection results in aspiration of virus directly into the lung and because HRSV in BALB/c mice is not directly cytopathic (Domachowske et al., 2004; Graham et al., 2002; Peebles and Graham, 2005). However, it has been reported that the primary target of HRSV in the mouse model is the alveolar epithelium, which differs to the infection in humans (Peebles and Graham, 2005). Bronchiolitis is associated with the presence of natural killer cells and CD8+ lymphocytes, both of which secrete IFNγ; clearance of the virus occurs alongside the rise in the number of CD8+ T cells (Graham et al., 1991; Peebles and Graham, 2005). However, CD4+ T cells are also required for viral clearance, unlike B cells, which although important for protection against subsequent infection, do not play a role in viral clearance (Hussell et al., 1997; Hussell and Openshaw, 1998). *In vivo* infection of mice leads to similar expression of cytokines as seen in human infection, namely RANTES, MCP-2, MIP-1α, MIP-2, IFN-inducible

protein 10 and the IL-8 homologue keratinocyte chemokine (Miller et al., 2004; Peebles and Graham, 2005; Power et al., 2001), many of which have pathogenic effects in HRSV infection. For example, RANTES and MIP-2 are associated with airway hyperresponsiveness, and mice with MIP-1α deficiency had reduced inflammation following HRSV infection (Miller et al., 2003; Miller et al., 2004).

1.3 *Orthomyxoviridae*

1.3.1 *Orthomyxoviridae* family

The *Orthomyxoviridae* family contains the genera *Influenzavirus A*, *Influenzavirus B*, *Influenzavirus C*, *Thogotovirus* and *Isavirus*; single stranded, negative sense RNA viruses (Wright et al., 2007). Influenza A viruses are further classified based on the haemaglutinin (HA) and neuraminidase (NA) molecules and named according to the type of virus, host of origin (if not human), place of isolation, strain number and year of isolation, for example, Influenza A/Mute Swan/MI/451072/06 (H5N1). The influenza virus was first isolated from swine in 1930 and from humans in 1933, which was named Influenza A; Influenza B, a genetically distinct virus was isolated in 1940 and Influenza C in 1947 (Wright et al., 2007).

1.3.2 *Influenzavirus A*

1.3.2.1 Natural history of *Influenzavirus A*

Influenza A virus infects a wide variety of species other than man, including birds, swine, horses, dogs, cats, whales and seals (Figure 1-3). As all known strains of HA and NA subtypes are found in aquatic birds (Aniseriformes [e.g. ducks, geese and swans] and Charadriiformes [e.g. gulls, terns]), they are considered the natural reservoir of Influenza A. The infection of ducks with most strains of Influenza A is asymptomatic, with viral replication occurring predominantly in the intestinal tract and, to a much lesser degree, in the respiratory tract. These avian viruses have evolved into strains which are host-specific for horses, pigs and humans, among others. Some strains have the ability to cross species barriers; hypotheses that swine are an intermediate host between humans and birds, with genetic mixing of strains within a swine host have been proposed, but evidence for this is contradictory (Webster et al.,

1992). This “mixing vessel” hypothesis has its basis in the fact that swine trachea contain both avian and human type receptors for Influenza virus, and can be simultaneously infected with strains from both avian and human hosts, leading to the potential for reassortment into new strains (Wright et al., 2007).

Avian influenza viruses are categorised as low pathogenicity or high pathogenicity avian influenza (LPAI or HPAI), depending on their pathogenicity in domestic chickens. LPAI causes mild respiratory disease, depression and/or a decrease in domestic egg production. HPAI viruses are classified as such according to criteria defined by the Animal Health OIE, including rate of mortality in 4 – 8 week old chickens following intravenous infection, growth in cell culture and the amino acid sequence of the haemaglutinin connecting peptide (Wright et al., 2007).

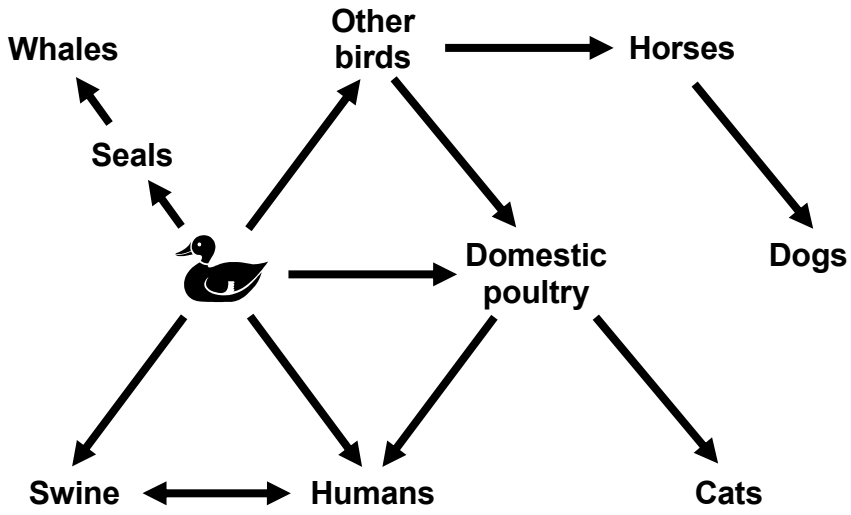

Figure 1-3 Transmission of Influenza A virus from waterfowl to other species. Modified from Wright et al., 2007.

Influenza viruses are continually circulating in the human population, and seasonal outbreaks occur in the winter, most likely due to the low indoor humidity during this time, which favours the survival of the virus within aerosols (Wright et al., 2007). Since 1977, subtypes H3N2 (the cause of the 1968 pandemic) and H1N1 have been circulating in the population (Webster et al., 1992). Pandemics have occurred every 8 to 41 years over the last few centuries and occur when a new influenza virus appears, immunity to which is

therefore low, and infection spreads globally (Taubenberger and Morens, 2008). New influenza viruses occur due to antigenic shift; the rearrangement of gene segments between two different (often human and avian) viruses present within one infected cell, and antigenic drift (point mutations that cause gradual antigenic changes). These changes, particularly those which occur in the HA gene, lead to viruses which are immunogenically distinct and to which the population has no immunity, which therefore have the potential to cause a pandemic (Wright et al., 2007).

An H1N1 virus was responsible for the catastrophic 1918-19 Influenza pandemic and also for the recent 2009 “Swine Flu” pandemic (Mauad et al., 2010; Taubenberger, 2006). The 1918-19 pandemic originated in the United States, despite its widely used “Spanish Influenza” moniker, spreading through Army camps and through movement of troops to Europe. The outbreak has been associated with pigs kept at the army camps, but may have originated from Kansas, from where recruits were sent to training camps at which the outbreaks were reported (Wright et al., 2007). Recent genetic analysis of the strain has shown that the virus had originally evolved within avian hosts and that this virus was the common ancestor for the current swine and human H1N1 viruses (Taubenberger, 2006). The 2009 pandemic was identified to originate in swine in Mexico (Centers for Disease Control and Prevention, 2009), and was transmissible not only person-to-person, but naturally occurring cases in several other species were also reported, including domestic turkeys, ferrets, cats and cheetahs (Lohr et al., 2010).

The H5N1 strain has been the cause of outbreaks of influenza in people in South East Asia since 1997. The first case was in Hong Kong, in a three year old boy and the infection was fatal. Prior to this, transmission of HPAI to humans had not been considered a risk and only three previous cases had been reported, all of which caused mild symptoms (Kuiken and Taubenberger, 2008; Wright et al., 2007). Further cases were reported in Hong Kong that year and the mortality rate was high (33 %), however no evidence of human to human transmission was found. H5N1 HPAI is now much more widely spread throughout Asia, the Middle East, Russia, south-eastern and central Europe

and parts of Africa. Mortality rates have increased to 59 % (in the period up to 2007) and evidence of some human to human transmission is reported, but is rare (Taubenberger and Morens, 2008; Wright et al., 2007).

1.3.2.2 Pathogenesis of *Influenzavirus A* in humans

Transmission of human influenza virus occurs by inhalation of infectious particles within droplets (aerosols) and possibly via fomites and self-inoculation of the upper respiratory tract and conjunctiva (Kuiken and Taubenberger, 2008). Infection occurs in the upper respiratory tract, with virus infecting predominantly ciliated epithelial cells in the trachea and bronchi. These cells express greater numbers of the receptor for human influenza virus, which have a terminal sialic acid, linked to a galactose by an alpha-2,6 linkage (Shinya et al., 2006). These receptors bind to the HA protein of the virus. In avian influenza (specifically, H5N1), the receptor differs and this leads to attachment of the virus lower in the respiratory tract (bronchioles and alveoli); H5N1 preferentially attaches to alveolar macrophages and type II pneumocytes (van Riel et al., 2007). This pattern of attachment might explain the high mortality rate in H5N1 infected humans, due to the increased likelihood of pneumonia with viral attachment at this location, even in the absence of tracheobronchial lesions (Korteweg and Gu, 2008; Kuiken and Taubenberger, 2008).

Uncomplicated influenza infection (i.e. that which does not lead to pneumonia) in humans causes diffuse, superficial necrotising tracheobronchitis, which increases in severity distally in the respiratory tract. The epithelium exhibits vacuolisation, oedema and loss of cilia, with extensive desquamation of epithelium in severe cases. Within the lamina propria, hyperaemia and oedema are present, with infiltration of neutrophils following epithelial necrosis and later inflammation dominated by lymphocytes and macrophages (Taubenberger, 2006; Walsh et al., 1961). Clinical symptoms are due to damage at these sites secondary to viral replication, and the local and systemic effects of cytokines and other inflammatory mediators (Eccles, 2005). When pneumonia occurs due to extension of viral infection into the lower respiratory tract, the primary target cells are the type I pneumocytes and ciliated bronchiolar epithelial cells, with non-ciliated epithelium, type II

pneumocytes and alveolar macrophages as secondary targets (van Riel et al., 2007). Damage to type I pneumocytes leads to leakage of fluid across the alveolar-capillary barrier and damage to type II pneumocytes reduces their ability to absorb this fluid, and produce surfactant, which assists in the clearance of fluid by reducing surface tension. The outcome of this is alveolar oedema alongside the alveolar necrosis and desquamation of pneumocytes into the alveolar lumen (Kuiken and Taubenberger, 2008). Oedema cells and necrotic pneumocytes, along with alveolar macrophages, fibrin and hyaline membranes fill the alveoli, and the interstitium is thickened by hyperaemic capillaries, oedema and infiltration by neutrophils with lesser eosinophils and capillary thrombosis (Kuiken and Taubenberger, 2008; Taubenberger and Morens, 2008). These changes, with necrotising bronchiolitis and tracheobronchitis similar to that described above are the histological lesions seen due to influenza virus and are the cause of severe, and occasionally fatal, respiratory dysfunction (Kuiken and Taubenberger, 2008). Secondary bacterial infection is a common sequel; it is thought that 96 % of deaths in the 1918-19 pandemic, were due to bacterial pneumonia and this may complicate the histological findings; the presence of neutrophils may be due to bacterial infection (Kuiken and Taubenberger, 2008; Taubenberger and Morens, 2008). The histological lesions seen in pandemics, including the 1918-19 pandemic, do not differ greatly from those seen in pneumonia caused by seasonal influenza (Taubenberger and Morens, 2008).

1.3.2.3 Experimental infection with *Influenzavirus A*

Mice, ferrets and pigs have all been used for the study of experimental infection of influenza virus. In the earliest experiments, it was shown that mice exhibit similar histological lesions to humans, but are unable to transmit the virus between individuals (Shope, 1935). Work since then has revealed that infection of mice leads to a highly variable response; most influenza viruses do not naturally cause disease in mice. Some strains, those replicated using embryonated chicken eggs, may replicate in the respiratory tract of mice, but cause no disease; whereas others, especially those which are mouse adapted by passage through mouse lungs, can cause severe morbidity and mortality, and lethal pneumonia (Tripp and Tompkins, 2009). Mouse adapted strains

cause similar lesions to those present in human lower respiratory tract infections. Despite the similarities between lesions, mice do not show the formation of hyaline membranes or capillary thrombosis that are a feature of infection in humans (Taubenberger and Morens, 2008).

Infection of BALB/c mice with a H1N1 virus reconstructed from genomic RNA from the 1918-19 pandemic showed marked virulence in mice, similar to the increased morbidity and mortality seen in humans during that pandemic, including, by day 4 pi, necrotising bronchitis and bronchiolitis with multifocal (peribronchiolar) to diffuse, moderate to severe alveolitis. The inflammatory infiltrate consisted of neutrophils and macrophages with a moderate to severe peribronchiolar and alveolar oedema (Tumpey et al., 2005).

Infection of mice with HPAI H5N1 results in bronchopneumonia with desquamation of epithelial cells, peribronchial and diffuse alveolar interstitial inflammation, and intraalveolar oedema at day 4 pi (Nishimura et al., 2000; Taubenberger and Morens, 2008). Immunohistology for viral antigen reveals that virus is present in epithelial cells of the upper and lower respiratory tract (bronchial and alveolar epithelium) by day 1 pi and increased numbers of epithelial cells (described as bronchial epithelium in the text but bronchiolar epithelium shown in the figures), as well as desquamated epithelial cells within bronchioles by day 4 pi (Lu et al., 1999; Nishimura et al., 2000). Lu et al. (1999) also described viral antigen-positive cells within mononuclear cells within the “subepithelial interstitium”. Infection of extra-pulmonary sites has also been described, with viral antigen present in neurons, ependymal cells and glial cells (Lu et al., 1999; Nishimura et al., 2000). Additionally, Nishimara et al. (2000) also described multifocal areas of adipocyte necrosis which were associated with positive staining for viral antigen and they speculated that this may be the cause of other scientists’ reports of virus isolation from other organs (e.g. liver, spleen, kidney, heart). Viraemia has been described in several papers, and is the suspected route of infection to the brain (Lu et al., 1999; Nishimura et al., 2000).

Reports of experimental infection of mice with LPAI H5N1 are not prevalent in the literature. Experimental infection of chickens and ducks has shown that these viruses are adapted for either one or the other group of birds; those isolated from chickens replicate less well in ducks and vice versa (Mundt et al., 2009; Spackman et al., 2007). A LPAI H5N1 virus isolated from a Mute Swan [A/Mute Swan/MI/451072/06 (H5N1)] intranasally inoculated into chickens and ducks, replicated better in ducks, with virus isolated from tracheal and cloacal swabs at days 2, 4 and 7 pi in ducks and only at day 2 pi in chickens. Seroconversion was similarly higher in ducks than chickens (Mundt et al., 2009). Histologically, chickens exhibited mild catarrhal tracheitis and mild BALT hyperplasia, whereas ducks exhibited mild catarrhal and multifocal lymphocytic tracheitis and moderate lymphocytic infiltrates and focal oedema within the lung. In contrast, chickens infected with chicken-adapted strains exhibited lesions in a variety of organs which were more severe (Mundt et al., 2009). LPAI H5N1 viruses used in these studies were found to be wild-bird adapted strains which were antigenically and genetically distinct from HPAI H5N1 (Spackman et al., 2007). The lower pathogenicity is thought to be due to differences in the HA protein; HA cleavage is required for function of this protein, in HPAI this can be achieved by endosomal proteases during virus entry and so has a wide cellular and organ tropism compared to LPAI viruses, in which extracellular proteases present in the respiratory and gastrointestinal tracts are required for cleavage, hence LPAI viruses are restricted to these systems. These differences are dependent on the amino acids present at the cleavage site of HA (Boycott et al., 1994; Mundt et al., 2009).

1.4 Interferon γ

The host response to viral infection is complex, with many cytokines, chemokines and cellular components involved. Interferon (IFN) γ is a cytokine within the innate immune response and its role in MHV-68 infection has been studied by several authors (Dutia et al., 1997; Ebrahimi et al., 2001; Gangadharan et al., 2008; Lee et al., 2009; Mora et al., 2007; Sarawar et al., 1997). IFNγ also is suggested to have a role in the regulation of the pulmonary proteins, CCSP and SPLUNC1 (Britto et al., 2010; Curran et al., 2009; Magdaleno et al., 1997; Yao et al., 1998a).

1.4.1 Interferons in viral infection

Infection of a host organism by a virus initiates an immune response, the aim of which is to eliminate or reduce the harmful effect of the virus. The adaptive immune system generates a pathogen-specific response via T and B cells, with the ability to establish memory of infection on the occasion of a subsequent exposure to the same stimulus. In the interim, the faster innate immune response provides a defence via non-specific receptors which recognise molecular structures conserved in infectious organisms but are not expressed within the host (Biron and Sen, 2007). This requires the actions of a pre-existing cell population, of which monocytes or macrophages, dendritic cells (DC), natural killer (NK) cells and polymorphonuclear leukocytes are from the immune system and express the appropriate receptors. Recognition of pathogen-associated molecular patterns (PAMPs) via these receptors initiates an innate immune response (Biron and Sen, 2007).

Toll-like receptors (TLR) are trans-membrane proteins which recognise PAMPs. Specifically relating to viral antigens, TLR3 recognises double-stranded RNA, TLR7 and 8 recognise single-stranded RNA and TLR9 is activated by DNA containing unmethylated cytidine-phosphate-guanosine (CpG) sequences. These TLRs are present within endosomes and, along with other cytoplasmic proteins including RNA-activated protein kinase (PKR) and RNA helicases, initiate downstream pathways which result in the transcription of genes which form the response to infection. Cytokines are a major product in this response, including the pro-inflammatory TNFα, interleukins IL- 1, 6, 18, 12 and interferons. Interferons are divided into three types; type I which includes IFNα, IFNβ, IFNε, IFNδ, IFNκ, IFNω and IFNτ, which can be synthesised by virtually any cell type in response to the appropriate stimulation; transcription of IFNα and IFNβ are the most important in response to viral infection. These interferons act to stimulate the transcription of further genes which act in many ways to inhibit viral replication via binding or cleaving of viral RNA, inhibition of cellular protein synthesis (required by RNA viruses to replicate) and promotion of apoptosis of the infected cell (Biron and Sen, 2007). The second type of interferons, type II, comprises IFNγ. Type III IFNs are more recently described and include IFNλ1, IFNλ2 and IFNλ3, also known

as IL-29, 28A and 28B, respectively. These IFNs are also induced by viral infection and use pathways similar to type I interferons (Randall and Goodbourn, 2008).

1.4.2 Interferon γ

IFNγ is produced by NK cells, monocytes/macrophages, DC, B cells, NKT cells (which have characteristics of both NK cells and T cells) and CD4+ Th1 cells and CD8+ T cells. Of these, the antigen presenting cells (APC; monocytes/macrophages, DC) and NK cells are important in early innate immunity (Schroder et al., 2004). APC are activated by the presence of antigen and secrete IL-12 and IL-18, which stimulates the production of IFNγ (Goodbourn et al., 2000; Schroder et al., 2004). In addition, macrophages also secrete chemokines (e.g. macrophage-inflammatory protein 1α [MIP-1α]) which attract NK cells to the site, which are then stimulated to produce IFNγ via IL-12. Inhibition of IFNγ production is mediated by IL-4, IL-10, transforming growth factor-β and glucocorticoids (Schroder et al., 2004). IFNγ receptors are expressed almost ubiquitously on the surface of cells (Huang et al., 1993b). The receptor is composed of two pairs of peptides; IFNγR1 (which bind to IFNγ) and IFNγR2 which transduce the signal (Bach et al., 1997; Schroder et al., 2004). This signal is transmitted though the Jak/STAT pathway, resulting in phosphorylated STAT1 molecules within the cell nucleus binding to the gamma activation sequence (GAS), a regulatory region upstream of IFNγ inducible genes, leading to the transcription of these genes (Goodbourn et al., 2000). This signalling is transient; *in vitro* transcription of genes occurs within 15-30 minutes of treatment with IFNγ, and STAT activation is inhibited within 1 hour. Following signal transduction by the receptor-ligand complex, the complex is internalised and enters the endosomal pathway where it is dissociated. In many cells types IFNγR1 is recycled to the cell surface, but in a dissociated form, otherwise IFNγ is degraded within the endosome (Schroder et al., 2004).

IFNγ-inducible genes are numerous and have varied functions. Specific anti-viral effects include production of protein kinase dsRNA-regulated (PKR), a kinase which is activated by dsRNA and inhibits viral protein synthesis;

dsRNA-specific adenosine deaminase (ADAR) which alters viral mRNA causing mistranslation and the generation of non-functional viral proteins; and guanylate-binding proteins which have anti-viral properties by an unknown mechanism (Goodbourn et al., 2000; Schroder et al., 2004). IFNγ also induces the expression of several cytokines and chemokines, including IL-12 which activates NK cells and drives CD4+ T cell development to Th1 cells, as well as being important in the production of IFNγ itself (Goodbourn et al., 2000). IFNγ causes several chemokines to be upregulated which act to attract different immune cells towards the site of inflammation, including IFN-inducible protein 10 (IP-10; monocytes and T cells), monocyte chemoattractant protein-1 (MCP-1; monocytes/macrophages), monokine-induced by IFNγ (MIG; T cells), macrophage-inflammatory protein-1α and -1β (MIP-1α and -1β; CD4+, CD8+ and memory T cells), RANTES (CD4+ T cells and monocytes/macrophages), ICAM-1 and VCAM-1 (adhesion molecules) (Schroder et al., 2004). Additionally, IFNγ upregulates genes which are involved in MHC class I and II antigen presentation, increasing the number and variety of viral proteins presented on the cell surface, thereby increasing the antigenic stimulation of T cells and the induction of cell-mediated immunity. Inhibition of cellular proliferation and increased apoptosis is also stimulated. Apoptosis is increased via upregulated IRF-1, caspase 1, PKR (which most likely induces Fas), death associated proteins, Fas and Fas ligand and increased sensitivity to TNFα-mediated apoptosis by promotion of TNFα receptor expression on the cell surface (Goodbourn et al., 2000; Malmgaard, 2004; Schroder et al., 2004). Lastly, via an increase of reactive oxygen species and NO, IFNγ increases cells' microbial killing ability (Schroder et al., 2004). It should be noted that there are differences in the levels of IFNγ in different strains of laboratory mice. For example, the T cells in C57BL/6 and C3H mice secrete significantly higher IFNγ levels than T cells in BALB/c mice (Schroder et al., 2004).

1.4.3 IFNγ in MHV-68 infection

The secretion of IFNγ in response to MHV-68 infection is consistent with that seen in other viral infections. IFNγ is produced in the spleen, mediastinal and cervical lymph node cells in response to infection, from as early as day 3 pi, peaking at 10 days pi, correlating with viral clearance from the lung (Sarawar

et al., 1996). Investigation of the wide ranging effects of IFNγ has been conducted using genetically engineered mice which either have a disruption to the IFNγ gene, or lack the IFNγ receptor (IFNγR), thereby functionally removing the action of IFNγ (Dalton et al., 1993; Huang et al., 1993b). In both cases, these mice develop normally and are healthy in the absence of infectious disease. However, IFNγ$^{-/-}$ mice exhibit deficits in the ability to deal with pathogens, for example, impaired production of macrophage antimicrobial products and reduced expression of macrophage MHC class II antigens (Dalton et al., 1993). Similarly, IFNγR$^{-/-}$ mice also show increased susceptibility to infectious agents (e.g. *Listeria monocytogenes* and vaccinia virus), despite normal cytotoxic and helper T cell responses, most likely due to decreased Ig switching causing decreased IgG2a responses (Huang et al., 1993b).

The role of IFNγ in clearing acute MHV-68 infection has been found to be both not essential and essential by different authors. Earlier reports found that MHV-68 infection in IFNγ$^{-/-}$ (BALB/c) mice resulted in elimination of the virus at a similar rate to that seen in wild type mice, despite a higher viral titre in the lung at day 13 pi (Sarawar et al., 1997). This was similar to the finding in IFNγR$^{-/-}$ (129/Sv/Ev) mice, where no differences were found in either the viral titre or the clearance of virus from the lung compared to wild type mice (Dutia et al., 1997). However, this was in contrast to the results of infection of IFNγ$^{-/-}$ (BALB/c) mice with MHV-68, which caused an acute bronchopneumonia characterised by a neutrophilic infiltrate, hyperaemia, interstitial and intra-luminal oedema and numerous viral inclusion bodies, which was fatal in some mice (>60 %) at 9-14 days pi. Those which survived had cleared the virus from the lung by day 14 (Lee et al., 2009). Lee et al. (2009) found that this was a dose dependent effect, seen with infectious doses of 4 x 10^5 PFU; at the lower dose of 4x10^3 PFU, IFNγ$^{-/-}$ mice survived the acute infection. The lower dose had also been used by Sarawar et al. (1997). The different background strain of the mice used may also explain the apparently conflicting results as T cells in BALB/c mice secrete lower levels of IFNγ compared to other strains (Schroder et al., 2004), or may be due to chemokine differences seen between BALB/c and C57Bl/6 mice (Weinberg et al., 2004). Additionally, as acute disease was not seen in IFNγ$^{-/-}$ mice infected with MHV-68 lacking viral cyclin

or bcl-2 genes, Lee et al. (2009) suggested that the severity of the acute disease may be due to early reactivation of latent virus as both of the genes are required to control latency. This is supported by the finding that *in vitro*, MHV-68-infected primary bone marrow-derived macrophages subsequently treated with IFNγ showed inhibition of lytic viral replication and decreased expression of the lytic gene switch 50, which is essential for reactivation. This suggests that absence of IFNγ activity may lead to earlier reactivation of the virus (Goodwin et al., 2010; Steed et al., 2007).

Intranasal infection of IFNγR$^{-/-}$ (C57BL/6) mice induces a more severe perivascular, peribronchiolar and subpleural inflammatory infiltration (lymphocytes, plasma cells, neutrophils, eosinophils) compared to wild type mice, and hyperplasia and hypertrophy of type II pneumocytes at 15 dpi. In wild type mice, the inflammation is less severe and resolves by day 45 pi, whereas B lymphocyte dominated infiltrates are still present in the same locations in the IFNγR$^{-/-}$ mice at this timepoint and additionally, subpleural fibrosis is seen (Mora et al., 2005). The distribution of pulmonary fibrosis is more extensive by day 150 pi, when the IFNγR$^{-/-}$ mice exhibit interstitial fibrosis with myofibroblasts and a five-fold increase in collagen deposition compared to wild type mice. These changes are associated with increased TGF-β expression in epithelial cells and alveolar macrophages and increased numbers of apoptotic cells (Mora et al., 2005). When IFNγR$^{-/-}$ were treated with an antiviral drug (cidofovir) from day 45 pi, the number of mice exhibiting severe pulmonary fibrosis decreased, which was associated with decreases in TGF-β, VEGF and macrophage activation markers, suggesting that these cytokines are a factor in the pathogenesis of the fibrosis (Mora et al., 2007).

Fibrosis in chronic MHV-68 infection of IFNγR$^{-/-}$ mice has been widely reported by many authors in several organs, specifically the spleen, mediastinal lymph node and liver in addition to the lung (Dutia et al., 1997; Ebrahimi et al., 2001; Gangadharan et al., 2009). In the spleen, acute intranasal infection of 129/Sv/Ev IFNγR$^{-/-}$ mice results in pale, shrunken spleens at day 17-18 pi, which histologically show mild white pulp hyperplasia (but less than that seen in the wild type mice) and granulocytes are present in the red pulp. At day 21

pi in IFNγR$^{-/-}$ mice, there is a mature fibrosis, with fewer granulocytes and at least ten-fold fewer cells are present in the spleen compared to infected wild type mice, although CD4+ T cells, CD8+ T cells and B cells are all present. The reduction in cell numbers returns to normal by day 45 pi (Dutia et al., 1997; Ebrahimi et al., 2001; Gangadharan et al., 2008). Presence of infectious virus and increased levels of latent virus in the IFNγR$^{-/-}$ spleens is insufficient to explain the dramatic reduction in cell number and although removal of CD8+ T cells results in the abrogation of the fibrosis and the increased number of latently infected cells, a decrease in cellularity remains. In contrast, removal of CD4+ T cells does not fully abrogate the fibrosis (Dutia et al., 1997). Apoptosis as a cause of the reduction in cells number has also been excluded. Concurrent with the reduction in spleen cellularity, an increase in circulating lymphocytes is observed, which peaks at day 23 pi and resolves by day 45. Labelling of peripheral blood leukocytes from the IFNγR$^{-/-}$ mice revealed that these cells were not found in the spleen of IFNγR$^{-/-}$ mice, but on infusion into the wild type mice, trafficking of these cells into the spleen occurred as normal (Ebrahimi et al., 2001). This was thought to be due to increased TNFα levels in the spleen of IFNγR$^{-/-}$ mice, which can inhibit cell migration. Chemokines were also thought to be a factor in the pathogenesis of fibrosis; in the IFNγR$^{-/-}$ mice increased levels of pro-fibroplastic genes TNFα, TNFβ and IL-1β are seen, whereas IFNγ is anti-fibrogenic, along with IP-10 and MIG, which are secreted at higher levels in the wild type mice (Ebrahimi et al., 2001). A role for alternatively activated macrophages has also been suggested, mediated by the secretion of IL-4 and IL-13 by Th2 cells, which predominate in the absence of IFNγ, as these macrophages are associated with tissue repair and fibrosis (Gangadharan et al., 2008). The viral *M1* gene appears to have a role in the induction of fibrosis in IFNγR$^{-/-}$ mice as infection of these mice with an M1 deletion mutant virus does not cause the mortality or splenic fibrosis seen with wild type MHV-68 infection (Clambey et al., 2000) and M1 has been shown to stimulate CD8+ T cells, which are required for secretion of IFNγ (Evans et al., 2008).

IFNγ has a critical role in reducing the reactivation of latent virus. In the absence of IFNγ, a latent infection is established, however, the administration

of IFNγ to latently infected cells *in vitro* was found to reduce the number of cells in which this infection was reactivated (Steed et al., 2006). Similarly, in wild type mice, the administration of neutralising antibodies to IFNγ at 16 dpi leads to a greater recrudescence of lytic infection (Christensen et al., 1999).

1.5 Expression of proteins in the lung in relation to MHV-68 *M3*

Previous work in this group has used microarray analysis to identify genes upregulated in response to infection of wood mice with *M3* deficient MHV-68 (M3.stop) compared to wild type (M3.MR) virus. This identified the expression of *SPLUNC1*, *CCSP* and *AGR3* as being higher in M3.MR infection (Hughes, 2006).

1.5.1 Clara cell secretory protein

1.5.1.1 Clara cells

Clara cell secretory protein (CCSP, also known as CC10, CC16, uteroglobin, secretoglobin (SCGB)1A and polychlorinated biphenyl binding protein) is the major secreted protein of Clara cells and one of the main secretory proteins in the lung (Broeckaert et al., 2000; Reynolds et al., 2002). Clara cells are non-ciliated epithelial cells of the respiratory tract. The number and distribution of these cells within the respiratory tract differs between species (Massaro et al., 1994; Plopper et al., 1997). Clara cells have morphological characteristics which can be used to identify them ultrastructurally with transmission electron microscopy, including lack of cilia, apical projection of the cell into the airway lumen, abundant smooth endoplasmic reticulum, electron dense “secretory-vesicle like inclusions” within the apical cytoplasm and a basal nucleus (Pack et al., 1980). Using these characteristics, Pack et al. (1980) found that although a large proportion of the luminal surface of the mouse trachea is ciliated, the ciliated cells were interspersed with a large number of non-ciliated cells. Within the trachea, between 49.4 and 57.5 % of the epithelial cells were Clara cells; in the primary bronchus 46 %; axial bronchus 61 % and distal airway 71 %, so the frequency of Clara cells within the respiratory epithelium increases distally in the respiratory tract (Pack et al., 1980; Pack et al., 1981). In contrast, in human respiratory epithelium, there is a complete absence of Clara cells in the trachea and bronchi, with very low numbers in the proximal

bronchioles and only approximately one in five epithelial cells are Clara cells in the most distal (respiratory) bronchioles (Boers et al., 1999). Clara cells in humans are also morphologically different; cells are cuboidal and do not project into the lumen, nuclei are central and other organelles are less prominent (Plopper et al., 1997). Additionally, different types of Clara cell, based on morphological variations, have also been described. These include the Common type, Type II Clara cells (which have more electron dense cytoplasm and fewer electron dense vesicles) and the vesiculated type (in which the cytoplasm contains numerous large vesicles containing a faint matrix). The latter were postulated to be in transition between Clara cells and mucous cells (Pack et al., 1981). Antibodies to CCSP have been widely used both as a marker for Clara cells and to locate the protein within the cell, which shows that CCSP granules are stored within the electron dense secretory vesicles described by Pack et al. (1980), which are located in the apical cytoplasm (Ray et al., 1996; Ryerse et al., 2001). These electron dense vesicles are absent from the cytoplasm of $CCSP^{-/-}$ mice, along with reduced amounts of endoplasmic reticulum; furthermore, the airway lining fluid did not contain CCSP (Stripp et al., 2002).

In addition to CCSP, Clara cells also secrete surfactant A, B and D proteins; Tryptase Clara (a protease); phospholipase, thought to be secreted and important in the regulation of surfactant lipids; β-galactosidase-binding lectins; a leukocyte protease inhibitor, which inhibits neutrophil elastase and a 55kDa protein (CC55) which has not yet been characterised (Singh and Katyal, 2000).

1.5.1.2 Function of CCSP

Clara cell secretory protein is thought to be an anti-inflammatory protein, although the precise role of this protein is not yet understood (Singh and Katyal, 1997; Wang et al., 2003). First identified as a protein in the uterus of pregnant rabbits (uteroglobin), CCSP is able to bind progesterone (Miele et al., 1987). CCSP also has been shown to bind polychlorinated biphenyl (PCB) metabolites, a potentially toxic environmental pollutant (Stripp et al., 1996). In the lung, several potential properties have been identified; the inhibition of

phospholipase A_2 (PLA_2) may reduce inflammation as PLA_2 is involved in the production of arachidonic acid and the availability of prostaglandins and leukotrienes (Broeckaert, 2000; Miele et al., 1987; Singh and Katyal, 2000). Other immunomodulatory functions described for CCSP include inhibition of IFNγ, TNFα and IL-1 and inhibition of leukocyte chemotaxis (Mukherjee et al., 1999; Singh and Katyal, 2000).

The generation of $CCSP^{-/-}$ mice has allowed further elucidation of the role of CCSP in the lung. In these mice higher levels of other secretory proteins are found, including other members of the secretoglobin family, SCGB3A1 and SCGB3A2, possibly to compensate for the lack of CCSP (Reynolds et al., 2002; Watson et al., 2001). $CCSP^{-/-}$ mice are also associated with increased levels of IgA, with IgA mRNA-positive peribronchiolar lymphocytes readily detected in $CCSP^{-/-}$ mice, but rare in wild type mice. This peribronchiolar distribution has been suggested to be consistent with that of BALT and therefore, CCSP may have a role in the formation of BALT (Watson et al., 2001). Other models of inflammation have suggested that CCSP has a role in the resolution of inflammation. Instillation of LPS leads to a rapid decrease of CCSP in the BAL fluid and *CCSP* mRNA in lung tissue (although the number of Clara cells remained constant) and the restoration of levels within seven days, coinciding with the resolution of the neutrophil-dominated inflammation (Arsalane et al., 2000; Snyder et al., 2010). This is a similar finding to the effect of acute naphthalane injury, which also leads to a reduction in *CCSP* mRNA levels (Stripp et al., 1995). Following hyperoxia, $CCSP^{-/-}$ mice exhibit reduced survival time (compared to wild type mice), increased mRNA for the proinflammatory cytokines IL-1β, IL-3 and IL-6 and greater pulmonary oedema at later timepoints (82 hours). These results and others suggest that the lack of CCSP leads to altered regulation of pulmonary inflammation and a proinflammatory state (Johnston et al., 1997; Reynolds et al., 2007).

1.5.1.3 CCSP in disease

A survey of human patients with acute respiratory distress syndrome found significantly higher levels of CCSP in BAL fluid compared to controls, and interestingly, that patients who survived had significantly higher levels of CCSP

compared to those who died (Jorens et al., 1995). Conversely, patients with chronic lung disease, such as chronic obstructive pulmonary disease, cystic fibrosis, asthma and exposure to cigarette smoke, are associated with reduced levels of CCSP (Ghafouri et al., 2002; Pilette et al., 2001; Robin et al., 2002; Snyder et al., 2010). A similar finding has been described in horses with equine recurrent airway obstruction (Katavolos et al., 2009).

Further evidence of an anti-inflammatory role includes the *in vitro* antichemotactic and antiphagocytic effects on macrophages, monocytes and neutrophils (Miele et al., 1987). The immunomodulatory protein annexin A1 (ANXA1) is abundant in macrophages, blood leukocytes and ciliated epithelial cells of the lung. Lack of CCSP leads to alteration in the post-translational modification of this protein, which may alter its function; for example ANXA1 antagonises neutrophil extravasation. Therefore a decrease in CCSP may alter the paracrine control of ANXA1 and contribute to increased inflammatory responses (Reynolds et al., 2007). Pulmonary macrophages from $CCSP^{-/-}$ mice following stimulation by LPS, show increased TNFα production and increased TLR4 expression, suggesting an increased inflammatory response in the absence of CCSP (Snyder et al., 2010). Interestingly, several authors have shown that TNFα also induces the transcription of *CCSP in vitro*. As TNFα is capable of activating phospholipases (PLA_2 is inhibited by CCSP), this appears to be a counterregulatory mechanism (Cowan et al., 2000; Yao et al., 1998b). This was in contrast to Harrod and Jaramillo (2002) who reported that both *in vitro* and *in vivo* systems showed a decrease in CCSP promoter activity, following *Pseudomonas aeruginosa* infection caused increases in TNFα (Harrod and Jaramillo, 2002).

IFNγ induces increased levels of *CCSP* mRNA, protein and secretion of the protein both *in vivo* and *in vitro* in a dose dependent manner (Magdaleno et al., 1997; Yao et al., 1998a). This is controlled via the Jak/STAT1 pathway, IRF-3 and the respiratory epithelium transcription factors HNF-3α and HNF-3β (Bingle et al., 1995; Ramsay et al., 2003). Interestingly, the presence of CCSP inhibited the expression of IFNγ by peripheral blood mononuclear cells *in vitro*. This was suggested to be mediated via IL-2, either via a decrease in the

cytokine level or inhibition of its interaction with its receptor, or, as IFNγ induces PLA_2, inhibition of PLA_2 may be involved in decreased signal transduction (Dierynck et al., 1995). This suggests that the interaction between Clara cells and IFNγ is an example of the modulation of epithelial cell function by a cytokine, with subsequent epithelial cell modulation of the inflammatory response, restricting intra-pulmonary inflammation (Ramsay et al., 2003; Yao et al., 1998a).

Clara cells have been identified as contributing to cell renewal in the bronchial epithelium of rodents and humans and are designated facultative progenitor cells (Boers et al., 1999; Breuer et al., 1990; Hong et al., 2001; Stripp and Reynolds, 2008). CCSP positive cells also have characteristics of mucus secreting cells, suggesting that they are progenitor cells for different cell types in the respiratory epithelium (Boers et al., 1999; Evans et al., 2004). Different types of Clara cell have been described based on ultrastructural variations which suggest that Clara cells may secrete mucus, or become goblet cells (Pack et al., 1981). Sensitisation and subsequent challenge with ovalbumin is a common model for allergy-based respiratory disease. In $CCSP^{-/-}$ mice this results in increased inflammation (neutrophils; consistent with increased MIP-2) and also increased mucus production (Wang et al., 2001). In another similar model, ATP-challenged mice showed a dramatic increase in CCSP and the number of mucous cells, moreover, mucin synthesis was localised to Clara cells, indicating that these cells are the origin of the mucous cells, which are scant in naïve mice (Evans et al., 2004). Further investigation of the transition of Clara cells to mucin producing cells has shown that this is mediated by SPDEF, TTF-1 and FoxA2, in response to EGFR activation and IL-13 (Chen et al., 2009; Curran and Cohn, 2010). It is now widely accepted that Clara cells are the primary mucin-secreting cells in the mouse and in the small airways of humans (Davis and Dickey, 2008).

In vitro, encephalomyocarditis virus-infected monocytes treated with recombinant CCSP exhibited reduced IFNγ-mediated antiviral activity (Dierynck et al., 1995). *In vivo*, lack of CCSP has consistently resulted in an increased inflammatory response following experimental infection with

microorganisms, consistent with the assertion that CCSP has an anti-inflammatory function. Infection of $CCSP^{-/-}$ mice with adenovirus revealed increased inflammatory cell counts in BAL fluid, within which the proportion of neutrophils was greater than that seen in similarly infected wild type mice (Harrod et al., 1998). This is compatible with the increase in MIP-2 and MIP-1α mRNA in the $CCSP^{-/-}$ mice, as these are neutrophil-attractant chemokines. In addition, IL-6, TNFα, IL-1β and MCP-1 are also increased compared to the infected wild type mice (Harrod et al., 1998). Histologically, infiltration by mononuclear cells and neutrophils is more extensive in the absence of CCSP at both 7 and 14 dpi, suggesting that CCSP reduces the influx of neutrophils and monocytes. The increased inflammatory response in $CCSP^{-/-}$ mice was suggested to be the underlying cause of the reduced virus load in these mice, compared to the wild type mice (Harrod et al., 1998). A similar outcome was described following infection with *Pseudomonas aeruginosa*, which led to increased numbers of neutrophils in the BAL fluid, and increased TNFα and IL-1β in the absence of CCSP (Hayashida et al., 2000). The increased inflammatory response was also suggested to be the explanation for the lower numbers of viable bacteria which were recoverable from $CCSP^{-/-}$ mice at 24 hpi, compared to infected wild type mice. Interestingly, the wild type mice exhibited a decrease in the levels of CCSP at days 1 to 5 following infection with *P. aeruginosa*, but recovered to baseline levels by day 14, at which time the inflammatory response was resolving. It was postulated by the authors that in the wild type mice, CCSP levels decreased to allow neutrophils to be recruited to the lung, which is otherwise inhibited by CCSP. How this is regulated is not clear, as the decrease in CCSP occurred prior to the decrease in *CCSP* mRNA levels and was not associated with Clara cell injury (Hayashida et al., 2000). However, the findings of Harrod and Jaramillo (2002) suggested that this may be due to TNFα mediated decreased in CCSP promoter activity. Infection of $CCSP^{-/-}$ mice with HRSV showed similar alterations in the inflammatory response, with an increase in total cell numbers in the BAL fluid at days 2 (neutrophils, lymphocytes) and 7 (macrophages, neutrophils, eosinophils) pi and increased peribronchiolar infiltrates described histologically, with concurrent increases in neutrophil-attractant chemokines (MIP-2 and KC) (Wang et al., 2003). In contrast to the previously described

experiments, however, this increased inflammatory response did not lead to increased viral clearance, but higher viral titres in the $CCSP^{-/-}$ mice than in the wild type mice (Wang et al., 2003). An increase in IL-13 was also recorded in the $CCSP^{-/-}$ mice, which was suggested to be a cause of mucous metaplasia characteristic of HRSV infection and demonstrated by increased numbers of AB-PAS positive cells at day 7 pi. Alternatively, the increase in mucus was suggested to be secondary to an increase in elastase, from the higher numbers of neutrophils present, which increases *MUC5AC* expression (Wang et al., 2003).

1.5.2 SPLUNC1

1.5.2.1 The PLUNC family of proteins

The PLUNC (palate lung and nasal epithelium clones) family of proteins are relatively recently described and are present in the oral, nasopharyngeal and respiratory epithelium (Bingle et al., 2004). These proteins are predicted to show structural similarity to LPS-binding protein (LBP) and bactericidal/permeability-increasing protein (BPI), which are critical to the host innate immune response to LPS. Both proteins bind LPS; LBP subsequently signals to the host of the presence of low amounts of LPS, whereas BPI renders LPS non-inflammatory (Bingle and Craven, 2002). These two proteins could therefore be described as pro-inflammatory and anti-inflammatory, respectively. The family of proteins have been divided into two subgroups, on the basis that some (the “short” PLUNCs; SPLUNC) have homology only to the N-terminal domain of BPI, while the remainder (the “long” PLUNCs; LPLUNC) have homology to both the N- and C- terminal domains of BPI. In humans, four short and six long *PLUNC* genes have been identified, although *LPLUNC5* is likely to be a pseudogene (Barnes et al., 2008; Bingle and Craven, 2003). The mouse genome contains homologues of all human *SPLUNC* and *LPLUNC* genes, with an additional *SPLUNC5* gene (Bingle et al., 2004; LeClair et al., 2004). Furthermore, homologues have been described in other mammalian species (rat, horse, cow and pig), in addition to birds (chicken), some amphibians, but not in fish; an indication as to when these genes evolved (Bingle et al., 2009). This family of proteins are one of the most rapidly evolving mammalian genes, which is characteristic for genes involved

in host defence. The clustering of the genes close together on the chromosome indicates gene duplication, but the relatively low amino acid homology (<25 %) between the paralogues suggests rapid evolution of the individual genes (Bingle et al., 2004).

1.5.2.2 SPLUNC1

SPLUNC1 (also known as *spurt*, *LUNX*, *PLUNC*) was first identified as a gene expressed in the palate and nasopharynx of the mouse embryo (Weston et al., 1999). In the murine respiratory tract, SPLUNC1 expression is present from two days of age and is restricted to the epithelial cells of the trachea and mainstem bronchi; distally to this levels drop abruptly, and in the bronchioles and the alveoli no expression is present (LeClair et al., 2001; Weston et al., 1999). These patterns persist into adulthood, but are not present in embryonic lung. In the human respiratory tract SPLUNC1 is present in the non-ciliated epithelial cells in the airway, cells of the submucosal glands in the upper airway, along with minor glands of the tongue and nasal cavity, and the mucous acini (but not serous cells) of salivary glands (Bingle et al., 2005; Di et al., 2003; Kim et al., 2006; Vargas et al., 2008). The type of cell in which SPLUNC1 is found within the submucosal gland has been variable between authors, with some identifying serous cells as positive, but mucous cells negative (Campos et al., 2004; Kim et al., 2006) and others the opposite, finding SPLUNC1 in mucous acini only (Bingle et al., 2005). The presence of SPLUNC1 within the ducts of submucosal glands and as an important component of the airway lining fluid demonstrates that this protein is secreted (Bingle et al., 2005).

1.5.2.3 SPLUNC1 in disease

In humans, SPLUNC1 has been investigated as a marker of respiratory disease. Analysis of nasal lavage fluid (NLF) in workers chronically exposed to dimethylbenzylamine (DBMA), shows that levels of SPLUNC1 are initially decreased compared to controls, but increase to higher levels than in controls in response to acute exposure to the chemical (Ghafouri et al., 2003; Lindahl et al., 2001). In contrast, control subjects exhibit a decrease in SPLUNC1 in response to the same acute exposure to DBMA (Lindahl et al., 2001).

SPLUNC1 was also found to be decreased in the NLF of smokers (Ghafouri et al., 2002; Ghafouri et al., 2003). Additionally, people with seasonal allergic rhinitis also had lower levels of SPLUNC1 in NLF during symptomatic periods, compared to non-symptomatic periods, or healthy controls (Ghafouri et al., 2006). In contrast, other studies have shown that SPLUNC1 expression is increased in the respiratory tract of patients with chronic respiratory conditions. In cystic fibrosis patients, SPLUNC1 was found to be increased in nasal cells (Roxo-Rosa et al., 2006) and in the epithelium and the mucus plugs within lumina of small airways [bronchioles] (Bingle et al., 2007). This is in contrast to cases of COPD, in which despite increased levels of SPLUNC1 being detected in sputum samples (Di et al., 2003), bronchiolar epithelial cells were not found to be positive (Bingle et al., 2007; Liu et al., 2010b). Comparison of lung tissue from stable and progressive Idiopathic Pulmonary Fibrosis revealed significantly higher levels of *SPLUNC1* mRNA in the lung tissue of progressive cases (Boon et al., 2009). Immunohistology localised SPLUNC1 to the epithelial cells and lumen of airways named as bronchi in the legend, but are morphologically comparable to those termed “small airways” [bronchioles] by Bingle et al. (2007). Moreover, Boon et al. (2009) described the positive cells to be of secretory/goblet type, which is contrary to the finding in cystic fibrosis, where goblet cells within the airways were negative for SPLUNC1 (Bingle et al., 2007).

In cancers of the lung, nasal and salivary tissues, SPLUNC1 has been variably reported as a marker, prognostic indicator and as downregulated, compared to non-neoplastic tissue. In a survey of glandular lung tumours, SPLUNC1 was shown by immunohistology to be expressed in pulmonary adenocarcinomas, muco-epidermoid carcinomas and bronchio-alveolar carcinomas (Bingle et al., 2005), and in salivary gland papillary cystadenocarcinoma (Vargas et al., 2008). Two other neoplasms have been investigated by several authors. Non-small cell lung cancer (NSCLC) is positive for *SPLUNC1* and 80 % of lymph nodes with metastases were also positive (Iwao et al., 2001); moreover, the presence of *SPLUNC1* in these metastases correlated with a poor prognosis of survival (Benlloch et al., 2009). In addition, the presence of *SPLUNC1* positive tumour cells in the peripheral blood has been suggested as a

diagnostic tool for NSCLC (Cheng et al., 2008; Mitas et al., 2003). In nasopharyngeal carcinoma (NPC), *SPLUNC1* is downregulated, and has been proposed as a putative tumour suppressor gene in this neoplasm (He et al., 2005; Zhang et al., 2003; Zhang et al., 2010). NPC has a higher occurrence within some human populations, which has been correlated with increased incidence of infection with Epstein-Barr virus. However, it has also been shown that within these populations, two single nucleotide polymorphisms in the *SPLUNC1* promoter gene show significant association with the susceptibility to NPC, which may affect the transcription of *SPLUNC1*. Furthermore, the potential antimicrobial function of the PLUNC proteins was suggested to be a link between this polymorphism, infection with EBV and the development of NPC (He et al., 2005). This is interesting in light of the finding of Zhou et al. (2007) that EBV-transformed B lymphocytes showed a significantly lower survival rate in culture in the presence of recombinant SPLUNC1, compared to similarly treated normal B lymphocytes, and that EBV DNA in the culture supernatant of SPLUNC1 treated cultures was also reduced (Zhou et al., 2008).

1.5.3.4 Function of SPLUNC1

SPLUNC1 is expressed by cells in culture; primary human bronchial epithelial cells (HBECs) grown at an air liquid interface initially express abundant SPLUNC1. Its expression decreases as cells de-differentiate, then is highly expressed as cells re-differentiate. It has been reported as the most highly expressed gene in HBECs (Campos et al., 2004; Ross et al., 2007) and is also expressed by primary tracheobronchial epithelial cells in culture (Bingle et al., 2007). However, *SPLUNC1* is also reported to be highly expressed in cultured alveolar type II cells; a cell type which does not express this gene *in vivo* (Ballard et al., 2010). Moreover, the same report also found that *CCSP* was expressed by type II alveolar cells in culture; again this gene is not expressed by this cell type *in vivo* (Ballard et al., 2010). Cell cultures require the addition of retinoic acid to maintain the mucociliary phenotype to express *SPLUNC1* (Bingle et al., 2007; Campos et al., 2004; Yeh et al., 2010). Expression of *SPLUNC1* was not affected by the action of the inflammatory mediators IL-1β or TNFα (Bingle et al., 2007) but was downregulated by IL-13 (Yeh et al.,

2010). SPLUNC1 has been isolated from and shown to be released by human peripheral neutrophils *in vitro*, in response to stimulation with secretagogues (Bartlett et al., 2008); however, this was not the finding of Bingle et al. (2007), who failed to detect SPLUNC1 in neutrophils in sections of lung tissue.

SPLUNC1 was upregulated in the nasal epithelium following olfactory bulbectomy in the rat; olfactory bulbectomy causes degeneration of olfactory receptor neurons, which are present within the olfactory epithelium. This increase was suggested to be in response to the injury of the respiratory epithelium (Sung et al., 2002). In contrast, studies using murine models of obliterative airway disease and asthma, have reported a decrease in *SPLUNC1* expression in these conditions (Follettie et al., 2006; Kuperman et al., 2005; Lande et al., 2005).

SPLUNC1 has been investigated as a putative antimicrobial protein in murine models of infectious and inflammatory disease. Infection of mice with *Mycoplasma pneumoniae* leads to increased *SPLUNC1* mRNA at 4 hours pi, but not at 72 hours pi, and treatment of mice with SPLUNC1 neutralising antibody lead to increased bacterial burdens and neutrophil counts in BAL fluid, suggesting that SPLUNC1 is decreased during the subacute inflammatory response (Chu et al., 2007). The same authors also found that IL-13 antibody treatment of allergic mice with *M. pneumoniae* infection led to decreased *SPLUNC1* and increased bacterial levels, suggesting that increased levels of IL-13 in models of allergy impaired SPLUNC1 expression and decreased bacterial clearance. This is consistent with the findings of Yeh et al. (2010) and Ghafouri et al. (2006) on the interaction between SPLUNC1 and IL-13. However, IL-4Ra1$^{-/-}$ mice, which lack the signalling pathway for IL-4 and IL-13, showed reduced levels of SPLUNC1 in an ovalbumin based model of airway inflammation (Britto et al., 2010). A similar murine allergy model also showed that SPLUNC1 inhibited eosinophilic inflammation in the lung, although the mechanism was not defined (Liu et al., 2010a). SPLUNC1$^{-/-}$ mice were more susceptible to infection with *M. pneumoniae*, with a two-fold increase in numbers of bacteria and higher neutrophil counts in BAL fluid. Similarly, transgenic mice which overexpressed *SPLUNC1* were protected,

with lower bacterial numbers and lower pro-inflammatory cytokine levels (Gally et al., 2010a). In addition, infection of SPLUNC1$^{-/-}$ mice with *M. pneumoniae* suggested that SPLUNC1 was required for the induction of TLR2 signalling in response to *M. pneumoniae*, and impaired expression of SPLUNC1 may be implicated in the bacterial infection of patients with chronic lung disease such as COPD (Gally et al., 2010b). In an ovalbumin stimulated model of inflammation, IFNγR$^{-/-}$ mice failed to show a reduction of SPLUNC1 following exposure to ovalbumin, a response seen in the wild type mice, suggesting that IFNγ is involved in the inhibition of SPLUNC1 in inflammatory response in the respiratory tract (Britto et al., 2010). In another study, naive IFNγR$^{-/-}$ mice exhibited increased SPLUNC1 in BAL fluid, in addition to IFNγR$^{-/-}$ mice with Th1 and Th2 induced inflammation, suggesting that SPLUNC1 regulates inflammation in the healthy lung, but during an inflammatory response, is inhibited by IFNγ (Curran et al., 2009).

An additional role for SPLUNC1 has been proposed in the regulation of epithelial sodium channels (ENaC) in the respiratory tract, with SPLUNC1 having been shown *in vitro* to inhibit ENaC in human bronchial epithelial cultures and *Xenopus laevis* oocytes, which would result in excess fluid within the airway lumen (Garcia-Caballero et al., 2009; Rollins et al., 2010). Investigation of SPLUNC1 as a surfactant showed that *in vitro*, the protein reduced surface tension at the air-liquid interface and inhibited biofilm formation by *Pseudomonas aeruginosa* (Gakhar et al., 2010).

1.5.3 AGR2 and AGR3

Anterior gradient homologue 2 (AGR2; also known as, or homologous in other species to, Agr2h, Gob-4, hAG-2, mAG-2 (Aberger et al., 1998; Fritzsche et al., 2006; Komiya et al., 1999; Zhang et al., 2005)) and anterior gradient homologue 3 (AGR3; homologous in other species to Gm888, BCMP11, hAG-3 (Fletcher et al., 2003)) are homologues of the genes XAG-2 and XAG-3, first identified in *Xenopus laevis*. XAG-2 encodes a secreted protein produced by the mucin-producing cement gland, which is located anteriorly in the ectoderm of the embryo and is the first ectodermal organ in the developing *Xenopus* embryo (Aberger et al., 1998; Liu et al., 2005). The cement gland functions to

attach the embryo to a solid support prior to swimming and feeding. Homologues of this protein have been described in varying locations in other species. In the mouse, AGR2 is expressed in another secretory cell, the intestinal goblet cell (Komiya et al., 1999) and in humans, homologues have been described in several tissues containing mucus secreting cells, including lung, trachea, pancreas, stomach, colon, prostate gland and small intestine (Fritzsche et al., 2006; Persson et al., 2005; Zhang et al., 2005), although the function is unclear (Fletcher et al., 2003; Liu et al., 2005).

It has been suggested that AGR2 may have a role as a differentiation factor in specifying the dorsal ectoderm to acquire an anterior fate and develop into the cement gland and forebrain, in *Xenopus* (Aberger et al., 1998) and injection of AGR2 into *Xenopus* embryos has been shown to cause enhanced cement gland development (Liu et al., 2005). Alternatively, AGR2 and AGR3 may function as endoplasmic reticulum oxidoreductases, which are members of the protein disulfide isomerase family and are part of the chaperone process, ensuring the correct folding of proteins during their synthesis (Persson et al., 2005). AGR2 has been shown not to be secreted, but tied to the endoplasmic reticulum and essential *in vivo* for the secretion of MUC2 mucin in the goblet cells of the intestine, where it forms disulfide bonds with MUC2 during processing of the glycoprotein (Park et al., 2009; Zhao et al., 2010). In Clara cells, AGR2 is associated with the expression of SPDEF, a gene required for the differentiation of these cells to goblet cells in response to allergen exposure-induced goblet cell hyperplasia (Chen et al., 2009; Curran and Cohn, 2010; Park et al., 2007).

AGR3 in humans (hAG-3) has been described as homologous to hAG-2, although has only been documented in the lung and the pancreas (Fletcher et al., 2003; Persson et al., 2005). The human homologues were originally cloned as a gene that is differentially expressed between oestrogen receptor positive and negative breast carcinomas (Fletcher et al., 2003; Persson et al., 2005), in which both hAG2 and hAG-3 have been suggested as biomarkers of prognosis (Adam et al., 2003; Fritzsche et al., 2006). AGR2 is also overexpressed in

another neoplasm of a secretory cell, namely prostate adenocarcinoma, with expression greatest in high-grade lesions (Zhang et al., 2005).

1.6 Aim of this thesis

The aim of this work was to investigate the expression of *CCSP*, *SPLUNC1*, *AGR2* and *AGR3* in relation to murine models of viral infection in the respiratory tract and in particular, to examine the effect of the MHV-68 *M3* gene on the transcription of these genes and the corresponding proteins. This was to include localisation of the anatomical sites within the respiratory tract and the temporal expression of these genes. Comparison of MHV-68 M3.stop and M3.MR infection was used to try and elucidate the role of this viral gene in the response to viral infection. As a comparison, the expression of *CCSP* and *SPLUNC1* in the context of other respiratory viruses was also investigated.

Chapter 2 Materials and Methods

2.1 Cell Culture

2.2 Viruses

2.3 Infection of mice

2.4 Tissue sampling, Fixation and Histology

2.5 Immunohistology

2.6 *In situ* hybridisation

2.7 Transmission Electron Microscopy

2.8 Molecular Biology

2.1 Cell Culture

Three cell lines were used in this work; human embryonic kidney 293T cells (Graham et al., 1977), mouse fibroblast cells NIH3T3 (Bojan et al., 1983) and a transformed fibroblast cell line derived from IFNαβR$^{-/-}$ 129/Sv mouse embryo fibroblasts (Muller et al., 1994), named αβSV1 cells (Hughes et al., 2009). All cell lines were maintained in Dulbecco's Modified Eagle Medium (DMEM, Lonza), supplemented with 10 % (v/v) Foetal Calf Serum (BioWest), 2mM L-glutamine (Invitrogen) and 100i.u./ml penicillin/streptomycin (Invitrogen). Cells were incubated in a humidified atmosphere at 37 °C, in 5 % CO_2. Cells were cultured in 150 cm^2 vented flasks (Iwaki) and were passaged when approaching confluency. Medium was removed from the flask and cells washed with pre-warmed (to 37 °C) sterile PBS. Cells were detached by the addition of 8ml Versene (Lonza) with 0.25 % (v/v) Trypsin (Gibco). After a short incubation period (30 – 60 seconds), 8 ml DMEM was added, cells harvested and centrifuged at 100 g for 5 minutes. The supernatant was decanted and the cell pellet resuspended in 10 ml DMEM. From this suspension a small sample was mixed with an equal volume of Trypan Blue and the cell density calculated using a haemocytometer. Suitable numbers of cells were then seeded in new flasks or plates as required.

2.2 Viruses

2.2.1 Viruses used in this thesis

2.2.1.1 MHV-68

2.2.1.1.1 MHV-68

MHV-68 working stocks were produced from sub-master stocks of clone g2.4 (Sunil-Chandra et al., 1992a).

2.2.1.1.2 MHV-68 M3.stop and M3.MR

Infection of wood mice was performed using recombinant viruses MHV-68 M3.stop and MHV-68 M3.MR which were kindly provided by Professors Virgin and Speck (Washington University School of Medicine and Emory University). Functional ablation of the *M3* gene was achieved by targeted disruption following the insertion of three in-frame translational stop codons, a frameshift mutation, and a novel *Avr*II site to generate the M3.stop virus. The M3 marker

rescue virus (MHV-68 M3.MR) was generated by cotransfection of the parental *M3*-containing plasmid with viral genome derived from the MHV-68-M3.stop viral stock. Further characterisation of these viruses has been published (van Berkel et al., 2002).

2.2.1.1.3 LHΔGFP

A recombinant virus with an inserted green fluorescent protein (GFP) was utilised in the infection of cell cultures (LHΔGFP). This virus was kindly provided by Dr. Bernadette Dutia, University of Edinburgh. The LHΔGFP virus had been constructed by co-transfection of viral DNA with DNA containing a human cytomegalovirus (HCMV) immediate-early promoter-driven green fluorescent protein cassette (CMV-GFP) into baby hamster kidney (BHK) cells (Dutia et al., 2004).

2.2.1.2 Sendai virus

The Sendai virus used was a recombinant virus with an inserted *eGFP* gene inserted between the Sendai virus *N* and *P* genes (rSeV/eGFP), produced and used in the laboratories of Dr. Ultan Power, Queens University, Belfast. Stocks were grown in embryonated chicken eggs and titrated on LLC-MK2 cells.

2.2.1.3 Human respiratory syncytial virus

Two strains of HRSV were used; a clinical isolate from a hospitalised infant with bronchiolitis in the Royal Belfast Hospital for Sick Children (BT2a) and a laboratory strain which has been commonly used in experimental work (RSV Long); both of which were grown on HEp-2 cells and used in the laboratories of Dr. Ultan Power, Queens University, Belfast.

2.2.1.4 Influenza A virus

Two strains of H1N1 were used in this work; Influenza A/NC/20/99 (H1N1) and Influenza A/Ca/04/09 (H1N1). Two strains of H5N1 were used, one of high pathogenicity [Influenza A/Vietnam/04/98 (H5N1)] and one of low pathogenicity [Influenza A/Mute Swan/MI/451072/06 (H5N1)]. All influenza viruses were provided by and utilised in the laboratories of Prof. Ralph Tripp, University of Georgia, Athens.

2.2.2 Production of MHV-68 stocks

Flasks (150 cm^2) were seeded with αβSV1cells at 2 x 10^6 cells per flask and infected at an MOI of 0.001 in 5ml of DMEM for 60-90 minutes at 37°C when cells achieved 70 % confluency. Cells were then washed twice with pre-warmed sterile PBS and DMEM with 1 % foetal calf serum, 2 mM L-glutamine and 100 i.u./ml penicillin/streptomycin. These cultures were monitored daily until 100 % cytopathic effect was observed. Cells were then scraped off the flasks into the medium and both decanted and centrifuged at 1000 *g* for 20 minutes at 4 °C. The resulting cell pellets were resuspended in approx. 0.3 ml sterile PBS/150 cm^2 flask and transferred to a dounce homogeniser which had been pre-chilled on ice, and homogenised to disrupt cell membranes and release intracellular virus. This suspension was then centrifuged at 2000 *g* for 20 minutes at 4 °C. The supernatant was removed and kept on ice, while the cell pellet was resuspended in sterile PBS, homogenised a second time in the douncer and the suspension centrifuged as before. The supernatants from both homogenisation steps were pooled, aliquoted and stored at -70 °C.

2.2.3 Titration of MHV-68 stocks

6 well plates (Iwaki) were seeded with approximately 2.5 x 10^5 NIH3T3 cells per well and 5ml DMEM with 10 % foetal calf serum, 2mM L-glutamine and 100 i.u./ml penicillin/streptomycin added per well, 24 hours prior to titration. Ten-fold serial dilutions of stock virus were prepared in DMEM from 10^{-4} to 10^{-9}. Medium was decanted from the 6 well plates and 1ml of diluted stock virus added per well, each dilution being performed in duplicate. Plates were incubated at 37 °C, 5 % CO_2 for 1 hour, then the inoculum removed and cells washed three times with pre-warmed sterile PBS and fresh DMEM added. Plates were then incubated as before, for 4 days. To examine the number of plaques, the medium was removed and cells fixed in 4 % PFA for 30 minutes, then stained with 0.1 % Toluidine Blue, rinsed in tap water and left to dry. Plaques were then counted and the titre calculated as follows:

$$\text{Titre (pfu/ml)} = \frac{\text{Number of plaques x dilution}}{\text{Final volume of sample}}$$

2.2.4 Infection of cell cultures

Transfected cells in 6 well plates were infected with a GFP-labelled MHV-68 virus (LHΔGFP) when cells were confluent, at an MOI of 0.5, in triplicate. The appropriate volume of stock virus in 1ml DMEM was inoculated onto cells and plates incubated at 37 °C, 5 % CO_2 for one hour. Cells were then washed twice with sterile PBS and 2ml DMEM with 10 % FCS, 2 mM L-glutamine and 100 i.u./ml penicillin/streptomycin added per well. Plates were incubated as before. At 12 hours post infection, plates were examined under fluorescent light and digital images at 40x magnification taken (ten per transfection). These images were then analysed using Nikon NIS-Elements Basic Research software v.3.0 (Nikon U.K. Ltd., Kingston, Surrey) to quantify the percentage area showing expression of GFP above a threshold, set to eliminate background fluorescence.

2.3 Infection of mice

All *in vivo* experiments were performed with at least three mice per group and were performed once each.

2.3.1 Infection of wood mice (*Apodemus sylvaticus*) with MHV-68

Wood mice were obtained from and housed by the Department of Veterinary Pathology, Faculty of Veterinary Science, University of Liverpool at the Leahurst Field Station. These laboratory-bred mice were 6 - 10 weeks old and had previously tested negative for MHV-68 by serology and PCR analysis. Mice were lightly anaesthetised using isoflurane and $4x10^5$ pfu of either MHV-68 M3.MR or MHV-68 M3.stop in 40 µl PBS administered intranasally. Mock-infection of mice with 40 µl PBS was performed and mice maintained in parallel. At either 7 or 14 days post infection, mice were euthanased by cervical dislocation following anaesthesia induced by isoflurane.

2.3.2 Infection of 129 wild type and IFNgR$^{-/-}$ mice with MHV-68

Wild-type 129/Sv/Ev mice and IFN-γR$^{-/-}$ 129/Sv/Ev (Huang et al., 1993a) were purchased from B & K Universal (Hull, UK) and bred in-house at the Royal (Dick) School of Veterinary Studies, University of Edinburgh, where the infection studies were performed. Mice were sex matched and aged 8-10

weeks. Mice were lightly anaesthetised using halothane and $4x10^5$ pfu MHV-68 in 40 µl PBS administered intranasally. Mice were euthanased at 8 or 12 days post infection by asphyxiation in CO_2. Uninfected mice were used as negative controls.

2.3.3 Infection of BALB/c mice with Sendai Virus and HRSV

BALB/c mice were housed at the Medical Biology Centre, Queen's University Belfast, where the infection studies were performed. Mice were all female and aged 8 – 10 weeks. General anaesthesia was induced by intra-peritoneal injection of xylazine and ketamine and 10^5 $TCID_{50}$ of either HRSV Long, HRSV BT2a or rSeV/eGFP in 50 µl PBS administered intranasally. Mock-infection of mice with 50µl PBS was performed and mice maintained in parallel. Mice were euthanased at days 1, 3, 5 and 7 post infection by cervical dislocation, following induction of anaesthesia with xylazine and ketamine as before.

2.3.4 Infection of BALB/c mice with Influenza A virus

BALB/c mice were housed at the Animal Health Research Center, University of Georgia, Athens, USA, where the infection studies were performed. Uninfected mice and mice which had been mock-infected with allantoic fluid were used as negative controls.

2.4 Tissue sampling, Fixation and Histology

Tissues were removed from mice immediately after euthanasia. From each wood mouse, the cardiac lobe of the lung was dissected and snap frozen in liquid nitrogen and later stored at -80 °C. Other tissues were fixed in 4 % PFA for 24 – 48 hours prior to embedding, with the exception of mice infected at the University of Georgia, Athens which following fixation in 4 % PFA for 24 - 48 hours were transferred into 70 % (v/v) ethanol and transported to the University of Liverpool where they were embedded. Tissues were routinely embedded in paraffin wax by the Histology Laboratory, Veterinary Laboratory Services, School of Veterinary Science, University of Liverpool. 5 µm sections of paraffin-embedded tissue were prepared and mounted on glass slides; for routine histopathology sections were mounted on plain slides (ColourSlides, Solmedia Laboratory Supplies), for immunohistology and *in situ* hybridisation

adhesive-coated slides were used (Polysine^{TM}, VWR International). Slides were deparaffinated in xylene and rehydrated through graded alcohols, followed by staining with haematoxylin (VWR International) for five minutes, blueing in running tap water for six minutes and eosin (VWR International) staining for two minutes. Sections were then dehydrated in 95 % and absolute alcohol, followed by clearing in xylene and mounted in DPX (VWR International).

2.5 Immunohistology

2.5.1 Preparation of slides

Immunohistology was performed by the Histology Laboratory, Veterinary Laboratory Services, School of Veterinary Science, University of Liverpool, on PFA-fixed and paraffin-embedded tissue sections using the peroxidase anti-peroxidase (PAP) technique (Kipar et al., 2001). Sections were placed in xylene to dissolve the paraffin wax for 10 minutes and rehydrated in graded alcohols (two 3 minute washes in 100 % ethanol, then one 3 minute wash in 96 % ethanol) followed by inactivation of endogenous peroxidase by 30 minute incubation in freshly prepared methanol with 0.5 % (v/v) H_2O_2 at room temperature (RT) (Perhydrol 30 %, Fisher Scientific) then washed twice in TBS. Slides were treated in 10mM citrate buffer (0.9 % [v/v] 0.1 M citric acid, 1 % [v/v] 0.1M sodium acetate [pH 6.0]) for 25-30 minutes at 97 °C for improved antigen retrieval. Slides were then placed in coverplates in Sequenza racks (Thermo Shandon) and washed with Tris buffered saline (TBS, pH 7.4). Non-specific binding of the anti-serum was blocked with 50 % swine serum in TBS for 10 minutes at RT. Slides were incubated with primary antibody diluted in 20 % swine serum in TBS (dilutions and antibodies in Table 2-1) for 15-18 hours at 4 °C, washed with TBS and incubated with swine anti-rabbit IgG (1:100 in 20 % swine serum in TBS, Stratech Scientific Ltd., Vector Laboratories, Peterborough, UK) for 30 minutes at RT. Following further washing with TBS, 30 minutes incubation with PAP-rabbit at RT (1:100 in TBS, Stratech Scientific Ltd.) was performed. Slides were washed again in TBS and then removed from the coverplates. Ten minutes incubation with 3,3′-diaminobenzidine tetrahydrochloride (DAB, Sigma-Aldrich Co. Ltd.) with 0.01 % H_2O_2 in 0.1 M imidazole buffer (0.1 M imidazole, 0.1 M HCl [pH 7.1]) at

RT was followed by three washes with TBS and one with distilled water, before counterstaining with Papanicolaou's haematoxylin, dehydration in ascending alcohols, clearing in xylene and coverslipping and mounting with DPX (VWR International).

Antigen	Primary antibody	Reference/Source
MHV-68	1:2000 Rabbit anti-MHV-68	Prof. James Stewart
CCSP	1:200 Rabbit anti-mouse CCSP	Kindly provided by Dr. Barry Stripp (Ray et al., 1996)
SPLUNC1	1:200 Rabbit anti-mouse SPLUNC1	Kindly provided by Dr. Colin Bingle
AGR2	1:100 Rabbit anti-human AG2	Novus Biologicals, Littelton, CO, USA
HRSV	1:50 Mouse anti- pan RSV (IgG1)	Abcam, Cambridge, UK

Table 2-1 Primary antibodies used in immunohistology.

2.5.2 Image Analysis of Immunohistological slides

Image analysis was performed at AstraZeneca, Alderley Park, Cheshire, with the kind assistance of Mrs. Alison Bigley of the Analytical Morphology Group. Analysis was performed on ACIS II (automated cellular imaging system), Chromavision, using ACIS Product version 2.4.8.0 (Clarient, Inc.) and Matrox® Imaging Library.

Each slide was digitally scanned. The resulting digital image was systematically examined at high power (40x); all tracheal and bronchial sections and the bronchiole (if any) nearest the centre of each high power field was analysed. Each analysed airway was outlined to exclude alveolar tissue, so only respiratory epithelium was analysed. Within these outlined areas the

intensity of DAB staining (on a scale of 0 - 255) and the percentage area of DAB-stained, haematoxylin-stained and the total stained area was calculated using measurements obtained by the ACIS II software.

Each airway was classified either as bronchiole, bronchus or trachea. The data from these areas were collated and analysed using Minitab v.15.1 (Minitab Ltd., Coventry, UK) and groups compared using two sample T-tests or ANOVA with Boneferroni post-tests. Data was judged to be significant when $P \leq 0.05$, or highly significant when $P \leq 0.005$.

2.6 *In situ* hybridisation

2.6.1 Synthesis of DIG-labelled RNA robe for ISH

2.6.1.1 Restriction enzyme digest; preparation of DNA template

To 5µg DNA extracted from a maxiprep of the appropriate plasmid (2.8.5.4), 5 µl of the appropriate restriction enzyme (Table 2-2), 5 µl of buffer and RNAse free water to a final volume of 30 µl were added and incubated at 37 °C for 2 hours. DNA was then extracted using Phenol:Chloroform:Isoamyl alcohol (25:24:1 [Sigma]), Chloroform:Isoamyl alcohol (24:1[Sigma]) and ethanol, resuspended in 30µl RNAse-free water and stored at -20 °C.

Gene	Vector	Enzyme used to create sense probe; buffer	Enzyme used to create anti-sense probe; buffer	Source
MHV-68 tRNA; pEH1.4	pBluescript	EcoRI; EcoR1 buffer (Biolabs)	HindIII; Buffer B (Roche)	Prof. Stacey Efstathiou
CCSP	pBluescript	XhoI; Buffer H (Roche)	EcoRI; EcoRI buffer (Biolabs)	Prof. James Stewart
SPLUNC1	pBluescript	EcoRV; Buffer B (Roche)	SmaI; Buffer 4 (Biolabs)*	
AG2	pCMV-SPORT6	EcoRI; EcoRI buffer (Biolabs)	XhoI; EcoRI buffer (Biolabs)	Dr. Colin Bingle
AG3	pCMV-SPORT6	EcoRI; EcoRI buffer (Biolabs)	XhoI; EcoRI buffer (Biolabs)	

Table 2-2 Restriction digest enzymes and buffers used to create DNA templates for RNA probes.
*incubated at 25°C, as per manufacturer's instructions.

2.6.1.2 *In vitro* RNA transcription

A DIG RNA labelling kit (Roche) was used to create digoxigenin-labelled RNA probes. 1 µg of purified template DNA was placed in an RNase-free reaction vial and RNase-free water added to make a total volume of 13 µl. This vial was placed on ice and the following reagents added: 2 µl 10xNTP labelling mixture, 2 µl 10x transcription buffer, 1 µl protector RNase inhibitor and 2 µl RNA polymerase. The specific RNA polymerase varied; all anti-sense probes were generated with T7 polymerase; sense probes were generated using T3 polymerase, except in the case of AG2 and AG3, when SP6 polymerase was used. The vials were incubated for 2 hours at 37 °C. To each vial, 2 µl DNase I was added to remove the template DNA and incubated at 37 °C for 15 minutes and then 2 µl 0.2M EDTA (pH 8.0) was added to stop the reaction. To the DNase digested probes, 1 µl of 1 mg/ml yeast tRNA was added followed by ethanol precipitation and resuspension in 45 µl RNase-free water.

2.6.1.3 Alkaline hydrolysis

The optimum length of an RNA probe is between 300 and 500 bp; probes longer than 500 bp may lead to non specific binding during *in situ* hybridisation (Brown, 1998) and so longer probes were shortened using alkaline hydrolysis. To the probe, 5 µl 0.4 M $NaHCO_3$ 0.6M Na_2CO_3 (pH 10.2) was added and incubated at 60°C for a period of time calculated thus:

$$T = \frac{L_i - L_f}{K \times L_i \times L_f}$$

where T = time/minutes, L_i = initial length of fragment, L_f = final length of fragment and K = 0.11 kb/min. Following incubation, the reaction was neutralised with 5 µl of 3 M sodium acetate (pH 4.6, Sigma) followed by ethanol precipitation. The pellet was dried and resuspended in 50 µl RNase-free water.

2.6.1.4 Dot blot analysis

Serial ten-fold dilutions of the DIG-labelled RNA probes in 10 µg/ml yeast tRNA were prepared and 5 µl volumes spotted onto an Hybond N+ membrane (Amersham Biosciences). Using a UV cross-linker the DNA was fixed onto the membrane. The membrane was washed in washing buffer (0.1 M maleic acid,

0.15 M NaCl [pH 7.5], 0.3 % (v/v) Tween 20) for two minutes, on a shaking platform at RT. It was then incubated in blocking solution (10x Blocking solution [Sigma] diluted in Maleic acid buffer [0.1 M maleic acid, 0.15 M NaCl, pH 7.5]) for 30 minutes, with shaking, as before. This was followed by incubation with antibody solution (anti-digoxigenin-AP FAb fragments [Roche] diluted 1:5000 in blocking solution) for 30 minutes, with shaking. The membrane was then washed twice with washing buffer for 15 minutes each time and then equilibrated in detection buffer (0.1 M Tris-HCl, 0.1 M NaCl, pH 9.5) for 3 minutes. One 4-nitro blue tetrazolium chloride (NBT)/5-bromo-4-chloro-3-indolyl-phosphate (BCIP) tablet (Roche) was dissolved in 10 ml double distilled water (final concentration 0.4 mg/ml NBT, 0.19 mg/ml BCIP, 100 mM Tris buffer pH 9.5, 50 mM $MgSO_4$) and used to incubate the membrane in the dark. The colour reaction occurred over the following 1 - 3 hours at which point the reaction was stopped by rinsing the membrane in TE buffer for 5 minutes.

2.6.2 *In situ* hybridisation (ISH)

2.6.2.1 Preparation of slides for ISH

RNA-ISH was performed on 4 % PFA fixed, paraffin wax embedded 5 µm tissue sections on Biobond (British Biocell International) coated slides. Slides were deparaffinised by washing in xylene twice for 5 minutes, in isopropanol twice for 5 minutes, followed by 5 minute washes in 96 % alcohol, 70 % alcohol and distilled DEPC-treated water. Slides were then transferred into coplin jars and washed with PBS for 5 minutes. Proteolysis was performed as follows; 20 minutes incubation with 0.2 M HCl, two 30 minute incubations in 2xSSC with 5 mM EDTA at 50 °C and digestion in proteinase K (1 µg/ml [Roche] in 20 mM Tris [pH 8.0] with 2 mM $CaCl_2$) for 15 minutes at 37°C. Slides were then washed in 0.2 % (v/v) glycine-PBS for 5 minutes and post-fixed for 4 minutes in 4 % PFA, washed twice for 1 minute in PBS and 15 minutes in PBS with 5 mM $MgCl_2$. Acetylation was the performed using 0.25 % (v/v) in 0.1 M triethanolamine (pH 7.5, VWR International) for 10 minutes and washed in PBS, twice for 1 minutes and then once for 15 minutes.

2.6.2.2 Prehybridisation and Hybridisation

Slides were prehybridised for 1 hour at 52 °C in pre-hybridisation buffer (0.1 mg/ml single stranded salmon sperm DNA (Sigma), 0.25 mg/ml yeast tRNA (Sigma), 6 x SSC, 45 % (v/v) deionised formamide (Qbiogene), 5 x Denhardt's solution (Qbiogene). Slides were removed from the coplin jar and placed in a humidity chamber and tissue sections covered with hybridization buffer (60 % [v/v] deionised formamide, 30 mM EDTA [pH 8.0], 30 mM piperazin-N,N'bis(2-ethanesulfate-acid) [PIPES, pH 7.0, Sigma], 0.9 M NaCl, 6x Denhardt's solution, 0.01 % [v/v] Triton X-100, 0.2 mg/ml yeast tRNA, 0.25 mg/ml single stranded salmon sperm DNA, 8000 U heparin [Sigma], 62.5 mg/ml dextransulfate solution) containing DIG-labelled probes at varying concentrations (1:100 to 1:500), depending on optimal staining results. Slides were covered with hydrophobic gel-bond film (Combrex Life Sciences) and sealed with rubber glue (Fix-O-Gum), then incubated at 37 °C for 15–18 hours. Following incubation, the gel-bond film was removed and slides returned to a coplin jar for post-hybridisation washing: two 15 minutes washes in 6x SSC with 45 % (v/v) formamide at 42 °C, two 5 minutes washes in 2x SSC at RT and two 15 minute washes in 0.2x SSC at 50°C.

2.6.2.3 Detection of hybridised probes

Prior to detection of the hybridised probes, slides were washed in buffer 1 (100 mM Tris, 100 mM NaCl, pH 7.5) for 1 minute, then 30 minutes in buffer 1 with 2 % (v/v) sterile neutral sheep serum (Sigma) and 0.3 % (v/v) Triton X-100, both at RT. Detection was performed with alkaline phosphatase-coupled anti-digoxigenin antibody (anti-digoxigenin-AP FAb fragments, 1:200, Roche) in buffer 1 with 1 % (v/v) neutral sheep serum and 3 % (v/v) Triton X-100 in a humidity chamber at RT for 2 hours. Slides were washed twice for 15 minutes in buffer 1, then once for 2 minutes in buffer 3 (100 mM Tris, 100 mM NaCl, 50 mM $MgCl_2$, pH 9.5). Detection of hybridised probes used 0.1875mg/ml 4-nitro blue tetrazolium chloride (NBT; VWR), 0.1 mg/ml 5-bromo-4-chloro-3-indolyl-phosphate (BCIP; Sigma) and 0.05 % (w/v) levamisole (Sigma) in buffer 3 at RT, in the dark, for between 2 and 16 hours. This reaction was stopped by a 10 minute wash in buffer 4 (10 mM Tris, 1 mM EDTA), also in the dark. Slides were finally washed in distilled water and then counterstained 10 seconds with

Papanicolaou's haematoxylin before mounting with glycer-gel (Dako) and coverslipping. They were left to dry in the dark.

2.7 Transmission Electron Microscopy

Sections of lung and trachea (no larger than 2 x 2 x 2mm) were fixed in 4 % PFA with 2.5 % glutaraldehyde in 0.1 M sodium cacodylate solution (pH 7.4) and kept at 4 °C (all reagents are supplied by TAAB Laboratories). For processing, these tissue sections were washed in 0.1M sodium cacodylate buffer and secondarily fixed in 1 % osmium tetroxide$_{(aq)}$ for 90 minutes. Tissue sections were washed in distilled water and stained en bloc with 2 % uranyl acetate in 0.69 % maleic acid for 90 minutes, then dehydrated in ascending concentrations of ethanol followed by acetone, before infiltration in 30 %, 70 % and 100 % (w/v) resin in acetone for an hour each. Tissue sections were then orientated in embedding capsules and left overnight in fresh resin at 60 °C to polymerise. Semi-thin sections (0.5 µm) were cut using an ultramicrotome (Reichert-Jung Ultracut) with a diamond knife (Diatome Ltd.) and were stained with Toluidine blue for viewing with a light microscope and selection of areas for ultrastructural examination. Ultrathin (60 nm) sections were cut with a diamond knife, mounted on copper grids, stained with Reynold's lead citrate and viewed (H600 Transmission electron microscope, Hitachi). TEM processing was performed by the Electron Microscopy Unit, Veterinary Laboratory Services, School of Veterinary Science, University of Liverpool.

2.8 Molecular Biology

2.8.1 Extraction of RNA from tissue

From tissue which had been stored at -80 °C, 30 mg sections were placed in 750 µl RLT buffer (Qiagen) which contained 1.43 mM β-mercaptoethanol and ground in a tissue homogeniser. A further 750 µl RLT buffer was added to the lysate and this was centrifuged at 20,000 *g* for 5 minutes to remove the cell debris. The supernatant was added to a further 1.5 ml buffer RLT and mixed with 3 ml 70 % (v/v) ethanol. This mixture was then filtered through an RNeasy Mini Spin column (Qiagen) in 700 µl loads by centrifugation at 20,000 *g* for 30 seconds. Following this, the RNA bound within the Mini Spin column was washed with 700 µl RW1 buffer (centrifuged for 1 minute at 20,000 *g*), 500 µl

RPE buffer (centrifuged for 15-30 seconds at 20,000 *g*), a further 500 µl RPE buffer (centrifuged for 2 minutes at 20,000 *g*) and finally subjected to a dry spin for 1 minute to ensure all buffers and ethanol were removed. The lysate within the column was then incubated with 50 µl of RNAse-free water for 20 - 25 minutes at RT prior to elution by centrifugation at 20,000 *g* for one minute. The RNA concentration was determined by UV spectroscopy by measuring the absorbency at 260 and 280 nm. To ensure removal of any remaining DNA, samples were treated with DNAse-1 (Invitrogen) as follows: 30 µg RNA was incubated with 10 µl 10x DNAse-1 buffer and 10 µl DNAse-1 in a total volume of 100 µl at RT for 15 minutes; 10 µl 25 mM EDTA was added to stop DNAse reactivity, followed by heat inactivation at 65 °C for 10 minutes. To this, 350 µl of RLT buffer and 250 µl 100 % ethanol were added, mixed well and transferred to an RNAeasy Mini Spin column and centrifuged at 20,000 *g* for 15 seconds. The column and RNA were washed twice with 500 µl RPE buffer and centrifuged at 20,000 *g* for 2 minutes, followed by a dry centrifugation step at 20,000 *g* for 1 minute to ensure removal of all buffers. 50 µl of RNAse-free water was then placed into the column and incubated at RT for 5 - 25 minutes, followed by elution at 20,000 *g* for 1 minute. RNA samples were stored at -80 °C.

2.8.2 Synthesis of cDNA

In a 0.2 ml RNase-free centrifuge tube, 2 µg of RNA was placed with 1 µl Oligo$(dT)_{15}$ primer (500 µg/ml), and 1 µl dNTPs (10 mM,) and RNase-free water to make a total volume of 13 µl. This was incubated at 65 °C for 5 minutes and then on ice for 1 minute. Then the following was added to the mixture: 4 µl 5x First strand buffer (250 mM Tris-HCl [pH 8.3], 375 mM KCL, 15 mM $MgCl_2$, Invitrogen), 1 µl DTT (0.1 M, Invitrogen), 1 µl RNase OUT (40 U, Invitrogen) and 1 µl SuperScript III reverse transcriptase (200 U, Invitrogen). This was incubated at 50 °C for 30 minutes, followed by inactivation of the reverse transcriptase by incubation at 75 °C for 15 minutes. Finally, 2 U RNase H (Invitrogen) was added and incubated at 37 °C for 20 minutes to remove any RNA complimentary to the cDNA. The cDNA was stored at -20 °C. The concentration of DNA was measured using UV spectrophotometry.

2.8.3 General PCR

Amplification of DNA was performed using cDNA generated from RNA extracted from wood mouse lung, using the primers listed in Table 2-3. Reactions were carried out in 0.2 ml thin walled tubes, with a total reaction mixture of 40 µl, comprising 1 µg cDNA, 10x PCR buffer (Invitrogen, final comcentration 20m M Tris-HCl [pH 8.4], 50 mM KCl), 1.5 mM $MgCl_2$, 0.2 mM each of dATP, dTTP, dCTP and dGTP (10 mM dNTP mix, Invitrogen), 40 ng of each of forward and reverse primers, 2 U DNA polymerase (Platinum *Taq* DNA polymerase, Invitrogen). Reaction mixtures were prepared in a Captair® Biohood (Erlab) in which elimination of contaminating DNA by exposure to ultraviolet light was performed prior to use. PCR reactions were carried out in Thermo Hybaid MBS thermo-cycler (Thermo Electron Corporation). The thermal cycling was as follows: 15 minutes at 95 °C, followed by 40 cycles of 30 seconds denaturation at 95 °C, 30 seconds annealing at 55 or 56 °C and 45 seconds extension at 72 °C, and final strand extension at 72 °C for 7 minutes.

Primer name	Gene	Primer Sequence 5'→3'	Anneal-ing temp	Product length
CCSP F1	*CCSP*	CCTCTGGCCTCTACCATGAA	55°C	351 bp
CCSP R1		GACAGGGGCCTTTAGCAGTA		
SP1 F1	*SPLUNC1*	ACTCAGACACCAAGAGAGAT	56°C	1011 bp
SP1 R5		CGTGAGGAGAAGGAAGACAT		

Table 2-3 Primers used in PCR.

PCR products were electrophoresed through 2 % (w/v) agarose gels (Invitrogen; with 0.1 µg/ml Ethidium Bromide [Sigma] in TAE buffer [40 mM Tris-base, 20 mM glacial acetic acid, 1 mM EDTA]), having been mixed 5:1 with loading buffer (50 % [v/v] glycerol, 100 mM Tris-HCl [pH 7.4], 10 mM EDTA, 0.02 % [w/v] orange G). Gels were electrophoresed in a horizontal elecrophoresis tank (BioRad), filled with TAE buffer, at 100 V. Gels were examined under ultraviolet light (Utraviolet Transilluminator, BioRad), digital

images taken and size of bands from PCR products compared with 1 kb Plus DNA ladder (Invitrogen).

2.8.4 Quantitative fluorescence real-time PCR (qPCR)

Gene-specific DNA was quantified using 200 ng total cDNA and an Opticon Monitor 2 real time PCR machine (MJ Research). Total reaction volume was 20 µl, including 200 ng cDNA, 10x Buffer (Invitrogen, final concentration 20 mM Tris-Hcl, 50 mM KCl), 2.5 mM $MgCl_2$ (Invitrogen), Sybr green (Lamb Biosciences), 0.25 mM dATP, dGTP, dCTP, dTTP (Amersham), 0.15 % (w/v) Triton X-100 (VWR International) 0.4 µg BSA (Promega) and 1 U of DNA polymerase (Platinum *Taq* DNA polymerase, Invitrogen) and 0.05 µM forward and reverse primers (Table 2-4).

The cycle parameters were as follows: 94 °C for 10 minutes (hot start), followed by 35 cycles of 10 seconds at 94 °C, 20 seconds at 60 °C, 15 seconds at 72 °C, 1 second at 75 °C to melt off primer dimers and a plate reading. The melting curve was created to analyse the specificity of the product by measuring fluorescence at 0.2 °C increments from 65 - 95 °C and the efficiency of the reaction calculated. The quantity of the gene of interest was standardised by comparison with ribosomal protein L8 (rpl8).

Standard curves were constructed by serial dilutions of plasmids containing the genes of interest. PCR products of these genes were cloned into pCR2.1 vector and DNA extracted using QIAGEN Maxi prep kits as described in 2.8.5.4. The DNA concentration was measured by UV spectrophotometry and converted to copy number using the following formula:

$$\frac{[\text{DNA/g}] \times [6.022\text{x}10^{23}]}{[\text{vector + insert/bp}] \times 660} = \text{copy number/µl}$$

where 660 = M_r of 2 nucleotides and $6.022\text{x}10^{23}$ is Avogadro's constant. Log graphs of the standards were used to set the threshold of fluorescence. Results were analysed using the Opticon Monitor software v.3.1.32 (MJ Geneworks Inc.) and statistical analysis (ANOVA) on Minitab.

Primer	Gene	Sequence 5'→3'	Product length
RPL8-f	*RPL8*	CAGTGAATATCGGCAATGTTTTG	163 bp
RPL8-r	*RPL8*	TTCACTCGAGTCTTCTTGGTCTC	
gp150-f	*gp150*	CTACTTCTTCATCGGACGCT	159 bp
gp150-r	*gp150*	CGGGATCTGTCGGACTGT	
CC10-f	*CCSP*	GATCGCCATCACAATCACTGTGG	156 bp
CC10-r	*CCSP*	GTCTGAGCCAGGGTTGAAAGG	
SPLUNC1-f	*SPLUNC1*	CAGCCTGAAAATCAGCTTGC	158 bp
SPLUNC1-r	*SPLUNC1*	TGCACCAGGGTGACATCCAAAC	

Table 2-4 Primers used for qPCR.

2.8.5 Molecular Cloning

2.8.5.1 Cloning of PCR products

PCR products were inserted into plasmids (pCR 2.1-TOPO [Invitrogen]) as follows: 4 µl of fresh PCR product was incubated for 5 minutes at RT with 1 µl salt solution (1.2 M NaCl, 0.06 M $MgCl_2$) and 1 µl vector (10 ng/µl linearised plasmid DNA, 50 % glycerol, 50 mM Tris-HCl [pH 7.4], 1 mM EDTA, 1 mM DTT, 0.1 % Triton X-100, 100 µg/ml BSA, phenol red). The reaction was then placed on ice prior to transformation.

2.8.5.2 Transformation of plasmids

The product of the cloning reaction, or 5 µl of DNA from a previous plasmid preparation, was added to competent *Escherichia coli* bacteria (Top 10 One Shot cells, Invitrogen) which were gently mixed, then incubated on ice for 30 minutes. The cells and plasmids were then heat-shocked at 42 °C for 60 seconds and incubated on ice for a further 5 minutes. 800 µl of Luria-Bertani medium (LB; 1 % [w/v] tryptone, 0.5 % [w/v] yeast extract, 1 % [w/v] NaCl) with 50 µl/ml ampicillin was added to the cells and incubated at 37 °C in an orbital shaker at 200 rpm, for 45 minutes. A 100 µl sample was plated onto LB agar. The remaining culture was centrifuged (2000 *g*, 5 minutes) and the pellet

resuspended in 100 µl LB, plated on LB agar and both plates incubated overnight at 37 °C. Individual colonies grown on the plate were added to 10 ml LB medium with 50 µg/ml ampicillin and incubated at 37 °C in an orbital shaker at 200 rpm overnight. From this, glycerol stocks were made (250 µl of LB medium in 750 µl 60 % (v/v) glycerol, vortexed and stored at -80 °C). From the remainder of the bacterial culture, the plasmid DNA was purified (minipreps).

2.8.5.3 Small scale purification of plasmid DNA (miniprep)

Cultures containing transformed bacteria in LB medium were pelleted by centrifugation at 4,000 *g* for 10 minutes. The supernatant was discarded and the pellet resuspended in 200 µl Solution I (50 mM glucose, 25 mM Tris-Cl [pH 8.0], 10 mM EDTA [pH 8.0], 1 mg/ml lysozyme [Sigma]) and incubated at RT for 5 minutes. To this 400 µl Solution II (denaturation solution; 0.2 M NaOH, 1 % [w/v] SDS) was added and incubated on ice for 5 minutes. Following this, 300 µl Solution III (neutralisation solution; 3 M potassium acetate, 11 % [v/v] glacial acetic acid [pH5.5]) was added and further incubated on ice for 5 minutes. The cells were then centrifuged at 20,000 *g* for 7 minutes and the supernatant collected and transferred to a new centrifuge tube. To the supernatant, 500 µl of isopropyl alcohol (Sigma) was added to precipitate the DNA and incubated on ice for 15 minutes. The precipitated DNA was pelleted by centrifugation at 20,000 *g* for 5 minutes and the supernatant removed and the pellet allowed to air dry, before resuspension in 200 µl TE (pH 8.0). To this 100 µl 7.5 M ammonium acetate (Sigma) was added and mixed well, followed by incubation on ice for 15 minutes. Debris was removed by centrifugation at 20,000 *g* for 5 minutes. The supernatant was removed and placed in a new centrifuge tube; to this 600µl 100 % ethanol was added and incubated at -20 °C for one hour. To pellet the DNA centrifugation for 10 minutes at 20,000 *g* was performed, the supernatant removed and the pellet air-dried. The DNA was then resuspended in 100 µl TE (pH 8.0) and stored at 4 °C.

2.8.5.4 Large scale purification of plasmid DNA (maxiprep)

To purify larger quantities of DNA, the QIAGEN Plasmid Maxi Kit (Qiagen) was used. Either a single colony grown on a selective LB agar plate or ~5 µl partially thawed glycerol stock was placed in 5 ml LB medium with 50 µg/ml

ampicillin and incubated with rotation (200 rpm) at 37 °C for 4 – 8 hours. This culture was then added to 400 ml LB medium with 50 µg/ml ampicillin in a 2 litre flask and incubated at 37 °C in an orbital shaker at 200 rpm overnight. The bacteria were then centrifuged at 6000 *g* for 15 minutes at 4 °C and the pellet resuspended in 10 ml buffer P1 (50 mM Tris-Cl [pH 8.0], 10 mM EDTA, 100µg/ml RNase A). The bacteria were then lysed by addition of 10 ml buffer P2 (200 mM NaOH, 1 % [w/v] SDS) which was mixed well by inverting the tube, then incubated at RT for 5 minutes. To this, 10 ml buffer P3 (neutralisation buffer; 3 M potassium acetate [pH 5.5]) was added and mixed thoroughly before incubation on ice for 20 minutes. The solution was centrifuged to remove debris at 20,000 *g* for 30 minutes at 4 °C and the supernatant containing the DNA promptly removed, which was centrifuged again at 20,000 *g* for 15 minutes at 4 °C to ensure all particles were removed. To a QIAGEN-tip 500 (equilibrated using 10 ml buffer QBT [750 mM NaCl, 50 mM MOPS [pH 7.0], 15 % isopropanol [v/v], 0.15 % triton X-100 [v/v]]) the supernatant was added and allowed to pass through the tip by gravity flow. The DNA was then washed twice with 30 ml buffer QC (1 M NaCl, 50 mM MOPS [pH 7.0], 15 % isopropanol [v/v]) prior to elution of the DNA in 15 ml buffer QF (1.25 M NaCl, 50 mM Tris-Cl [pH 8.5], 15 % isopropanol [v/v]). To the eluate 10.5 ml isopropanol (Sigma) was added and the mixture centrifuged at 15,000 *g* for 30 minutes at 4 °C and the supernatant removed. The resulting pellet was washed with 5 ml 70 % ethanol and centrifuged again at 15,000 *g* for 10 minutes. The supernatant was removed, the pellet air dried and the DNA dissolved in 500 µl TE buffer (pH 8.0). The yield of DNA was calculated using UV spectrophotometry.

2.8.5.5 Transfection

293T cells were seeded in either 6 well plates at a density of $2.5x10^5$ cells per well, or T25 flasks at $5x10^5$ cells per flask, one day prior to transfection; cells should be 50 – 80 % confluent at the time of transfection. For T25 flasks, the following quantities of DNA and solutions were doubled. On the day of transfection, the cell culture medium (DMEM, with 10 % FCS, 2 mM L-glutamine and 100 i.u./ml penicillin/streptomycin) was replaced 1 – 4 hours prior to transfection. DNA consisted of plasmids with inserted genes of interest,

or GFP as a positive control. For each well to be transfected, 250 µl 0.25 M $CaCl_2$ was added to 12.5 µg DNA, which was then added drop-wise, with gentle agitation, to 250 µl 2xHepes-buffered saline (HEBS; 140 mM NaCl, 1.5 mM $Na_2HPO_4 \cdot 2H_2O$, 50 mM HEPES [4-(2-Hydroxyethyl)-piperazine-1-ethanesulfonic acid, N-(2-Hydroxyethyl)-piperazine-N′-(2-ethanesulfonic acid)]) and incubated at RT for 20 minutes. This solution was then added slowly to the cell culture medium in the plates, with gentle agitation to mix the solutions. Cells were incubated at 37 °C, with 5 % CO_2 for 18 hours. The calcium phosphate containing medium was then removed, cells washed twice with pre-warmed sterile PBS and 2 ml cell culture medium added to each well. Cells were again incubated at 37 °C, with 5 % CO_2 until 48 hours after the initial transfection. At this point, cells which had been transfected with a GFP containing plasmid were examined under fluorescent light for evidence of transfection efficiency. Transfected cells were infected with MHV-68 at this point (2.4.4); for analysis of proteins (2.8.6), cells were washed in pre-warmed sterile PBS and detached with versene/trypsin as before (2.1) and seeded 1:4 in new flasks and cells and supernatant were harvested 24 hours later.

2.8.6 Analysis of proteins

2.8.6.1 Collection of cells and supernatant

Supernatant from transfected cells was collected and centrifuged at 2500 *g*, 4°C for 5 minutes. The supernatant was then aliquoted and stored at -20 °C. The cells from flasks were scraped off the plastic, washed with sterile PBS and combined with the cell pellet from the previous centrifugation and centrifuged a second time at 2500rpm, 4 °C for 5 minutes. The supernatant was discarded and the cell pellet resuspended in 150 µl PBS. To this, 50 µl sample buffer (1 M Tris [pH 6.8], 4 % [w/v] SDS [Sigma], 20 % [v/v] glycerol, 4 % [v/v] βmercaptoethanol, 0.04 % [w/v] bromophenol blue) was added and samples were boiled for 10 minutes, then stored at -20 °C.

2.8.6.2 SDS-PAGE

Samples were mixed with equal volumes of sample buffer with 10 % (v/v) 1 M dithiothreitol (DTT, Sigma) and incubated at 95 °C for 10 minutes, followed by centrifugation for 30 seconds to pellet any insoluble precipitate. Samples were

electrophoresed at 200 V (20 mA per gel) through 10 % acrylamide (Bio-Rad) gels (10 % [w/v] 40 % acrylamide, 375 mM Tris [pH 8.8], 0.1 % [w/v] SDS, 0.06 % [w/v] ammonium persulphate, 0.08 % [v/v] TEMED [Sigma]), with 10 µl samples loaded onto wells within a 5 % acrylamide stacking gel (5 % [w/v] 40 % acrylamide, 125 mM Tris [pH 6.8], 0.1 % [w/v] SDS, 0.8 % [w/v] ammonium persulphate, 0.2 % [v/v] TEMED) in a Mini-PROTEAN®3 Electroporesis system (Bio-Rad) filled with running buffer (2.5 mM Tris [pH 8.3], 250 mM Glycine, 0.1 % [w/v] SDS). A standard marker for Western Blots (Bio-Rad Precision Plus C) was used to indicate the size of proteins.

2.8.6.3 Western Blotting

Proteins were transferred from the SDS-PAGE gel onto a PVDF membrane (Immobilon-P, Millipore), using a Bio-Rad Mini Trans Blot cell, at 100 v (350 mA) for one hour, in transfer buffer (running buffer with 20 % [v/v] ethanol). Immunodetection of proteins was performed as follows; the membrane was rinsed in PBS for 2 minutes, then incubated in blocking buffer (TBS with 0.1 % [v/v] Tween-20 (VWR International), 1 % [v/v] goat serum, 5 % [w/v] skimmed milk powder), with agitation for one hour at RT, then washed in washing buffer (TBS with 0.1 % [v/v] Tween-20) twice for 5 minutes each. Antibody detection was performed either using an HRP-conjugated anti-V5 antibody (anti-V5-HRP [Invitrogen]) for transfected proteins expressed in a vector with a V5 epitope (1:2500 in blocking buffer) for 1 hour at RT, with agitation, or rabbit anti-actin antibody (Sigma, 1:300 in blocking buffer) for 2 hours at RT with agitation followed by a secondary HRP conjugated antibody (goat anti-rabbit Ig [Harlan Sera Labs] 1:10,000 in blocking buffer) for 1 hour at RT, with agitation, for detection of actin as a positive control. Detection of the standard marker was performed using StrepTactin-HRP (Bio-Rad, 1:5000). Membranes were rinsed in washing buffer, twice, for 5 minutes at RT.

Proteins were visualised using Detection Amersham ECL Western Blotting System (GE Life Sciences) which elicits a peroxidase-catalysed oxidation of luminol and the light detected by exposure of radiographic film (Hyperfilm ECL Western, GE Life Sciences), as per the manufacturer's protocol.

2.8.7 DNA Sequencing

PCR products generated with CCSP and SPLUNC1 specific primers (Table 2-3), were cloned into pCR2.1 plasmids, transformed and the resulting DNA extracted, as above. Sequencing was performed by Eurofins MWG (Ebersberg, Germany) and sequences compared using BLAST (Basic Local Alignment Search Tool) programmes, available at http://blast.ncbi.nlm.nih.gov/Blast.cgi (Altschul et al., 1990). Comparison of nucleotide sequences between species was performed using ClustalW2, available at http://www.ebi.ac.uk/Tools/clustalw2/index.html (Larkin et al., 2007) and displayed using the BoxShade programme, available at http://www.ch.embnet.org/software/BOX_form.html. cDNA sequences were translated into amino acid sequences using the ExPASy translate tool, available from the Swiss Institute of Bioinformatics website, available at http://www.expasy.ch/tools/dna.html (Gasteiger et al., 2003). Sequences were then compared and displayed using BLAST and BoxShade as before.

Chapter 3 Results

3.1 MHV-68 infection and its effect on the expression of CCSP and SPLUNC1

3.1.1 MHV-68 infection in *Apodemus sylvaticus*

3.1.2 MHV-68 infection in 129 wild type and IFNγR$^{-/-}$ mice

3.1.3 MHV-68 infection *in vitro*

3.2 Paramyxovirus infection and its effect on the expression of CCSP and SPLUNC1

3.3 Influenza A virus infection and its effect on the expression of CCSP and SPLUNC1

3.1 MHV-68 infection and its effect on the expression of CCSP and SPLUNC1

3.1.1 MHV-68 infection in *Apodemus sylvaticus*

3.1.1.1 Quantification of *CCSP* and *SPLUNC1* expression

RNA was extracted from the cardiac lung lobe of wood mice infected with MHV-68 M3.MR (M3.MR), MHV-68 M3.stop (M3.stop) or mock-infected (mock) with PBS, and cDNA was generated by *in vitro* reverse transcription. cDNA (200 ng) was used in each reaction with gene-specific primers to quantify the copy numbers of *CCSP* and *SPLUNC1*. These copy numbers were compared to known copy numbers of serial ten-fold dilutions of a plasmid (pCR2.1) containing the gene of interest, which was used to generate a standard curve. The values obtained were normalised against the copy number of the cellular ribosomal gene *RPL8*, which was similarly quantified in comparison to a standard curve of ten-fold dilutions of a plasmid containing *RPL8*. Melting point analysis was performed to ensure specific amplification of the product.

qPCR data for *CCSP* showed that mRNA copy numbers (measured using cDNA as a surrogate) at day 7 pi were similar in mock-infected and both infected groups, but M3.stop and M3.MR infected woodmice at day 14 showed higher *CCSP* expression, compared to mock-infected controls (Figure 3-1). However, these differences were not statistically significant (comparison of M3.MR and mock, P = 1.0; M3.stop and mock, P = 0.0507 [ANOVA]). Moreover, the M3.stop infected mice showed a higher expression of *CCSP* at day 14 pi than the M3.MR infected mice, but again, this increase was not significant (P = 0.1231 [ANOVA]). This was in contrast to that seen in previous experiments which showed significantly higher expression of *CCSP* at day 14 in M3.MR infected wood mice compared to M3.stop infected wood mice (D. Hughes, unpublished observations). There was an increase in gene expression at day 14 pi, compared to day 7 pi, in both the M3.MR and M3.stop infected wood mice, However, this was also not a significant change (M3.MR day 7 to day 14 pi, P = 0.054; M3.stop day 7 to day 14 pi, P = 0.056 [two sample T-test]).

SPLUNC1 expression as quantified by qPCR revealed no difference in the mock, M3.MR and M3.stop infected mice at day 7 pi (Figure 3-2). At day 14 pi mock and M3.MR infected wood mice exhibited similar copy numbers of mRNA, but an increase in copy number in M3.stop infected wood mice compared to M3.MR and mock-infected wood mice, although this increase was not significant (mock and M3.stop P = 0.4542, M3.MR and M3.stop P = 0.470 [ANOVA]).

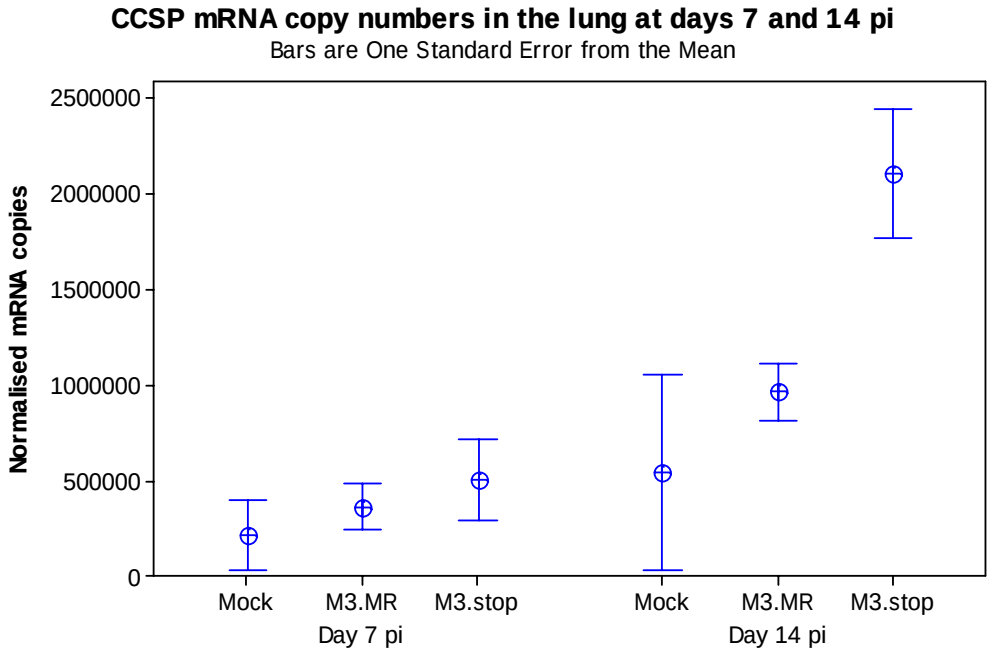

Figure 3-1 Quantification of mRNA copies of CCSP from wood mice either infected with M3.MR, M3.stop or mock-infected, at days 7 and 14 pi.

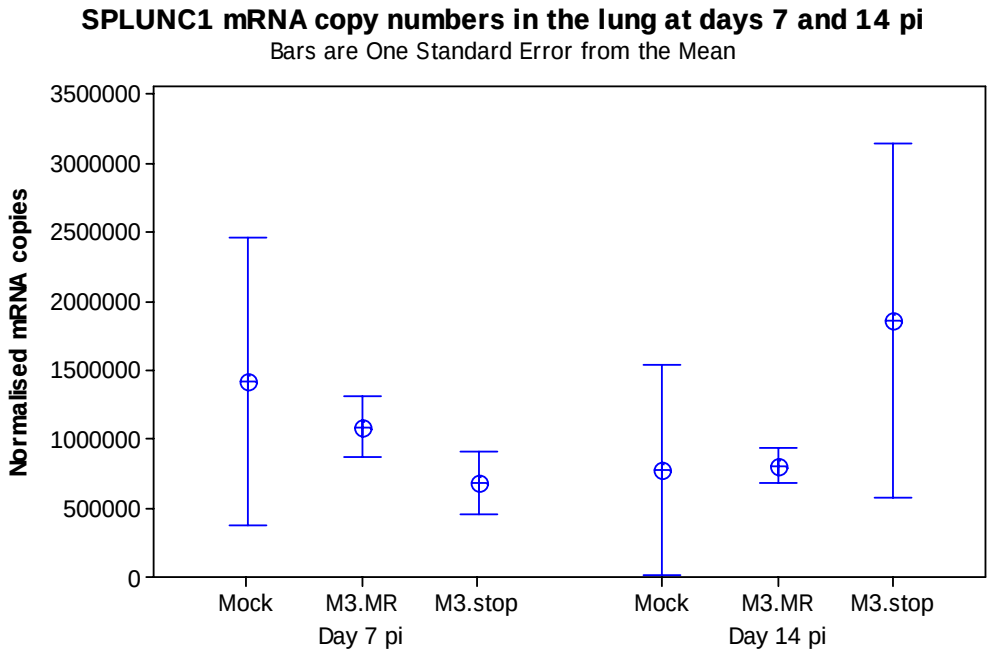

Figure 3-2 Quantification of mRNA copies of SPLUNC1 in wood mice either infected with M3.MR, M3.stop or mock-infected, at days 7 and 14 pi.

In both Figures 3-1 and 3-2, 200 ng cDNA was used per reaction and the copy number was normalised against *RPL8*. Data are the mean of experiments from three mice per group; bars represent the standard error of the mean. Two sample T-tests showed no significant differences between the groups.

3.1.1.2 The inflammatory response in MHV-68 infected *Apodemus sylvaticus*

3.1.1.2.1 MHV-68 M3.MR infection

At 7 days pi, M3.MR infection in wood mice elicited a moderate to occasionally severe, multifocal to coalescing, predominantly peribronchiolar inflammatory infiltration, composed of lymphocytes and macrophages, with fewer neutrophils (Figure 3-3a). Within these inflammatory foci there were scattered necrotic or apoptotic cells and debris. The bronchiolar epithelium was unaltered and no changes were seen in the trachea or bronchi.

At day 14 pi, infiltration by inflammatory cells was mild to moderate, predominantly either perivascular or peribronchiolar and macrophage-dominated, with fewer lymphocytes than were seen at day 7 (Figure 3-3b). Additionally, mild multifocal granulomatous infiltration was seen within the parenchyma. No alteration was present within the bronchiolar epithelium, bronchi or trachea.

3.1.1.2.2 MHV-68 M3.stop infection

Multifocal, mild to moderate mixed (macrophages, with lesser neutrophils and lymphocytes) peribronchiolar and perivascular infiltration was present at day 7 pi (Figure 3-3c). No alterations in the bronchiolar epithelium, the bronchi or trachea were observed.

At day 14 pi, mild to moderate, multifocal (perivascular and peribronchiolar) inflammatory infiltration was observed, consisting of macrophages and lymphocytes (Figure 3-3d). These infiltrates were less macrophage-dominated than those seen in M3.MR infected wood mice at the comparable timepoint.

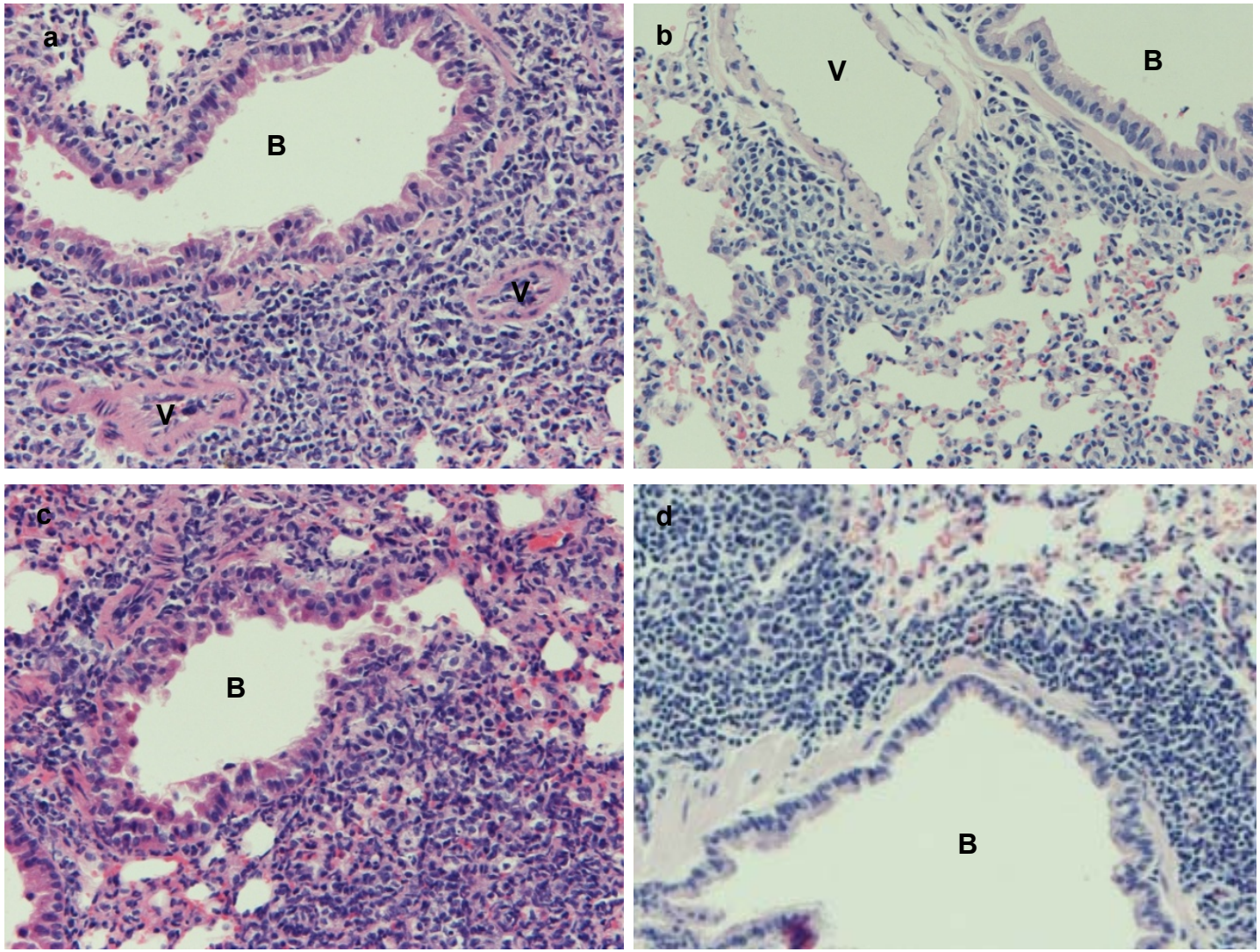

Figure 3-3 Histology of lungs from M3.MR and M3.stop infected wood mice.

(a) M3.MR infected wood mouse at day 7 pi, showing macrophage and lymphocyte dominated peribronchiolar infiltration (20x, HE). (b) M3.MR infected wood mouse at day 14 pi showing macrophage dominated peri-vascular and peribronchiolar infiltration (20x, HE). (c) M3.stop infected wood mouse lung at day 7 pi, with peribronchiolar infiltrate comprising macrophages with lesser lymphocytes and neutrophils (20x, HE). (d) M3.stop infected wood mouse at day 14 pi, with macrophages and lymphocytes in the peri-bronchiolar infiltration (20x, HE). B = bronchiole, V = vessel.

3.1.1.3 Immunohistology and *in situ* hybridisation

3.1.1.3.1 CCSP expression in *Apodemus sylvaticus*

qPCR data had shown that *CCSP* is constitutively expressed in wood mouse lung, but there appeared to be marked variation between samples. *CCSP* is expressed in Clara cells, which vary in number at different levels of the respiratory tract. *In situ* hybridisation using *CCSP* riboprobes and immunohistology with CCSP-specific antibodies was used to investigate where CCSP genes and proteins were expressed.

3.1.1.3.1.1 *In situ* hybridisation for *CCSP*

In mock-infected wood mice, used to assess constitutive expression, moderate transcription was seen, represented by a moderately intense signal within infrequent epithelial cells in the trachea (Figure 3-4a), and the number of positive epithelial cells increased distally in the respiratory tract; cells were frequently positive in the bronchi and proximal bronchioles (Figure 3-4b) and in the distal bronchioles the majority of epithelial cells were weakly positive, with scattered cells exhibiting stronger signal (Figure 3-4c). Alveolar cells were negative (Figure 3-4d).

Following infection of wood mice with either M3.MR or M3.stop, the expression of *CCSP* (detected by RNA-ISH) altered, most notably in the bronchioles. At 7 dpi, staining was highly variable. In some bronchioles numerous cells exhibited strong staining (Figure 3-5a), whereas some bronchioles exhibited reduced staining with many negative cells and scattered strongly positive cells (Figure 3-5b). These bronchioles often exhibited prominent peribronchiolar inflammation. At day 14 pi, the signal for *CCSP* was more frequent in epithelial cells within the bronchioles of both M3.MR (Figure 3-5c) and M3.stop infected wood mice (Figure 3-5d). The trachea and bronchi showed a similar staining pattern to the mock-infected wood mice; the alveoli were consistently negative.

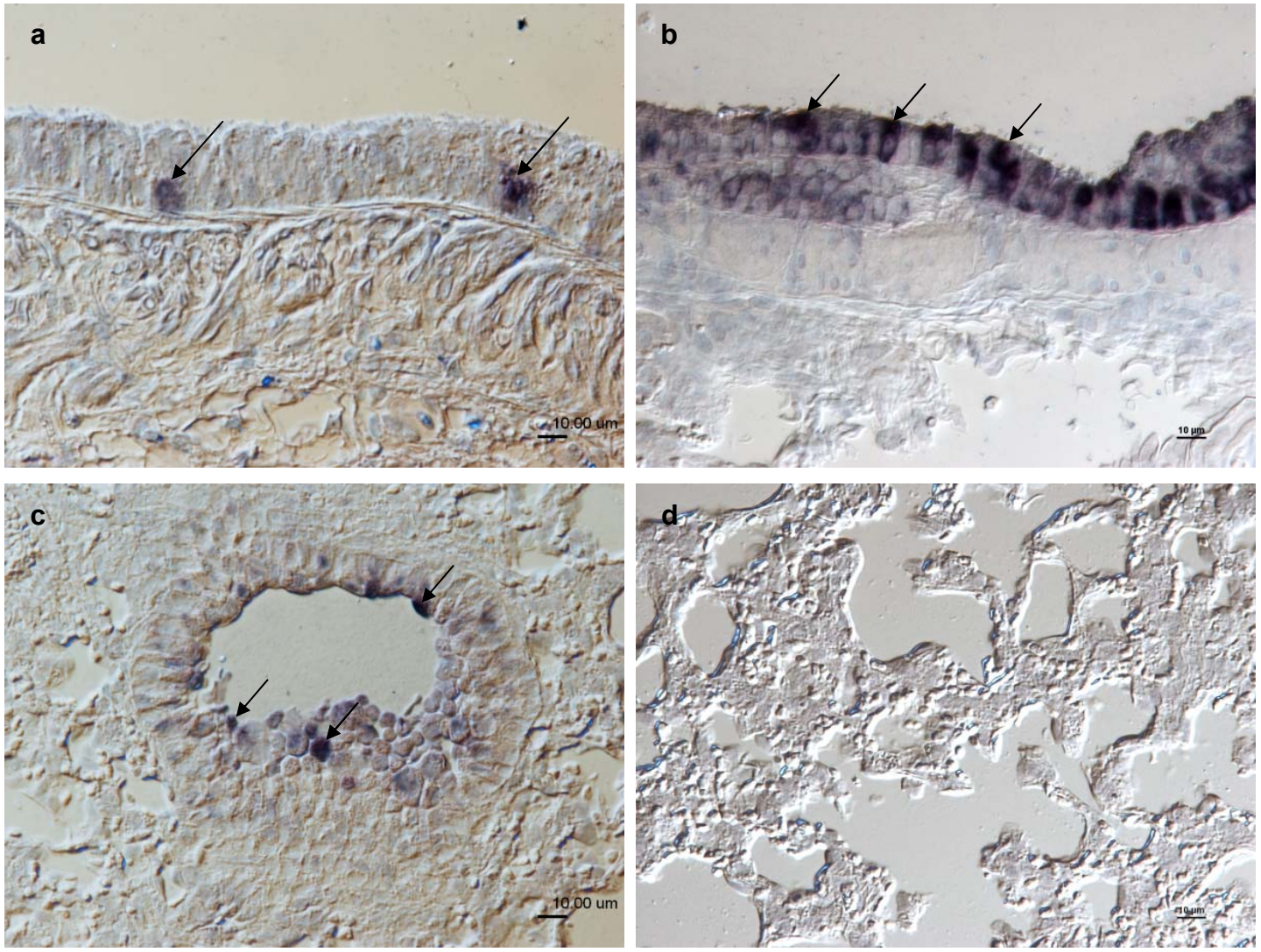

Figure 3-4 ISH for *CCSP* in mock-infected wood mice.

(a) Trachea of a mock-infected wood mouse showing infrequent epithelial cells exhibiting positive signal for *CCSP* (arrows; 40x). (b) Proximal bronchiole of mock-infected wood mouse showing numerous positive cells (arrows; 40x). (c) Bronchiole of mock-infected wood mouse in which the majority of epithelial cells are positive for *CCSP* (arrows; 40x). (d) Alveoli were consistently negative for *CCSP* (40x).

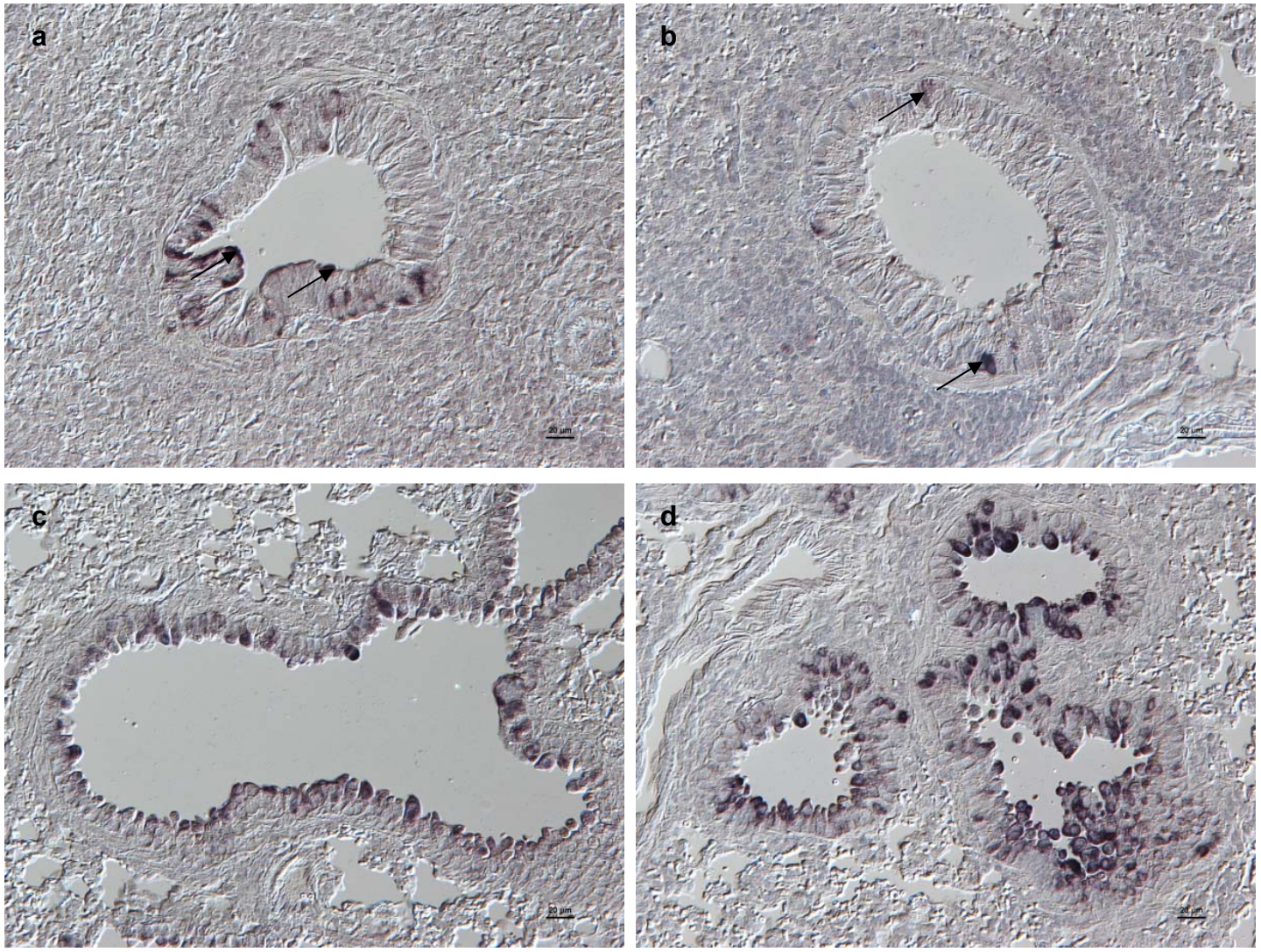

Figure 3-5 ISH for *CCSP* in the bronchioles of M3.MR and M3.stop infected wood mice.

(a) M3.MR infection at day 7 pi showing a strong signal for *CCSP* in some epithelial cells (arrows; 20x). (b) M3.stop infection at day 7 pi showing low numbers of cells with a signal for *CCSP* (arrows; 20x). (c) Bronchiolar epithelial cells positive for *CCSP* were more numerous in M3.MR infection at day 14 dpi (20x). (d) M3.stop infected wood mice at day 14 pi also exhibited numerous *CCSP* positive cells (20x).

3.1.1.3.1.2 Immunohistology for CCSP

Immunohistology for CCSP antigen in mock-infected wood mice was used to establish the pattern and intensity of constitutive expression of the protein. Immunohistology for this antigen is also used in the literature to identify Clara cells (Broeckaert et al., 2000). In the trachea of these wood mice, positive staining for CCSP was present distally, approximately from the level of the mediastinal lymph node, from where cells at regular intervals exhibited specific, granular intra-cytoplasmic staining of variable intensity (Figure 3-6a). The intra-cytoplasmic staining was similar in pattern in the bronchi, but the number of positive cells was increased (Figure 3-6b). Within the bronchioles, the number of Clara cells increased dramatically and the majority of the epithelial cells were positive for CCSP (Figure 3-6c). Alveolar cells were negative (Figure 3-6d).

Quantitative analysis of the immunohistological staining for CCSP was performed. The intensity of expression of CCSP (on a scale of 0 – 255), an indication of the quantity of protein within cells, and also in the percentage area of CCSP positive tissue within the respiratory epithelium, indicating the number of cells which are expressing the protein, was determined by analysis of immunohistological staining using image analysis software. In the mock-infected wood mice, this confirmed that Clara cells were most numerous in the bronchioles, as this was the site of the largest percentage area of CCSP staining (Figure 3-7b). There was a significantly greater percentage of positive cells in the bronchi (12.5 %) than the trachea (3.1 %; $P = 0.003$, two sample T-test) and a greater percentage of positive cells in the bronchioles (48.8 %) than the bronchi ($P = 0.001$, two sample T-test). In addition, the greatest intensity of staining also occurred in the bronchioles (Figure 3-7a), which was significantly greater than the staining in the bronchi ($P= 0.001$, two sample T-test).

The quantitative analysis allowed comparison of the percentage area stained and intensity of staining between the mock-infected and the infected wood mice. Changes were most marked and consistent in the bronchioles, although changes in the trachea were also observed. At day 7 pi there were significant decreases in both intensity of staining ($P = 0.034$, two sample T-test) and

percentage area stained (P = 0.003; two sample T-test) in response to infection with M3.MR, within the bronchioles. In the trachea there was a similar significant decrease in response to infection with M3.stop (intensity P = 0.001, percentage area P = 0.036; two sample T-test). Changes following infection with M3.MR in the trachea or either virus in the bronchi were not significant (Figure 3-8a,b). This indicates that in the first 7 days following infection with MHV-68, both the quantity of CCSP and the number of CCSP positive cells in the bronchiolar epithelium decreases. Moreover, there were differences between the two groups of infected wood mice; the M3.stop wood mice exhibited a significant decrease in the intensity of staining in bronchioles (P = 0.001, two sample T-test) and trachea (P = 0.011, two sample T-test), when compared to the M3.MR infected wood mice (Figure 3-8a), although the percentage area of tissue stained remained similar (Figure 3-8b). This suggests that the lack of M3 protein exacerbated this decrease in the quantity of CCSP in Clara cells at day 7 pi.

At day 14 pi there were significant differences seen in the bronchioles only, where an increase in both the intensity (P = 0.001, two sample T-test) and the percentage area stained (P = 0.001, two sample T-test) were seen between M3.MR infected and mock-infected wood mice (Figure 3-10a,b). Significant increases in both intensity of staining (P = 0.002, two sample T-test) and percentage area stained (P = 0.001, two sample T-test) were also present between the M3.stop infected and mock-infected wood mice (Figure 3-10a,b). At this timepoint, the consequence of infection appeared to be in contrast to that seen at day 7; both of the infected groups showed a significant increase in intensity of staining and percentage area stained in the bronchioles, suggesting that the quantity of protein and the number of cells containing protein had increased. Consistent with the effect present at day 7, was the observation that within the bronchioles, M3.stop infected wood mice showed significantly lower intensity (P = 0.039, two sample T-test) and percentage area stained (P = 0.001, two sample T-test), than the M3.MR mice, suggesting that despite the overall increase in CCSP expression at this timepoint, the absence of M3 reduced the production of CCSP (Figure 3-10a,b).

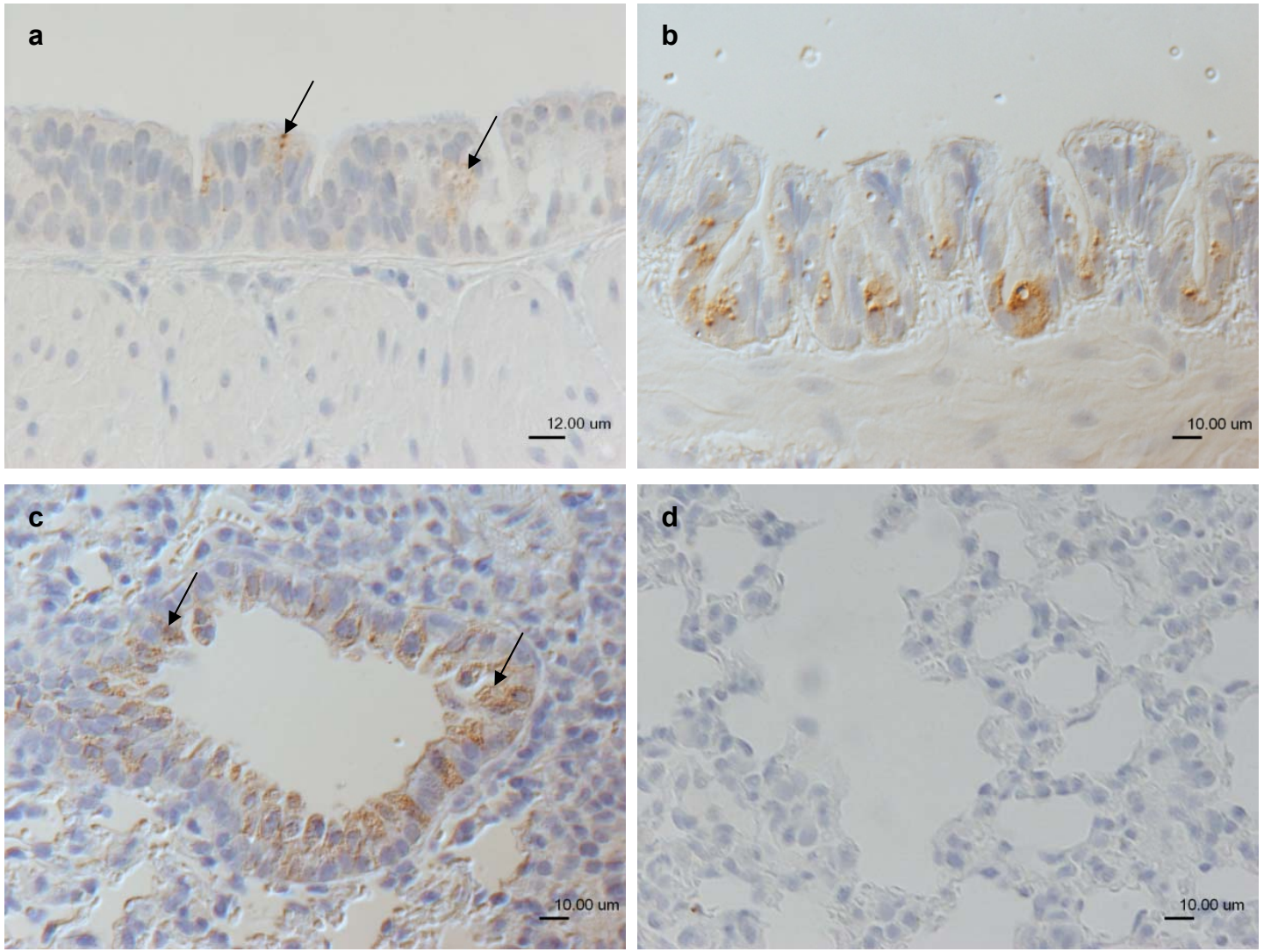

Figure 3-6 Immunohistology for CCSP in mock-infected wood mice.

(a) Trachea: Clara cells identified by CCSP expression, are infrequent. They exhibit granular, cytoplasmic staining of variable intensity (arrows; 40x). (b) Bronchus exhibiting a larger number of Clara cells, compared to the trachea (40x). (c) Bronchi-ole: the majority of epithelial cells are positive for CCSP (arrows; 40x). (d) Cells within the alveoli are negative (40x).

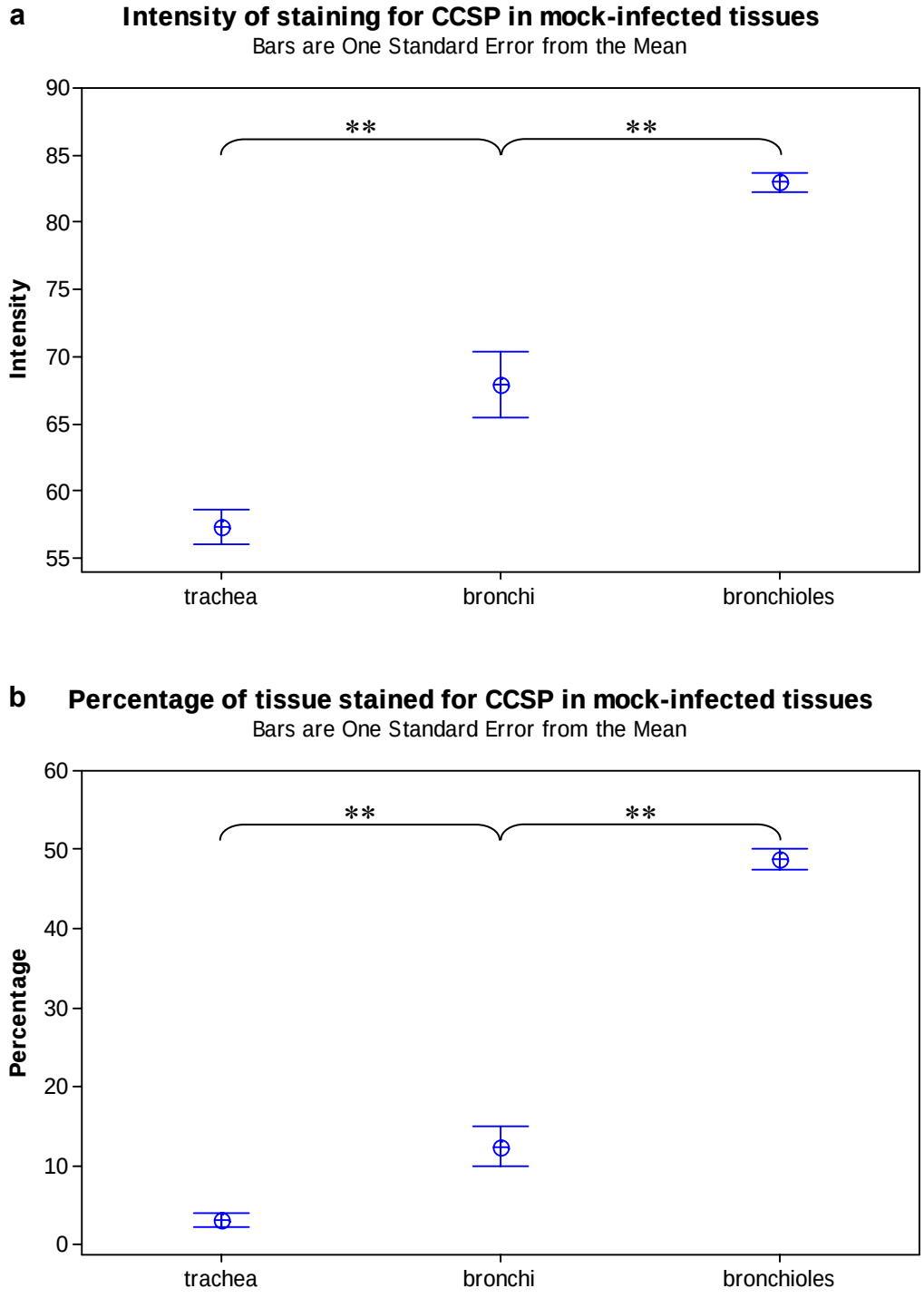

Figure 3-7 Quantitative analysis of immunohistological staining for CCSP in mock-infected wood mice at different levels of the respiratory tract.
(a) Intensity of staining for CCSP in the respiratory epithelium (b) Percentage area of respiratory epithelium stained for CCSP. Data are the mean of analysis of tissue from six mice per group; bars represent the standard error of the mean. ** P< 0.005 (two sample T-test).

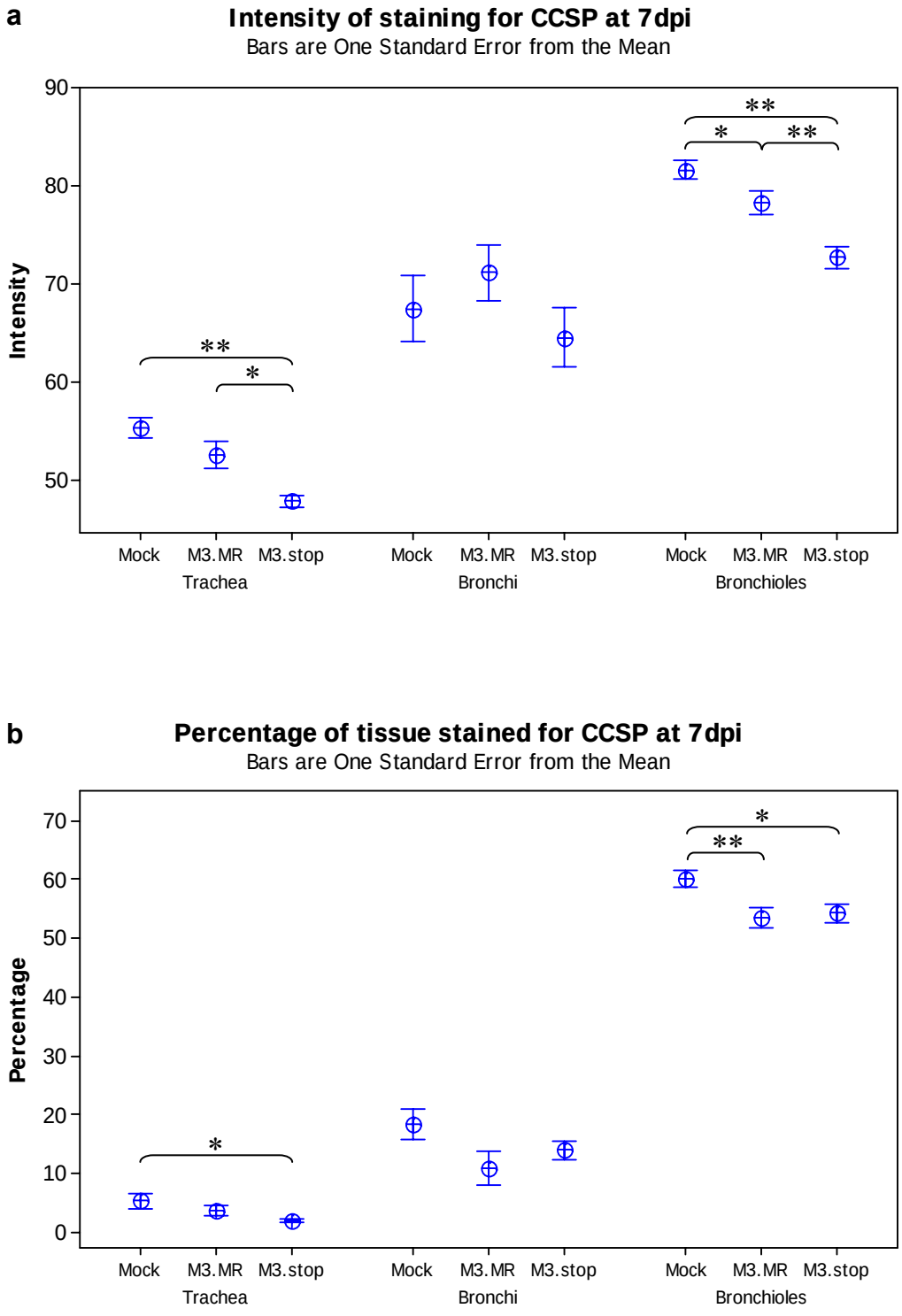

Figure 3-8 Quantitative analysis of immunohistological staining for CCSP in wood mice at different levels of the respiratory tract, following infection with either M3.MR or M3.stop at 7 dpi.
(a) Intensity of staining for CCSP in respiratory epithelium (b) Percentage area of respiratory epithelium stained for CCSP. Data are the mean of analysis of tissue from three mice per group; bars represent the standard error of the mean. ∗ P< 0.05; ∗∗ P< 0.005 (two sample T-test).

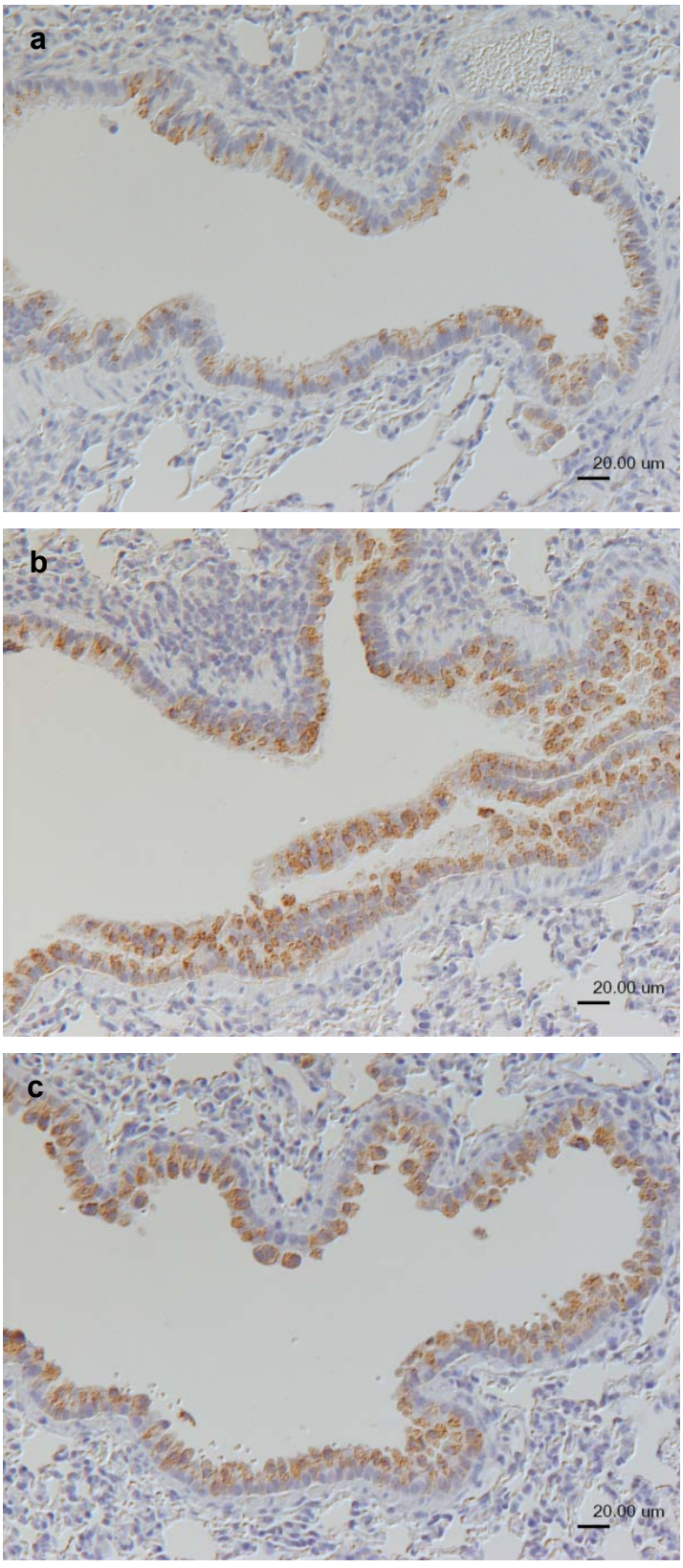

Figure 3-9 Immuno-histology for CCSP in mock-infected, M3.MR and M3.stop infected wood mouse bronchi-oles at day 14 pi.

(a) Mock-infected wood mouse bronchiole (20x) (b) M3.MR infected wood mouse bronchiole showing predominantly strong staining in the majority of epithelial cells (20x). (c) M3.stop infected wood mouse bronchiole, which exhibits less intense staining than the M3.MR infected bronchiole, but greater intensity than that seen in the mock-infected wood mouse (20x).

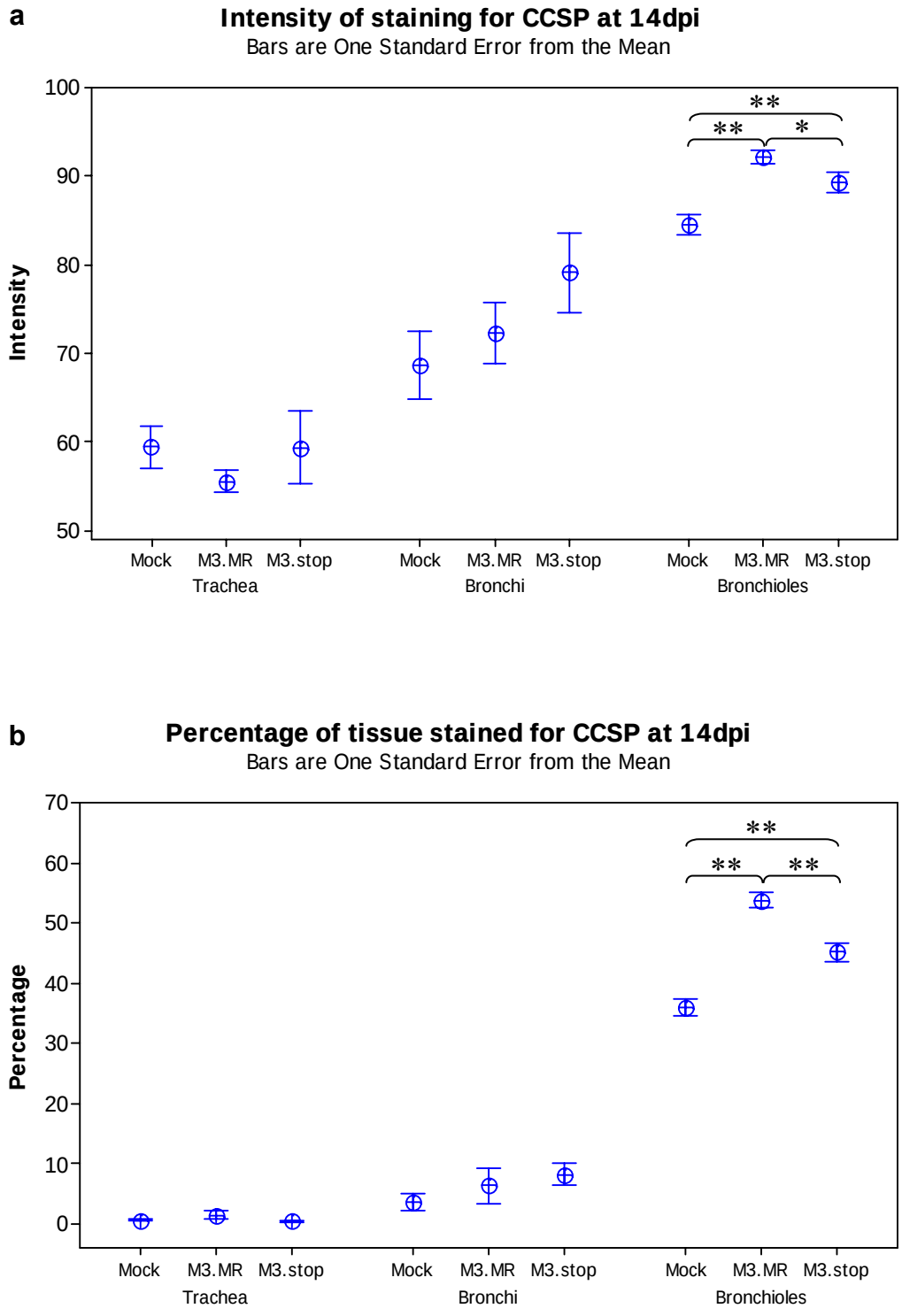

Figure 3-10 Quantitative analysis of immunohistological staining for CCSP in wood mice at different levels of the respiratory tract, following infection with either M3.MR or M3.stop at day 14 pi.
(a) Intensity of staining for CCSP in respiratory epithelium (b) Percentage area of respiratory epithelium stained for CCSP. Data are the mean of analysis of tissue from three mice per group; bars represent the standard error of the mean. * P< 0.05; ** P< 0.005 (two sample T-test).

3.1.1.3.2 SPLUNC1 expression in *Apodemus sylvaticus*

3.1.1.3.2.1 *In situ* hybridisation for *SPLUNC1*

In situ hybridisation analysis was used in mock-infected wood mice to establish the distribution and levels of constitutive expression of *SPLUNC1* in wood mice (Figure 3-11). ISH revealed moderate to strong signal in numerous non-ciliated epithelial cells in the trachea, as well as in the epithelial cells in several, but not all, submucosal glands (Figure 3-11a). The number of cells in the bronchi was also high, showing a similar frequency of signal as seen in the trachea (Figure 3-11b). Distal to the bronchi, however, there was a dramatic difference; in bronchioles very few cells exhibited only a very faint signal, which could be difficult to distinguish from background (Figure 3-11c). The alveoli were negative in all wood mice examined (Figure 3-11d).

Following infection, there was little alteration in the distribution of signal for *SPLUNC1* in wood mice. This was of note, especially as there was little upregulation of signal in the bronchioles, where alterations in response to infection had been observed in *CCSP* expression. Despite the lack of signal in the mock-infected mice at this anatomical location, as it is the section of the respiratory airway closest to the site of infection and the accompanying inflammatory response, it was thought that this site may also show alteration in response to infection. However, although rare cells exhibited positive signal, the change was very minor (Figure 3-12).

Tissue from a wood mouse that had been infected with MHV-68 at day 3 pi was also examined using ISH to investigate whether any upregulation of *SPLUNC1* had occurred prior to day 7 pi, but this also exhibited a faint signal in very rare cells, similar to that observed in M3.MR infected wood mice at day 7 pi (data not shown).

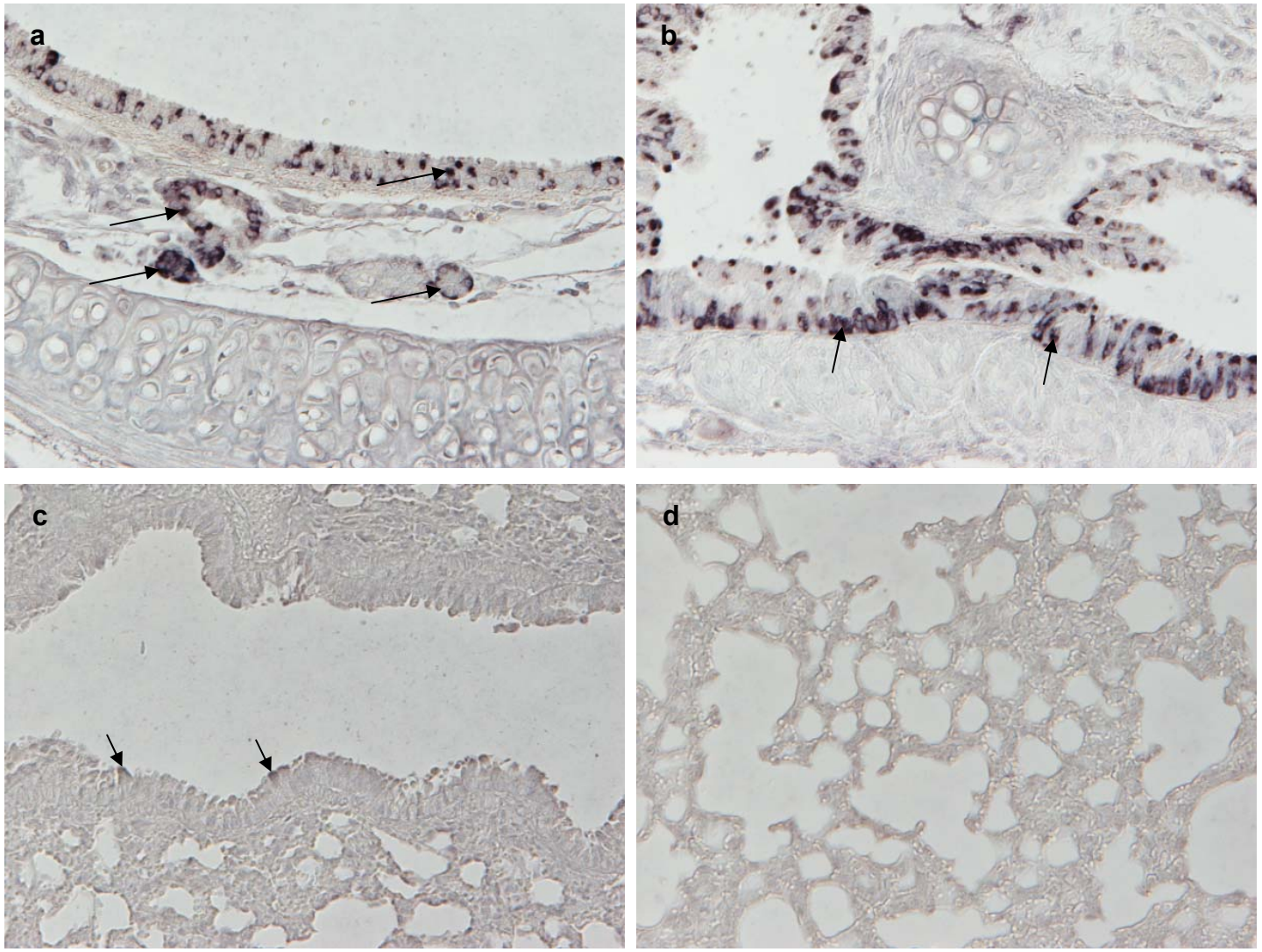

Figure 3-11 ISH for *SPLUNC1* in mock-infected wood mice at different levels of the respiratory tract.

(a) Trachea and sub-mucosal glands exhibit frequent cells positive for *SPLUNC1* (arrows; 20x). (b) Bronchial epithelium also exhibits frequent strongly positive cells (arrows; 20x). (c) Within the bronchiole, rare cells exhibit a weak signal for *SPLUNC1* (arrows; 20x). (d) Alveoli are negative for *SPLUNC1* (20x).

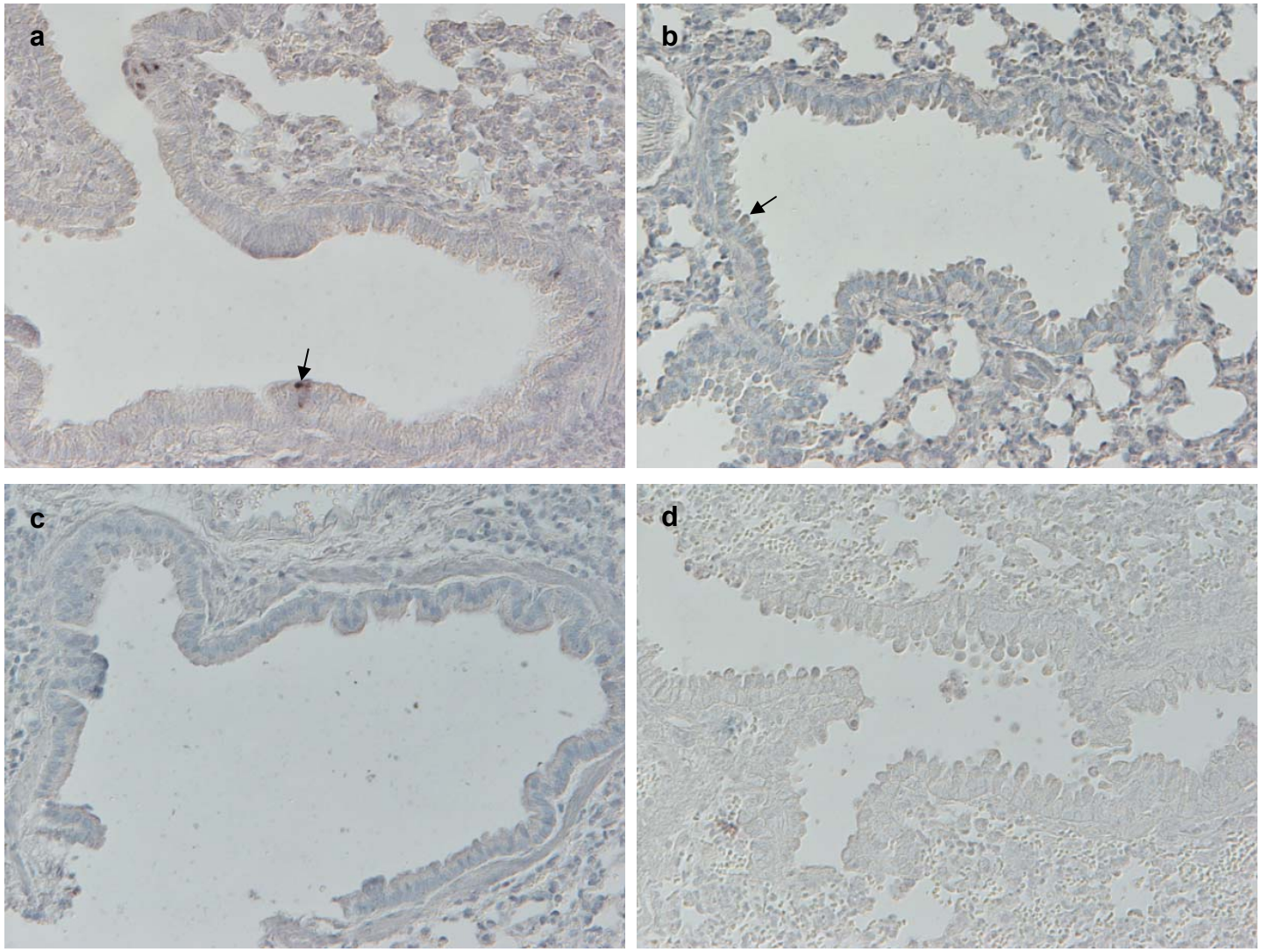

Figure 3-12 ISH for *SPLUNC1* in the bronchioles of M3.MR and M3.stop infected wood mice.

(a) Rare positive cells are present in the M3.MR infected wood mouse bronchiole, day 7 pi (arrow; 20x). (b) Rare faintly positive cells are present in the M3.stop infected wood mouse bronchiole at day 7 pi (arrows; 20x). (c) M3.MR infected wood mouse bronchioles at day 14 pi are negative for *SPLUNC1* (20x). (d) M3.stop infected wood mouse bronchioles at day 14 pi are negative for *SPLUNC1* (20x).

3.1.1.3.2.2 Immunohistology for SPLUNC1

Immunohistology for SPLUNC1 using an antibody to the murine protein, was utilised to examine the distribution of this protein within the respiratory tract. In the mock-infected animals, staining for the protein was most intense in the tracheal and bronchial non-ciliated epithelium, with little discernable difference between these two areas (Figure 3-13a,b). In addition, there was strong staining in many cells of the submucosal glands, similar to the pattern of *SPLUNC1* expression demonstrated by ISH (Figure 3-11). Distal to the bronchi, the intensity of staining decreased, the proximal bronchioles exhibiting stronger staining than the distal bronchioles (Figure 3-13c,d). This finding was intriguing as no, or a very low signal for *SPLUNC1* had been observed in the bronchioles following RNA-ISH (Figure 3-11c).The alveolar cells were negative in all sections examined.

Quantitative analysis of the intensity and percentage area stained for SPLUNC1 by immunohistology in mock-infected wood mice confirmed that expression of the protein was similar in the trachea and the bronchi, and significantly lower, in both the percentage area stained ($P = 0.001$, two sample T-test) and the intensity of staining ($P = 0.001$, two sample T-test), in the bronchioles (Figure 3-14).

Following infection with either M3.MR or M3.stop at 7 dpi, alterations in the intensity of staining and the percentage area of tissue stained were both seen within the bronchioles. There was a highly significant decrease in intensity of staining in both M3.MR ($P = 0.001$, two sample T-test) and M3.stop ($P = 0.004$, two sample T-test) infected wood mice, compared to the mock-infected wood mice at this timepoint (Figure 3-15a). Similarly, there was a significant decrease in the percentage area of tissue stained in both the M3.MR ($P = 0.048$, two sample T-test) and M3.stop ($P = 0.032$, two sample T-test) infected wood mice, compared to mock-infected controls (Figure 3-15b). This was a similar pattern to the changes observed in CCSP expression in the bronchioles at this timepoint. However, the effect of M3 was different in SPLUNC1 expression; the absence of M3 was associated with a higher staining intensity than M3.MR infection ($P = 0.012$, two sample T-test), although this did not

abrogate the effect of infection (Figure 3-15a), in contrast to CCSP, where the absence of M3 was associated with further reduction of staining intensity at day 7 pi (Figure 3-8a).

The consequence of infection at day 14 pi was in complete contrast to that seen at day 7, as SPLUNC1 intensity and percentage area stained were increased in response to infection at this timepoint. This was seen in the bronchioles, as before, where highly significant increases were observed in response to infection by both M3.MR (intensity P = 0.001, percentage area P = 0.001, two sample T-test) and M3.stop (intensity P = 0.001, percentage area P = 0.001, two sample T-test), although here were no significant differences in intensity or percentage area stained between the two types of infection (intensity P = 0.976, percentage area P = 0.293, two sample T-test; Figure 3-16a,b). Interestingly, a similar increase in the intensity of staining was also seen in the bronchi (P = 0.001, two sample T-test) and the trachea (P = 0.006, two sample T-test) following infection with M3.MR; percentage area of SPLUNC1 staining in the bronchi was also increased (P = 0.013, two sample T-test). However, these anatomical sites, like the bronchioles did not show any difference between M3.MR infected and M3.stop infected wood mice.

The presence of SPLUNC1 protein detected by immunohistology in the bronchiolar epithelium, in the absence of ISH signal for *SPLUNC1* was confirmed using a combination of these two techniques on a single slide. This showed that SPLUNC1 protein was present in the trachea and bronchi where *SPLUNC1* is expressed (as demonstrated by RNA-ISH), whereas in the bronchiole, protein was present in higher quantities and more distally, in terminal bronchioles, than signal for *SPLUNC1* (Figure 3-17). This would suggest that SPLUNC1 protein is not produced at this location, despite of the increased quantity at this timepoint, following infection. As previously stated, no signal for *SPLUNC1* was seen in the distal bronchioles at 3, 7 or 14 days pi.

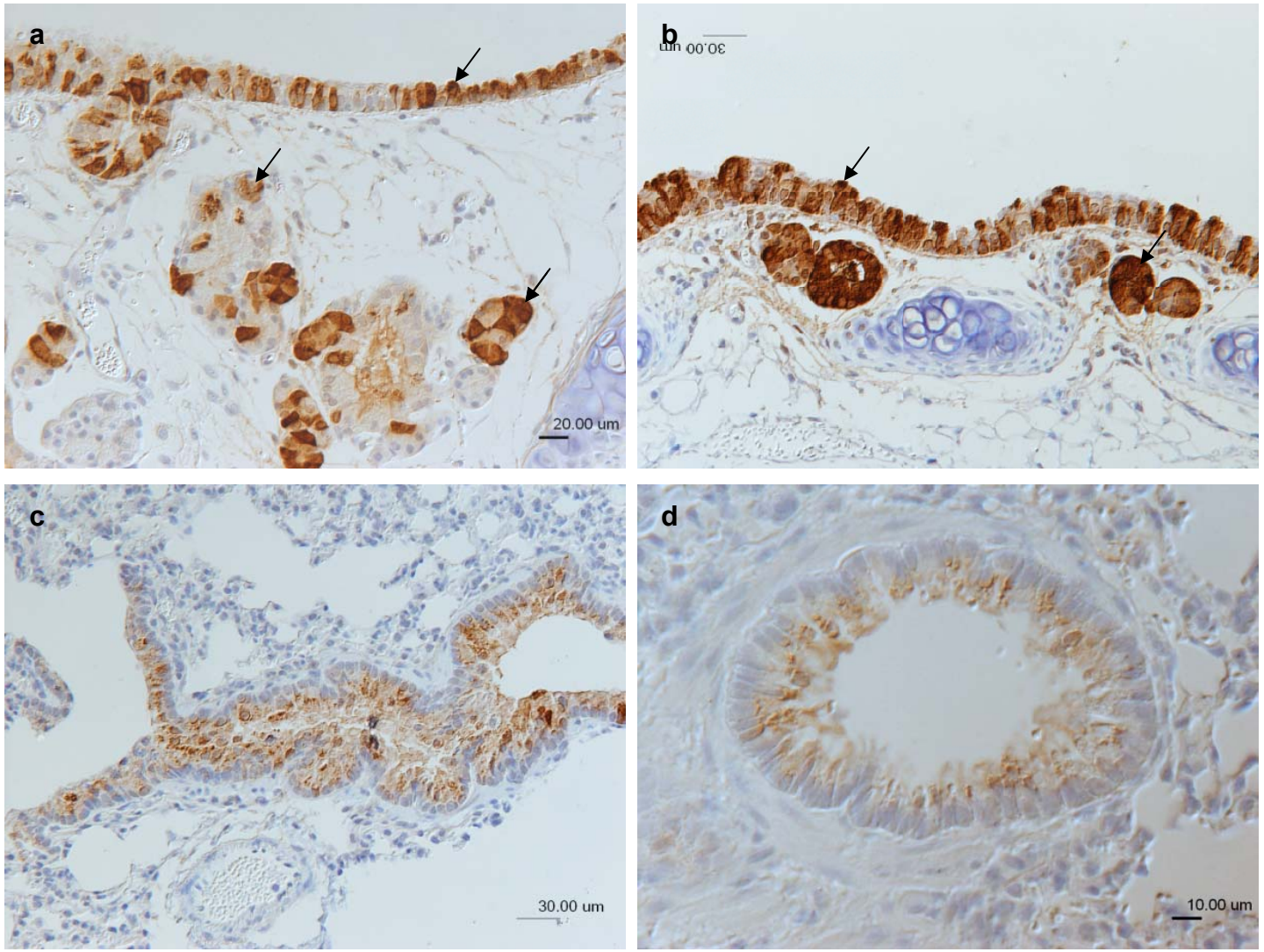

Figure 3-13 Immuno-histology for SPLUNC1 in mock-infected wood mice at different levels of the respiratory tract.

(a) Trachea showing positive staining in non-ciliated respiratory epithelial cells and submucosal glands (arrows; 20x). (b) Bronchi with strong staining in respiratory epithelium and submucosal glands (arrows; 20x). (c) Proximal bronchiole where numerous epithelial cells are positive, but with reduced intensity compared to the upper respiratory tract (20x). (d) Distal bronchiole with reduced intensity of staining for SPLUNC1 (40x).

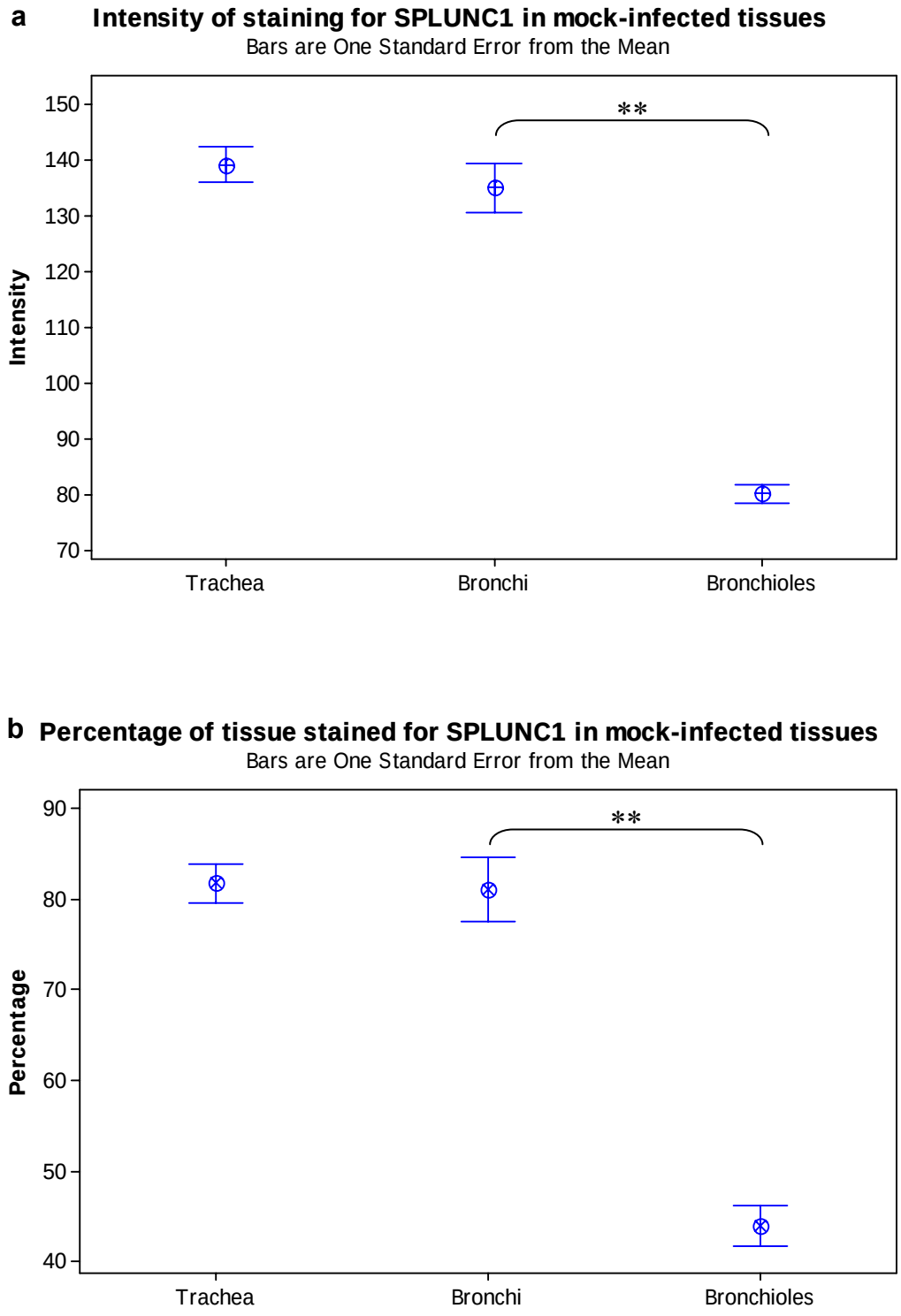

Figure 3-14 Quantitative analysis of immunohistological staining for SPLUNC1 at different levels of the respiratory tract in mock-infected wood mice.
(a) Intensity of staining for SPLUNC1 in respiratory epithelium (b) Percentage area of respiratory epithelium stained for SPLUNC1. Data are the mean of analysis of tissue from three mice per group; bars represent the standard error of the mean. * P< 0.05; ** P< 0.005 (two sample T-test).

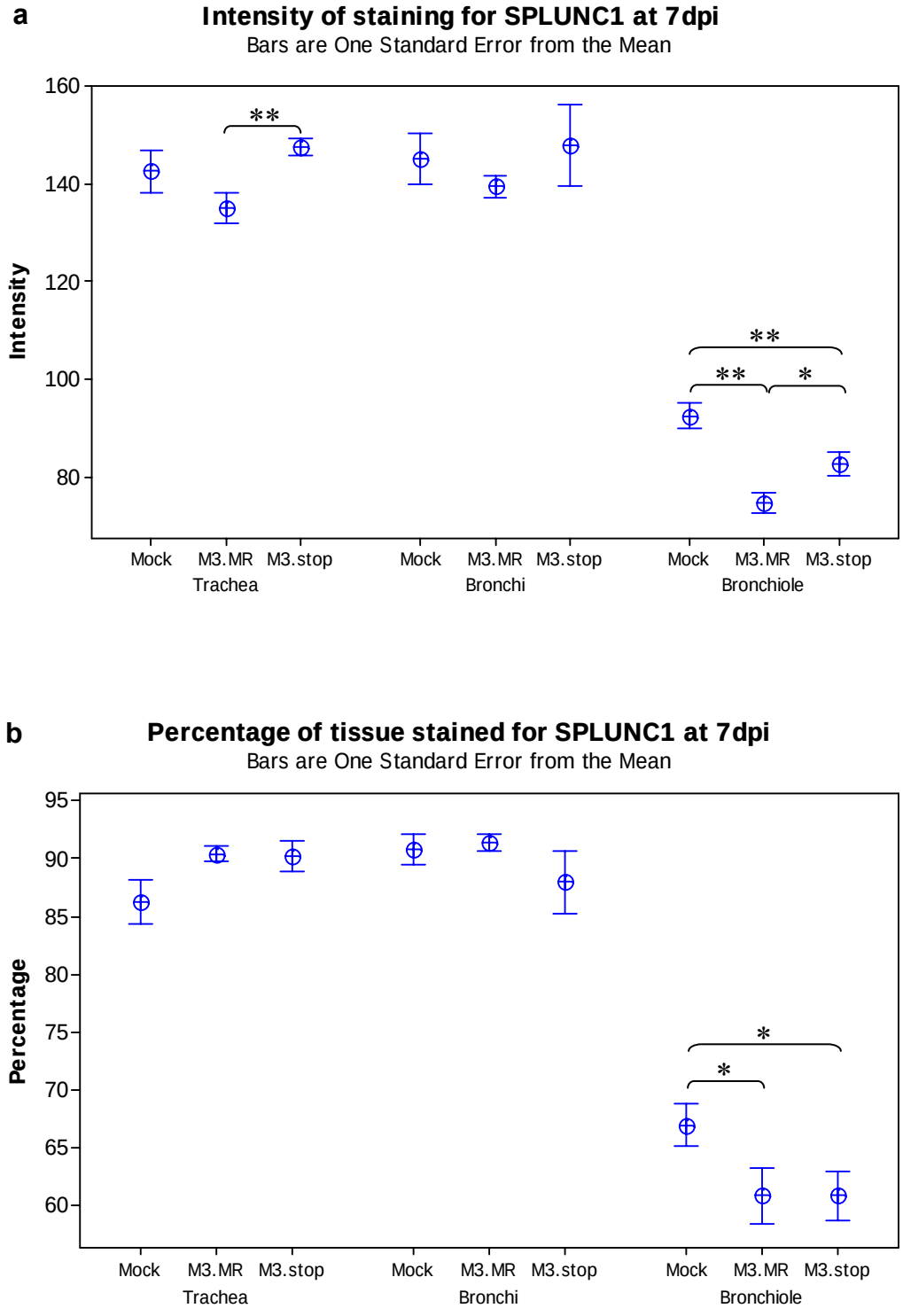

Figure 3-15 Quantitative analysis of immunohistological staining for SPLUNC1 in wood mice at different levels of the respiratory tract, following infection with either M3.MR or M3.stop, at day 7 pi.
(a) Intensity of staining for SPLUNC1 in respiratory epithelium (b) Percentage area of respiratory epithelium stained for SPLUNC1. Data are the mean of analysis of tissue from three mice per group; bars represent the standard error of the mean. * P< 0.05; ** P< 0.005 (two sample T-test).

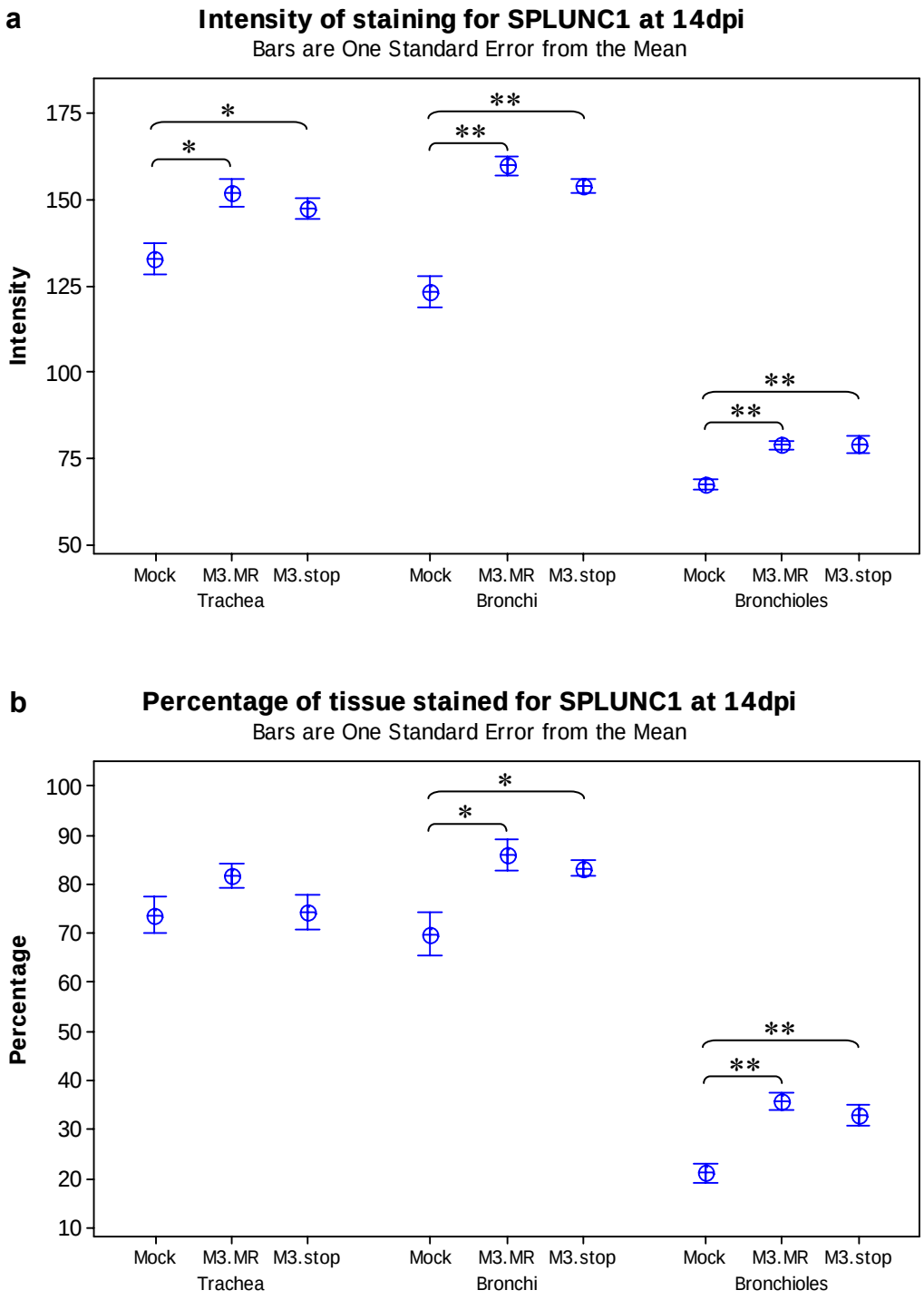

Figure 3-16 Quantitative analysis of immunohistological staining for SPLUNC1 in wood mice at different levels of the respiratory tract, following infection with either M3.MR or M3.stop, at day 14 pi.
(a) Intensity of staining for SPLUNC1 in respiratory epithelium (b) Percentage area of respiratory epithelium stained for SPLUNC1. Data are the mean of analysis of tissue from three mice per group, bars represent the standard error of the mean. * $P < 0.05$; ** $P < 0.005$ (two sample T-test).

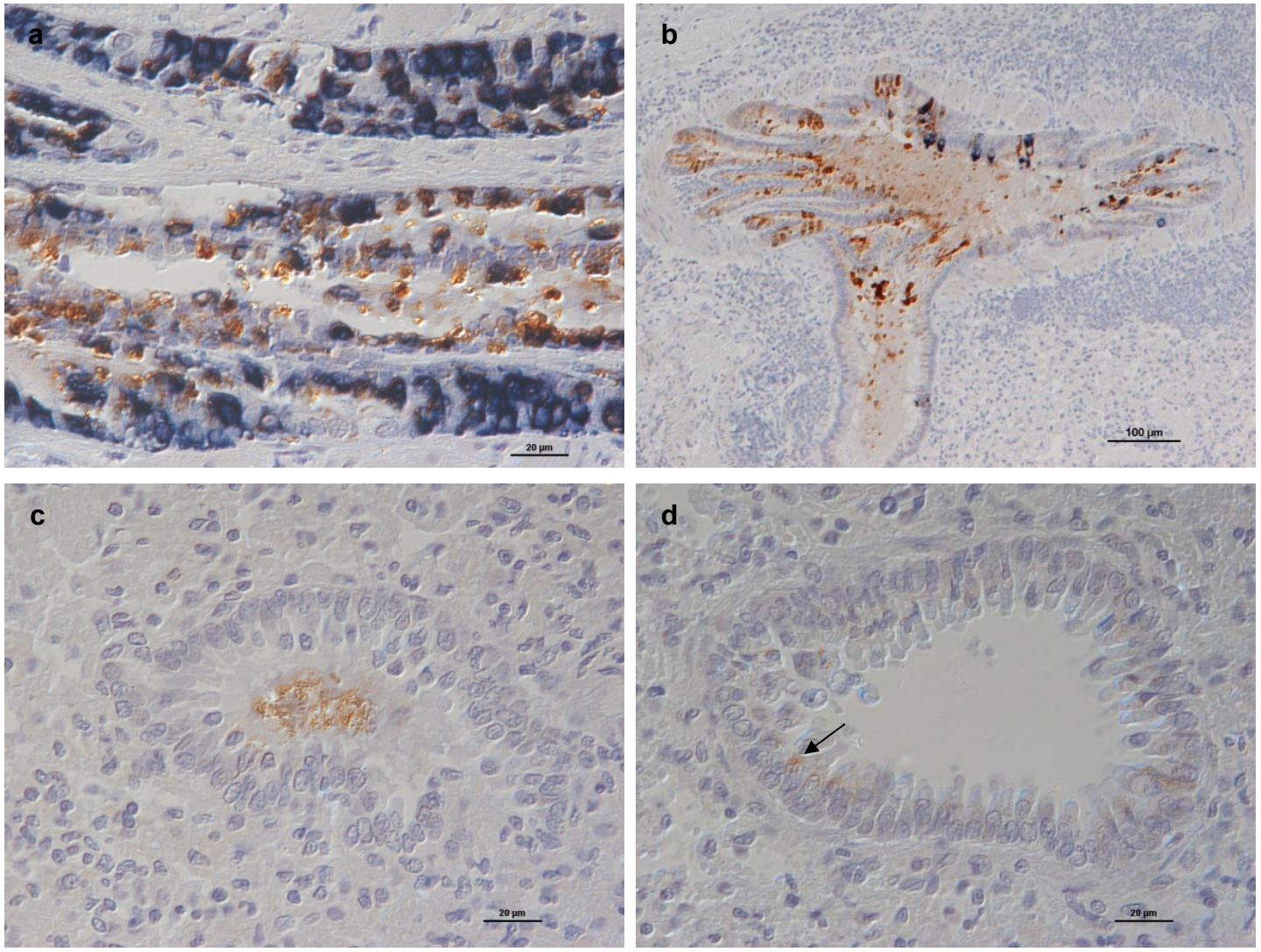

Figure 3-17 ISH-IH for *SPLUNC1* and SPLUNC1 protein at different levels of the respiratory tract in a M3.MR infected wood mouse at day 14 pi.

(a) Bronchus showing extensive signal for *SPLUNC1* (blue-black staining) and frequent cells positive for SPLUNC1 protein (brown staining) (40x). (b) Proximal bronchiole with scattered cells exhibiting a signal for *SPLUNC1* and numerous cells and intra-luminal material exhibiting positive staining for SPLUNC1 protein (10x). (c) Distal bronchiole with positive intra-luminal staining for SPLUNC1 protein (40x). (d) Distal bronchiole with scattered cells exhibiting intracellular staining for SPLUNC1 protein (arrow) in the absence of signal for *SPLUNC1* (40x).

3.1.1.3.3 Cellular localisation of SPLUNC1

SPLUNC1 was shown to be transcribed and translated within non-ciliated cells in the upper respiratory tract (Figure 3-13a). Clara cells are present in the upper respiratory tract, but are not as frequent as *SPLUNC1* positive cells. To demonstrate whether Clara cells are capable of transcribing *SPLUNC1*, immunohistology for CCSP (to demonstrate Clara cells) and ISH for *SPLUNC1* was performed on the same tissue section (Figure 3-18). Some non-ciliated cells exhibited positive staining for both CCSP and *SPLUNC1*, whereas others were positive for either CCSP or *SPLUNC1* alone. This suggests that not only Clara cells but also other non-ciliated cells transcribe *SPLUNC1*. In addition, sections undergoing immunohistology for SPLUNC1 were counterstained with Alcian blue and Periodic acid Schiff stains, which stain polysaccharides and are commonly used to identify mucins. This showed AB-PAS positive cells in the bronchi and bronchiolar epithelium, and in submucosal glands that also stained for SPLUNC1 (Figure 3-19). This suggests that cells of the mucous cell type can also transcribe and secrete SPLUNC1.

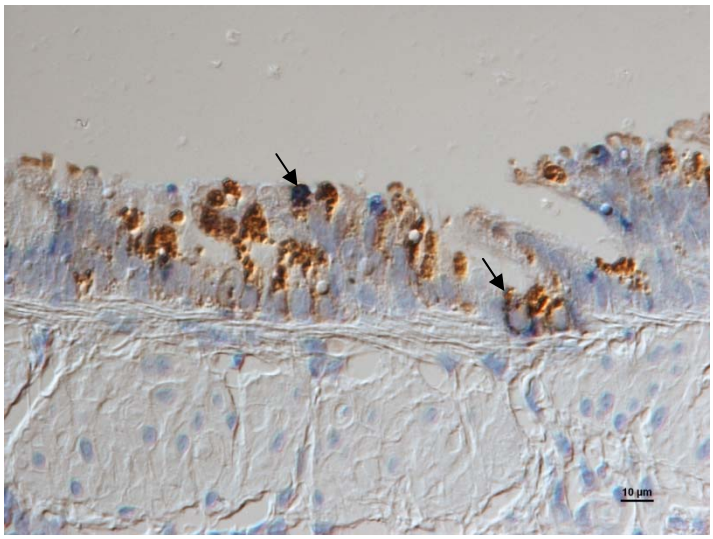

Figure 3-18 Immunohistology for CCSP and ISH for *SPLUNC1*, in the bronchus of a M3.MR infected wood mouse at 14 dpi.
Non-ciliated cells show positive staining for CCSP and *SPLUNC1* mRNA (arrows, 40x).

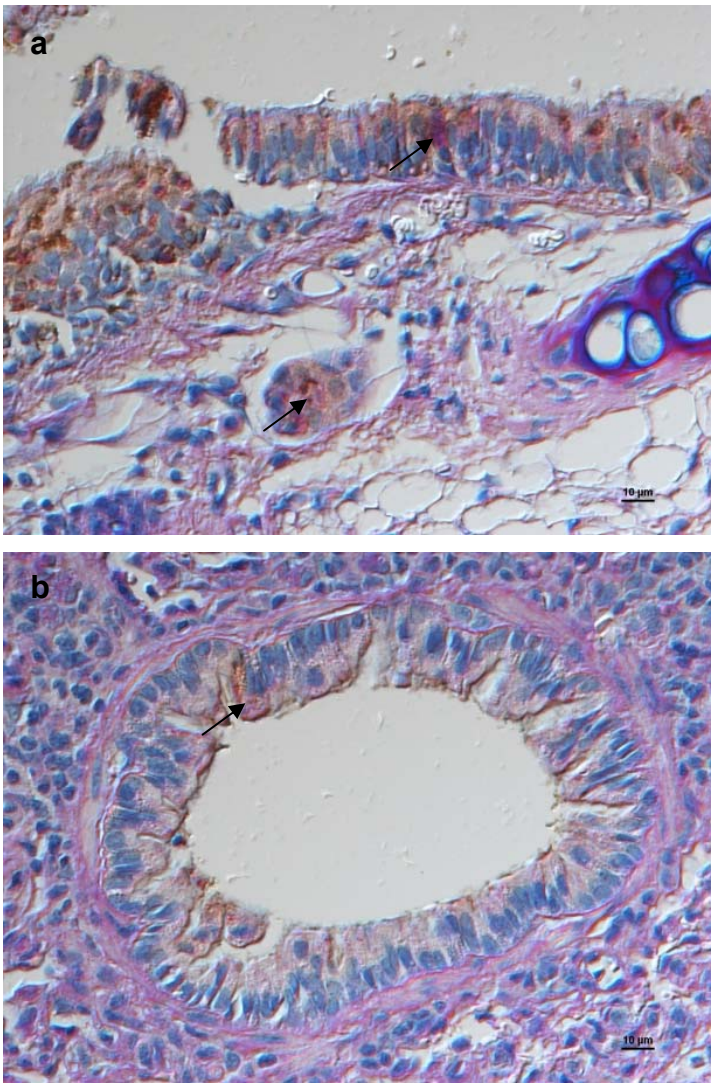

Figure 3-19 Immunohistology for SPLUNC1 in a M3.MR infected wood mouse, counterstained with AB-PAS for polysaccharides.
(a) Bronchial epithelium and submucosal gland in which cells that are AB-PAS positive (indicative of mucous cells) and positive for SPLUNC1 are present (arrows; 40x). (b) Bronchioles exhibited fewer cells which were AB-PAS and SPLUNC1 positive (arrow, 40x).

3.1.1.3.4 AGR2 and AGR3 expression in *Apodemus sylvaticus*

AGR3 was one of the genes identified as upregulated in the presence of the viral *M3* gene in M3.MR infected mice, compared to M3.stop infected wood mice (Hughes, 2006). *AGR2* is thought to be a homologue of *AGR3*. As little is known about the function of these genes, particularly in mice, *in situ* hybridisation and immunohistology were used to describe their locations within the lung of wood mice.

In the trachea there was a weak signal for *AGR2* using ISH, in the non-ciliated cells of the respiratory epithelium and also in some of the submucosal glands (Figure 3-20a). In the distal airway, the signal was stronger in the bronchioles, predominantly in the apical portion of the non-ciliated epithelial cells (Figure 3-20b). In M3.MR and M3.stop infected mice at 14 dpi, the signal was reduced, in both the trachea (Figure 3-20c) and in the bronchioles (Figure 3-20d).

Immunohistology for AGR2 protein showed a similar distribution in uninfected wood mice; the protein was present in the respiratory epithelium in the non-ciliated cells of the bronchi and bronchioles (Figure 3-21a,b).

AGR3 distribution and expression was similarly surveyed using ISH. The location of cells showing signal in uninfected wood mice was similar to that seen for *AGR2*, with some non-ciliated cells in the respiratory epithelium of the trachea positive and also cells within submucosal glands exhibiting positive staining (Figure 3-22a). In the bronchioles more frequent cells exhibited a signal, consistent with higher numbers of non-ciliated cells in this location (Figure 3-22b). In response to infection, in the trachea M3.MR infected wood mice exhibited a stronger signal in a similar distribution to that seen in uninfected wood mice (Figure 3-22c), however, M3.stop wood mice showed little or no signal (Figure 3-22d). Interestingly, bronchioles showed little or no signal in either M3.MR or M3.stop infected wood mice (data not shown).

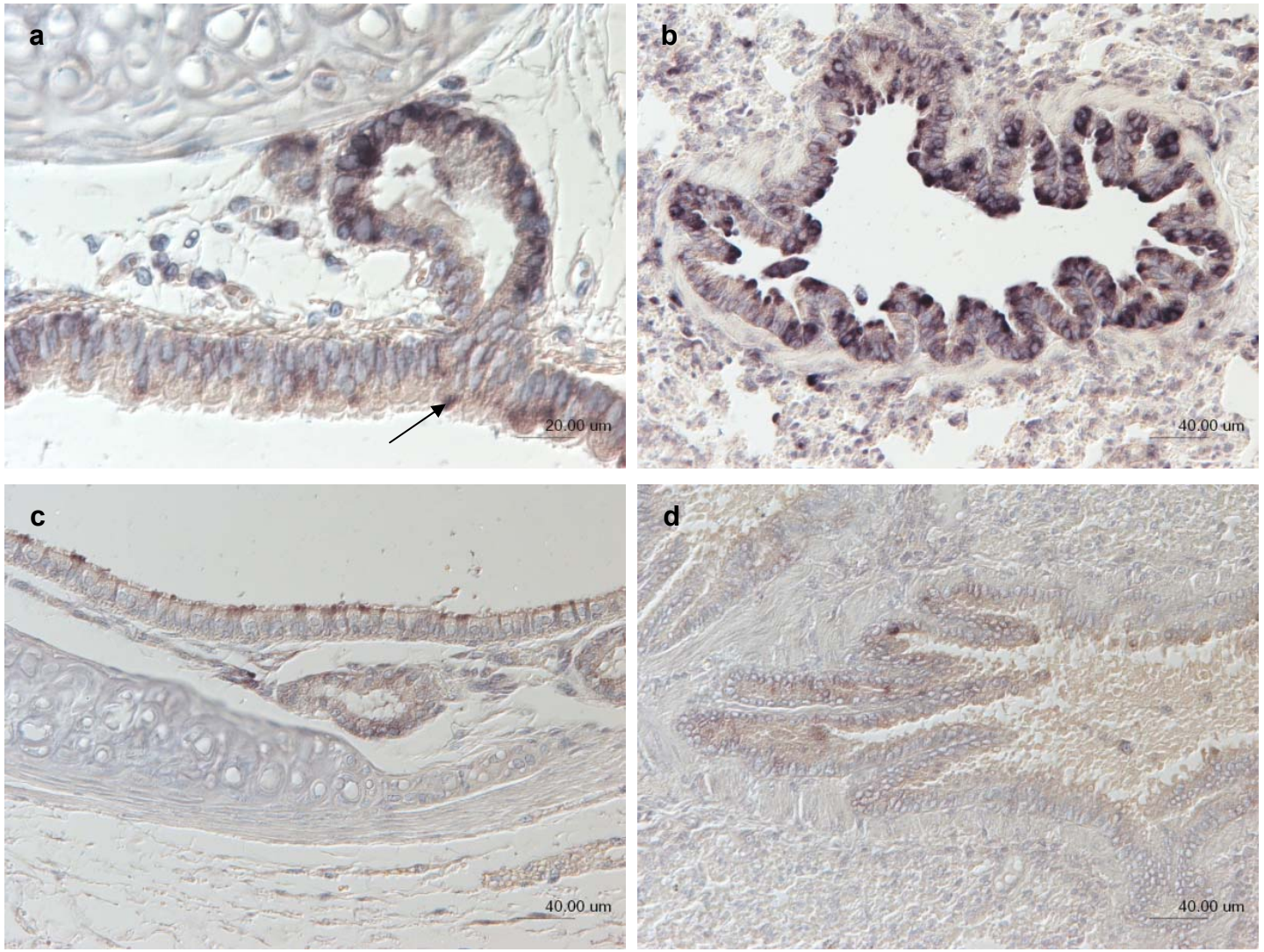

Figure 3-20 *AGR2* expression demonstrated by ISH at different levels of the respiratory tract in the wood mouse.

(a) Uninfected trachea and submucosal gland epithelium exhibiting signal for *AGR2*; the non-ciliated respiratory epithelium exhibits signal (arrow; 40x). (b) Bronchiole in uninfected wood mouse lung exhibiting signal for *AGR2* (20x). (c) Trachea and submucosal gland of an M3.MR infected wood mouse at 14 dpi, showing reduced signal for *AGR2* compared to an uninfected wood mouse (20x). (d) Bronchiole of an M3.stop infected wood mouse showing reduced signal for *AGR2* compared to an uninfected wood mouse (20x).

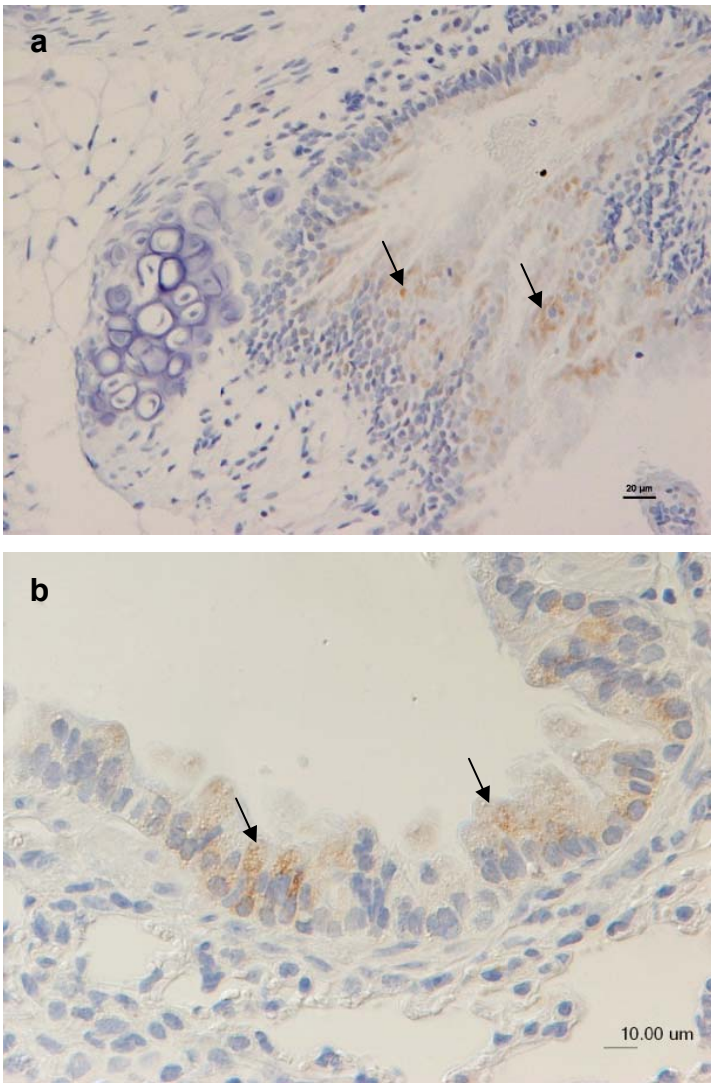

Figure 3-21 Immunohistology for AGR2 in the respiratory epithelium of an uninfected wood mouse.
(a) AGR2 positive cells are present in the bronchial epithelium (arrows, 20x). (b) Positively stained epithelial cells in the bronchioles are non-ciliated (arrows, 40x).

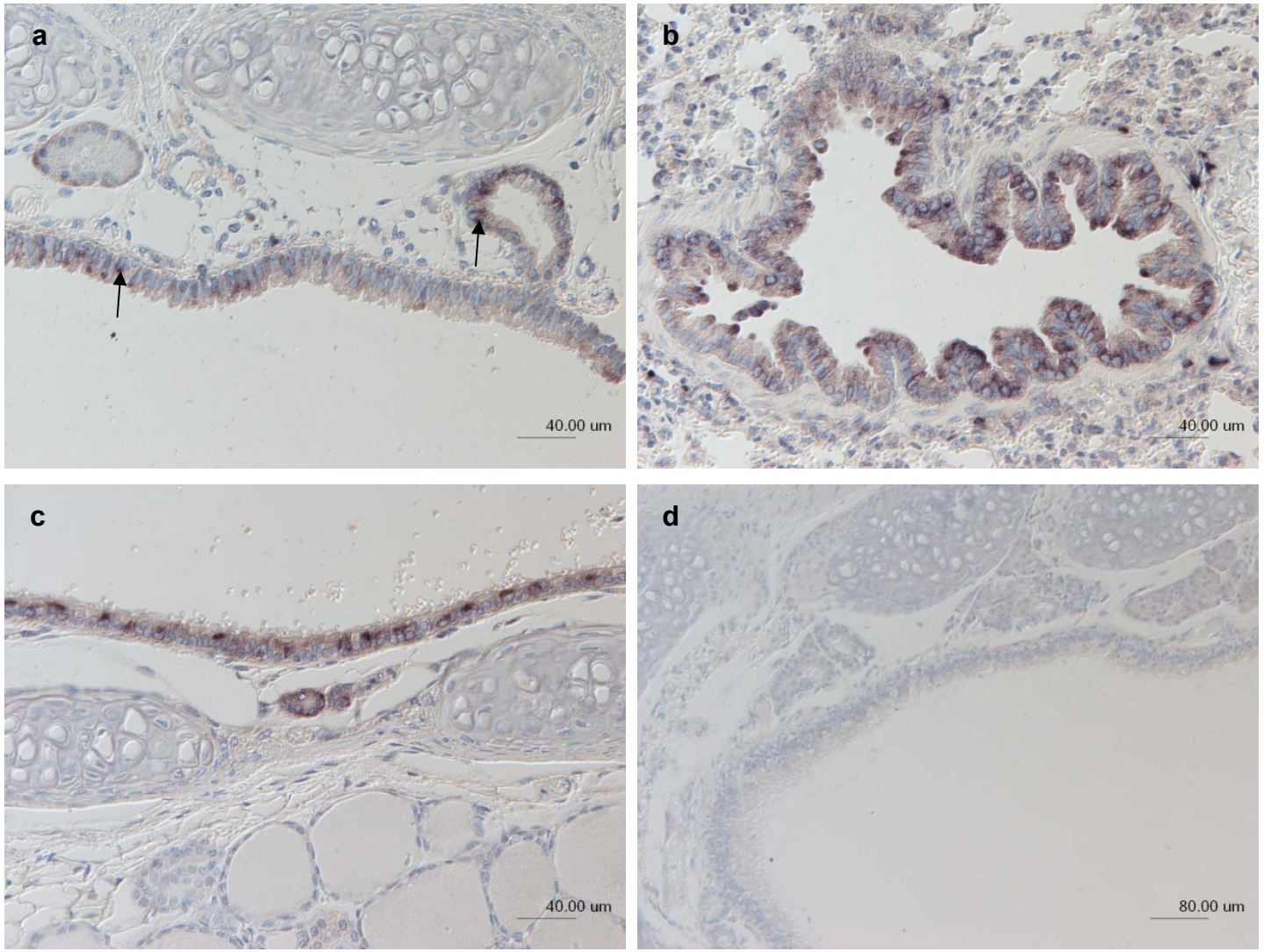

Figure 3-22 ISH for *AGR3* at different levels of the respiratory tract in the wood mouse.

(a) Trachea of an uninfected wood mouse showing ISH signal for *AGR3* in non-ciliated cells in the respiratory epithelium and within the submucosal glands (arrows; 20x). (b) Bronchiole of an uninfected wood mouse showing frequent cells exhibiting positive signal for *AGR2* (20x). (c) Trachea of an M3.MR infected wood mouse at day 14 pi showing more frequent cells in the respiratory epithelium exhibiting positive signal, compared to the uninfected wood mouse (20x). (d) Trachea of an M3.stop infected wood mouse showing no signal for *AGR3* (10x).

3.1.1.4 Ultrastructural morphology and location of Clara cells in *Apodemus sylvaticus*

Transmission electron microscopy (TEM) was used to examine the trachea, bronchi and bronchioles of mock-infected and M3.MR infected wood mice at day 14 pi. In particular, the morphology of Clara cells was examined, to distinguish the different types of Clara cells as described by Pack et al (1981), as well as to establish the proportion of respiratory epithelium that are Clara cells in the wood mouse. These results should be interpreted with caution, however, as the number of animals that were examined was low (one mock-infected wood mouse, two M3.MR infected wood mice).

Firstly, the overall numbers of ciliated versus non-ciliated cells was established as this data is not known in wood mice. The highest proportion of ciliated cells occurs in the trachea, with the proportion decreasing distally within the airway, where they constitute the minority of cells, in common with other murine species (Figure 3-23). Proportions were similar for mock-infected and M3.MR infected wood mice.

Within the non-ciliated proportion of epithelial cells in the respiratory tract, three types of Clara cells have been described, on the basis of ultrastructural morphological properties (Pack et al., 1981). The most frequent type of Clara cells seen in the wood mice are those described by Pack et al (1981) as the “Common Type”. These cells have a basal nucleus and cytoplasm of moderate electron density containing smooth endoplasmic reticulum, mitochondria and “mitochondria-like bodies” and vesicles, most commonly in the apical part of the cell, adjacent to the luminal membrane, filled with electron dense material, though to be CCSP (Figure 3-25a). These cells are of a relatively consistent height within the respiratory epithelium, so appear to project further into the lumen in the distal airway, where the bronchiolar ciliated epithelium is cuboidal rather than columnar (Figure 3-25b). In mock-infected wood mice, this was the overwhelmingly dominant type of Clara cell observed (Figure 3-24). The “Type II Clara cell” has a more electron dense cytoplasm than the Common type, with less smooth endoplasmic reticulum and less frequent electron-dense vesicles (Figure 3-25c). This type was consistently seen at all levels of the

airway in M3.MR infected wood mice, but infrequently in the mock-infected wood mouse (Figure 3-24). The third type of Clara cell is the “Vesiculated Clara cell”, in which most or all of the cytoplasm is vesiculated; these vacuoles may or may not contain a faint matrix (Figure 3-25d). This type of cell was not observed in the mock-infected wood mouse, but was a feature in the M3.MR infected wood mice, and represented a growing proportion of the Clara cell population in the distal respiratory tract (Figure 3-24).

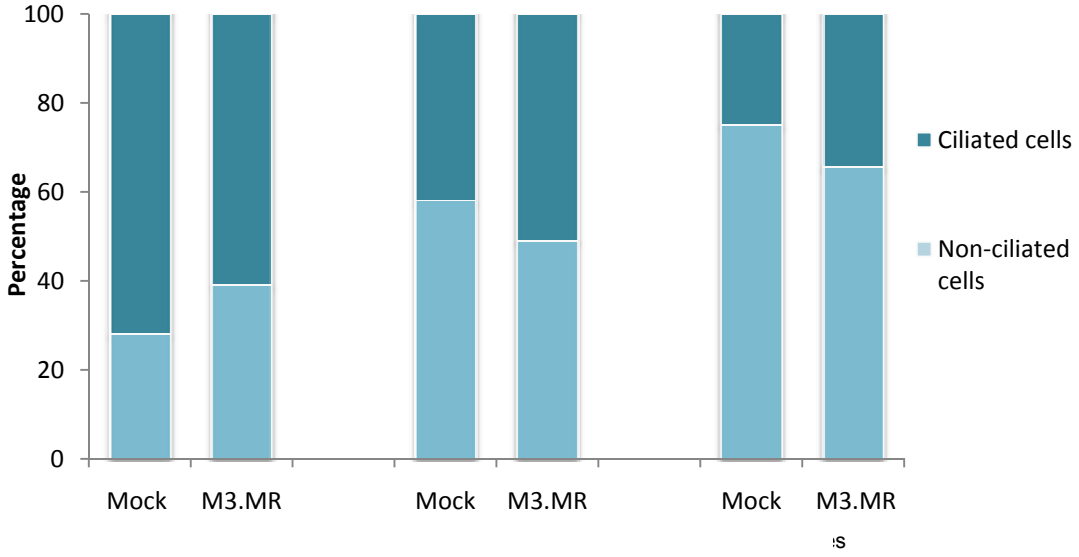

Figure 3-23 Proportion of ciliated and non-ciliated epithelial cells as determined by transmission electron microscopy at different levels of the respiratory tract of mock-infected and M3.MR infected wood mice.
Data represent the mean results from one (mock-infected) or two (M3.MR infected) mice per group.

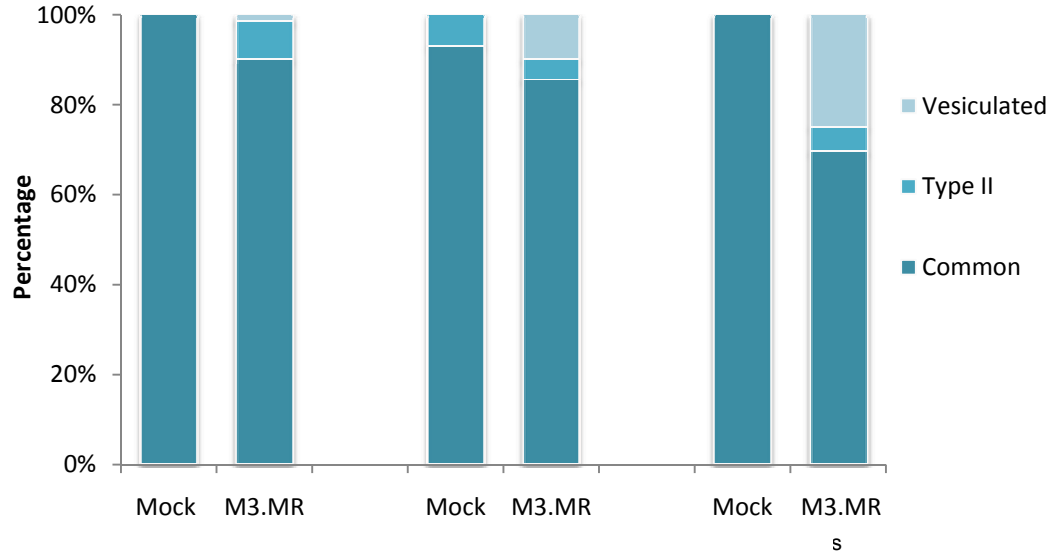

Figure 3-24 Different types of Clara cell present as determined by transmission electron microscopy at different levels of the respiratory tract of mock-infected and M3.MR infected wood mice at day 14 pi.
Data represent the mean results from one (mock-infected) or two (M3.MR infected) mice per group.

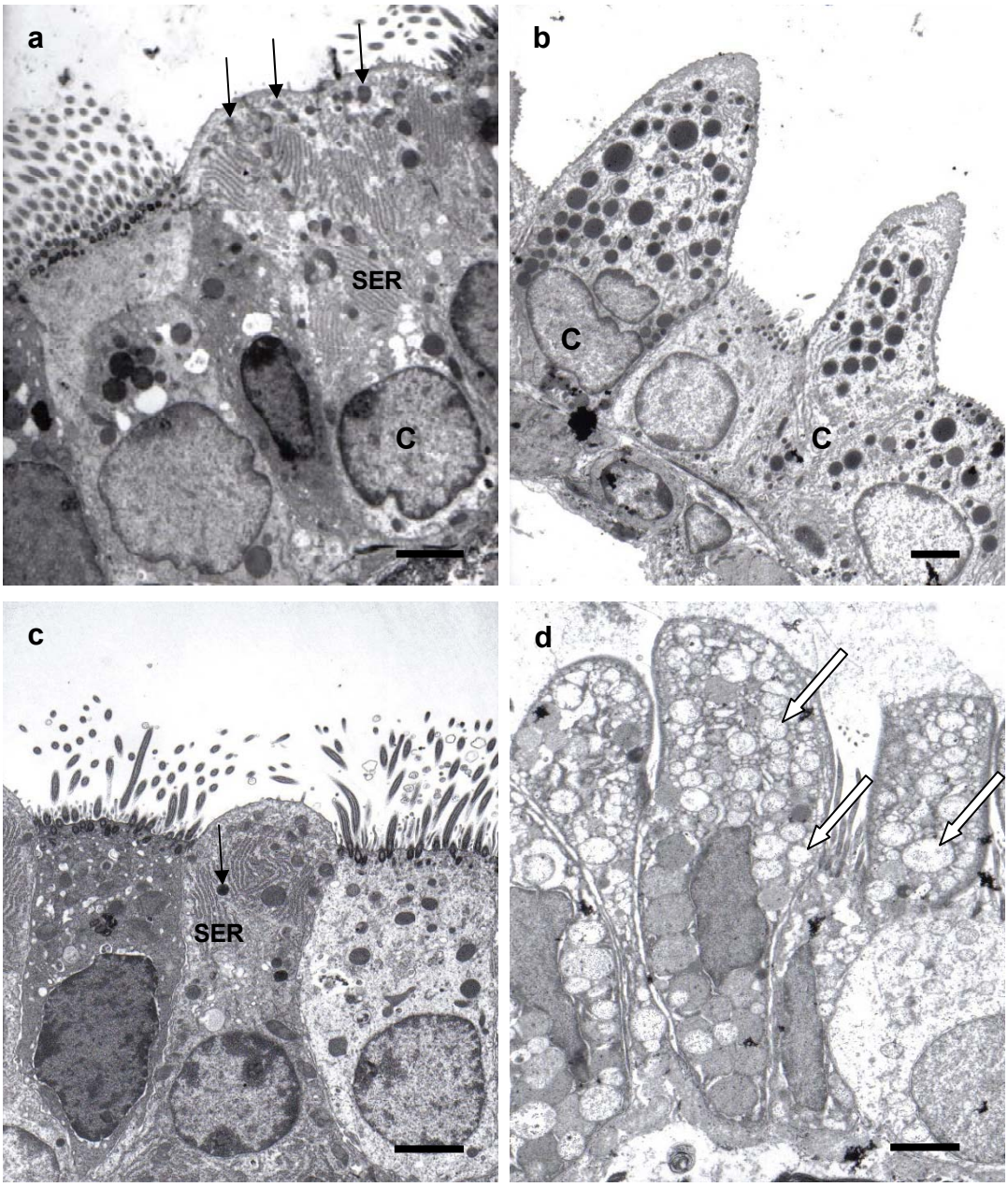

Figure 3-25 TEM of Clara cells in mock-infected and M3.MR infected wood mice.
(a) Common type of Clara cell in the trachea of a mock-infected wood mouse with abundant SER and electron dense vesicles (4000x). (b) Common type of Clara cell in the bronchiole of a mock-infected wood mouse exhibiting numerous electron dense vesicles and prominent apical projection into the lumen (3000x). (c) Type II Clara cell in the trachea of an M3.MR infected wood mouse, with more electron dense cytoplasm (4000x). (d) Vesiculated Clara cell in the bronchiole of an M3.MR infected wood mouse, with numerous intracytoplasmic vesicles, which contain electron lucent material (3500x). Bars = 2.5µm, C = Clara cell, SER = smooth endoplasmic reticulum, black arrows = electron dense vesicles, white arrows = vesicles containing matrix.

3.1.1.5 CCSP and SPLUNC1 sequences in *Apodemus sylvaticus*

3.1.1.5.1 CCSP sequence in *Apodemus syvaticus*

CCSP-specific primers were designed and used to amplify cDNA, generated from the lungs of wood mice and the PCR products were then cloned into plasmids and transformed in *E.coli*. Several clones were then sequenced, of which four resulted in identical sequences of 351 bp in length, which was submitted to GenBank (*Apodemus sylvaticus* clara cell secreted protein mRNA. Accession number HM008619. **2010)**. This sequence was then compared to other known sequences using BLAST, which revealed strong sequence homology, particularly in other *Rodentia* species (*Rattus norvegicus* 91 %, *Mus musculus* 92 %, *Mesocricetus auratus* 84 %, *Neomotodon alstoni* 79 %) but also in other species (*Oryctolagus cuniculus* 71 %, *Homo sapiens* 70 % [Figure 3-26]).

This sequence was translated using the ExPASy Translate tool (Gasteiger et al., 2003) and the various potential translations (different frame shifts) analysed (Figure 3-27). The first 15bp of the 5' region are untranslated, followed by a 292bp coding region and a 44bp 3' untranslated region. The predicted sequence has 96 amino acids (aa), the first 19 of which are consistent with signal peptide and the last 77 with mature secretory protein.

The predicted amino acid sequence was compared to that of other species using BLAST (Altschul et al., 1997) and exhibited strong homology with other rodents, including the rat (86 %), mouse (87 %), Hamster (79 %), Mexican volcano mouse (74 %), but different from other species, for example 54 % homology with human CCSP and 55 % with the rabbit (Figure 3-28).

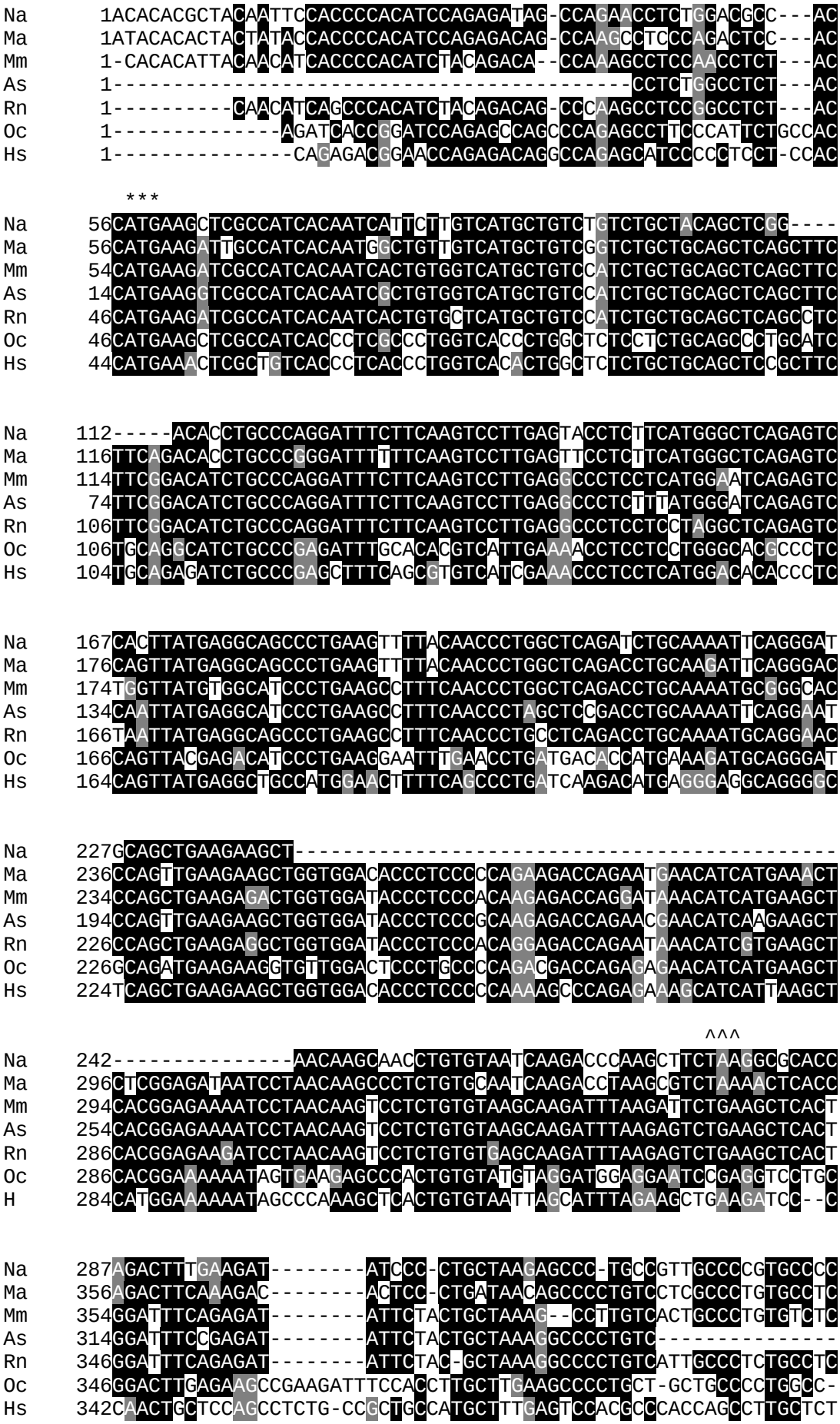
Na 1ACACACGCTACAATTCCACCCCACATCCAGAGATAG-CCAGAACCTCTGGACGCC---AC
Ma 1ATACACACTACTATACCACCCCACATCCAGAGACAG-CCAAGCCTCCCAGACTCC---AC
Mm 1-CACACATTACAACATCACCCCACATCTACAGACA--CCAAAGCCTCCAACCTCT---AC
As 1----------CCTCTGGCCTCT---AC
Rn 1----------CAACATCAGCCCACATCTACAGACAG-CCCAAGCCTCCGGCCTCT---AC
Oc 1--------------AGATCACCGGATCCAGAGCCAGCCCAGAGCCTTCCCATTCTGCCAC
Hs 1---------------CAGAGACGGAACCAGAGACAGGCCAGAGCATCCCCCTCCT-CCAC
***
Na 56CATGAAGCTCGCCATCACAATCATTCTTGTCATGCTGTCTGTCTGCTACAGCTCGG----
Ma 56CATGAAGATTGCCATCACAATGGCTGTTGTCATGCTGTCGGTCTGCTGCAGCTCAGCTTC
Mm 54CATGAAGATCGCCATCACAATCACTGTGGTCATGCTGTCCATCTGCTGCAGCTCAGCTTC
As 14CATGAAGGTCGCCATCACAATCGCTGTGGTCATGCTGTCCATCTGCTGCAGCTCAGCTTC
Rn 46CATGAAGATCGCCATCACAATCACTGTGCTCATGCTGTCCATCTGCTGCAGCTCAGCCTC
Oc 46CATGAAGCTCGCCATCACCCTCGCCCTGGTCACCCTGGCTCTCCTCTGCAGCCCTGCATC
Hs 44CATGAAACTCGCTGTCACCCTCACCCTGGTCACACTGGCTCTCTGCTGCAGCTCCGCTTC
Na 112-----ACACCTGCCCAGGATTTCTTCAAGTCCTTGAGTACCTCTTCATGGGCTCAGAGTC
Ma 116TTCAGACACCTGCCCGGGATTTTTTCAAGTCCTTGAGTTCCTCTTCATGGGCTCAGAGTC
Mm 114TTCGGACATCTGCCCAGGATTTCTTCAAGTCCTTGAGGCCCTCCTCATGGAATCAGAGTC
As 74TTCGGACATCTGCCCAGGATTTCTTCAAGTCCTTGAGGCCCTCTTTATGGGATCAGAGTC
Rn 106TTCGGACATCTGCCCAGGATTTCTTCAAGTCCTTGAGGCCCTCCTCCTAGGCTCAGAGTC
Oc 106TGCAGGCATCTGCCCGAGATTTGCACACGTCATTGAAAACCTCCTCCTGGGCACGCCCTC
Hs 104TGCAGAGATCTGCCCGAGCTTTCAGCGTGTCATCGAAACCCTCCTCATGGACACACCCTC
Na 167CACTTATGAGGCAGCCCTGAAGTTTTACAACCCTGGCTCAGATCTGCAAAATTCAGGGAT
Ma 176CAGTTATGAGGCAGCCCTGAAGTTTTACAACCCTGGCTCAGACCTGCAAGATTCAGGGAC
Mm 174TGGTTATGTGGCATCCCTGAAGCCTTTCAACCCTGGCTCAGACCTGCAAAATGCGGGCAC
As 134CAATTATGAGGCATCCCTGAAGCCTTTCAACCCTAGCTCCGACCTGCAAAATTCAGGAAT
Rn 166TAATTATGAGGCAGCCCTGAAGCCTTTCAACCCTGCCTCAGACCTGCAAAATGCAGGAAC
Oc 166CAGTTACGAGACATCCCTGAAGGAATTTGAACCTGATGACACCATGAAAGATGCAGGGAT
Hs 164CAGTTATGAGGCTGCCATGGAACTTTTCAGCCCTGATCAAGACATGAGGGAGGCAGGGGC
Na 227GCAGCTGAAGAAGCT----------
Ma 236CCAGTTGAAGAAGCTGGTGGACACCCTCCCCCAGAAGACCAGAATGAACATCATGAAACT
Mm 234CCAGCTGAAGAGACTGGTGGATACCCTCCCACAAGAGACCAGGATAAACATCATGAAGCT
As 194CCAGTTGAAGAAGCTGGTGGATACCCTCCCGCAAGAGACCAGAACGAACATCAAGAAGCT
Rn 226CCAGCTGAAGAGGCTGGTGGATACCCTCCCACAGGAGACCAGAATAAACATCGTGAAGCT
Oc 226GCAGATGAAGAAGGTGTTGGACTCCCTGCCCCAGACGACCAGAGAGAACATCATGAAGCT
Hs 224TCAGCTGAAGAAGCTGGTGGACACCCTCCCCCAAAAGCCCAGAGAAAGCATCATTAAGCT
^^^
Na 242---------------AACAAGCAACCTGTGTAATCAAGACCCAAGCTTCTAAGGCGCACC
Ma 296CTCGGAGATAATCCTAACAAGCCCTCTGTGCAATCAAGACCTAAGCGTCTAAAACTCACC
Mm 294CACGGAGAAAATCCTAACAAGTCCTCTGTGTAAGCAAGATTTAAGATTCTGAAGCTCACT
As 254CACGGAGAAAATCCTAACAAGTCCTCTGTGTAAGCAAGATTTAAGAGTCTGAAGCTCACT
Rn 286CACGGAGAAGATCCTAACAAGTCCTCTGTGTGAGCAAGATTTAAGAGTCTGAAGCTCACT
Oc 286CACGGAAAAAATAGTGAAGAGCCCACTGTGTATGTAGGATGGAGGAATCCGAGGTCCTGC
H 284CATGGAAAAAATAGCCCAAAGCTCACTGTGTAATTAGCATTTAGAAGCTGAAGATCC--C
Na 287AGACTTTGAAGAT--------ATCCC-CTGCTAAGAGCCC-TGCCGTTGCCCCGTGCCCC
Ma 356AGACTTCAAAGAC--------ACTCC-CTGATAACAGCCCCTGTCCTCGCCCTGTGCCTC
Mm 354GGATTTCAGAGAT--------ATTCTACTGCTAAAG--CCTTGTCACTGCCCTGTGTCTC
As 314GGATTTCCGAGAT--------ATTCTACTGCTAAAGGCCCCTGTC---------------
Rn 346GGATTTCAGAGAT--------ATTCTAC-GCTAAAGGCCCCTGTCATTGCCCTCTGCCTC
Oc 346GGACTTGAGAAGCCGAAGATTTCCACCTTGCTTGAAGCCCCTGCT-GCTGCCCCTGGCC-
Hs 342CAACTGCTCCAGCCTCTG-CCGCTGCCATGCTTTGAGTCCACGCCCACCAGCCTTGCTCT

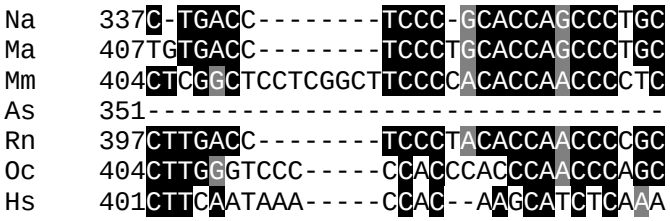

Figure 3-26 cDNA sequence alignment for *CCSP*, comparing the *Apodemus sylvaticus* sequence with those for *CCSP* of other species.
White characters on black background indicate consensus nucleotides; white characters on grey background indicate partial consensus nucleotides; black characters on white background indicate non-consensual nucleotides.
*** = start codon ^^^ = stop codon
Na = *Neotomodon alstoni* (Mexican volcano mouse; AJ583234.1)
Ma = *Mesocricetus auratus* (Golden hamster; L37041.1)
Mm = *Mus musculus* (Mouse; NM_011681.2)
As = *Apodemus sylvaticus* (Wood mouse; HM008619)
Rn = *Rattus norvegicus* (Brown Rat; BC069174.1)
Oc = *Oryctolagus cuniculus* (Rabbit; NM_001082237.1)
Hs = *Homo sapiens* (Human; NM_003357.3)

```
CCTCTGGCCTCTACCATGAAGGTCGCCATCACAATCGCTGTGGTCATGCTGTCCATCTGCTGCAGCTCA
              MetK  V  A  I  T  I  A  V  V  MetL  S  I  C  C  S  S
GCTTCTTCGGACATCTGCCCAGGATTTCTTCAAGTCCTTGAGGCCCTCTTTATGGGATCAGAGTCCAAT
A  S  S  D  I  C  P  G  F  L  Q  V  L  E  A  L  F  MetG  S  E  S  N
TATGAGGCATCCCTGAAGCCTTTCAACCCTAGCTCCGACCTGCAAAATTCAGGAATCCAGTTGAAGAAG
Y  E  A  S  L  K  P  F  N  P  S  S  D  L  Q  N  S  G  I  Q  L  K  K
CTGGTGGATACCCTCCCGCAAGAGACCAGAACGAACATCAAGAAGCTCACGGAGAAAATCCTAACAAGT
L  V  D  T  L  P  Q  E  T  R  T  N  I  K  K  L  T  E  K  I  L  T  S
CCTCTGTGTAAGCAAGATTTAAGAGTCTGAAGCTCACTGGATTTCCGAGATATTCTACTGCTAAAGGCC
P  L  C  K  Q  D  L  R  V  Stop
CCTGTC
```

Figure 3-27 Predicted amino acid sequence from cDNA for CCSP in the wood mouse.

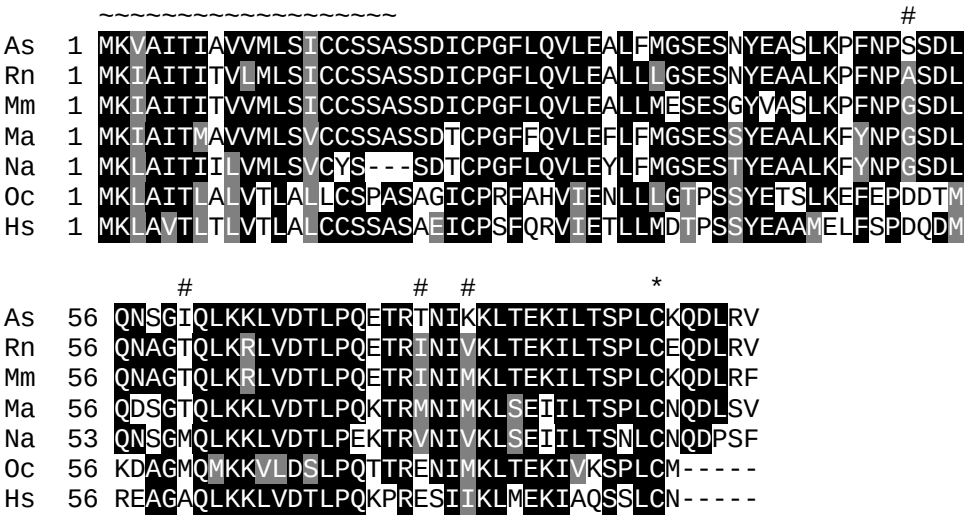

Figure 3-28 Amino acid sequence for CCSP from the wood mouse, aligned with those from other species, using ClustalW-XXL and Boxshade.
White characters on black background indicate consensus amino acids; white characters on grey background indicate partial consensus amino acids; black characters on white background indicate non-consensual amino acids.
~~~ = signal peptide; * = conserved cysteine for stabilisation of homodimers
# = amino acids in the wood mouse that are not conserved in any other species.
As= *Apodemus sylvaticus* (Wood mouse)
Rn = *Rattus norvegicus* (Brown Rat; sp|P17559|UTER_RAT)
Mm = *Mus musculus* (Mouse; sp|Q06318|UTER_MOUSE)
Ma = *Mesocricetus auratus* (Golden hamster; sp|Q8VD96|UTER_MESAU)
Na = *Neotomodon alstoni* (Mexican volcano mouse; sp|Q65C83|UTER_NEOAS)
Oc = *Oryctolagus cuniculus* (Rabbit; sp|P02779|UTER_RABIT)
Hs = *Homo sapiens* (Human; sp|P11684|UTER_HUMAN)
~~~

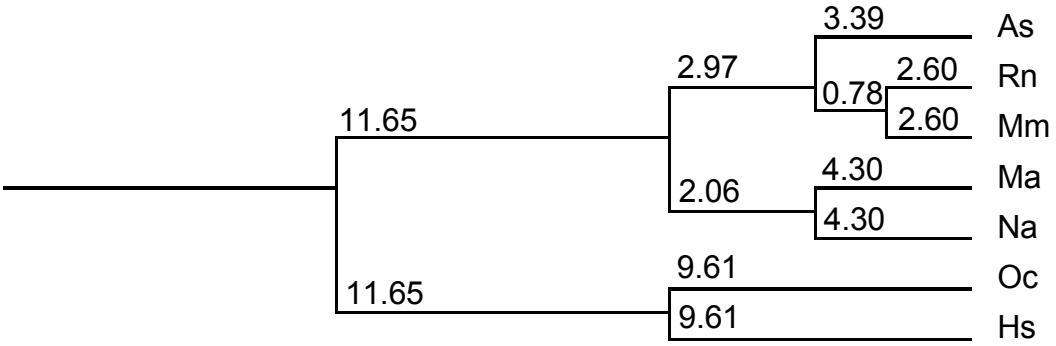

Figure 3-29 Phylogram for CCSP based on amino acid comparisons.
The tree was constructed using the ClustalW program by pair-group clustering method. The numerical values indicate mutation distances.
As= *Apodemus sylvaticus* (Wood mouse)
Rn = *Rattus norvegicus* (Brown Rat)
Mm = *Mus musculus* (Mouse)
Ma = *Mesocricetus auratus* (Golden hamster)
Na = *Neotomodon alstoni* (Mexican volcano mouse)
Oc = *Oryctolagus cuniculus* (Rabbit)
Hs = *Homo sapiens* (Human)

3.1.1.5.2 SPLUNC1 sequence in *Apodemus sylvaticus*

SPLUNC1 specific primers were used to amplify cDNA generated from the lung of wood mice. Following cloning, sequencing and translation of this product it was found that, in comparison to the amino acid sequence for *Mus musculus*, 10 amino acids were absent at the 5' end. Therefore 5'RACE was utilised to obtain this end of the sequence. This enabled the sequencing of a 1011 bp cDNA sequence for SPLUNC1 in *Apodemus sylvaticus*, which was submitted to GenBank (*Apodemus sylvaticus* short palate, lung and nasal epithelium associated (SPLUNC1) mRNA: HM008620. **2010**).

Alignment of this sequence using BLAST revealed high levels of homology with other rodent species; *Mus musculus* (93 %) and *Rattus norvegicus* (88 %). The rodents' sequences for SPLUNC1 contain an additional exon, when compared to other species (Figure 3-30), however, either side of this, high homology was also seen between *Apodemus sylvaticus* and *Homo sapiens* (72 and 78 %), *Bos taurus* (78 and 74 %) and *Sus scrofa* (73 and 79 %).

The cDNA sequence obtained for SPLUNC1 from *Apodemus sylvaticus* was translated using ExPASy Translate tool and the potential translations analysed to select the correct frameshift (Figure 3-31). The sequence contains a 53 bp untranslated 5' region and a 55bp 3' untranslated region, with an open reading frame comprising 834 bp (278 codons). This is highly similar to that described for *Mus musculus* (Weston et al., 1999).

The predicted amino acid sequence was compared to that of other species using BLAST (SIB) and exhibited strong homology with the mouse (92 %) and the rat (87 %), and lower homology with other species, for example the pig (61 %), the cow (63 %) and human (66 %). The wood mouse sequence exhibited the additional sequence in exon 2 found in other rodent species, but not present in non-rodent species (Figure 3-32; aa 23-46). The wood mouse shows high homology with *Mus musculus* in this region (83 %).

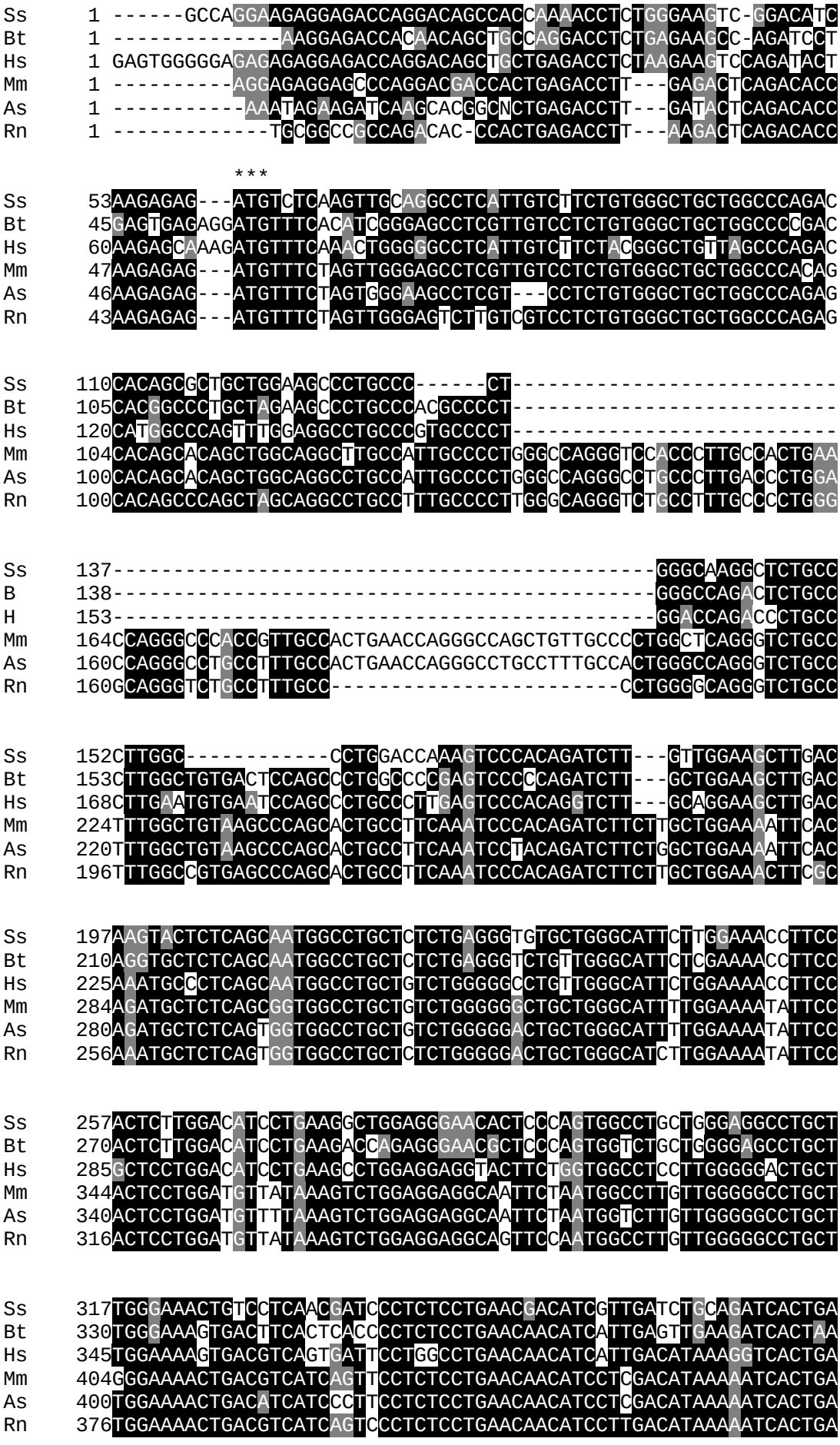
Ss 1 ------GCCAGGAAGAGGAGACCAGGACAGCCACCAAAACCTCTGGGAAGTC-GGACATC
Bt 1 --------------AAGGAGACCACAACAGCTGCCAGGACCTCTGAGAAGCC-AGATCCT
Hs 1 GAGTGGGGGAGAGAGAGGAGACCAGGACAGCTGCTGAGACCTCTAAGAAGTCCAGATACT
Mm 1 ----------AGGAGAGGAGCCCAGGACGACCACTGAGACCTT---GAGACTCAGACACC
As 1 ----------AAATAGAAGATCAAGCACGGCNCTGAGACCTT---GATACTCAGACACC
Rn 1 ------------TGCGGCCGCCAGACAC-CCACTGAGACCTT---AAGACTCAGACACC
***
Ss 53AAGAGAG---ATGTCTCAAGTTGCAGGCCTCATTGTCTTCTGTGGGCTGCTGGCCCAGAC
Bt 45GAGTGAGAGGATGTTTCACATCGGGAGCCTCGTTGTCCTCTGTGGGCTGCTGGCCCCGAC
Hs 60AAGAGCAAAGATGTTTCAAACTGGGGGCCTCATTGTCTTCTACGGGCTGTTAGCCCAGAC
Mm 47AAGAGAG---ATGTTTCTAGTTGGGAGCCTCGTTGTCCTCTGTGGGCTGCTGGCCCACAG
As 46AAGAGAG---ATGTTTCTAGTGGGAAGCCTCGT---CCTCTGTGGGCTGCTGGCCCAGAG
Rn 43AAGAGAG---ATGTTTCTAGTTGGGAGTCTTGTCGTCCTCTGTGGGCTGCTGGCCCAGAG
Ss 110CACAGCGCTGCTGGAAGCCCTGCCC------CT--------------------------
Bt 105CACGGCCCTGCTAGAAGCCCTGCCCACGCCCCT--------------------------
Hs 120CATGGCCCAGTTTGGAGGCCTGCCCGTGCCCCT--------------------------
Mm 104CACAGCACAGCTGGCAGGCTTGCCATTGCCCCTGGGCCAGGGTCCACCCTTGCCACTGAA
As 100CACAGCACAGCTGGCAGGCCTGCCATTGCCCCTGGGCCAGGGCCTGCCCTTGACCCTGGA
Rn 100CACAGCCCAGCTAGCAGGCCTGCCTTTGCCCCTTGGGCAGGGTCTGCCTTTGCCCCTGGG
Ss 137---GGGCAAGGCTCTGCC
B 138---GGGCCAGACTCTGCC
H 153---GGACCAGACCCTGCC
Mm 164CCAGGGCCCACCGTTGCCACTGAACCAGGGCCAGCTGTTGCCCCTGGCTCAGGGTCTGCC
As 160CCAGGGCCTGCCTTTGCCACTGAACCAGGGCCTGCCTTTGCCACTGGGCCAGGGTCTGCC
Rn 160GCAGGGTCTGCCTTTGCC-----------------------CCTGGGGCAGGGTCTGCC
Ss 152CTTGGC------------CCTGGACCAAAGTCCCACAGATCTT---GTTGGAAGCTTGAC
Bt 153CTTGGCTGTGACTCCAGCCCTGGCCCCGAGTCCCCCAGATCTT---GCTGGAAGCTTGAC
Hs 168CTTGAATGTGAATCCAGCCCTGCCCTTGAGTCCCACAGGTCTT---GCAGGAAGCTTGAC
Mm 224TTTGGCTGTAAGCCCAGCACTGCCTTCAAATCCCACAGATCTTCTTGCTGGAAAATTCAC
As 220TTTGGCTGTAAGCCCAGCACTGCCTTCAAATCCTACAGATCTTCTGGCTGGAAAATTCAC
Rn 196TTTGGCCGTGAGCCCAGCACTGCCTTCAAATCCCACAGATCTTCTTGCTGGAAACTTCGC
Ss 197AAGTACTCTCAGCAATGGCCTGCTCTCTGAGGGTGTGCTGGGCATTCTTGGAAACCTTCC
Bt 210AGGTGCTCTCAGCAATGGCCTGCTCTCTGAGGGTCTGTTGGGCATTCTCGAAAACCTTCC
Hs 225AAATGCCCTCAGCAATGGCCTGCTGTCTGGGGGCCTGTTGGGCATTCTGGAAAACCTTCC
Mm 284AGATGCTCTCAGCGGTGGCCTGCTGTCTGGGGGGCTGCTGGGCATTTTGGAAAATATTCC
As 280AGATGCTCTCAGTGGTGGCCTGCTGTCTGGGGGACTGCTGGGCATTTTGGAAAATATTCC
Rn 256AAATGCTCTCAGTGGTGGCCTGCTCTCTGGGGGACTGCTGGGCATCTTGGAAAATATTCC
Ss 257ACTCTTGGACATCCTGAAGGCTGGAGGGAACACTCCCAGTGGCCTGCTGGGAGGCCTGCT
Bt 270ACTCTTGGACATCCTGAAGACCAGAGGGAACGCTCCCAGTGGTCTGCTGGGGAGCCTGCT
Hs 285GCTCCTGGACATCCTGAAGCCTGGAGGAGGTACTTCTGGTGGCCTCCTTGGGGGACTGCT
Mm 344ACTCCTGGATGTTATAAAGTCTGGAGGAGGCAATTCTAATGGCCTTGTTGGGGGCCTGCT
As 340ACTCCTGGATGTTTTAAAGTCTGGAGGAGGCAATTCTAATGGTCTTGTTGGGGGCCTGCT
Rn 316ACTCCTGGATGTTATAAAGTCTGGAGGAGGCAGTTCCAATGGCCTTGTTGGGGGCCTGCT
Ss 317TGGGAAACTGTCCTCAACGATCCCTCTCCTGAACGACATCGTTGATCTGCAGATCACTGA
Bt 330TGGGAAAGTGACTTCACTCACCCCTCTCCTGAACAACATCATTGAGTTGAAGATCACTAA
Hs 345TGGAAAAGTGACGTCAGTGATTCCTGGCCTGAACAACATCATTGACATAAAGGTCACTGA
Mm 404GGGAAAACTGACGTCATCAGTTCCTCTCCTGAACAACATCCTCGACATAAAAATCACTGA
As 400TGGAAAACTGACATCATCCCTTCCTCTCCTGAACAACATCCTCGACATAAAAATCACTGA
Rn 376TGGAAAACTGACGTCATCAGTCCCTCTCCTGAACAACATCCTTGACATAAAAATCACTGA

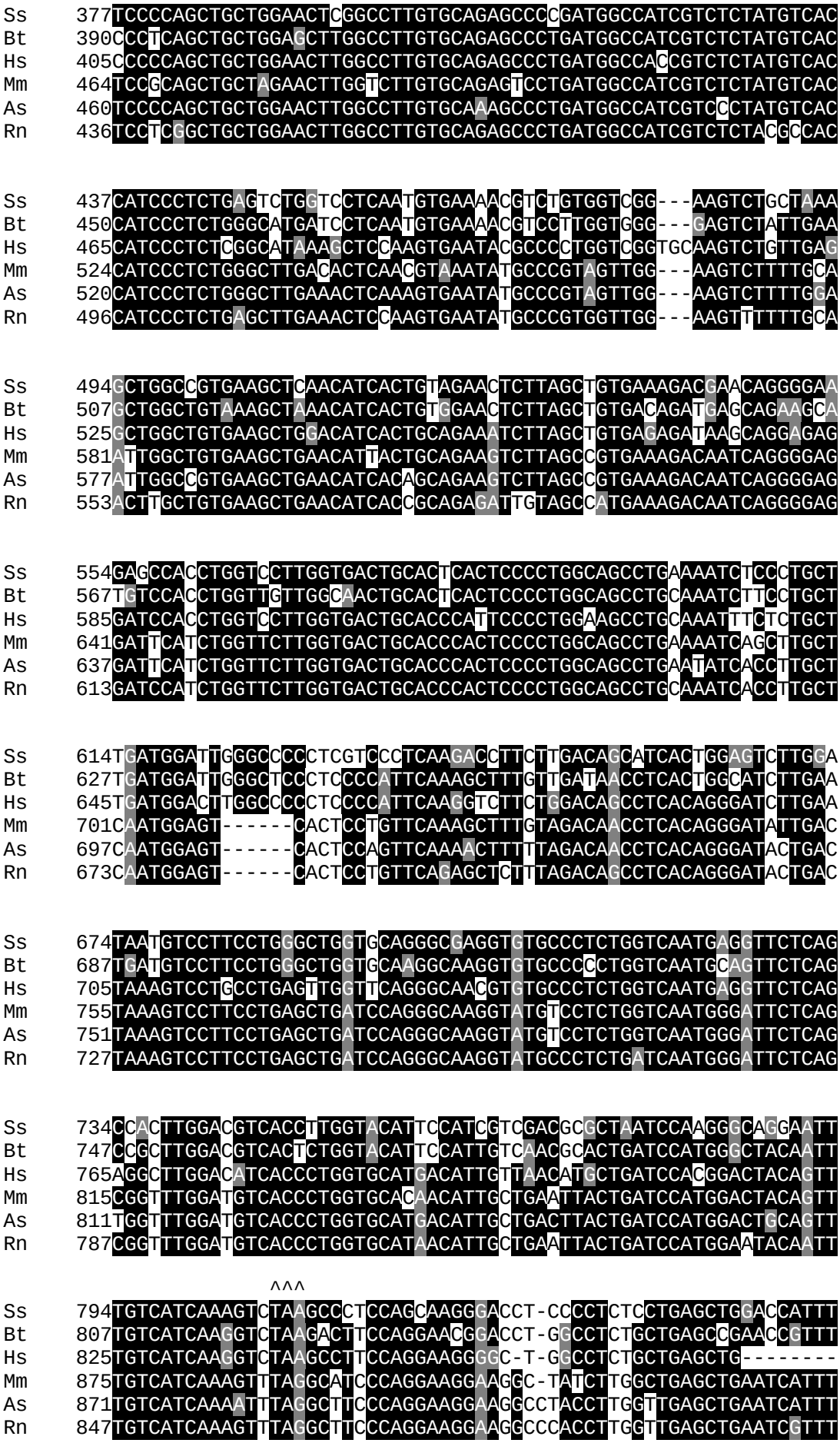
Ss 377TCCCCAGCTGCTGGAACTCGGCCTTGTGCAGAGCCCCGATGGCCATCGTCTCTATGTCAC
Bt 390CCCTCAGCTGCTGGAGCTTGGCCTTGTGCAGAGCCCTGATGGCCATCGTCTCTATGTCAC
Hs 405CCCCAGCTGCTGGAACTTGGCCTTGTGCAGAGCCCTGATGGCCACCGTCTCTATGTCAC
Mm 464TCCGCAGCTGCTAGAACTTGGTCTTGTGCAGAGTCCTGATGGCCATCGTCTCTATGTCAC
As 460TCCCCAGCTGCTGGAACTTGGCCTTGTGCAAAGCCCTGATGGCCATCGTCCCTATGTCAC
Rn 436TCCTCGGCTGCTGGAACTTGGCCTTGTGCAGAGCCCTGATGGCCATCGTCTCTACGCCAC
Ss 437CATCCCTCTGAGTCTGGTCCTCAATGTGAAAACGTCTGTGGTCGG---AAGTCTGCTAAA
Bt 450CATCCCTCTGGGCATGATCCTCAATGTGAAAACGTCCTTGGTGGG---GAGTCTATTGAA
Hs 465CATCCCTCTCGGCATAAAGCTCCAAGTGAATACGCCCCTGGTCGGTGCAAGTCTGTTGAG
Mm 524CATCCCTCTGGGCTTGACACTCAACGTAAATATGCCCGTAGTTGG---AAGTCTTTTGCA
As 520CATCCCTCTGGGCTTGAAACTCAAAGTGAATATGCCCGTAGTTGG---AAGTCTTTTGGA
Rn 496CATCCCTCTGAGCTTGAAACTCCAAGTGAATATGCCCGTGGTTGG---AAGTTTTTTGCA
Ss 494GCTGGCCGTGAAGCTCAACATCACTGTAGAACTCTTAGCTGTGAAAGACGAACAGGGGAA
Bt 507GCTGGCTGTAAAGCTAAACATCACTGTGGAACTCTTAGCTGTGACAGATGAGCAGAAGCA
Hs 525GCTGGCTGTGAAGCTGGACATCACTGCAGAAATCTTAGCTGTGAGAGATAAGCAGGAGAG
Mm 581ATTGGCTGTGAAGCTGAACATTACTGCAGAAGTCTTAGCCGTGAAAGACAATCAGGGGAG
As 577ATTGGCCGTGAAGCTGAACATCACAGCAGAAGTCTTAGCCGTGAAAGACAATCAGGGGAG
Rn 553ACTTGCTGTGAAGCTGAACATCACCGCAGAGATTGTAGCCATGAAAGACAATCAGGGGAG
Ss 554GAGCCACCTGGTCCTTGGTGACTGCACTCACTCCCCTGGCAGCCTGAAAATCTCCCTGCT
Bt 567TGTCCACCTGGTTGTTGGCAACTGCACTCACTCCCCTGGCAGCCTGCAAATCTTCCTGCT
Hs 585GATCCACCTGGTCCTTGGTGACTGCACCCATTCCCCTGGAAGCCTGCAAATTTCTCTGCT
Mm 641GATTCATCTGGTTCTTGGTGACTGCACCCACTCCCCTGGCAGCCTGAAAATCAGCTTGCT
As 637GATTCATCTGGTTCTTGGTGACTGCACCCACTCCCCTGGCAGCCTGAATATCACCTTGCT
Rn 613GATCCATCTGGTTCTTGGTGACTGCACCCACTCCCCTGGCAGCCTGCAAATCACCTTGCT
Ss 614TGATGGATTGGGCCCCCTCGTCCCTCAAGACCTTCTTGACAGCATCACTGGAGTCTTGGA
Bt 627TGATGGATTGGGCTCCCTCCCCATTCAAAGCTTTGTTGATAACCTCACTGGCATCTTGAA
Hs 645TGATGGACTTGGCCCCCTCCCCATTCAAGGTCTTCTGGACAGCCTCACAGGGATCTTGAA
Mm 701CAATGGAGT------CACTCCTGTTCAAAGCTTTGTAGACAACCTCACAGGGATATTGAC
As 697CAATGGAGT------CACTCCAGTTCAAAACTTTTTAGACAACCTCACAGGGATACTGAC
Rn 673CAATGGAGT------CACTCCTGTTCAGAGCTCTTTAGACAGCCTCACAGGGATACTGAC
Ss 674TAATGTCCTTCCTGGGCTGGTGCAGGGCGAGGTGTGCCCTCTGGTCAATGAGGTTCTCAG
Bt 687TGATGTCCTTCCTGGGCTGGTGCAAGGCAAGGTGTGCCCCCTGGTCAATGCAGTTCTCAG
Hs 705TAAAGTCCTGCCTGAGTTGGTTCAGGGCAACGTGTGCCCTCTGGTCAATGAGGTTCTCAG
Mm 755TAAAGTCCTTCCTGAGCTGATCCAGGGCAAGGTATGTCCTCTGGTCAATGGGATTCTCAG
As 751TAAAGTCCTTCCTGAGCTGATCCAGGGCAAGGTATGTCCTCTGGTCAATGGGATTCTCAG
Rn 727TAAAGTCCTTCCTGAGCTGATCCAGGGCAAGGTATGCCCTCTGATCAATGGGATTCTCAG
Ss 734CCACTTGGACGTCACCTTGGTACATTCCATCGTCGACGCGCTAATCCAAGGGCAGGAATT
Bt 747CCGCTTGGACGTCACTCTGGTACATTCCATTGTCAACGCACTGATCCATGGGCTACAATT
Hs 765AGGCTTGGACATCACCCTGGTGCATGACATTGTTAACATGCTGATCCACGGACTACAGTT
Mm 815CGGTTTGGATGTCACCCTGGTGCACAACATTGCTGAATTACTGATCCATGGACTACAGTT
As 811TGGTTTGGATGTCACCCTGGTGCATGACATTGCTGACTTACTGATCCATGGACTGCAGTT
Rn 787CGGTTTGGATGTCACCCTGGTGCATAACATTGCTGAATTACTGATCCATGGAATACAATT
^^^
Ss 794TGTCATCAAAGTCTAAGCCCTCCAGCAAGGGACCT-CCCCTCTCCTGAGCTGGACCATTT
Bt 807TGTCATCAAGGTCTAAGACTTCCAGGAACGGACCT-GGCCTCTGCTGAGCCGAACCGTTT
Hs 825TGTCATCAAGGTCTAAGCCTTCCAGGAAGGGGC-T-GGCCTCTGCTGAGCTG--------
Mm 875TGTCATCAAAGTTTAGGCATCCCAGGAAGGAAGGC-TATCTTGGCTGAGCTGAATCATTT
As 871TGTCATCAAAATTTAGGCTTCCCAGGAAGGAAGGCCTACCTTGGTTGAGCTGAATCATTT
Rn 847TGTCATCAAAGTTTAGGCTTCCCAGGAAGGAAGGCCCACCTTGGTTGAGCTGAATCGTTT

```
Ss    853CCTGCTGCCC---CATCCACTCCCTGCCCAGCACCCGAGGGCTCACAGAAGGCCAGCCCA
Bt    866CCTGAGGCTG---GATTCACTGCCTGCCC-------GAGGGCTCACAGAAGGCTGGCCCA
Hs    875-----------------------CTTCCC--------AGTGCTCACAGATGGCTGGCCCA
Mm    934CTTGCTGCTCAGTCTCCTGCCTCTTGCCCAGTCTCCCATGGCTCACAGAAAGG-GGCCCA
As    931CTTGCTGCTCAGTCTCCCGCCTCTTGCCCAGTCTCCCATGGCTCACAGAAAGG-GGCCCA
Rn    907CTCGATGCTC--TCTCCTGCCTCTTGCCCAGTTTCCCATGGCTCACAGAAAGG-GACCCA

Ss    910TGTCCCGGACAAGGACAC---CAGGTCTGGAGACCAGAGCAGCCCGCCCTCCAAGGAA-C
Bt    916TGTCCTGGACAATGACACAGCCATGTTTGGAGACCAGAGCAGCCTTCTCACCAAGGAAAC
Hs    904TGTGCTGGAAGATGACAC-------------------AGTTGCCTTCTCTCCGAGGAACC
Mm    993CATCCTGGAAAA-T-TAT-------------------GTCTTCCTTCTCCTCACGGAGCC
As    990CATCCTGGAAAAAT-TAT-------------------GTCT-------------------
Rn    964CGTCCTGGAAAATCATAT-------------------GCCTGCCTTCTCCTCACAGAGTC

Ss    966CGCTCCCCCTGCTTCCCCACCAGGCATGTGTGACATTCCCTGTTACTTGCGCAATAAAAT
Bt    976TTCTCCCTTTGCTTTCCCACCAAGCATGTGT--CATTCCTCGTTCATCACCAAATAAAAC
Hs    945TGCCCCCTCTCCTTTCCCACCAGGCGTGTGTAACATCCCATGTGCCTCACCTAATAAAAT
Mm   1032TGATCTCTTCCCATCAGGCACGATTA--------ATCCTGTGATCCTCACTAAATAAAA
As   1011-----------------------------------------------------------
Rn   1005TGCTCTCTTTTCCCATCAGACA-----------------TGATTAATCCTAAATAAAA

Ss   1026CGCCCTTTCTCGGCAAAAAAAAAAAAAAAAAAAAAAAAAAA-------------------
Bt   1034TGCCCTTTCTCTGCAAAAAAAAAAAAAAAAAAAAAAAAAAAAAAAAAAAAAAAAAACAAAAA
Hs   1005GGCTCTTCTTCTGCATCAAAAAAAAAAAAA-----------------------------
Mm   1084TAGCCCTTCATCTGCAAAAAAAAAAAAAA------------------------------
As   ---------------------------------------------------------------
Rn   1047TAGTTCTTCATCTGCAAAAAAAAAAAAAAAAAA---------------------------

Ss   1067-----------
Bt   1094AAAAAAAAAAA
Hs   1035-----------
Mm   1112-----------
As   ---------------
Rn   1079-----------
```

Figure 3-30 cDNA sequence alignment for SPLUNC1, comparing the *Apodemus sylvaticus* sequence with those published for SPLUNC1 in other species.
White characters on black background indicate consensus nucleotides; white characters on grey background indicate partial consensus nucleotides; black characters on white background indicate non-consensual nucleotides.
*** = start codon, ^^^ = stop codon
Ss = *Sus scrofa* (pig; AK238256.1)
Bs = *Bos taurus* (cow; BC114803.1)
Hs = *Homo sapiens* (Human; NM_016583.3)
As = *Apodemus sylvaticus* (wood mouse; HM008620)
Mm = *Mus musculus* (mouse; NM_011126.3)
Rn = *Rattus norvegicus* (brown rat; NM_172031.1)

```
 AAATAGAAGATCAAGCACGGCNCTGAGACCTTGATACTCAGACACCAAGAGAGATGTTTCTAGTGGGA
                                                        MetF  L  V  G
AGCCTCGTCCTCTGTGGGCTGCTGGCCCAGAGCACAGCACAGCTGGCAGGCCTGCCATTGCCCCTGGGC
S  L  V  L  C  G  L  L  A  Q  S  T  A  Q  L  A  G  L  P  L  P  L  G
CAGGGCCTGCCCTTGACCCTGGACCAGGGCCTGCCTTTGCCACTGAACCAGGGCCTGCCTTTGCCACTG
Q  G  L  P  L  T  L  D  Q  G  L  P  L  P  L  N  Q  G  L  P  L  P  L
GGCCAGGGTCTGCCTTTGGCTGTAAGCCCAGCACTGCCTTCAAATCCTACAGATCTTCTGGCTGGAAAA
G  Q  G  L  P  L  A  V  S  P  A  L  P  S  N  P  T  D  L  L  A  G  K
TTCACAGATGCTCTCAGTGGTGGCCTGCTGTCTGGGGGACTGCTGGGCATTTTGGAAAATATTCCACTC
F  T  D  A  L  S  G  G  L  L  S  G  G  L  L  G  I  L  E  N  I  P  L
CTGGATGTTTTAAAGTCTGGAGGAGGCAATTCTAATGGTCTTGTTGGGGGCCTGCTTGGAAAACTGACA
L  D  V  L  K  S  G  G  G  N  S  N  G  L  V  G  G  L  L  G  K  L  T
TCATCCCTTCCTCTCCTGAACAACATCCTCGACATAAAAATCACTGATCCCCAGCTGCTGGAACTTGGC
S  S  L  P  L  L  N  N  I  L  D  I  K  I  T  D  P  Q  L  L  E  L  G
CTTGTGCAAAGCCCTGATGGCCATCGTCCCTATGTCACCATCCCTCTGGGCTTGAAACTCAAAGTGAAT
L  V  Q  S  P  D  G  H  R  P  Y  V  T  I  P  L  G  L  K  L  K  V  N
ATGCCCGTAGTTGGAAGTCTTTTGGAATTGGCCGTGAAGCTGAACATCACAGCAGAAGTCTTAGCCGTG
MetP  V  V  G  S  L  L  E  L  A  V  K  L  N  I  T  A  E  V  L  A  V
AAAGACAATCAGGGGAGGATTCATCTGGTTCTTGGTGACTGCACCCACTCCCCTGGCAGCCTGAATATC
K  D  N  Q  G  R  I  H  L  V  L  G  D  C  T  H  S  P  G  S  L  N  I
ACCTTGCTCAATGGAGTCACTCCAGTTCAAAACTTTTTAGACAACCTCACAGGGATACTGACTAAAGTC
T  L  L  N  G  V  T  P  V  Q  N  F  L  D  N  L  T  G  I  L  T  K  V
CTTCCTGAGCTGATCCAGGGCAAGGTATGTCCTCTGGTCAATGGGATTCTCAGTGGTTTGGATGTCACC
L  P  E  L  I  Q  G  K  V  C  P  L  V  N  G  I  L  S  G  L  D  V  T
CTGGTGCATGACATTGCTGACTTACTGATCCATGGACTGCAGTTTGTCATCAAAATTTAGGCTTCCCAG
L  V  H  D  I  A  D  L  L  I  H  G  L  Q  F  V  I  K  I  Stop
GAAGGAAGGCCTACCTTGGTTGAGCTGAATCATTTCTTGCTGCTCAGTCTCCCGCCTCTTGCCCAGTCT

CCCATGGCTCACAGAAAGGGGCCCACATCCTGGAAAAATTATGTCT
```

Figure 3-31 Predicted amino acid sequence from cDNA for SPLUNC1 in the wood mouse.
Generated using the cloned cDNA sequence and translated using ExPASy (Gasteiger et al., 2003).

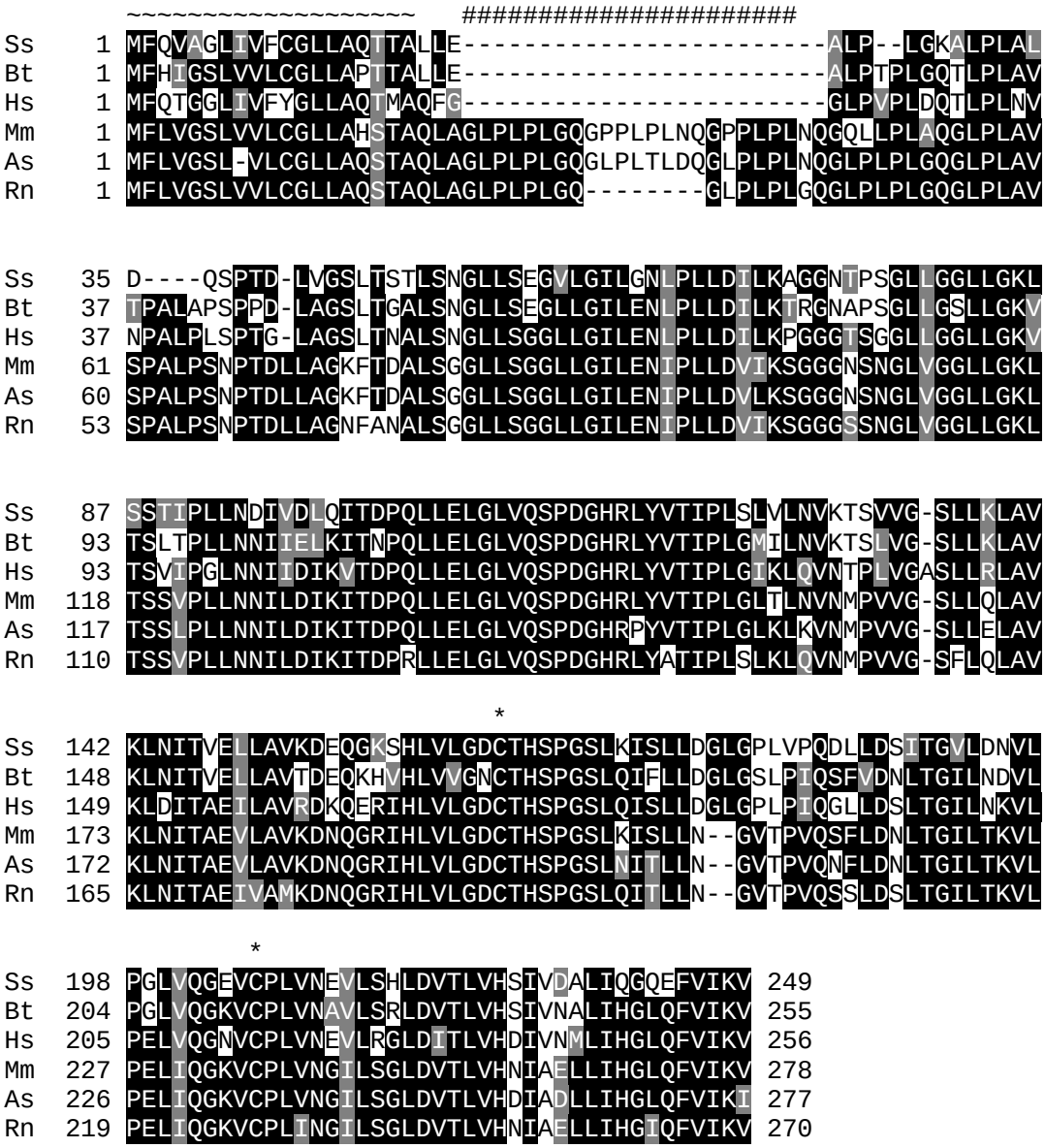

Figure 3-32 Predicted amino acid sequence of SPLUNC1from *Apodemus sylvaticus* compared to published sequences of other species.
White characters on black background indicate consensus amino acids; white characters on grey background indicate partial consensus amino acids; black characters on white background indicate non-consensual amino acids.
~~~ = signal peptide; * = conserved cysteines required for binding between BPI N-terminal domain and LPS; ### = ($G^{L}/_{P}/_{Q}{}^{P}/_{L}$LPL) repeat present in the enlarged exon 2 of rodent species.
Ss = *Sus scrofa* (pig; sp|Q5XW65.1|PLUNC_PIG)
Bs = *Bos taurus* (cow; sp|Q8SPU5.1|PLUNC_BOVIN)
Hs = *Homo sapiens* (human; sp|Q9NP55.1|PLUNC_HUMAN)
As = *Apodemus sylvaticus (*wood mouse; HM008620)
Mm = *Mus musculus* (mouse; sp|P97361.3|PLUNC_MOUSE)
Rn = *Rattus norvegicus* (brown rat; sp|Q8K4I4.1|PLUNC_RAT)
~~~

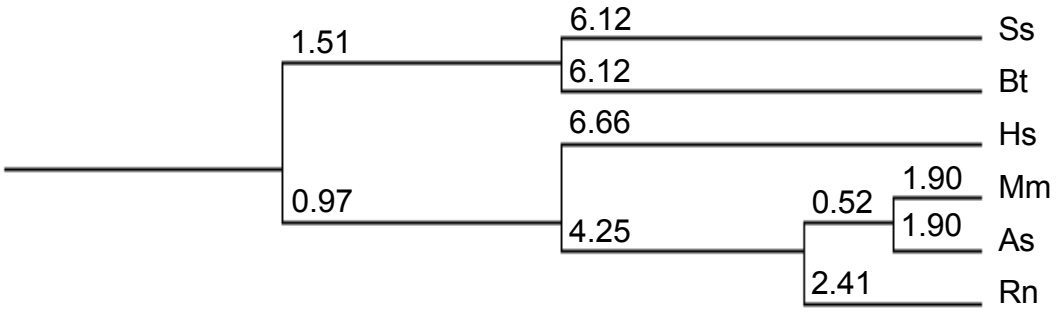

Figure 3-33 Phylogram for SPLUNC1 based on amino acid comparisons.
The tree was constructed using the ClustalW program by pair-group clustering method. The numerical values indicate mutation distances.
Ss = *Sus scrofa* (pig; sp|Q5XW65.1|PLUNC_PIG)
Bs = *Bos taurus* (cow; sp|Q8SPU5.1|PLUNC_BOVIN)
Hs = *Homo sapiens* (human; sp|Q9NP55.1|PLUNC_HUMAN)
As = *Apodemus sylvaticus (*wood mouse; HM008620)
Mm = *Mus musculus* (mouse; sp|P97361.3|PLUNC_MOUSE)
Rn = *Rattus norvegicus* (brown rat; sp|Q8K4I4.1|PLUNC_RAT)

3.1.2 MHV-68 infection in 129 wild type and IFNγR$^{-/-}$ mice

3.1.2.1 The inflammatory response in MHV-68 infected 129 wild type and IFNγR$^{-/-}$ mice

129 wild type (wt) and 129 interferon gamma receptor knock out (IFNγR$^{-/-}$) mice were infected with a wild type strain of MHV-68 intranasally, euthanased at 8 and 12 dpi and the lungs examined by light microscopy including immunohistology, using formalin fixed, paraffin embedded tissue specimens kindly provided by Dr. Bernadette Dutia, University of Edinburgh.

At day 8 pi, the wild type mouse lungs exhibited mild multifocal aggregates of macrophages, lymphocytes and neutrophils (both viable and degenerate), admixed with necrotic debris. These inflammatory foci were occasionally perivascular or peribronchiolar, but more frequently were randomly situated within the alveolar spaces and septa (Figure 3-34). Occasional lymphocyte-dominated accumulations were observed close to large bronchioles in one mouse. The endothelium within blood vessels was activated and showed adherent leukocytes, indicating migration of leukocytes from the blood into the surrounding lung tissue.

The IFNγR$^{-/-}$ mice exhibited a more severe inflammatory response at day 8 pi; a variably intense (mild to marked), multifocal to coalescing, predominantly peribronchiolar and perivascular infiltrate (neutrophils, lesser lymphocytes, macrophages) was seen which effaced the alveolar architecture at the centre of foci, and filled the alveolar spaces at the periphery. Mixed with the inflammatory cells were erythrocytes, necrotic cellular debris and fibrin (Figure 3-35). In addition, there was a mild diffuse, mixed infiltrate (lymphocytes, neutrophils, plasma cells, macrophages) surrounding the bronchi, which extended into the pleura and the surrounding adipose tissue.

By day 12 pi, wild type mice exhibited more numerous multifocal inflammatory infiltrates (lymphocytes, plasma cells, lesser neutrophils and macrophages), which were mild to moderate and predominantly perivascular or peribronchiolar (Figure 3-36). These inflammatory foci also occasionally

contained necrotic cells. Mild lymphoplasmacytic accumulations adjacent to bronchi were also seen.

At day 12 pi, IFNγR$^{-/-}$ mice exhibited multifocal marked (and focally extensive) accumulations of macrophages, admixed with neutrophils, lesser lymphocytes and cellular debris (Figure 3-37a,b). Additionally there were moderate, multifocal to coalescing (perivascular and peribronchiolar, with “bridges” in between), lymphoplasmacellular infiltrates with lesser neutrophils and macrophages (Figure 3-37c,d). Without these foci, alveoli exhibit mild to moderate hyperaemia and a mild increase in the number of alveolar macrophages.

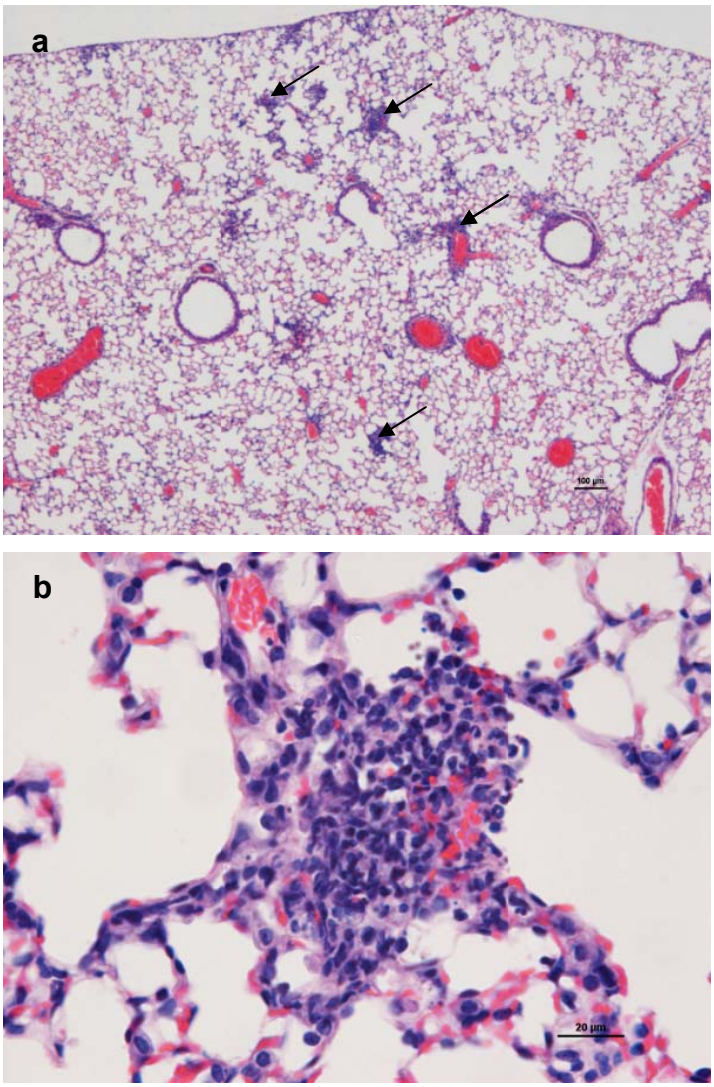

Figure 3-34 Histology of the lungs from 129 wild type mice infected with MHV-68 at day 8 pi.
(a) Mild multifocal infiltrates randomly positioned throughout the lung (arrows; 4x, HE). (b) Focus of inflammatory cells (macrophages, lymphocytes, neutrophils) within the alveolar wall and spaces (40x, HE).

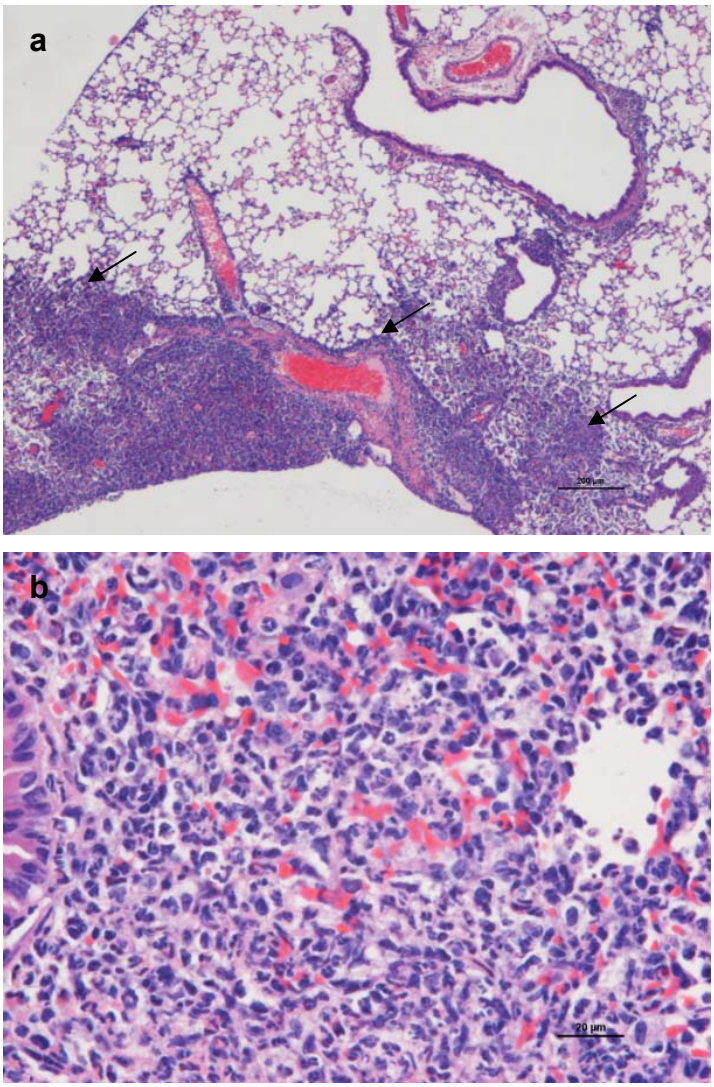

Figure 3-35 Histology of the lungs from MHV-68 infected 129 IFNγR$^{-/-}$ mice at day 8 pi.
(a) Multifocal to coalescing variably intense perivascular and peribronchiolar infiltrates (arrows; 4x, HE). (b) Inflammatory infiltrates efface the alveoli at the centre of inflammatory foci (40x, HE).

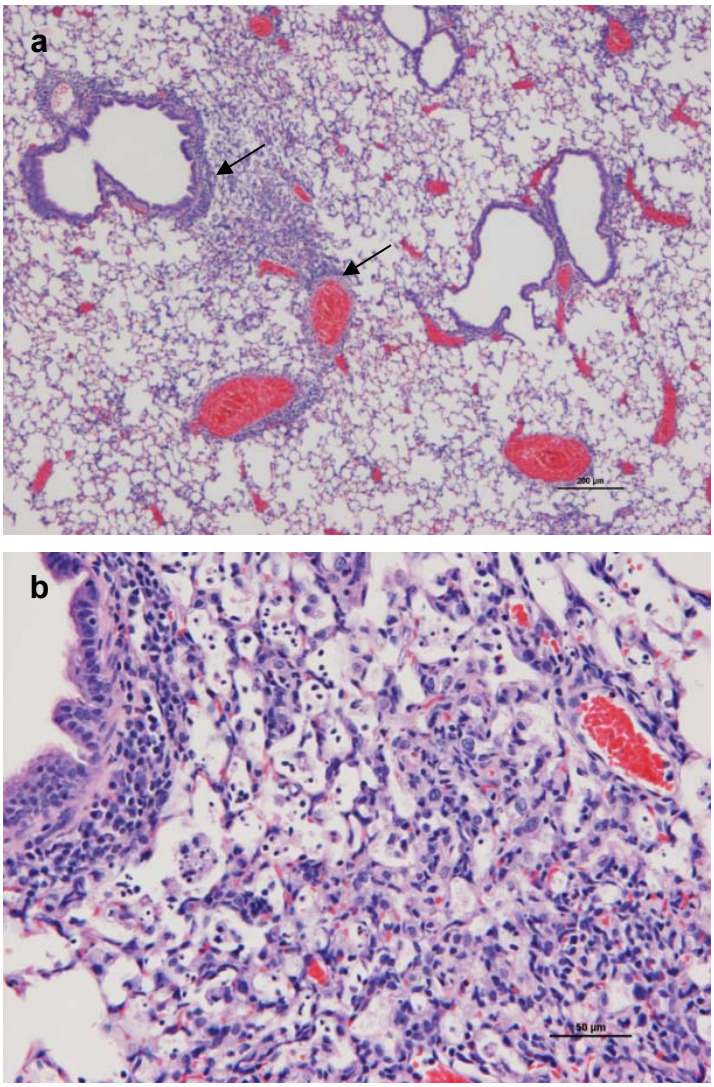

Figure 3-36 Histology of the lung from MHV-68 infected 129 wild type mice at day 12 pi.
(a) Wild type mouse lung showing mild to moderate multifocal infiltrates, which are predominantly perivascular and peribronchiolar (arrows; 4x, HE). (b) Mixed inflammatory infiltrate adjacent to a bronchiole and within alveolar spaces (20x, HE).

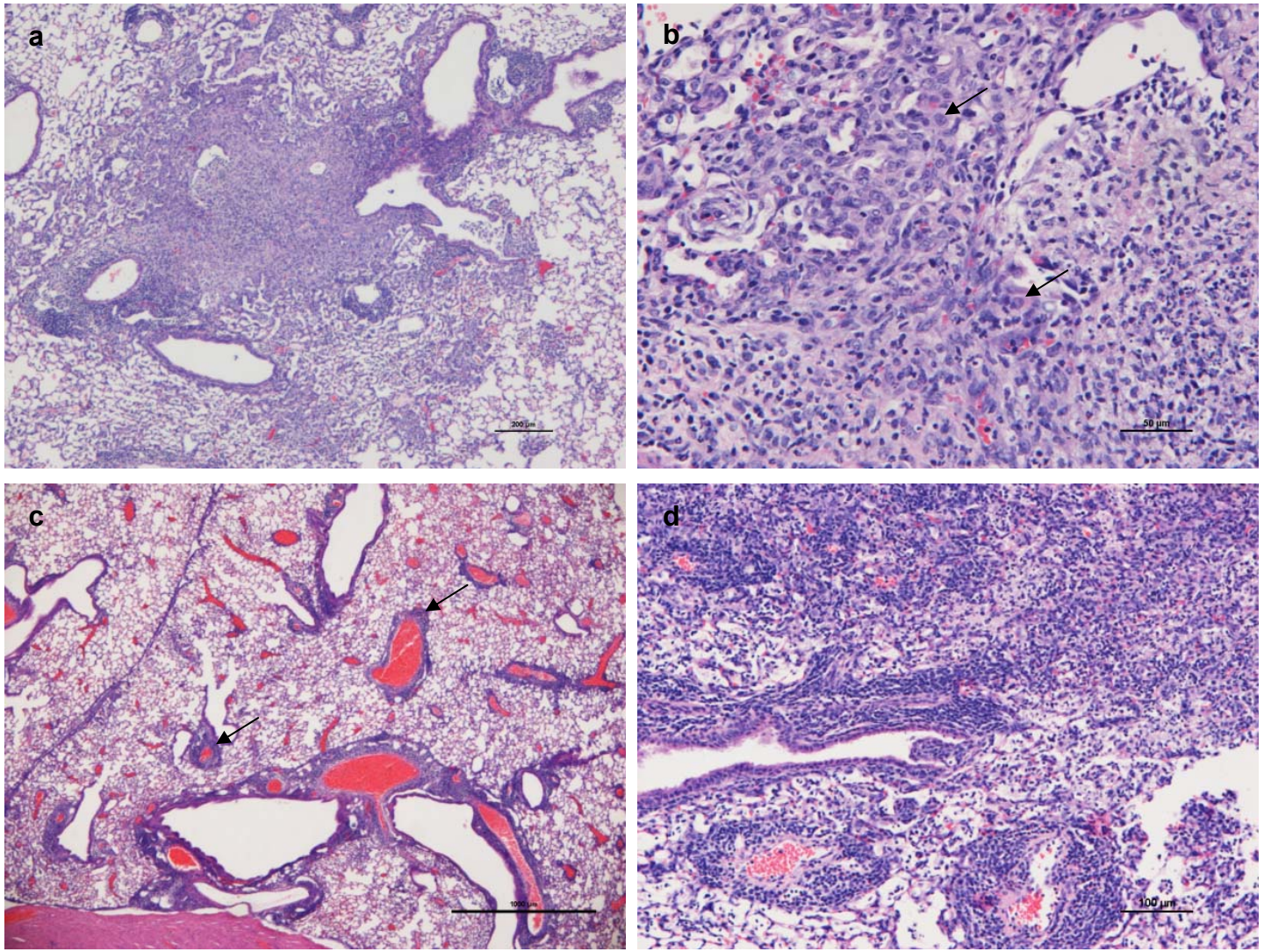

Figure 3-37 Histology of the lung from MHV-68 infected 129 IFNγR$^{-/-}$ mice at day 12 pi.

(a) Focally extensive macrophage dominated infiltrates (4x, HE). (b) Macrophage (arrows) dominated infiltrates, with admixed neutrophils and lymphocytes (20x, HE). (c) Moderate, multifocal to coalescing lymphoplasmacellular perivascular and peribronchiolar infiltrates (arrows; 2x, HE). (d) Lymphoplasmacellular perivascular and peribronchiolar infiltrates (20x, HE).

3.1.2.2 Immunohistology in 129 wild type and IFNγR$^{-/-}$ mice

3.1.2.2.1 CCSP expression in 129 wild type and IFNγR$^{-/-}$ mice

Immunohistological staining for CCSP antigen was performed and slides examined visually and quantitatively analysed as before (see 3.1.1.3.1.2). Overall, the pattern of distribution of CCSP in uninfected wild type and IFNγR$^{-/-}$ mice was similar to that seen in the wood mice; the intensity of staining and number of cells stained both increased distally in the respiratory tract. Even within the trachea the frequency of positive cells was greater in the distal trachea than the proximal trachea. The staining in wild type mice was generally more intense (Figure 3-38a,b), compared to that seen in IFNγR$^{-/-}$ mice (Figure 3-38c,d). In the IFNγR$^{-/-}$ mice, CCSP positive cells tended to project further in to the lumen than those of wild type mice; this was most notable in the trachea, where the difference in height between the non-ciliated Clara cell and ciliated respiratory epithelium is usually minimal (Figure 3-38c).

Quantitative comparison of wild type and IFNγR$^{-/-}$ mice at different timepoints in the various anatomical locations revealed that in the trachea, IFNγR$^{-/-}$ mice exhibited a significantly lower percentage area of tissue stained, at both day 0 pi (uninfected; P = 0.025, two sample T-test) and day 12 pi (P = 0.001, two sample T-test); no data is available for day 8 pi (Figure 3-39b). The IFNγR$^{-/-}$ mice also exhibited reduced intensity of staining in the trachea at days 0 and 12 pi, although these data were not significantly different (P = 0.052 and 0.272 respectively, two sample T-test [Figure 3-39a]). In the bronchi, both parameters showed considerable overlap at all timepoints and there was no significant difference between wild type and IFNγR$^{-/-}$ mice.

In the bronchioles, the percentage area of tissue stained was very similar between wild type and IFNγR$^{-/-}$ mice at all timepoints, however, there was a small but significant decrease in the intensity of staining for CCSP at all timepoints (day 0, P = 0.001; day 8, P = 0.003; day 12, P = 0.023; two sample T-test [Figure 3-39a]).

In addition to the differences between wild type and IFNγR$^{-/-}$ mice at the various timepoints and levels of the respiratory epithelium, the results over the

time-course of infection were also examined. The trachea exhibited a decrease in CCSP in response to infection, as shown by the significant decrease in percentage area of tissue stained in both wild type (P = 0.0019, ANOVA) and IFNγR$^{-/-}$ mice (P = 0.0004, ANOVA), between day 0 and day 12 pi (Figure 3-40b); in addition there were decreases in the intensity of staining for CCSP (Figure 3-40a), which were significant in the wild type mice (P = 0.0379, ANOVA), but not the IFNγR$^{-/-}$ mice (P = 0.1827, ANOVA). The data for the bronchi showed a large variation (as shown by the large standard error of the mean [SEM]) and overlap between groups, so that the differences between timepoints were not significant.

In the bronchioles there were decreases in intensity of staining for CCSP both between days 0 and 8 pi and days 8 and 12 dpi; these decreases were significant in the wild type mice between day 0 and day 12 (P = 0.0001, ANOVA) and day 8 and day 12 (P = 0.0002, ANOVA) and also in the IFNγR$^{-/-}$ mice between day 0 and day 8 (P = 0.0303, ANOVA) and day 0 and day 12 (P = 0.0001, ANOVA; Figure 3-40a). The percentage area of tissue stained showed a slightly different pattern; there were significant decreases between day 0 and day 8 in both the wild type mice (P=0.0001, ANOVA) and the IFNγR$^{-/-}$ mice (P = 0.0001, ANOVA), however, between days 8 and 12, there was an increase in percentage area stained, again in both wild type mice (P = 0.0001, ANOVA) and IFNγR$^{-/-}$ mice (P = 0.0029, ANOVA). This increase between days 8 and 12 pi, however, remained significantly less than the percentage area stained at day 0 for both wild type mice (P = 0.0001, ANOVA) and IFNγR$^{-/-}$ mice (P = 0.0001, ANOVA; Figure 3-40b).

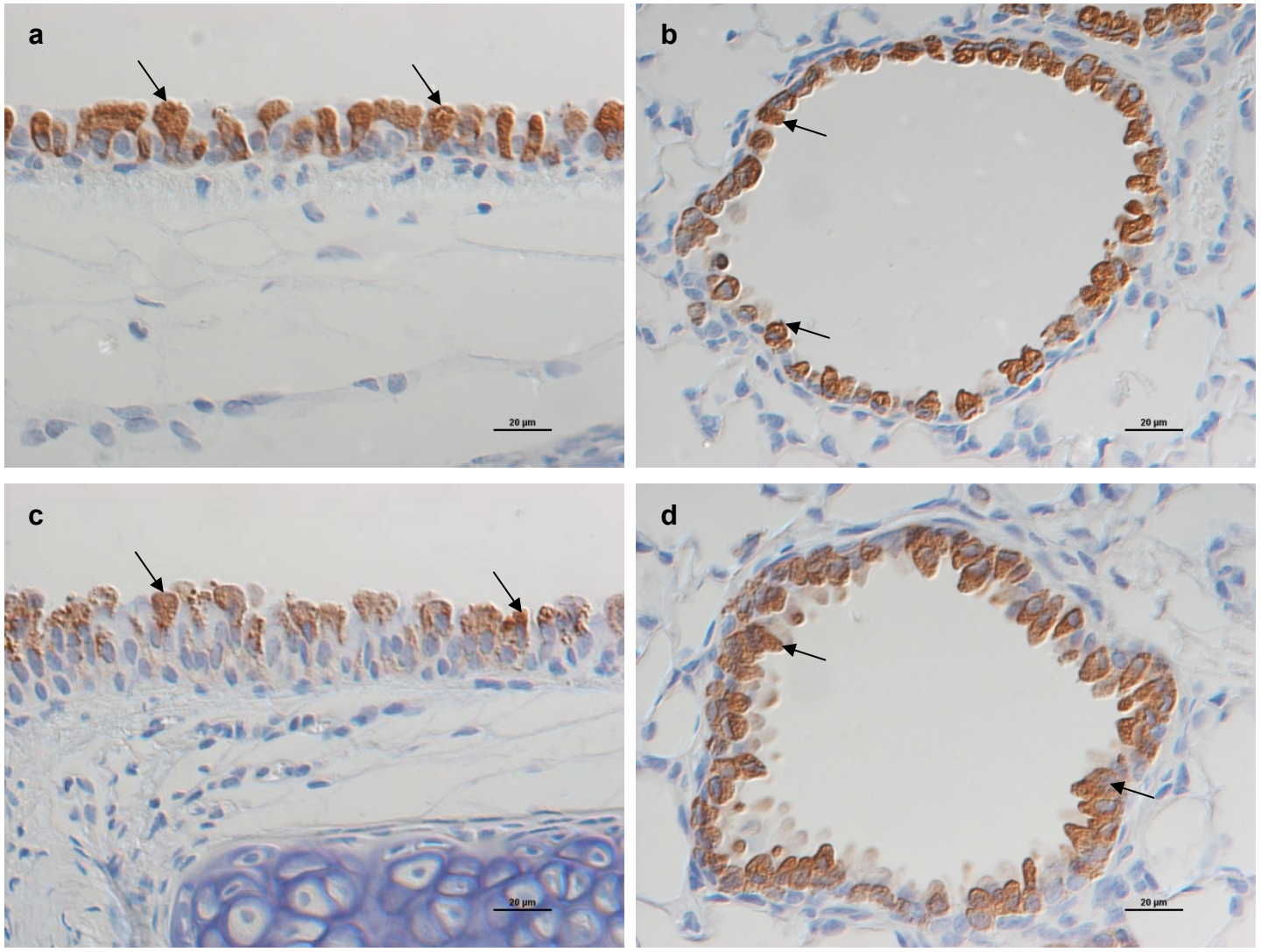

Figure 3-38 Immuno-histology for CCSP in the respiratory tract of uninfected (day 0) 129 wild type and IFNγR$^{-/-}$ mice.

(a) Trachea in an uninfected (day 0) wild type mouse exhibits numerous CCSP cells within the respiratory epithelium (arrows; 40x). (b) Bronchiole of an uninfected (day 0) wild type mouse with several cells strongly stained for CCSP (arrows; 40x). (c) Trachea of an uninfected (day 0) IFNγR$^{-/-}$ mouse with numerous positive cells, which are less strongly stained than those in the wild type mice (arrows; 40x). (d) Bronchiole of an uninfected (day 0) IFNγR$^{-/-}$ mouse exhibiting cells which are less strongly stained than in wild type mice, and project further into the lumen of the bronchiole (arrows; 40x).

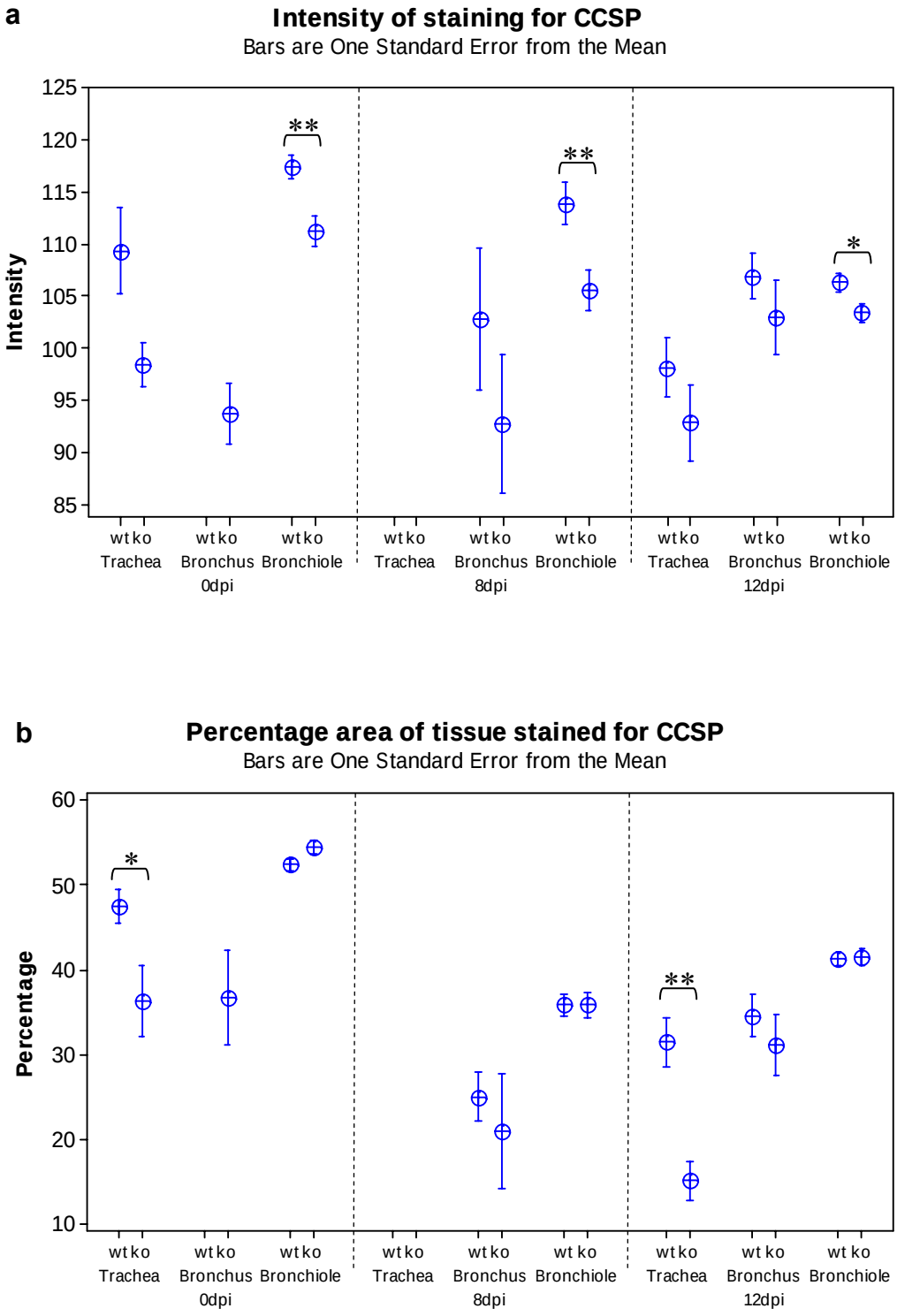

Figure 3-39 Quantitative analysis of immunohistological staining for CCSP at different levels of the respiratory tract in 129 wild type (wt) and IFNγR$^{-/-}$ (ko) mice before and after infection with MHV-68.
(a) Intensity of staining for CCSP in respiratory epithelium (b) Percentage area of respiratory epithelium stained for CCSP. Data are the mean of analysis of tissue from two or three mice per group, bars represent the standard error of the mean. ∗ P< 0.05; ∗∗ P< 0.005 (two sample T-test).

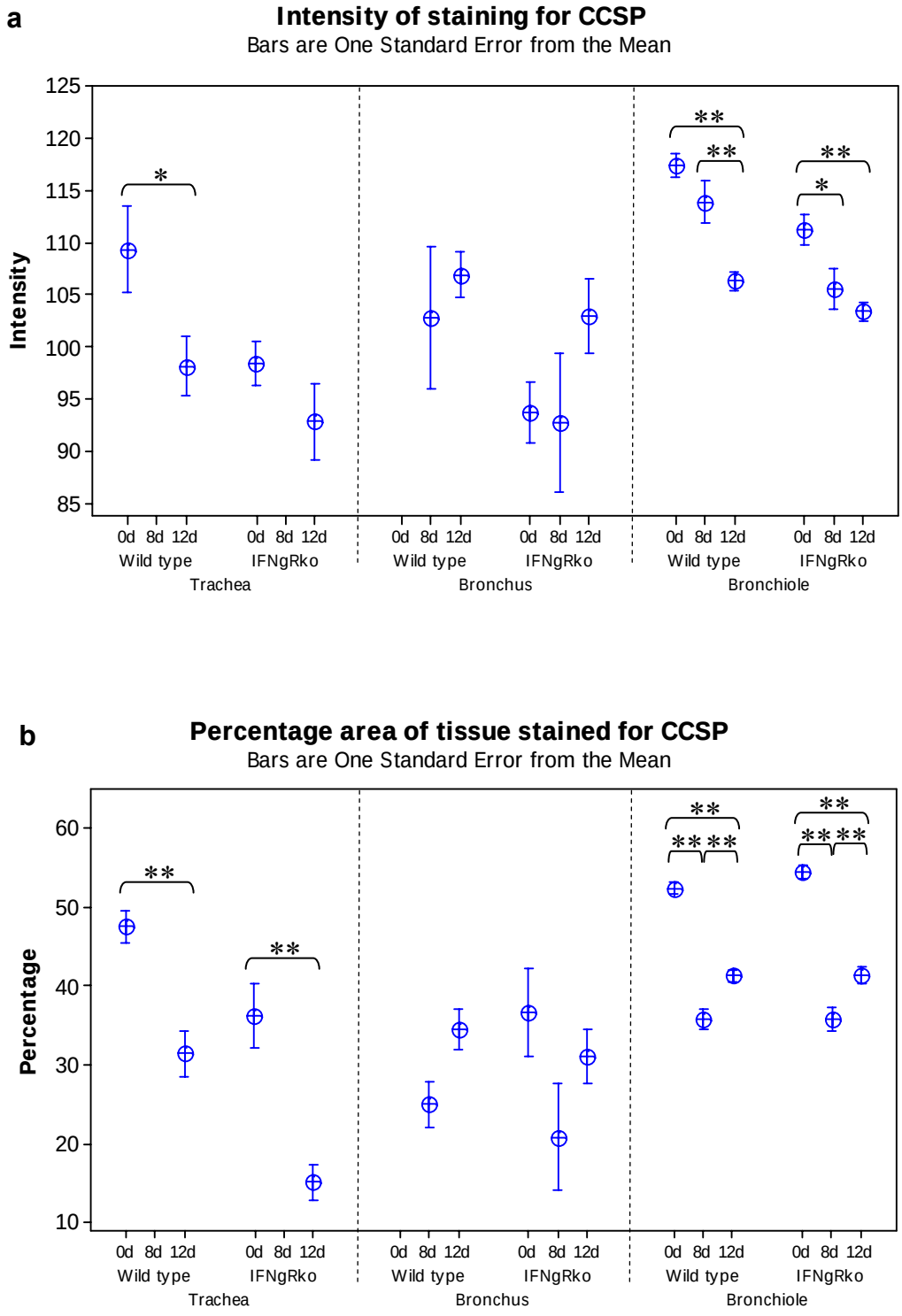

Figure 3-40 Quantitative analysis of immunohistological staining for CCSP at different levels of the respiratory tract in 129 wild type and IFNγR$^{-/-}$ (IFNγRko) mice, before and after infection with MHV-68.
(a) Intensity of staining for CCSP in respiratory epithelium (b) Percentage area of respiratory epithelium stained for CCSP. Data are the mean of analysis of tissue from two or three mice per group, bars represent the standard error of the mean. ∗ P< 0.05; ∗∗ P< 0.005 (ANOVA).

3.1.2.2.2 SPLUNC1 expression in 129 wild type and IFNγR$^{-/-}$ mice

Immunohistology for SPLUNC1 antigen was performed on sections of formalin fixed paraffin embedded lung tissue and viewed visually and quantitatively analysed as previously. In the uninfected (day 0) wild type mice, numerous cells within the trachea were positive, but exhibited varying intensity of staining. Those cells which exhibited moderate to intense staining were non-ciliated. In addition, some ciliated cells exhibited faint staining (Figure 3-41a). No submucosal glands or bronchi were present on the sections examined. Bronchioles were overwhelmingly negative with very rare positive cells within the more proximal bronchioles (Figure 3-41b).

In the trachea of IFNγR$^{-/-}$ mice, the proportion of cells positive for SPLUNC1 was similar to that seen in the wild type mice; the pattern of staining was similar however, in that non-ciliated cells were moderately to strongly positive and the ciliated cells faintly positive (Figure 3-41c). Submucosal glands present were variably stained; some (predominantly acinar serous-type glands) exhibited strong cytoplasmic and luminal staining, whereas others (mucous-type tubular glands) were predominantly negative (Figure 3-41d). Bronchi were not present on the sections examined. As in the wild type mice, bronchiolar epithelial cells were negative, with rare positive cells within proximal bronchioles.

Quantitative comparison of wild type and IFNγR$^{-/-}$ mice immunohistology showed that there were essentially no differences between wild type and IFNγR$^{-/-}$ mice in the intensity of staining at day 0 in either the trachea ($P = 0.993$, two sample T-test) or the bronchioles ($P = 0.415$, two sample T-test); data are not available for the bronchi. The percentage area of tissue stained was very similar in both groups of mice, in the trachea ($P = 0.246$, two sample T-test) and the bronchioles ($P = 0.773$, two sample T-test [Figure 3-42a,b]). Following infection, bronchi exhibited a significantly lower intensity ($P = 0.019$, two sample T-test) and percentage area of tissue stained ($P = 0.027$, two sample T-test) in IFNγR$^{-/-}$ mice than wild type mice at 8dpi. However, this relationship was reversed at 12 dpi, when the percentage area was significantly higher ($P = 0.009$, two sample T-test) in IFNγR$^{-/-}$ mice compared

to wild type mice; the intensity of staining was also increased in IFNγR$^{-/-}$ mice, but this difference was not significant (P = 0.053, two sample T-test [Figure 3-42a,b]).

In the trachea at day 12 pi (no data are available for day 8) IFNγR$^{-/-}$ mice exhibited a highly significant increase in intensity of staining, compared to wild type mice (P = 0.001, two sample T-test [Figure 3-42a]), but no difference in the percentage area stained (P = 0.607, two sample T-test [Figure 3-42b]). The bronchioles showed very little difference between the wild type and the IFNγR$^{-/-}$ mice, with the exception of the intensity of staining at day 12 pi, in which the IFNγR$^{-/-}$ mice exhibited a small, but significantly higher intensity (P = 0.011, two sample T-test [Figure 3-42a]).

The quantitative analysis of immunohistological staining for SPLUNC1 was also examined to assess the effect of infection at each location in the wild type and IFNγR$^{-/-}$ mice. In the trachea of wild type mice, there was a decrease in both the intensity (P = 0.0607, ANOVA) and percentage area stained (P = 0.2739, ANOVA) following infection (at day 12 pi), but neither of the alterations were significant (Figure 3-43a,b). In the bronchi, IFNγR$^{-/-}$ mice exhibited an increase in both intensity of staining (P = 0.0068, ANOVA) and percentage area of tissue stained (P = 0.0009, ANOVA) between days 8 and 12 pi. In contrast, the wild type mice exhibited no significant difference between these two timepoints (Figure 3-43a,b).

In the bronchioles, there were small, but significant increases in both the intensity of staining and the percentage area stained in response to infection in both wild type and IFNγR$^{-/-}$ mice; moreover, these increases were maintained from day 8 to day 12 pi (Figure 3-43a,b). In the wild type mice, between day 0 and day 8, the intensity of staining increased (P=0.0001, ANOVA); followed by a small, not significant decrease at day 12 (P = 0.0742, ANOVA). The intensity at day 12, however, remained significantly higher than that at day 0 (P = 0.0075, ANOVA). A very similar pattern was observed in the percentage area of tissue stained, with a highly significant increase between days 0 and 8 pi (P = 0.0033, ANOVA), followed by a similar percentage at day 12, which

remained significantly higher than that seen at day 0 (P = 0.0116, ANOVA). This pattern of alteration in response to infection is preserved in the IFNγR$^{-/-}$ mice (Figure 3-43a,b), which exhibited a significant increase in both intensity (P = 0.0001, ANOVA) and percentage area (P = 0.0102, ANOVA) between days 0 and 8 pi, which were maintained between days 8 and 12pi, so that the increased intensity and percentage area stained remained significantly higher in day 12, compared to day 0 (P = 0.0001 and 0.0002, respectively; ANOVA).

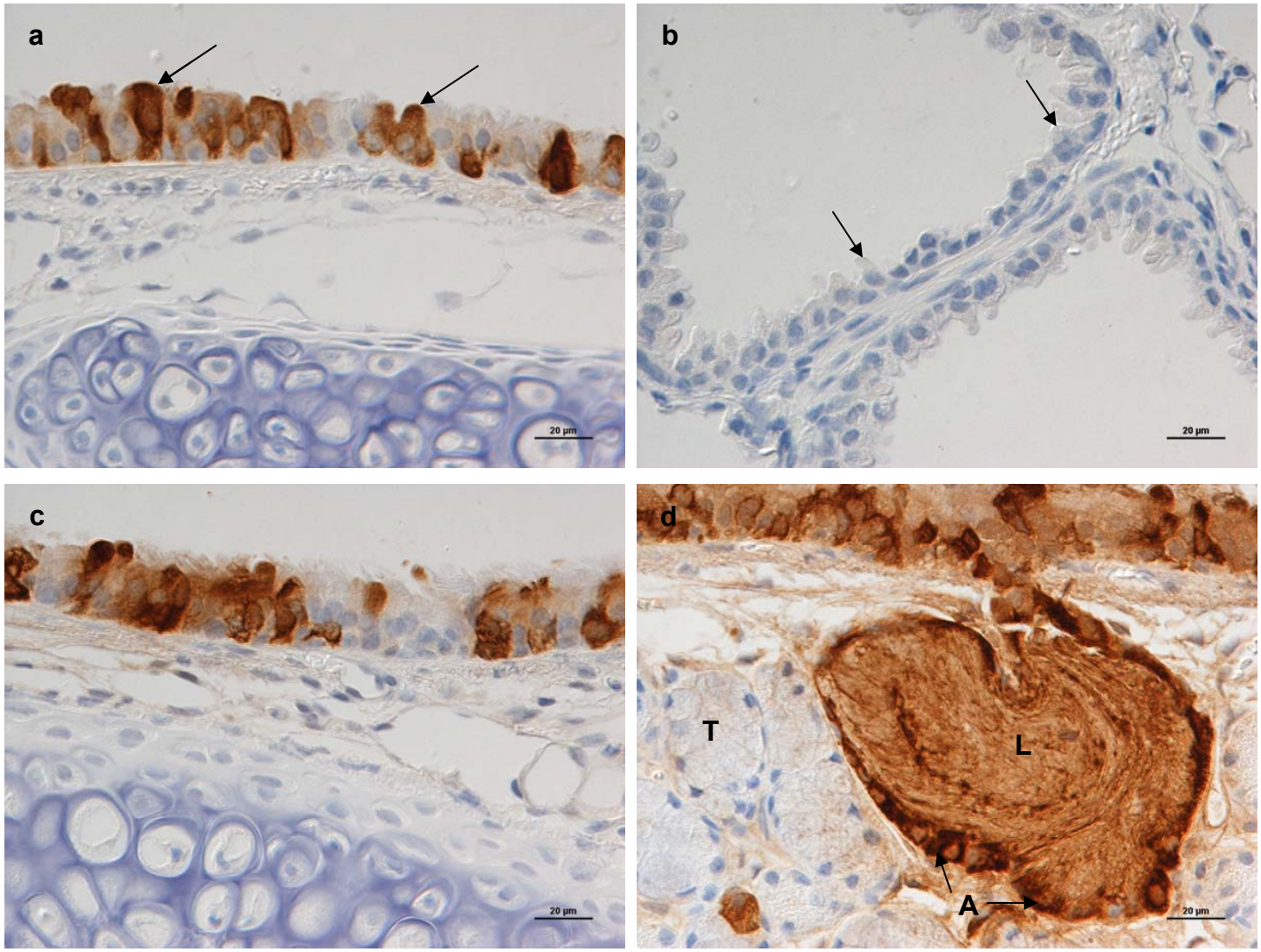

Figure 3-41 Immuno-histology for SPLUNC1 in uninfected (day 0) 129 wild type and IFNγR$^{-/-}$ mice.

(a) Trachea from day 0 wild type mouse showing strongly stained non-ciliated epithelial cells (arrows; 40x). (b) Bronchiole from day 0 wild type mouse, where the epithelial cells, including Clara cells [arrows], are negative (40x). (c) Trachea from a day 0 IFNγR$^{-/-}$ mouse showing strongly positive non-ciliated epithelial cells (40x). (d) Submucosal glands from a day 0 IFNγR$^{-/-}$ mouse; the acinar cells [A], and lumen [L] are strongly positive for SPLUNC1; whereas the mucous-type tubular cells [T] are negative (40x).

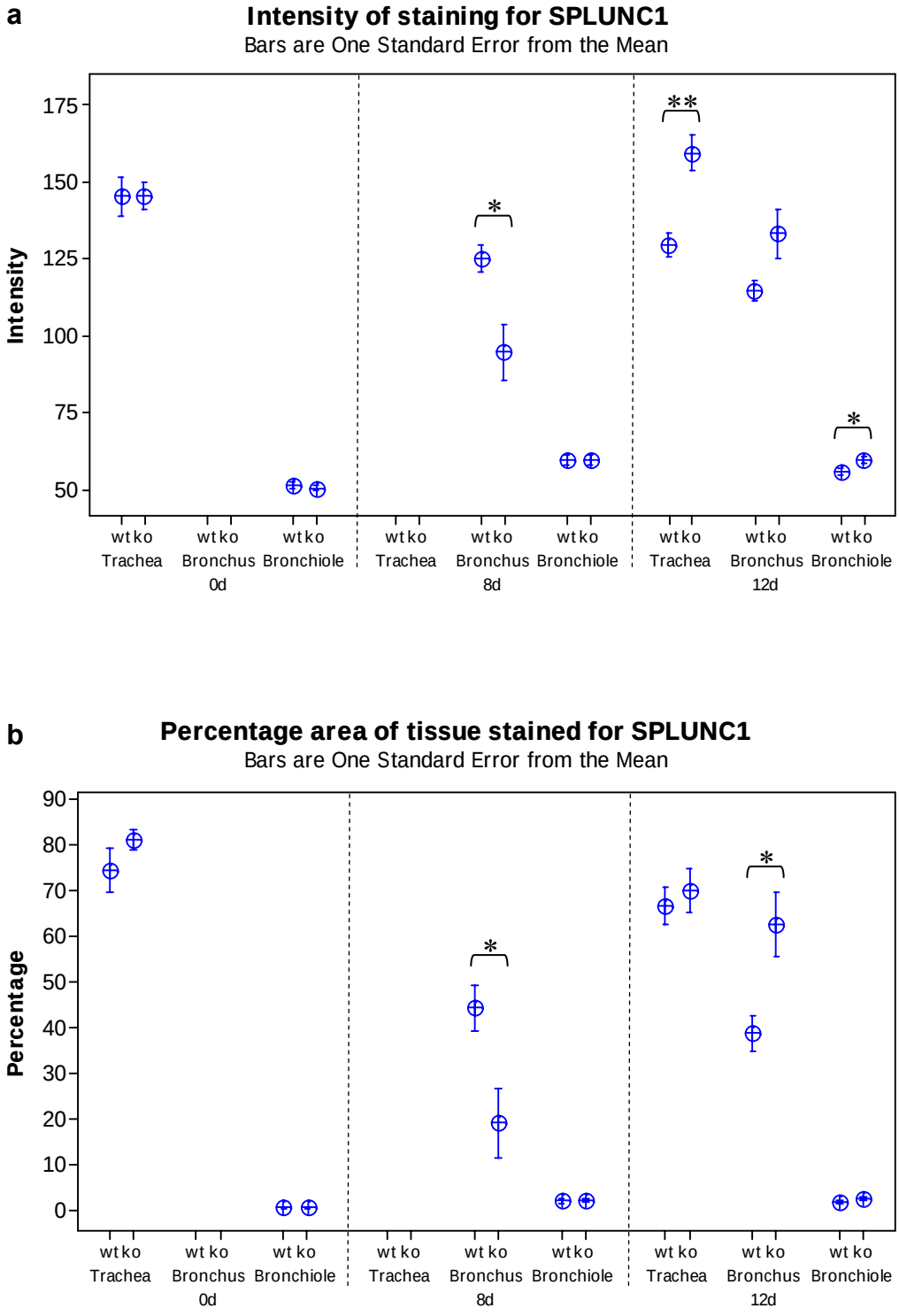

Figure 3-42 Quantitative analysis of immunohistological staining for SPLUNC1 at different levels of the respiratory tract in129 wild type (wt) and IFNγR$^{-/-}$ (ko) mice, before and after infection with MHV-68.
(a) Intensity of staining for SPLUNC1 in respiratory epithelium (b) Percentage area of respiratory epithelium stained for SPLUNC1. Data are the mean of analysis of tissue from two or three mice per group, bars represent the standard error of the mean. ∗ P< 0.05; ∗∗ P< 0.005 (two sample T-test).

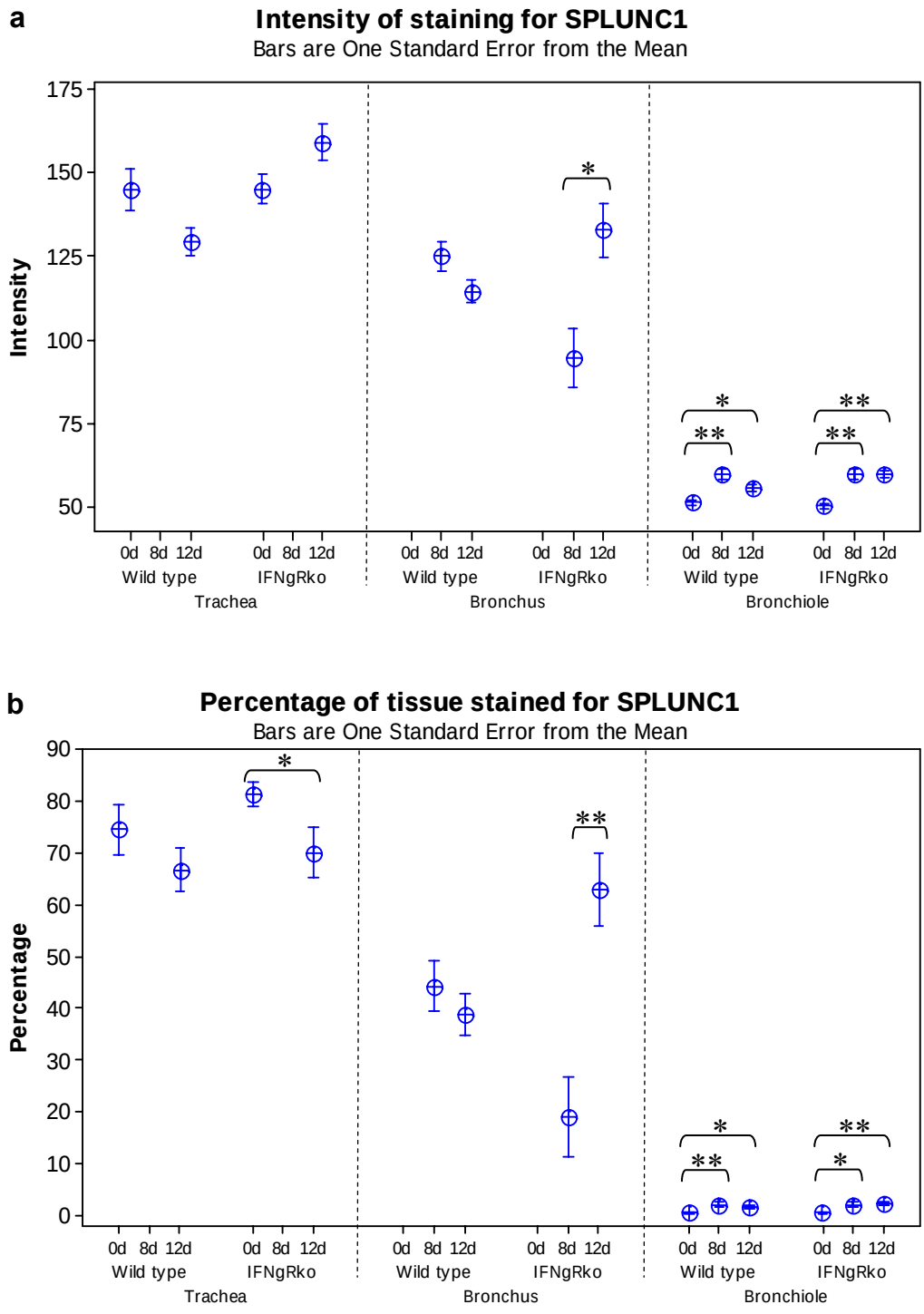

Figure 3-43 Quantitative analysis of immunohistological staining for SPLUNC1 at different levels of the respiratory tract in 129 wild type and IFNγR$^{-/-}$ mice (IFNγRko), before and after infection with MHV-68.
(a) Intensity of staining for SPLUNC1 in respiratory epithelium (b) Percentage area of respiratory epithelium stained for SPLUNC1. Data are the mean of analysis of tissue from two or three mice per group, bars represent the standard error of the mean. ∗ P< 0.05; ∗∗ P< 0.005 (ANOVA).

3.1.3 MHV-68 infection *in vitro*

3.1.3.1 Transfection of 293T cells

Transfection of cells using a vector containing *GFP* was used as a positive control to assess the efficiency of transfection. Approximately 48 hours after applying the transfection solution, cells were viewed under fluorescent light and approximately 40 % of cells transfected with the *GFP* containing vector were expressing GFP. Supernatants from transfected cell cultures were harvested and analysed for the presence of protein from the vector, using an anti-V5 antibody to detect the V5 tag present in the vector used (pcDNA5/FRT/V5-His-TOPO®, Invitrogen), and also actin as a control, using SDS-PAGE and Western Blotting. Although all samples examined were positive for actin, the proteins from the genes of interest inserted in the vector could not be detected.

3.1.3.2 Infection of transfected cells with MHV-68

Transfection of 293T cells with pcDNA5/FRT/V5-His-TOPO® vector containing inserts for the human genes *CCSP, AGR3, SPLUNC1* and *SPLUNC1* Cys mut (which contained a cysteine mutation, thought to be critical to the three dimensional structure and therefore for binding functions) was performed. 24 hours after the removal of the transfection solution, cells were infected with a recombinant virus which contained an inserted GFP (LHΔGFP). At 12 hpi, images were taken under fluorescent light and subsequently analysed to quantify the percentage area that was positive for GFP. The experiment was repeated twice, however, due to different thresholding of the images obtained, cannot be combined and so are presented separately.

In both experiments, cells transfected with *CCSP* exhibited a reduction in the percentage of cells infected with LHΔGFP, when compared to the control transfection (a vector with no insert). The reductions were 0.552 and 0.363-fold, respectively in the two experiments (Figure 3-44). This reduction was statistically significant in both experiments ($P = 0.020$ and 0.033, respectively; two sample T-test). Both *SPLUNC1* and *SPLUNC1* Cys mut showed an increase in the percentage of cells infected, but these increases were not statistically significant. *AGR3* exhibited a decrease in the first experiment, and

a small increase in the second; neither of these changes were significant (Figure 3-44).

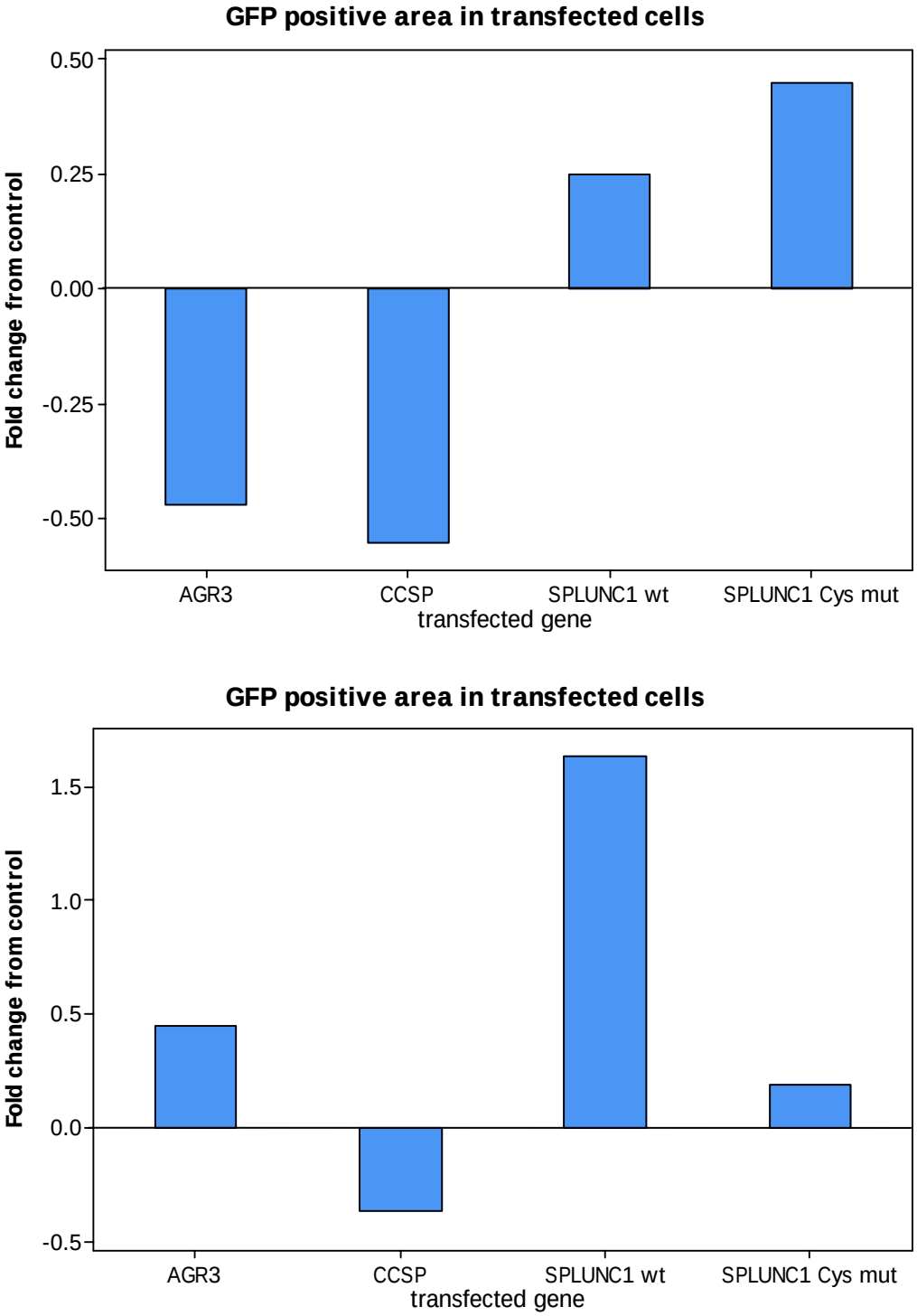

Figure 3-44 Alteration in the mean GFP positive area of cell cultures transfected with different gene-containing vectors compared to cells transfected with an empty vector, following infection with MHV-68 LHΔGFP. Data represent the mean of ten high power fields per transfection. Two replicates of the same experiment.

3.2 Paramyxovirus infection and its effect on the expression of CCSP and SPLUNC1

3.2.1 The inflammatory response to HRSV and SeV infection

To ascertain whether the pattern of alteration in expression of CCSP and SPLUNC1 was solely a MHV-68 related phenomenon, or a non-specific response to a pneumotropic virus, lungs from animals infected with other respiratory viruses were investigated. Mice were infected with either Human respiratory syncytial virus (HRSV)-BT2a (a clinical isolate), HRSV-Long (a laboratory strain), Sendai virus (SeV) or mock-infected and euthanased at days 1, 3, 5 and 7 post infection.

At day 1 pi, lungs from two out of four HRSV-BT2a infected mice exhibited scattered mild to moderate foci of viable and degenerate neutrophils, with lesser macrophages and admixed with necrotic cellular debris adjacent to either bronchioles or vessels (Figure 3-45a). By day 3 pi, all mice exhibited mild to moderate multifocal (peribronchiolar and perivascular) infiltrates which remained neutrophil-dominated, with lesser macrophages, lymphocytes and eosinophils and necrotic cellular debris (Figure 3-45b). In addition, mild diffuse type II pneumocyte hyperplasia was seen (Figure 3-45c). Immunohistology for HRSV revealed antigen predominantly within the cytoplasm of pneumocytes and less frequently in type II pneumocytes and macrophages (Figure 3-45d). Rare bronchiolar epithelial cells were also positive for HRSV antigen.

At day 5 pi, inflammatory infiltrates remained predominantly perivascular and peribronchiolar but were less neutrophil-dominated and contained increased numbers of lymphocytes. Low numbers of neutrophils were seen in the interstitium surrounding foci of inflammation. Within larger bronchioles, scattered necrotic epithelial cells were observed. Immunohistology for HRSV revealed that viral antigen was present in a similar pattern to that seen at day 3 pi. By day 7, the severity of the perivascular and peribronchiolar infiltrates had decreased, and neutrophils were less dominant than seen at earlier timepoints. Type II pneumocyte hyperplasia was still observed at a similar level to earlier timepoints; however, the level of viral antigen detected by immunohistology was reduced.

HRSV-Long infected mice at day 1 pi showed a similar response to HRSV-BT2a infected mice; two out of four mice exhibited small multifocal accumulations of viable and degenerate neutrophils. Similar inflammatory cells were occasionally seen within bronchiolar lumina (Figure 3-46a). Mice euthanased at day 3 pi exhibited mild diffuse neutrophil-dominated interstitial infiltrates (Figure 3-46b), opposed to the multifocal mixed infiltrates seen in the HRSV-BT2a infected mice. Additionally, immunohistology for HRSV antigen revealed fewer positive cells in HRSV-Long infected mice (Figure 3-46c). By day 5 pi, the diffuse neutrophilic interstitial infiltrate persisted and in addition there were mild multifocal aggregates of lymphocytes and histiocytes present in two out of four mice. All mice at day 7 pi exhibited mild, multifocal infiltrates that were more mixed (lymphocytes, lesser neutrophils, macrophages), predominantly in perivascular and peribronchiolar locations (Figure 3-46d). Interstitial neutrophils were still present, but in reduced numbers compared to previous timepoints.

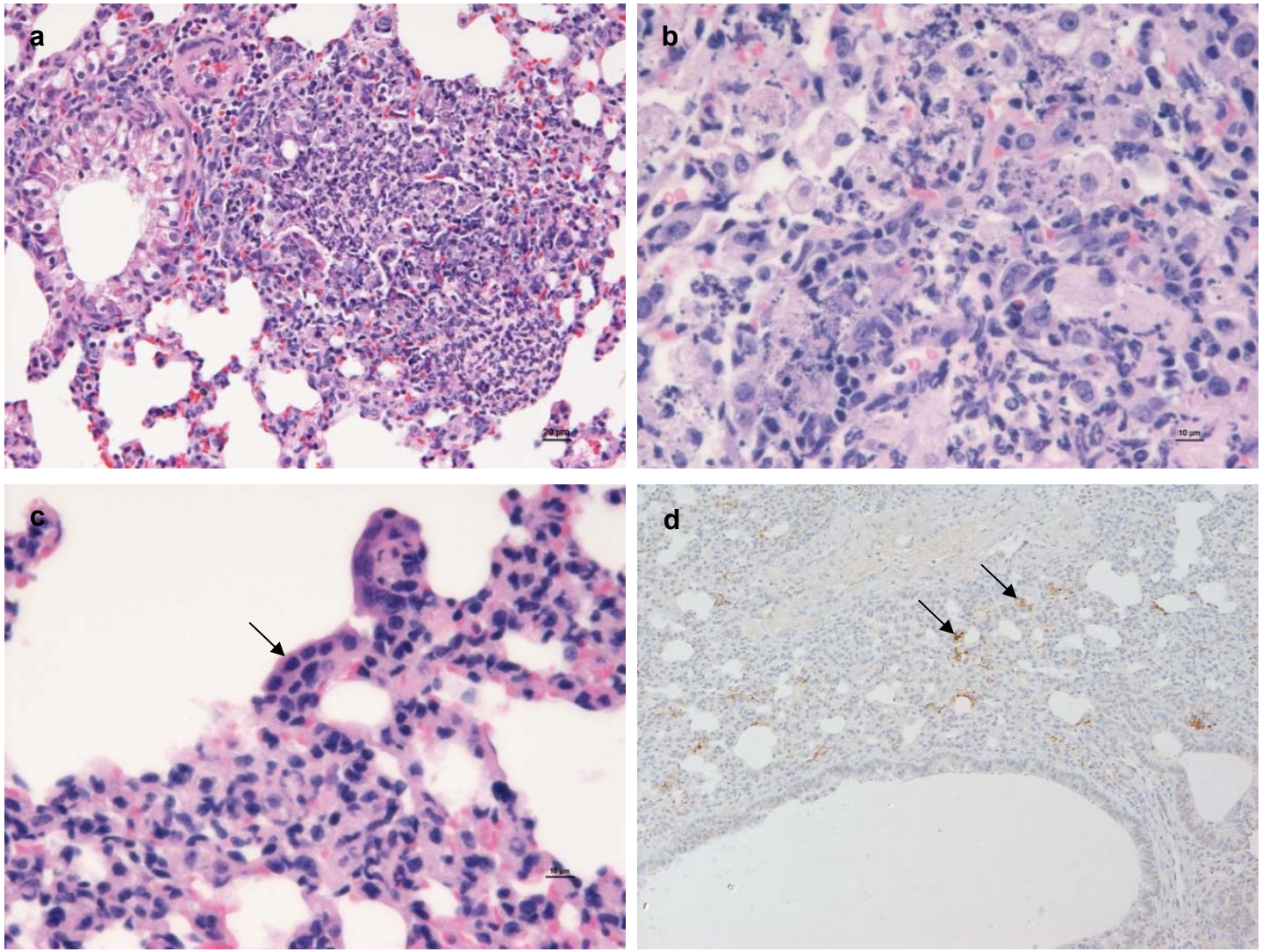

Figure 3-45 Histology of lung tissue from HRSV-BT2a infected BALB/c mice at days 1 and 3 post infection.

(a) A focal infiltrate of viable and degenerate neutrophils, macrophages and necrotic cellular debris at day 1 pi (HE, 20x). (b) Mixed inflammatory infiltrate and necrotic debris typical of that seen in mice at day 3 pi (HE, 40x). (c) Example of type II pneumocyte hyper-plasia seen at day 3 pi (arrow, HE, 40x). (d) Immunohistology for HRSV antigen demonstrates that virus is present and is predominantly seen in pneumocytes (arrows, 10x).

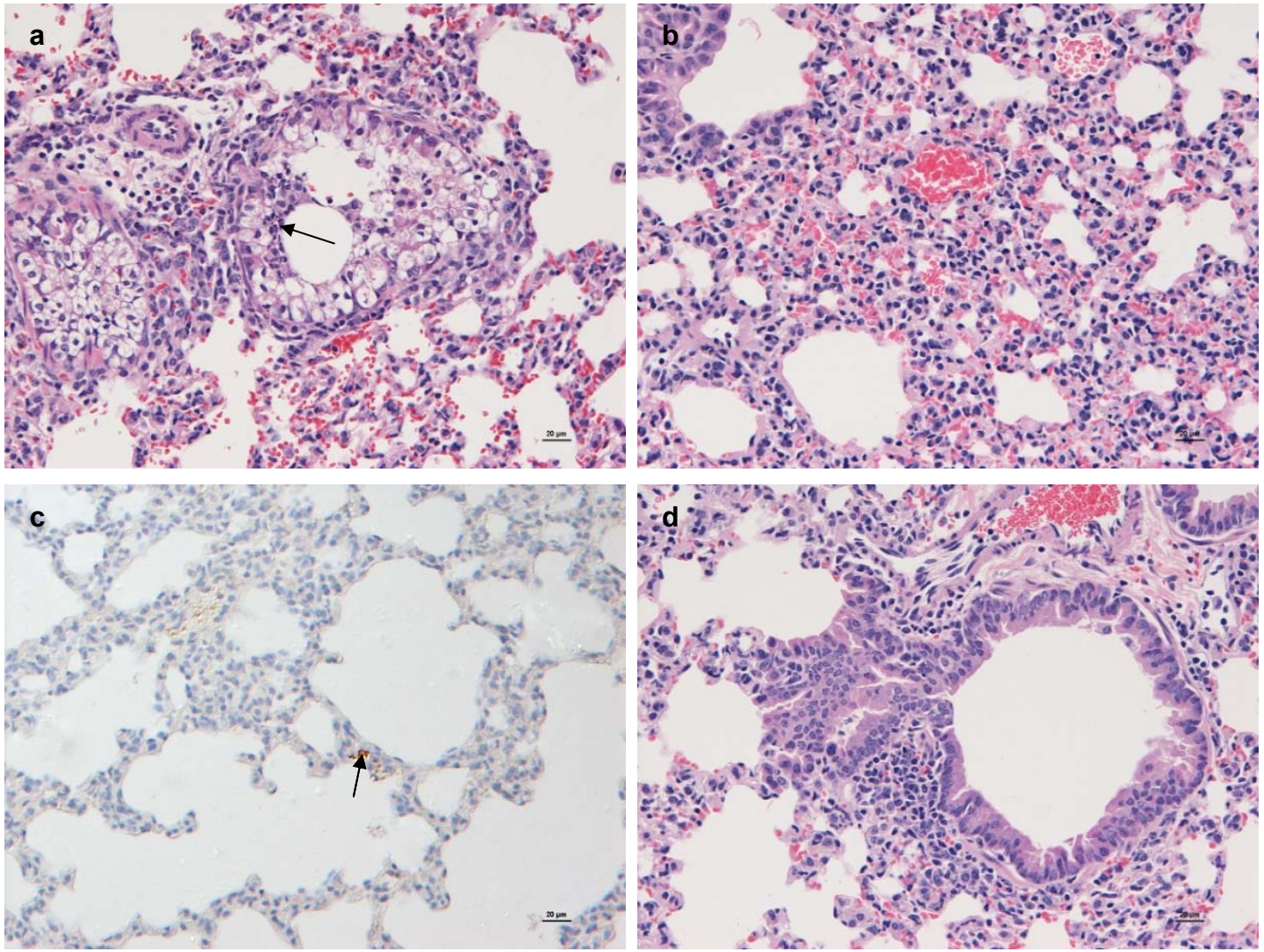

Figure 3-46 Histology of lung tissue from HRSV-Long infected BALB/c mice.

(a) Lung at day 1 pi showing mild infiltrates of peri-bronchiolar and intraluminal neutrophils (arrow, HE, 20x). (b) Mild diffuse interstitial neutrophilic infiltrate, day 3 pi (HE, 20x). (c) Immuno-histology for HRSV antigen revealed fewer cells expressing viral antigen in HRSV-Long infected mice at day 3 pi (arrow, 20x). (d) Mixed perivascular and peribronchiolar infiltrates at day 7 pi (HE, 20x).

Infection of mice with SeV led to a different response to that seen with MHV-68 and HRSV, as this virus induced a necrotising inflammation. At day 1 pi mice infected with SeV exhibited mild, scattered multifocal neutrophilic infiltration, with frequently degenerate neutrophils and lesser macrophages mixed with necrotic cellular debris. By day 3 pi these infiltrates were more frequent, mild to moderate and exhibited a perivascular and peribronchiolar distribution (Figure 3-47a). Infiltrates remained predominantly composed of neutrophils, with fewer lymphocytes and macrophages. Along with the necrotic cellular debris in these areas, scattered necrotic-apoptotic epithelial cells were present within bronchiolar epithelium (Figure 3-47b). The alveoli surrounding the inflammatory foci had mildly to moderately increased numbers of neutrophils within the interstitium.

5 days pi, the inflammatory response was similar in composition to that seen on day 3, but had increased in severity and distribution. Peribronchiolar and perivascular infiltrates were moderate, and extended into the surrounding alveoli, with neutrophils present within alveolar spaces, along with increased numbers of alveolar macrophages and necrosis of pneumocytes (Figure 3-47c). Bronchioles exhibited increased epithelial cell necrosis, and neutrophils were present within the respiratory epithelium and the lumen of airways, along with macrophages and cellular debris (Figure 3-48d).

In contrast to the HRSV infected mice, which exhibited evidence of resolution of inflammation by day 7 pi, the SeV infected mice at this timepoint had more severe inflammation than at the previous timepoint. The lungs exhibited moderate to severe, predominantly pyogranulomatous infiltrates with numerous degenerate neutrophils, cellular debris and fibrin, centred on bronchioles and vessels but extending far into the surrounding parenchyma, filling alveolar spaces (Figure 3-48e). Within pyogranulomatous infiltrates small foci of lymphocytes and plasma cells were present (Figure 3-48f). Bronchiolar lumina were frequently lined and occasionally occluded by degenerate neutrophils and cellular debris; the epithelium variably exhibited necrosis or attenuation (Figure 3-48f).

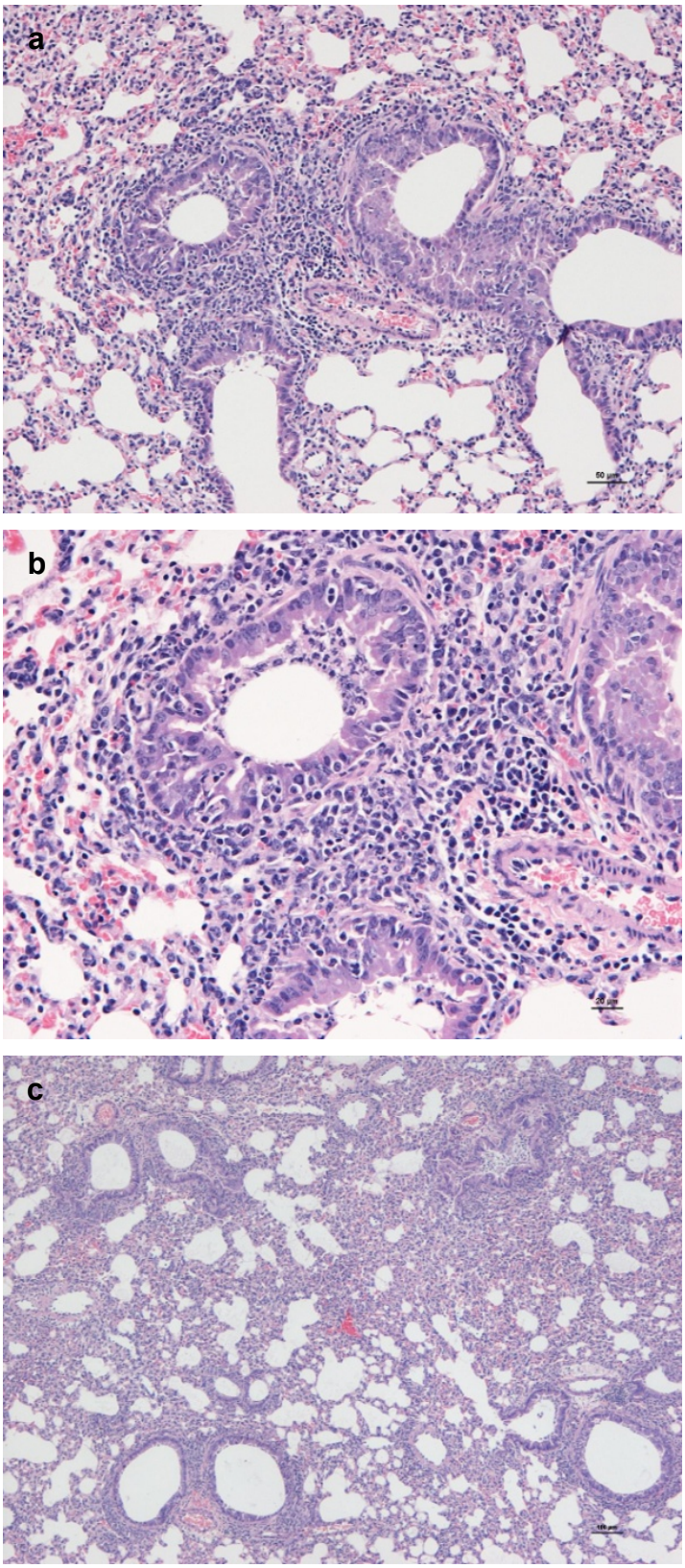

Figure 3-47 Histology of lung tissue from Sendai virus infected BALB/c mice.

(a) Mild to moderate peribronchiolar and perivascular infiltrates at day 3 pi (HE, 10x). (b) Mixed peribronchiolar infiltrates and neutrophils within the bronchiolar epithelium and lumen; day 3 pi (HE, 20x). (c) Perivascular and peribronchiolar infiltrates extend into the surrounding parenchyma on day 5 pi (HE, 4x).

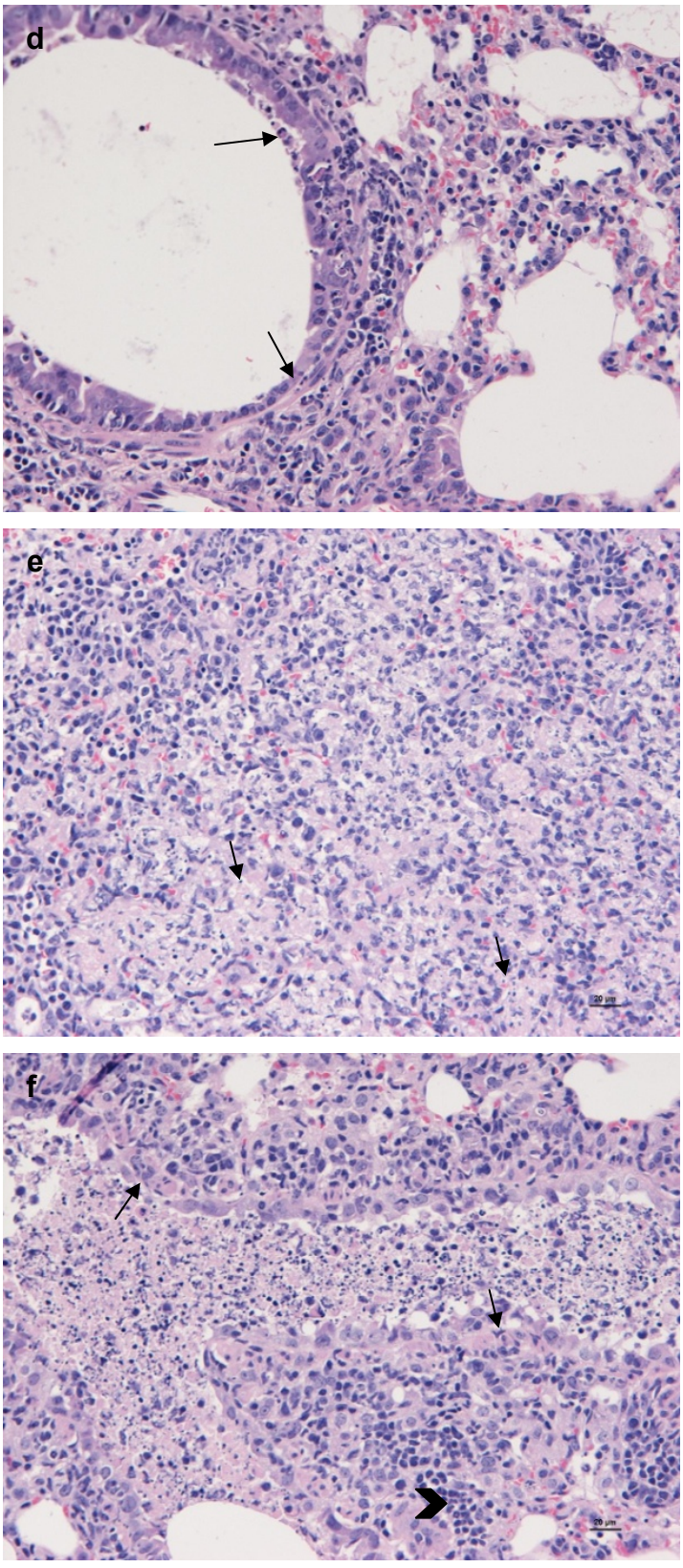

Figure 3-48 Histology of lung tissue from Sendai virus infected BALB/c mice.

(d) Mixed peribronchiolar infiltrates are seen, with neutrophils present within the respiratory epithelium, which exhibits evidence of necrosis; day 5 pi (arrows, HE, 20x). (e) Loss of alveolar structure with moderate to severe inflammation and evidence of pneumocyte necrosis [arrows]; day 7 pi (HE, 20x). (f) Bronchiolar lumen occluded with inflammatory cells and debris, necrosis and loss of respiratory epithelial cells [arrow]. Additionally, small foci of lymphocytes are present within the peribronchiolar infiltrates [arrowhead]; day 7 pi (HE, 20x).

3.2.2 Immunohistology in HRSV and SeV infected BALB/c mice

3.2.2.1 CCSP expression in response to HRSV and SeV infection

Immunohistology for CCSP in mock-infected BALB/c mice revealed a similar pattern of expression of the protein to that seen in the wood mice. The trachea had scattered positive cells in the respiratory epithelium (Figure 3-49a) and similarly, the bronchi exhibited infrequent positive cells (Figure 3-49b). In the bronchioles, the majority of respiratory epithelial cells were positive, but staining was not strong (Figure 3-49c), with the exception of mice at day 1 pi, which exhibited diffusely stronger staining for CCSP (Figure 3-49d). This phenomenon was also present in the infected mice and so is discounted in the following discussion as to the effect of infection on the expression of CCSP.

Infection of mice with either HRSV-Long or HRSV-BT2a revealed little alteration in the expression of CCSP. The majority of the epithelium remained positive and staining was generally faint to moderate with small foci of moderate to strong staining (Figure 3-50a). In the SeV infected mice, days 1 and 3 pi were similar in the frequency and strength of staining for CCSP as that seen in mock-infected mice, however, there was a decrease in the strength of staining and marked reduction in the number of positive bronchiolar epithelial cells at days 5 and 7 pi. This was most marked in association with peribronchiolar inflammatory infiltration (Figure 3-50b-d).

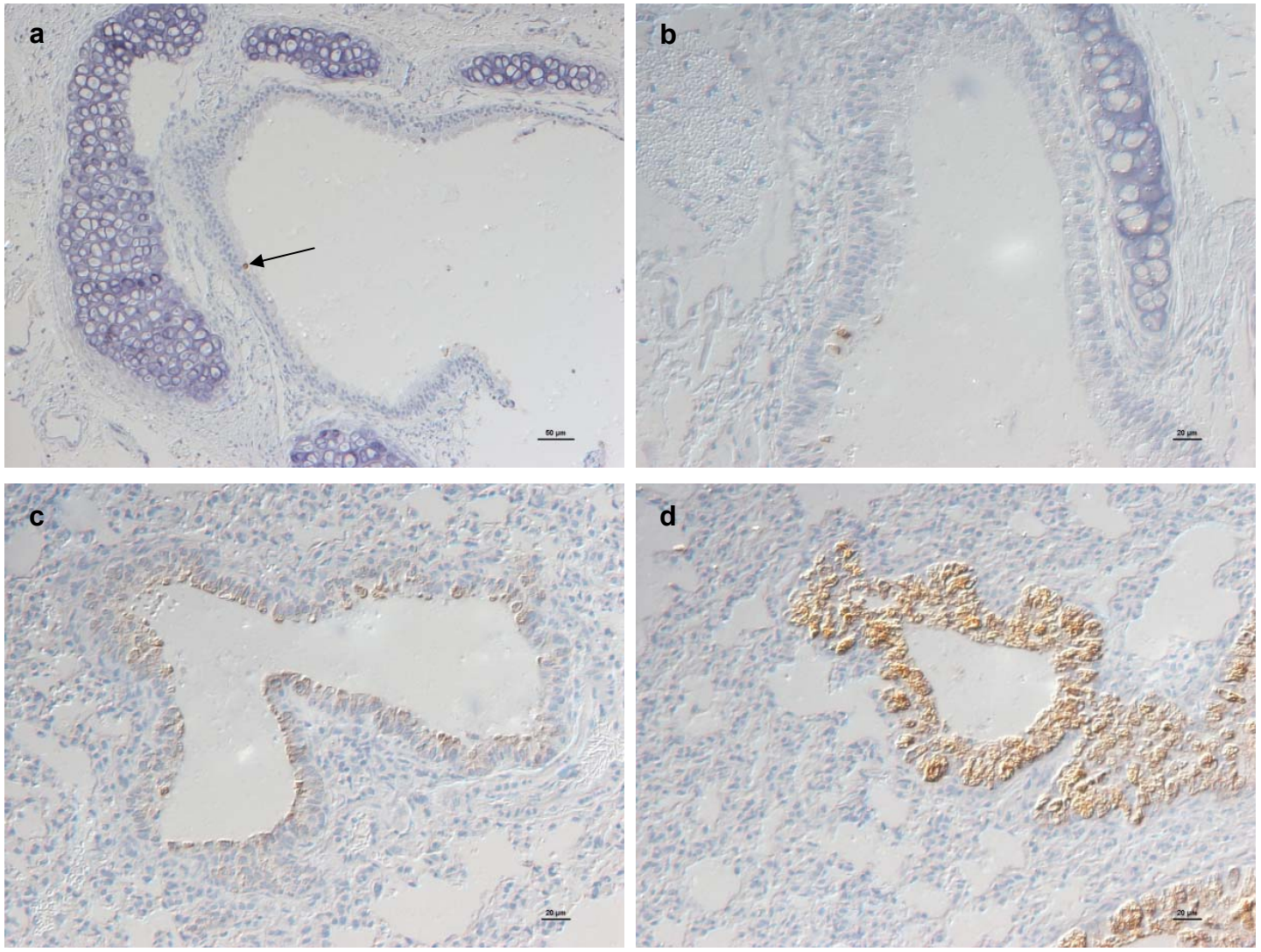

Figure 3-49 Immuno-histology for CCSP in mock-infected BALB/c mice.

(a) Scattered CCSP positive cells are seen in the trachea (arrow, 10x). (b) The bronchi exhibit scattered positive epithelial cells (20x). (c) Bronchioles contain numerous moderately positive cells at days 3, 5 and 7 pi (20x). (d) Bronchiolar staining for CCSP at day 1 pi shows a stronger reaction than that seen at later timepoints (20x).

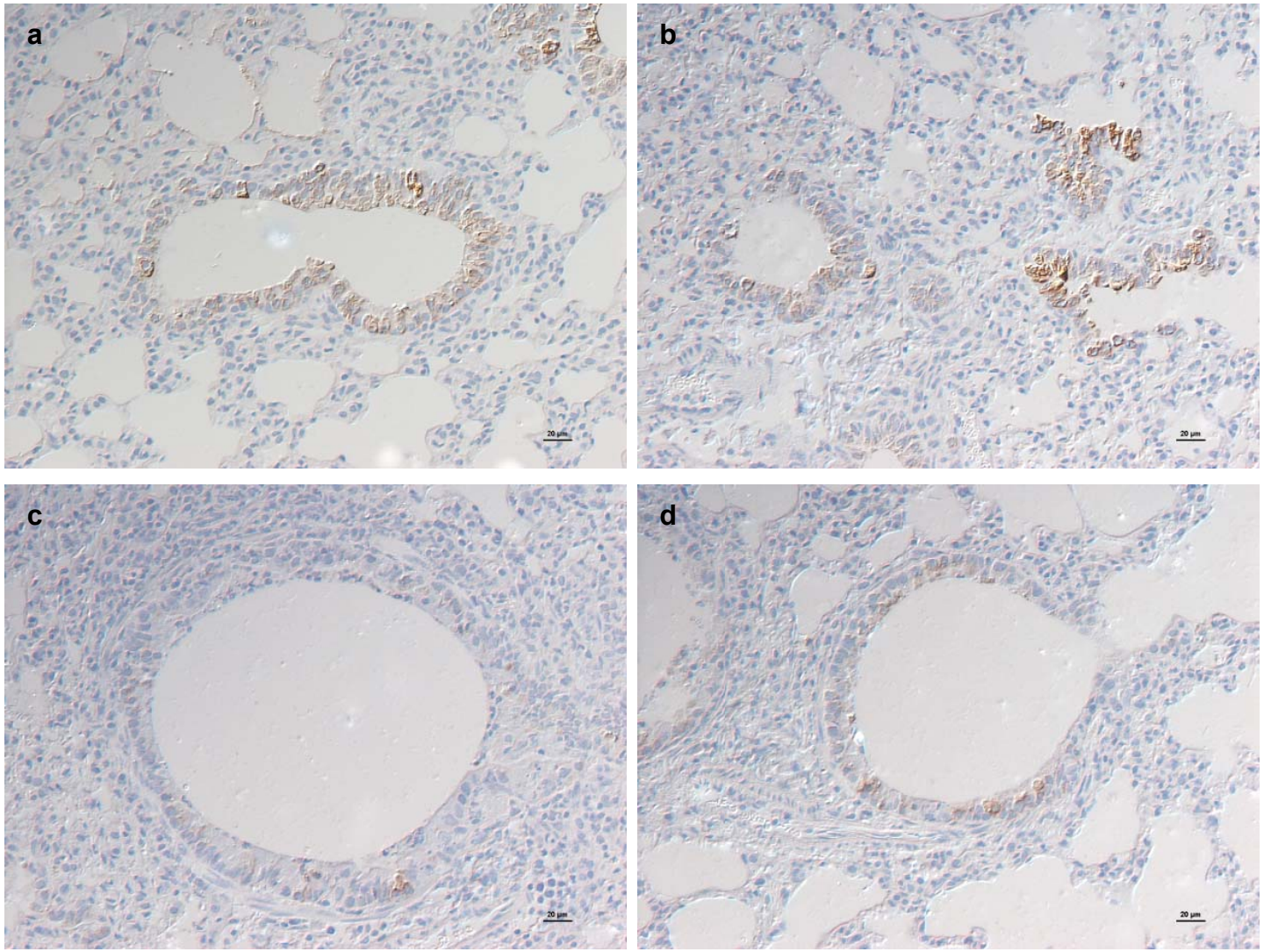

Figure 3-50 Immuno-histology for CCSP in HRSV and SeV infected BALB/c mice.

(a) HRSV-BT2a infected mouse (day 7pi); the distribution and expression of CCSP in HRSV infected mice was similar to that in mock-infected BALB/c mice (20x). (b) SeV infected mouse at day 3 pi showing similar distribution and strength of staining to mock-infected mice (20x). (c) SeV infection at day 5 pi was associated with a reduction in the number of CCSP positive cells (20x). (d) SeV infected mouse at day 7 pi; reduced number of CCSP positive cells are seen (20x).

3.2.2.2 SPLUNC1 expression in response to HRSV and SeV infection

Immunohistology for SPLUNC1 in mock-infected BALB/c mice was most prevalent in the trachea, where moderately to strongly positive non-ciliated cells in the respiratory epithelium were frequent and in addition, staining was seen in some of the submucosal gland epithelium and the glandular lumen (Figure 3-51a). Within the bronchi, the number of positive cells was slightly less than that seen in the trachea, however, the strength of staining remained high (Figure 3-51b). Immediately adjacent to the bronchi, the proximal bronchioles exhibited a transitionary area, in which bronchiolar epithelium exhibited relatively frequent positive cells (Figure 3-51c), compared to the bronchioles generally, in which only very rare positive cells were seen (Figure 3-51d). In contrast to the immunohistology for CCSP, there was no difference seen between any of the timepoints.

Very little difference was observed in the pattern or intensity of staining for SPLUNC1 as a result of infection with either HRSV or SeV. The proximal bronchioles continued to exhibit a “transitionary” zone between the bronchial and bronchiolar staining pattern; bronchioles were overwhelmingly negative. Occasional positive cells were observed in the bronchioles of SeV infected mice after day 3 pi, but these were infrequent and quantitative analysis would be required to establish whether this was a significant increase compared to mock-infected mice.

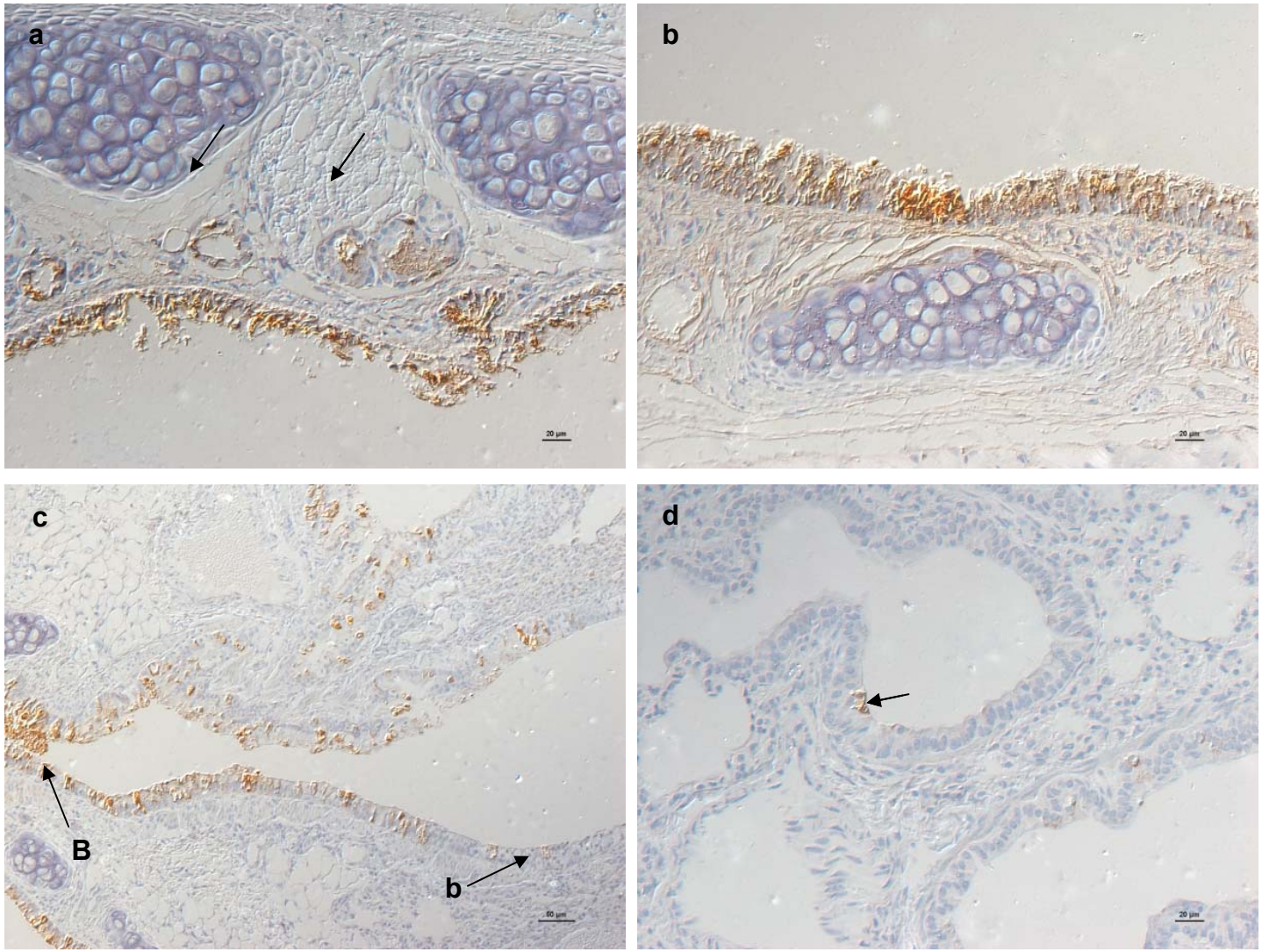

Figure 3-51 Immuno-histology for SPLUNC1 in the respiratory tract of mock-infected BALB/c mice.

(a) Trachea in which numerous cells are positive within the respiratory epithelium, in addition to positive cells within the submucosal glands (arrows, 20x). (b) Bronchial epithelium with numerous positive cells (20x). (c) The proximal bronchiole, in which the transition from the frequently positive bronchial epithelium [B] to the predominantly negative bronchiolar epithelium [b] can be seen (10x). (d) Bronchioles exhibit only very rare cells positive for SPLUNC1 (arrow; 20x).

3.3 Influenza A virus infection and its effect on the expression of CCSP and SPLUNC1

3.3.1 The inflammatory response to Influenza A virus infection

BALB/c mice were infected with one of four strains of Influenza A virus; Influenza A/Ca/04/09 (H1N1) [Ca H1N1], Influenza A/NC/20/99 (H1N1) [NC H1N1], Influenza A/Vietnam/04/98 (H5N1) [HPAI H5N1] or Influenza A/Mute Swan/MI/451072/06 (H5N1) [LPAI H5N1], and were euthanased at 12, 24, 48 and 72 hpi. Controls consisted of uninfected mice and mice which had had intranasal administration of allantoic fluid; allantoic fluid-treated mice were euthanased at 12 and 24 hpi.

Mice from the allantoic fluid-treated group exhibited mild multifocal aggregates of either neutrophils alone or neutrophils and macrophages within alveoli, often with amphophilic material in the centre (Figure 3-52a,b).

Infection with Influenza A virus induced a necrotising bronchiolitis, which was most severe in the HPAI H5N1 infected mice and increased in severity up to 72 hpi (the latest timepoint). In the lungs of mice infected with the other strains the inflammation was less severe and bronchiolar epithelial cell necrosis less widespread. The severity of the inflammatory infiltration increased up to 48 hpi, and was maintained between 48 and 72 hpi.

In NC H1N1 infected mice at 12 hpi, mild multifocal neutrophil-dominated infiltrates were present, variably peribronchiolar or intra-alveolar. Additionally, neutrophils were occasionally present within bronchiolar lumina. At 24 hpi, neutrophilic infiltrates were similarly distributed to those seen at 12 hpi, with additional perivascular infiltrates. By 48 hpi mild multifocal neutrophil-dominated peribronchiolar infiltrates also contained low numbers of macrophages, and the bronchiolar epithelium exhibited mild multifocal necrosis (Figure 3-53a). 72 hpi the inflammatory response was very similar to that at 48 hpi, additionally, mild multifocal perivascular oedema was present (Figure 3-53b).

Ca H1N1 infected mice at 12 hpi exhibited mild multifocal to coalescing thickening of the alveolar interstitium by neutrophils (Figure 3-54a), occasionally with neutrophils and eosinophilic acellular fluid (oedema) within alveolar spaces. Similar interstitial infiltrates were also observed at 24 hpi. By 48 hpi, mild multifocal necrosis of bronchiolar epithelium was present; bronchiolar lumina variably contained viable and degenerate neutrophils, macrophages and necrotic cellular debris. Mild multifocal peribronchiolar infiltration (neutrophils, lesser macrophages) and mild multifocal perivascular oedema are present (Figure 3-54b). At 72 hpi, necrosis of bronchiolar epithelium remained mild but was more widespread; other changes were similar to those seen than at 48 hpi.

Mice infected with HPAI H5N1 at 12 and 24 hpi exhibited occasional mild, multifocal pyogranulomatous infiltration, which were predominantly peribronchiolar and more frequent in the cranial lung lobes and occasionally extended into the lumen of bronchioles (Figure 3-55a). At 48 hpi, within alveoli, small necrotic foci with mild infiltration of neutrophils and macrophages were present (Figure 3-55b). Within bronchioles and also the trachea, small foci of necrotic epithelial cells were seen, with neutrophils within the epithelial layer and adjacent to the airway. Mild multifocal neutrophilic tracheitis was present at 72 hpi, whereas the bronchioles exhibit diffuse necrosis and loss of epithelium with mild to moderate mixed peribronchiolar infiltration (neutrophils, lymphocytes, macrophages [Figure 3-55b]). Multifocally, alveoli also contained cellular debris, neutrophils, macrophages and proteinaceous fluid (oedema) with mild to moderate interstitial infiltration (neutrophils) and mild to moderate perivascular oedema.

Mice infected with LPAI H5N1 exhibited similar changes at 12, 24 and 48 hpi; mild multifocal, neutrophil-dominated infiltrates, predominantly peribronchiolar, but also, less frequently, within alveoli or bronchiolar lumina (Figure 3-56a). By 48 hpi, rare necrotic cells were present within bronchioles. At 72 hpi, the inflammatory infiltrate was more mixed (neutrophils, lymphocytes, macrophages) and present within alveoli (Figure 3-56b) and as peribronchiolar aggregates. Fewer lymphocyte-dominated perivascular infiltrates were seen.

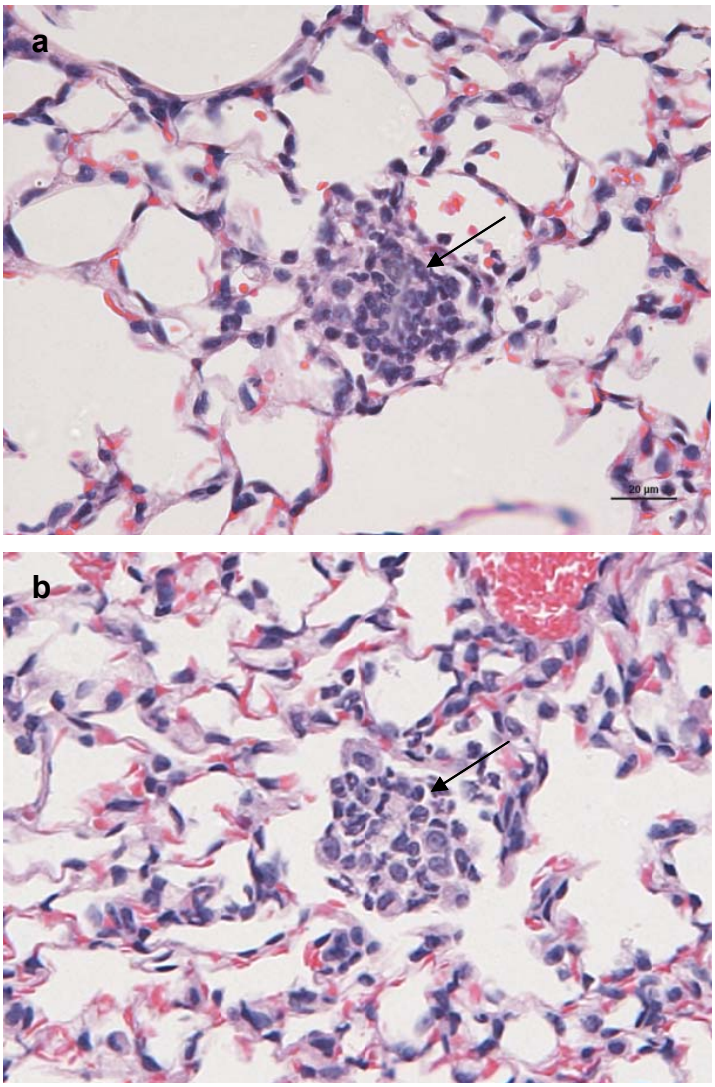

Figure 3-52 Histology of lung tissue from allantoic fluid-treated BALB/c mice. (a) Neutrophil-dominated alveolar infiltrate surrounding amphophilic material in mouse 12 hours after allantoic fluid administration (arrow; HE, 40x). (b) Pyogranulomatous infiltrate within an alveolus of a mouse 24 hours after allantoic fluid administration (arrow; HE, 40x).

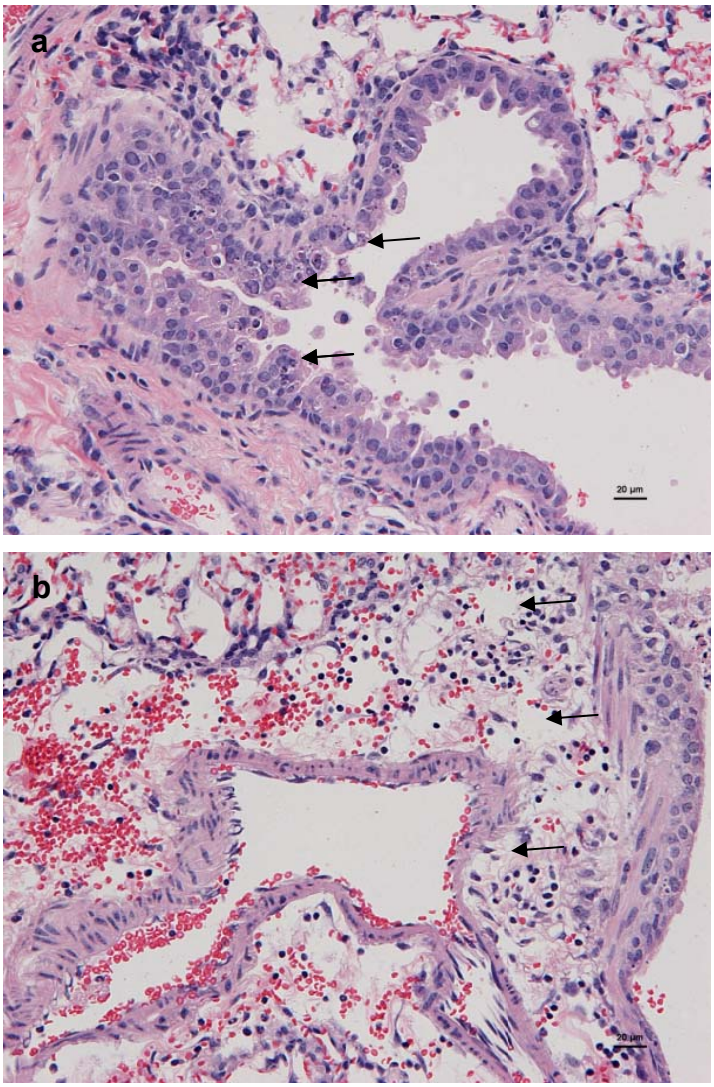

Figure 3-53 Histology of lung tissue from NC H1N1 infected BALB/c mice. (a) Mild necrosis of the bronchiolar epithelium at 48 hpi (arrows; HE, 20x). (b) Mild perivascular oedema at 72 hpi (arrows; HE, 20x).

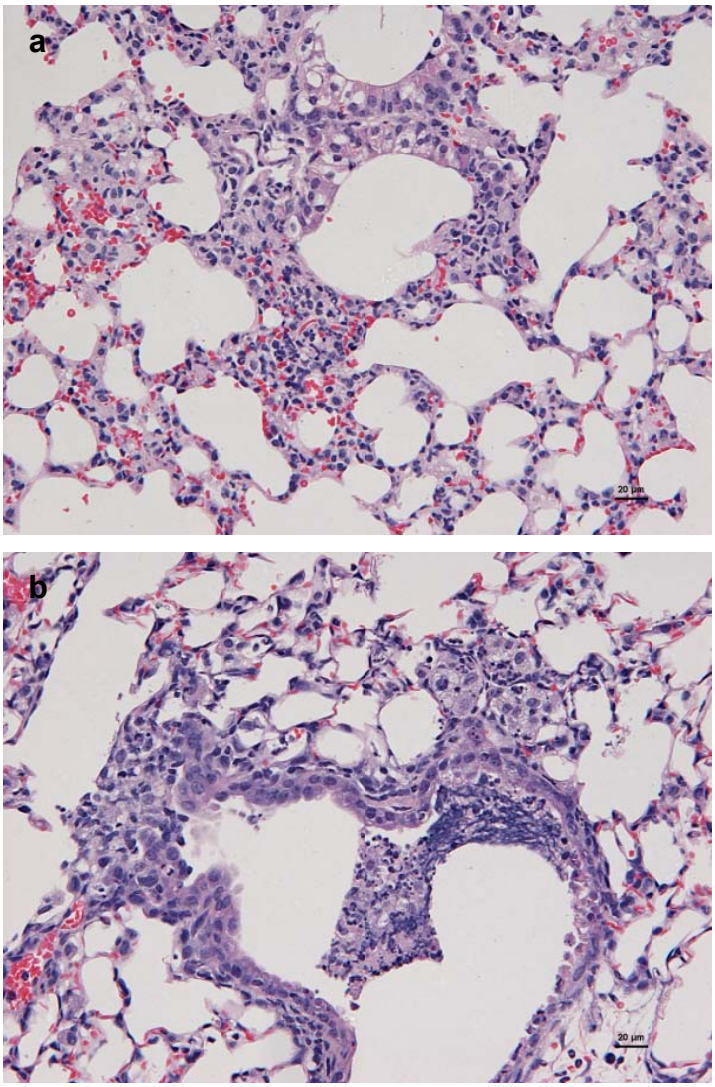

Figure 3-54 Histology of lung tissue from Ca H1N1 infected BALB/c mice. (a) Mild multifocal interstitial neutrophil-dominated infiltrates are seen at 12 hpi (HE, 20x). (b) Bronchioles exhibit mild multifocal necrosis and intra-luminal neutrophils, macrophages and cellular debris at 48 hpi (HE, 20x).

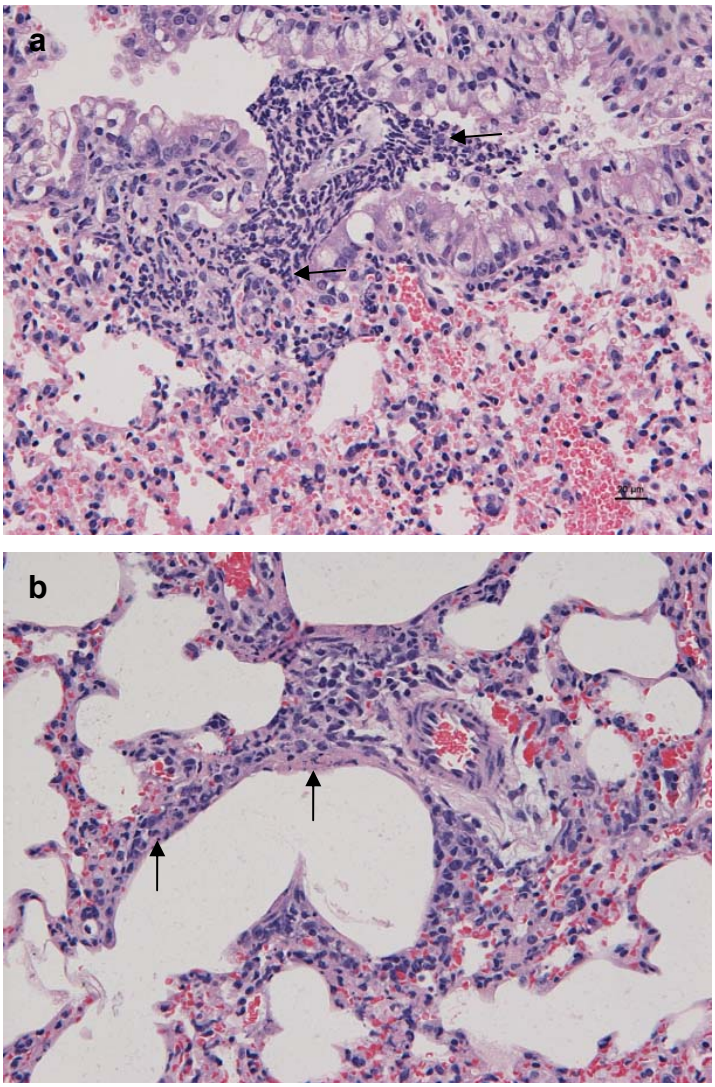

Figure 3-55 Histology of lung tissue from HPAI H5N1 infected BALB/c mice. (a) Mild pyogranulomatous infiltrates present within and around bronchioles at 12 hpi (arrows; HE, 20x). (b) Bronchioles exhibit necrosis and loss of epithelium with mild to moderate mixed peribronchiolar infiltrates at 72 hpi (arrows; HE, 20x).

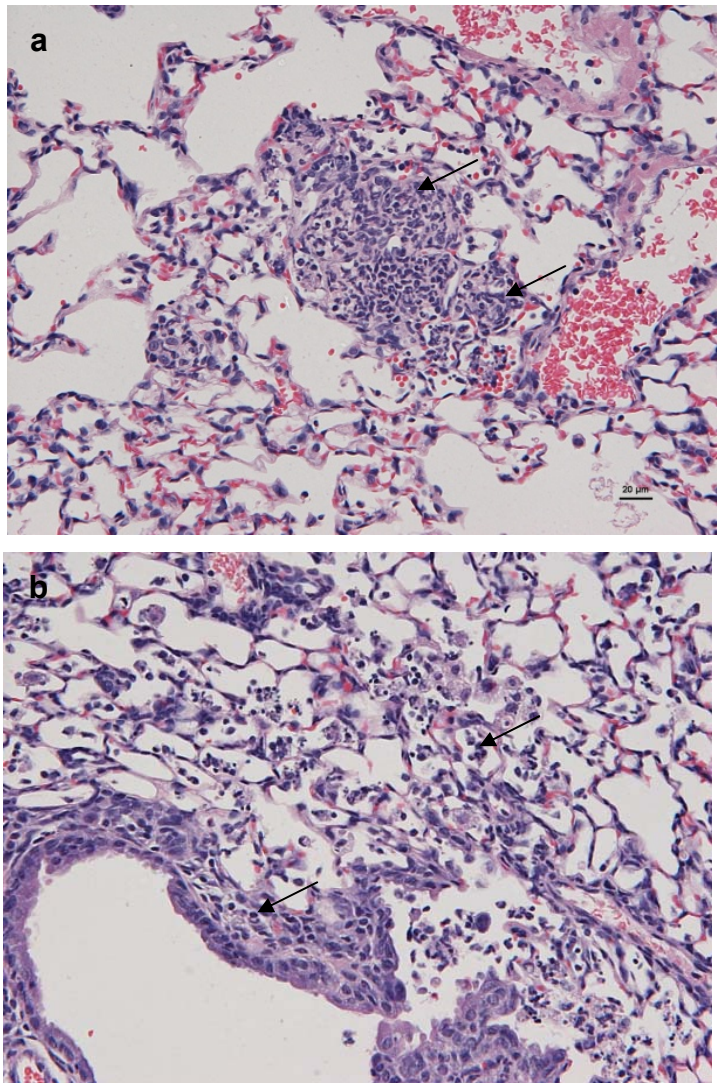

Figure 3-56 Histology of lung tissue from LPAI H5N1 infected BALB/c mice. (a) Alveolar neutrophil-dominated infiltrate at 24 hpi (arrows; HE, 20x). (b) Mild peribronchiolar mixed infiltrate, with inflammatory cells also present in the surrounding alveolar spaces at 72 hpi (arrows; HE, 20x).

3.3.2 Immunohistology in Influenza A virus infected BALB/c mice

3.3.2.1 CCSP expression in response to Influenza A virus infection

Immunohistology for CCSP in uninfected mice was similar to that described previously for control mice (Figure 3-49). Both mice treated with allantoic fluid and Influenza virus infected mice exhibited stronger staining in bronchiolar epithelium at 12 hpi (Figure 3-57a), similar to that described previously in HRSV and SeV infected mice at the first timepoint. The intensity of staining in allantoic fluid treated mice was similar (faint to moderate) to the uninfected mice by 24 hpi (Figure 3-57b). Similar increases seen at 12 hpi in infected mice will therefore not highlighted further.

In NC H1N1 infected mice, generally the intensity and distribution of staining for CCSP was similar to that seen in the uninfected mice, with the exception of bronchioles with mild or moderate peribronchiolar inflammatory infiltration, which tended to have far fewer positive epithelial cells (Figure 3-58a).

Ca H1N1 infected mice also showed a reduction in intensity of staining for CCSP in bronchioles, at 48 and 72 hpi. Association between this decreased staining and peribronchiolar inflammatory infiltration was less strong in this group, and a higher proportion of cells remained positive, but with lesser intensity (Figure 3-58b).

HPAI H5N1 infected mice exhibited a different pattern of staining; at 48 and 72 hpi , bronchioles with peribronchiolar inflammatory infiltration contained some epithelial cells which exhibited stronger staining than the majority of bronchioles in these mice, which generally exhibited only faint positivity overall (Figure 3-58c).

LPAI H5N1 infected mice did not show any remarkable difference in the distribution or intensity of staining, other than the common increase at 12 hpi seen in all groups. At 48 and 72 hpi, bronchiolar epithelium was frequently positive, with faint to moderate intensity of staining (Figure 3-58d).

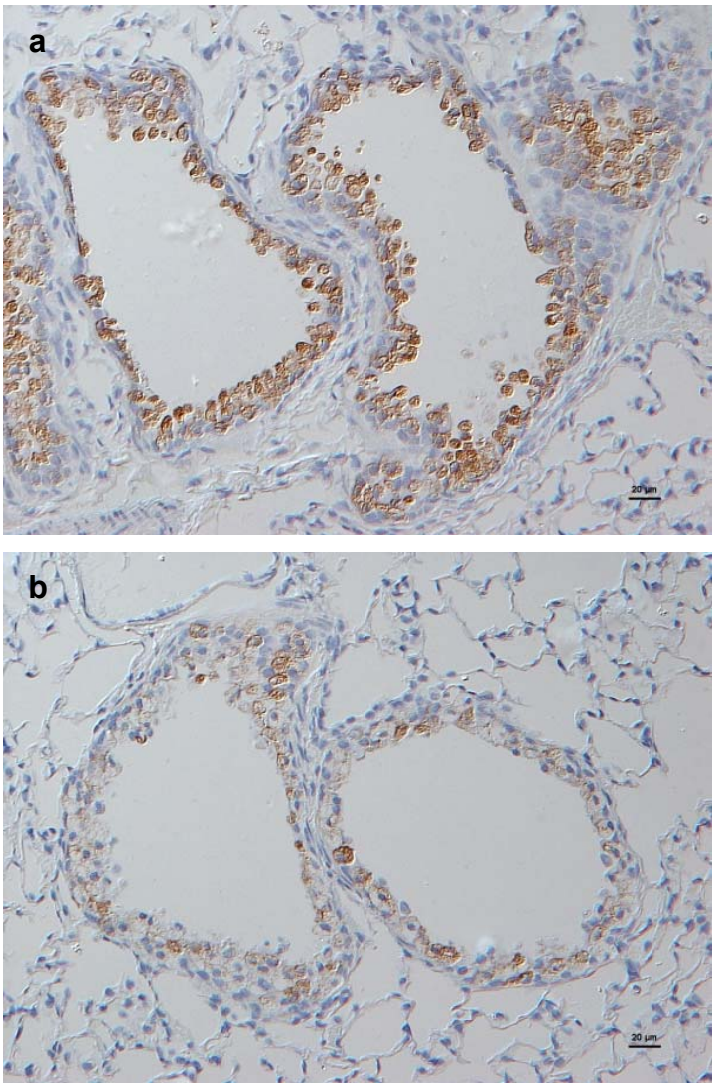

Figure 3-57 Immunohistology for CCSP in BALB/c mice treated with allantoic fluid.
(a) Bronchioles at 12 hpi exhibited increased intensity of staining (20x). (b) At 24 hpi, the intensity of staining was reduced and similar to the constitutive level of staining seen in uninfected mice (20x).

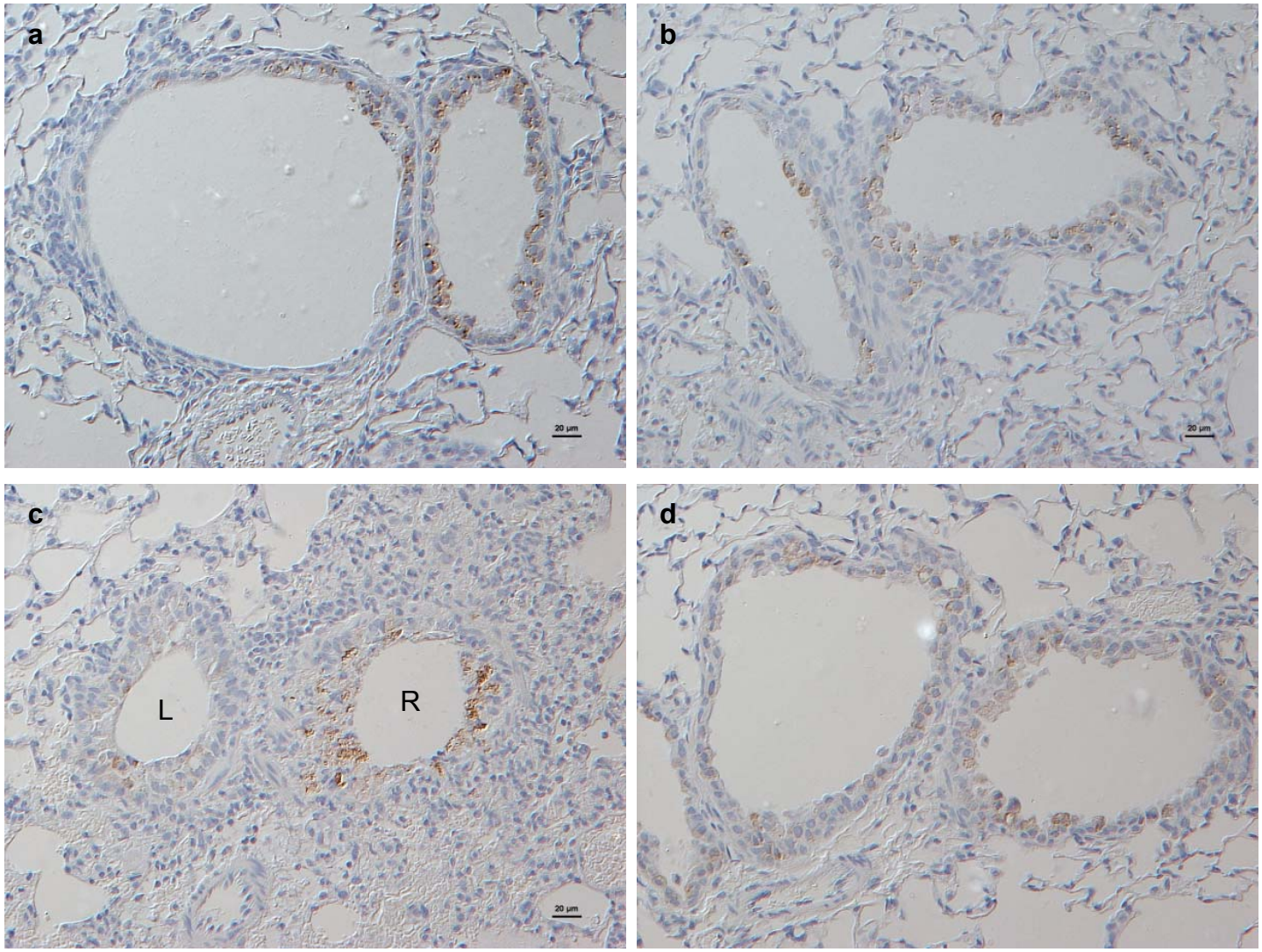

Figure 3-58 Immuno-histology for CCSP in Influenza A virus infected BALB/c mice.

(a) NC H1N1 infected mouse at 72 hpi; bronchioles with peribronchiolar inflammatory infiltration exhibit fewer CCSP positive epithelial cells (20x). (b) Ca H1N1 infected mouse at 48 hpi; bronchiolar epithelium exhibits overall reduced intensity of staining for CCSP (20x). (c) HPAI H5N1 infected mouse at 72 hpi; the left bronchiole (L) exhibits staining typical for these mice at this timepoint, whereas the right bronchiole (R), which has moderate peribronchiolar inflammatory infiltration, exhibits slightly stronger staining. This was seen in mice at 48 and 72 hpi (20x). (d) LPAI H5N1 infected mouse at 48 hpi exhibiting faint to moderate staining of the bronchiolar epithelium (20x).

3.3.2.2 SPLUNC1 expression in response to Influenza A virus infection

Immunohistology for SPLUNC1 in uninfected and allantoic fluid-treated mice yielded staining similar to that previously described in control BALB/c mice (Figure 3-51); frequency and intensity of staining was greatest in the trachea and bronchi, with a “transitionary zone” in the proximal bronchiole where the proportion of positive cells and the intensity of staining decreased rapidly. Bronchioles distal to this zone were negative.

In infected mice, two anatomical areas exhibited differences from the control mice. The “transitionary zone” in the proximal bronchiole in NC H1N1, and LPAI H5N1 infected mice, at later timepoints (48 and 72 hpi), exhibited staining in this area that extended distally to that seen in the control mice (Figure 3-59a), so a greater number of cells were positive for SPLUNC1 (Figure 3-60). Conversely, in HPAI H5N1 infection, staining within the “transitionary zone” was much weaker at 72hpi, despite having been unaltered at previous timepoints (Figure 3-59b). Lastly, bronchioles in several of the infected mice exhibited rare or occasional epithelial cells positive for SPLUNC1; staining was either widespread throughout the cytoplasm of scattered cells (Figure 3-59c) or concentrated in the apical cytoplasm or on the luminal surface of the cell (Figure 3-59d). However, this pattern of staining was inconsistent within groups of mice and so conclusions as to whether the viral infection caused these changes cannot be drawn.

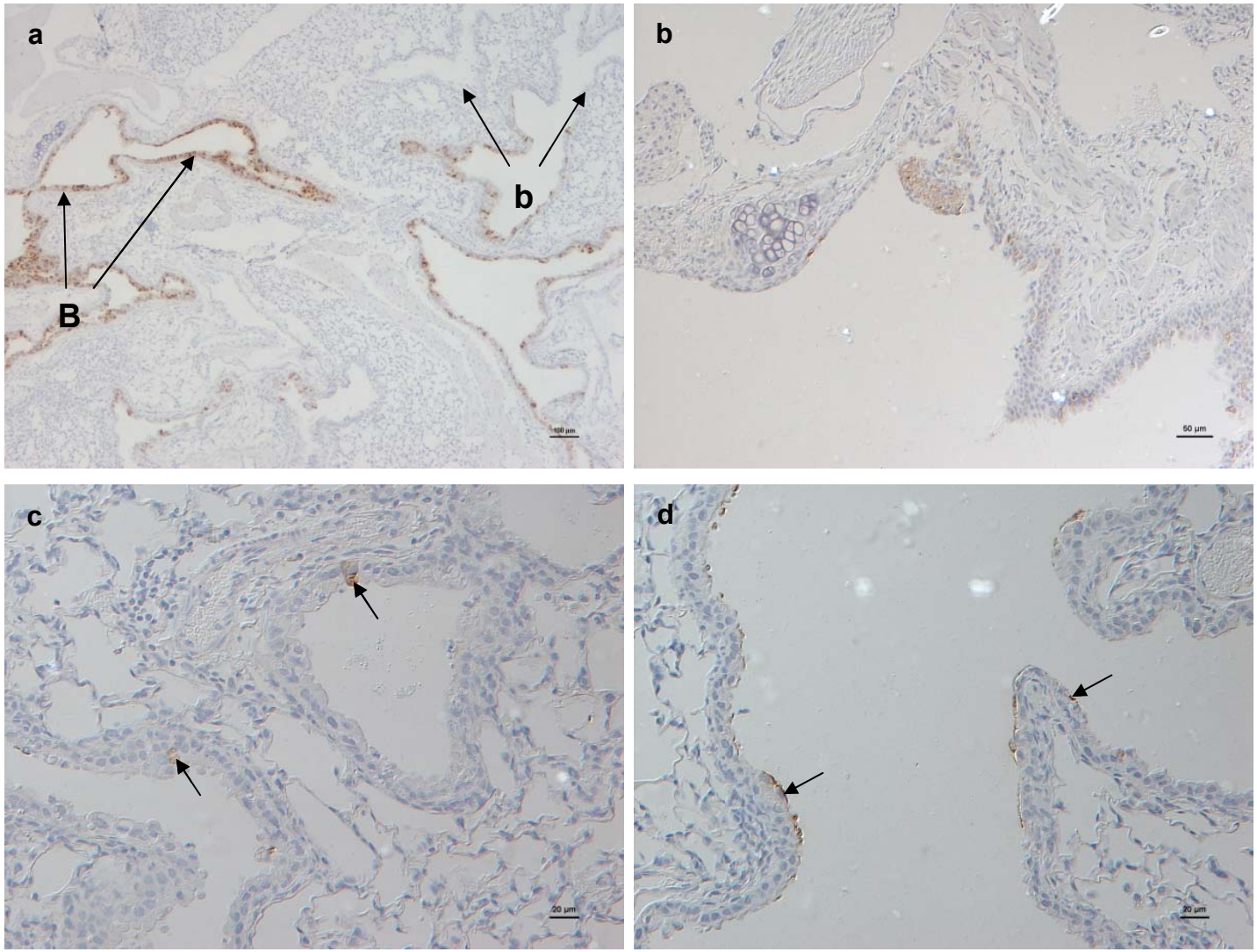

Figure 3-59 Immuno-histology for SPLUNC1 in the lung of Influenza A virus infected BALB/c mice.

(a) Bronchial-bronchiolar junction (“transition zone”), in an allantoic fluid treated mouse showing strongly positive epithelium close to the bronchus [B] and negative bronchioles distally [b] (4x). (b) Bronchial-bronchiolar junction in a HPAI H5N1 infected mouse at 72 hpi showing reduced staining for SPLUNC1 (10x). (c) Scattered bronchiolar cells were positive for SPLUNC1; Ca H1N1 infected mouse, 48 hpi (arrows; 20x). (d) In some mice, the luminal surface of bronchiolar epithelial cells was positive for SPLUNC1; NC H1N1 infected mouse, 48hpi (arrows; 20x).

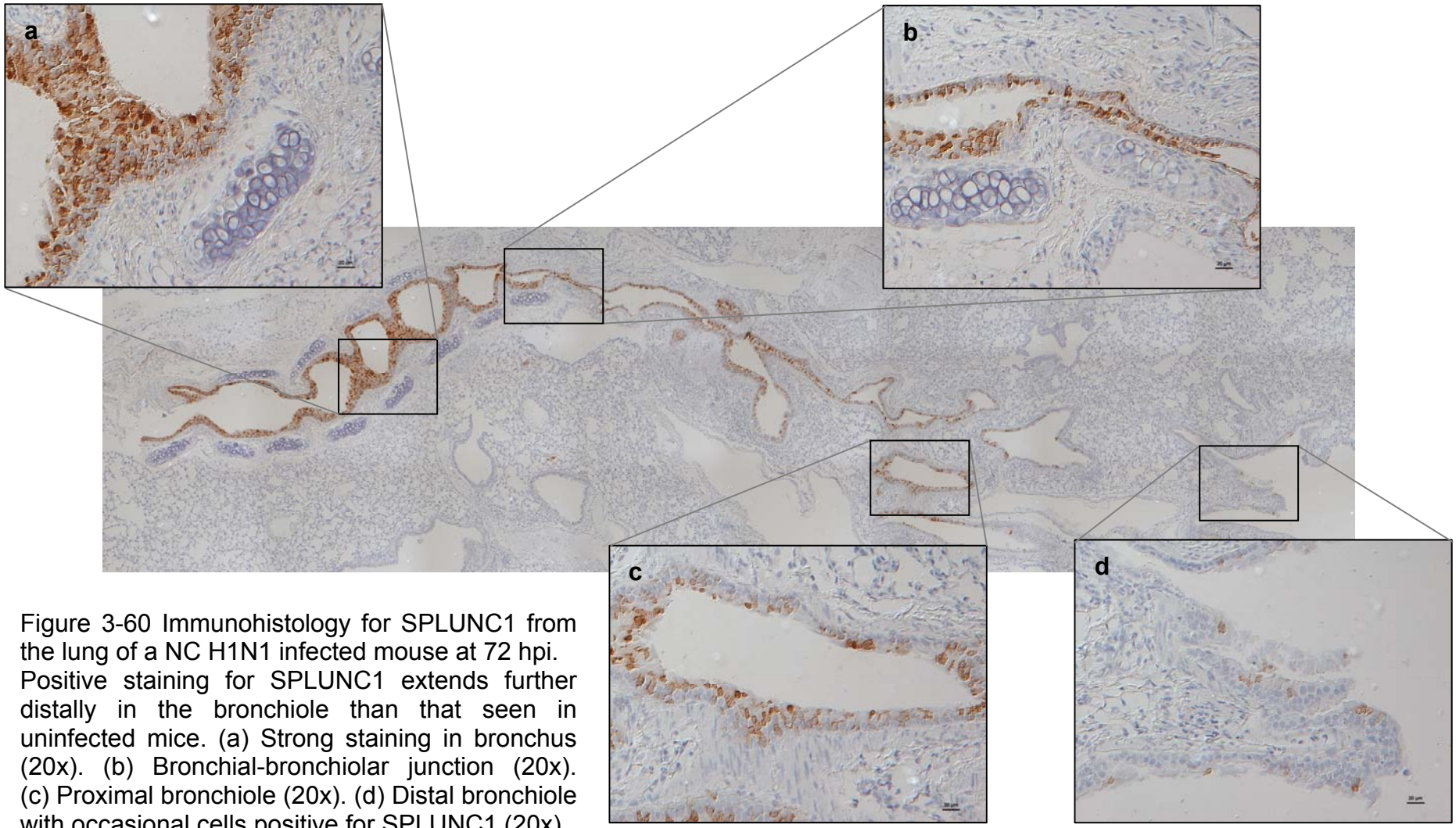

Figure 3-60 Immunohistology for SPLUNC1 from the lung of a NC H1N1 infected mouse at 72 hpi. Positive staining for SPLUNC1 extends further distally in the bronchiole than that seen in uninfected mice. (a) Strong staining in bronchus (20x). (b) Bronchial-bronchiolar junction (20x). (c) Proximal bronchiole (20x). (d) Distal bronchiole with occasional cells positive for SPLUNC1 (20x).

Chapter 4 Discussion and Conclusions

4.1 MHV-68 infection in a natural host

4.2 Protein expression in the mock-infected *Apodemus sylvaticus* lung

4.3 Influence of viral infection on the expression of CCSP

4.4 Influence of viral infection on the expression of SPLUNC1

4.5 Conclusions

4.1 MHV-68 infection in a natural host

4.1.1 Pulmonary inflammatory response to MHV-68

Experimental infection of wood mice has shown that there are significant differences between infection of *Apodemus sylvaticus* and *Mus musculus* (Hughes et al., 2010). Infectious virus is detectable in the lung for a shorter period and at a titre three folds lower in wood mice than that seen in comparable infection in BALB/c mice; however viral antigen persists for longer in the wood mouse lung and is present in the lung in macrophages and peribronchiolar and perivascular lymphocytes at 14 dpi (Hughes et al., 2010). The most dominant inflammatory feature in the lungs of wood mice at 7 dpi is the perivascular and peribronchiolar lymphocytic infiltration, which is composed predominantly of B cells; these infiltrates are far less significant in BALB/c mice (Hughes et al., 2010). At 14 dpi, BALB/c mice exhibit a mild to moderate interstitial inflammation, which is composed of both B and T cells; whereas, in wood mice, the perivascular and peribronchiolar lymphocytes remain, and in addition iBALT (which consists predominantly of B cells and exhibits germinal centre formation) is seen (Hughes et al., 2010).

4.1.2 The effect of the M3 protein

The *M3* gene of MHV-68 encodes a unique viral chemokine binding protein, which binds to a wide range of chemokines *in vitro* and *in vivo* (Table 1-3) and subsequently has the potential to alter the inflammatory response to MHV-68 infection. M3 has been shown to bind a range of T cell chemokines, but does not bind, or inefficiently binds, B cell chemokines (Parry et al., 2000; van Berkel et al., 2000). Considering the prevalence of B lymphocytes in the inflammatory response in the lungs of MHV-68 infected wood mice, the action of this gene was investigated using MHV-68 with a stop codon inserted in the *M3* gene (M3.stop), disabling expression of the chemokine binding protein (van Berkel et al., 2002). In the M3.stop infected wood mice, the B cell dominated infiltrates were replaced with mixed B and T cell infiltrates, and the iBALT seen at 14 dpi in the wild type infected wood mice was absent (Hughes, 2006). This is consistent with the alteration in chemokine expression in the absence of M3 compared to wild type MHV-68 infection, which consisted of increased levels of the T cell recruiting chemokines MIP-1α, RANTES, and

MIP-3β and the decrease in the B cell attracting SDF-1α and BLC, (Hughes, 2006). As the B lymphocyte is a major site of latency for this virus, recruitment of this cell type to the site of infection clearly confers a survival advantage for MHV-68, the role cited as the evolutionary stimulus for these proteins (Alcami, 2003). This suggests that M3 plays an important role in the pathogenesis of MHV-68 infection in the wood mouse, a natural host.

In addition to the direct chemokine binding effect of M3, the presence of this protein during MHV-68 infection was also found to affect the expression of a number of host genes. These included *CCSP* (Clara cell secretory protein), *SPLUNC1* (short palate lung and nasal epithelium clone 1) and *AGR3* (anterior gradient 3). These genes were identified by microarray analysis as having higher expression in the lungs of wood mice infected with wild type (M3.MR) MHV-68, compared to M3.stop (Hughes, 2006). These data were verified using quantitative RT-PCR, to measure the levels of *CCSP* and *SPLUNC1* mRNA (James Stewart, unpublished observations). The expression of these genes and their proteins in the lung in response to viral infection has been the focus of this thesis.

4.2 Protein expression in the mock-infected *Apodemus sylvaticus* lung

4.2.1 Clara cell secretory protein

Clara cells secrete a number of proteins, including several surfactant proteins, enzymes and immunomodulatory proteins (Singh and Katyal, 2000). These cells are identified by morphological characteristics and by the presence of CCSP, most frequently by immunohistology (Pack et al., 1980; Ray et al., 1996; Ryerse et al., 2001). Clara cells are non-ciliated, with basal nuclei, abundant smooth endoplasmic reticulum and contain electron dense vesicles, which are located in the apical cytoplasm of the cell. In *Mus musculus* Clara cells are columnar, therefore in the distal respiratory tract where the ciliated cells are cuboidal, they project into the lumen of the airway. Clara cells in the wood mouse are very similar in morphology, with small apical projections in the upper respiratory tract and pronounced projections into the lumina of bronchioles (Figure 3-25).

The proportion of the respiratory epithelium which consists of Clara cells in the wood mouse identified using TEM was compared to data published for *Mus musculus*. The wood mouse differed slightly, although as the sample sizes for electron microscopy were small, these data are not statistically valid. In the mock-infected wood mouse trachea, only 28 % of epithelial cells were Clara cells, compared to 49 – 57 % in the laboratory mouse (Pack et al., 1980). Distally, there is greater similarity between the two species as wood mice had 58 % Clara cells in bronchi, compared to 46 – 61 % in laboratory mice, and in the bronchioles 75 % and 71 % of cells were Clara cells in wood mice and laboratory mice, respectively (Figure 3-23). The difference in the trachea is interesting, as this appears to be the site of greatest variation between species. For example, in humans, Clara cells are not found in the trachea or bronchi and comprise only approximately 20 % of the epithelial cells of the bronchioles (Boers et al., 1999). One of the reasons for this difference has been suggested to be due to the lack of mucous or goblet cells in the murine respiratory epithelium, and the paucity of submucosal glands compared to other species (Pack et al., 1981). The small diameter of the airway of mice means that overproduction of mucus quickly leads to obstruction of the airways. This may explain the lack of mucous cells, even in the event of allergy type stimulation, in the distal airways in this species (Evans et al., 2004).

The differences in the proportion of Clara cells in the respiratory epithelium within each anatomical location as identified by TEM, was similar to the percentage of area stained for CCSP using immunohistology, in the mock-infected wood mice (Figure 3-6). These data reflect the area within the cells which contain CCSP, not the cell as a whole, and subsequently the figures are lower. There were also differences between the day 7 and day 14 pi wood mice, which suggests that the intranasal instillation of PBS had an effect on the expression of CCSP (Figure 3-8 and Figure 3-10). Nevertheless, the percentage area stained for CCSP increased significantly between the trachea and bronchi, and the bronchi and bronchioles ($p=0.003$ and $p=0.001$, respectively; Figure 3-7). This is consistent with the number of Clara cells increasing in a similar manner (Figure 3-23). Interestingly, the intensity of staining for CCSP also increased significantly in the distal respiratory tract

(trachea and bronchi, p=0.001; bronchi and bronchioles p=0.001 [Figure 3-7]). This implies that aside from the number of Clara cells increasing in the distal airway, they are also more productive.

In situ hybridisation for *CCSP* showed that the gene was constitutively transcribed at all levels of the respiratory tract. However, the proportion of cells positive for signal for *CCSP* mRNA varied greatly with relatively few positive cells in the trachea, increasing distally to the bronchioles where cells were frequently positive (Figure 3-4). This is consistent with the increased intensity of immunohistological staining in this location. The anatomical variation in the frequency of cells exhibiting mRNA signal is the most likely explanation for the variation in the quantitative RT-PCR results (Figure 3-1), as, although these results were normalised against the housekeeping gene *RPL8*, this gene is expressed in all cells and does not differentiate between alveolar cells and respiratory epithelium. Therefore the number of bronchioles in the sample could differ, in addition to variation due to the inclusion or otherwise of bronchial tissue.

In summary, Clara cells in wood mice showed similar morphology to laboratory mice. The number of Clara cells (shown by transcription of *CCSP*, presence of CCSP by immunohistology and morphology) increased from approximately one in four cells in the trachea to three in four cells in the bronchioles. The intensity of staining for CCSP was also greatest in the bronchioles, suggesting that this anatomical location is the major site of production of this protein.

mRNA extracted from the lungs of wood mice was used to generate cDNA which was amplified, cloned and sequenced to obtain the cDNA sequence for CCSP from *Apodemus sylvaticus*, which has been submitted to Genbank. The cDNA sequences revealed highest homology with other rodent species (Figure 3-26). Translation of the cDNA to obtain the amino acid sequence showed similarly high homology with other rodent species (*Rattus norvegicus* 86 %, *Mus musculus* 87 %, *Mesocricetus auratus* 79 % and *Neomotodon alstoni* 74 %; Figure 3-28). The 19 amino acid signal peptide is almost completely conserved within these species, with the exception of a single amino acid (3rd;

valine in the wood mouse, isoleucine in other rodents) and *Neotomodon alstoni* has a shorter, 16 amino acid signal peptide (Macias et al., 2004). *CCSP* is encoded across three exons; the signal peptide is encoded within the first exon at the amino terminus and directs the protein to the endoplasmic reticulum for post-translational modification. The signal peptide is then cleaved prior to secretion (Gupta and Hook, 1988; Stripp et al., 1994). The second exon encodes the majority of the mature protein (61 amino acids), of which four in the wood mouse are not conserved in any of the other rodent species (Figure 3-28). All of the remaining amino acids in this region are homologous with at least one of the rodent species. The remaining 16 amino acids are encoded by exon three, which represents the carboxyl terminal portion; this includes a conserved cysteine which is required for the stabilisation of homodimers. Once secreted, CCSP is present as a homodimer (Stripp et al., 1994). The similarity of the rodent species' CCSP, and the differences from the protein in other mammals, is demonstrated by the clustering of the rodents in the phylogenetic tree in a separate clade from the other mammals (Figure 3-29). Similarly, this demonstrates the homology between *Apodemus sylvaticus, Mus musculus* and *Rattus norvegicus*.

4.2.2 Short palate lung and nasal epithelium clone 1

SPLUNC1 is abundantly and uniformly expressed in the trachea and bronchi of *Mus musculus*. Distal to the division of the mainstem bronchi, expression decreases abruptly. Epithelia within the terminal bronchioles, respiratory bronchioles and alveoli are negative (LeClair et al., 2001; Weston et al., 1999). The precise cellular location of *SPLUNC1* transcription is poorly characterised in mice, with descriptions of strong uniform staining of the respiratory mucosa (LeClair et al., 2001). In contrast, human respiratory epithelium appears to be a relatively minor site of SPLUNC1 expression, with occasional non-ciliated cells being described as positive in the trachea, but the main source in the upper respiratory tract are the submucosal glands and the associated ductular epithelium (Bingle et al., 2005; Campos et al., 2004; Di et al., 2003). However, there are conflicting reports as to whether it is the mucous or serous glands which express SPLUNC1, with both types being described as either positive or negative by different authors (Bingle et al., 2005; Campos et al., 2004; LeClair

et al., 2001). These glands are more numerous in humans than in mice, which may be the reason for the higher levels of *SPLUNC1* transcription in the respiratory epithelium in mice (Campos et al., 2004).

In the wood mouse, immunohistology for SPLUNC1 protein revealed cells of the respiratory mucosa in the trachea and bronchi were frequently, but not uniformly, stained (Figure 3-13a). Within these cells, those that are stained for SPLUNC1 show lack of cilia and small apical protrusions into the lumen of the airway, characteristic of Clara cells. In the bronchi, the number of cells positively stained for SPLUNC1 is very similar to the trachea (Figure 3-13b). The percentage area stained within the trachea and bronchi are 81.7 % and 81.1 %, respectively (Figure 3-14b). Therefore, many more cells are identified as containing SPLUNC1 than are positive for CCSP in these locations. As a visual comparison between the marker of Clara cells (CCSP) and cells which transcribe *SPLUNC1*, combined immunohistology for CCSP and RNA-*in situ* hybridisation for *SPLUNC1* was performed (Figure 3-18). This showed that cells which transcribed *SPLUNC1* included Clara cells, but occasionally other cells which were CCSP negative also transcribed *SPLUNC1.* These CCSP negative cells are non-ciliated and morphologically similar to Clara cells. This suggests that not all Clara cells in the trachea and bronchi may stain for CCSP constitutively, and that Clara cells are one of the major sources of SPLUNC1 in the respiratory epithelium of the wood mouse.

In addition to the respiratory mucosa, the submucosal glands are a source of SPLUNC1 in both the laboratory mouse and in humans. Within the submucosal glands in the respiratory tract of wood mice, cells were variably either strongly stained or negative (Figure 3-13a,b). Identification as to whether the SPLUNC1 positive cells are mucous or serous cells is problematic, as both cell types are often present within single acini. An attempt to clarify this was made using an Alcian blue - periodic acid Schiff (AB-PAS) stain, which stains polysaccharides and therefore highlights mucus. This showed that although PAS positive cells in the respiratory mucosa were also SPLUNC1 positive, within the submucosal glands the PAS positive cells appeared to be less strongly stained for SPLUNC1 (Figure 3-19). Some cells within the glandular

acini which were PAS negative (and therefore are most likely serous cells) were also positive for SPLUNC1 (Figure 3-19). In addition, in the submucosal glands of IFNγR$^{-/-}$ mice, cells with serous type morphology were strongly positive for SPLUNC1 and adjacent mucous cells were negative (Figure 3-41d). The conflicting reports in the literature suggest that the cell type which secretes SPLUNC1 may vary between species, or under different influences, with both serous and mucous cells having the ability to express SPLUNC1.

In the bronchioles both the intensity of staining and the percentage area stained for SPLUNC1 was significantly lower than in the bronchi (Figure 3-14). In the proximal bronchioles relatively frequent epithelial cells are positive and staining is quite strong, but these both decrease rapidly in the distal bronchiole (Figure 3-13c,d). This is in contrast to *Mus musculus*, in which the airways are negative for SPLUNC1 distal to the mainstem bronchi (LeClair et al., 2001; Weston et al., 1999), and humans, which also do not express SPLUNC1 in bronchioles in non-diseased states (Bingle et al., 2005). In the wood mouse bronchioles, non-ciliated cells are stained for SPLUNC1, suggesting that Clara cells are the source of the protein. However, signal for *SPLUNC1* mRNA detected by *in situ* hybridisation was very low in the bronchioles of mock-infected wood mice (Figure 3-11c). This suggests that either the protein is not transcribed in these cells, or that the levels of transcription in the non-diseased lung are very low and the protein is stored intracellularly. The dramatic difference in the transcription of *SPLUNC1* between the bronchi and the distal bronchioles may explain the wide range of values obtained by quantitative RT-PCR in mock-infected mice (Figure 3-2).

In summary, SPLUNC1 is expressed at higher levels in the upper respiratory tract, specifically in the trachea and the bronchi. Both non-ciliated cells in the respiratory mucosa and the submucosal gland epithelium are shown to transcribe and translate the gene. The precise type of glandular cell (i.e. serous or mucous) is not clear, but it is likely that both express SPLUNC1 in the wood mouse. Additionally, in the wood mouse, SPLUNC1 protein is constitutively present in the bronchiolar epithelium, which is in contrast to *Mus musculus* and humans.

mRNA extracted from the lungs of wood mice was used to generate cDNA, which was amplified, cloned and sequenced to obtain the cDNA sequence for SPLUNC1 from *Apodemus sylvaticus*, which has been submitted to Genbank. The cDNA sequences revealed greatest homology with other rodent species (Figure 3-30). Translation of the cDNA to obtain the amino acid sequence showed similarly high homology with other rodent species (*Rattus norvegicus* 87 %, *Mus musculus* 92 %), with lower homology with non-rodent mammalian species (pig, cow, human; Figure 3-30). SPLUNC1 comprises nine exons, of which exons 2 - 8 are coding and exons 1 and 9 are non-coding (LeClair et al., 2001; LeClair et al., 2004). The signal peptide (19 aa) is encoded in the 2nd exon and is almost completely conserved between *Apodemus sylvaticus* and the other rodent species examined, with the exception of the loss of an amino acid at position 8 in the *Apodemus sylvaticus* sequence (Figure 3-32). The second exon is enlarged in the *Mus musculus* and *Rattus norvegicus* and this enlargement is also present in the sequence for *Apodemus sylvaticus* (Figure 3-32). This region contains a repeat sequence [G($^{L}/_{P}/_{Q}$)($^{P}/_{L}$)LPL] which is repeated four times in the house mouse and the wood mouse, and three times in the rat protein (Larsen et al., 2005). That this repeat is not present in any of the other *PLUNC* genes suggests that this sequence is not essential to the function of the protein (Larsen et al., 2005). This difference most likely represents a deletion within the protein of humans and other species (Bingle and Bingle, 2000; LeClair et al., 2001). Towards the carboxyl terminal portion two conserved cysteine residues are present and are also conserved in the wood mouse, at amino acids 203 and 244; these are of interest as they are homologous to those required for the binding between the N-terminal domain of BPI and LPS (Larsen et al., 2005). The similarity of the rodent species' SPLUNC1, and the differences with other mammals, is demonstrated by the clustering of the rodents in the phylogenetic tree (Figure 3-33). Similarly, this demonstrates the homology between *Apodemus sylvaticus*, *Mus musculus* and *Rattus norvegicus*.

4.2.3 AGR2 and AGR3

AGR2 is associated with the secretion of mucin in the goblet cells of the small intestine of mice (Park et al., 2009; Zhao et al., 2010) and in Clara cells with

the differentiation of these cells to a goblet cell phenotype in a murine model of goblet cell hyperplasia in response to allergen exposure (Chen et al., 2009; Curran and Cohn, 2010; Park et al., 2007). In humans, AGR3 has been described as homologous to AGR2, but this has not been confirmed in mice (Fletcher et al., 2003; Persson et al., 2005). AGR2 is present in neoplasms of other secretory organs, including prostate gland and breast carcinomas (Fletcher et al., 2003; Persson et al., 2005; Zhang et al., 2005).

In uninfected wood mice, AGR2 was present at all levels of the respiratory tract, and in both the respiratory epithelium and the submucosal glands in the trachea (Figure 3-20a,b and Figure 3-21). Within the bronchiolar epithelium, the protein was localised to the non-ciliated cells, which is consistent with the reports in the literature cited above that this gene is associate with secretion of proteins or mucins (Figure 3-21b).

AGR3 showed a similar distribution in the uninfected wood mouse (Figure 3-22a,b); *in situ* hybridisation showed that the gene was transcribed in the respiratory and submucosal gland epithelium in the trachea and also within the bronchiolar epithelium. This gene was less frequently detected than *AGR2.*

Limited analysis as to the effect of infection on the expression of these genes was performed, due to the limited amount of tissue available. On the small sample sizes studied, AGR2 appeared to be downregulated in the trachea and the bronchiole at 14 dpi following infection (Figure 3-20c,d), which was in contrast to AGR3, which appeared to be upregulated in the trachea in M3.MR infection, but downregulated following M3.stop infection (Figure 3-22c,d). However, further analysis needs to be performed to confirm these results. Work is underway to further describe the distribution of these genes in the mouse and the effect of viral infection on their transcription.

4.3 Influence of viral infection on the expression of CCSP

CCSP has a postulated role as an anti-inflammatory protein, although the mechanisms of induction or function of this role are poorly understood. Investigation of the action of CCSP in response to viral infection, to date, has

focused on the use of CCSP$^{-/-}$ mice and the examination of the alteration in the inflammatory response in the absence of CCSP. Both adenovirus and Human respiratory syncytial virus infection in CCSP$^{-/-}$ mice led to increased inflammatory responses in the lung (Harrod et al., 1998; Wang et al., 2003). In adenovirus infection, lack of CCSP was associated with increased inflammatory cell counts in BAL fluid and more extensive infiltration of lung tissue by inflammatory cells, along with increased transcription of pro-inflammatory chemokines and cytokines (Harrod et al., 1998). Similarly, following HRSV infection, mice lacking CCSP showed increases in numbers of inflammatory cells in the BAL fluid, increased peribronchiolar infiltrates and increased chemokine levels (Wang et al., 2003). Furthermore, restoration of CCSP by intra-tracheal instillation of recombinant human CCSP prior to infection with HRSV, lead to abrogation of these increased inflammatory responses (Wang et al., 2003).

A similar response in CCSP$^{-/-}$ mice infected with *Pseudomonas aeruginosa* was also observed, with increased neutrophils and cytokines (TNFα and IL-1β) in BAL fluid. Moreover, in the simultaneously infected wild type mice, a decrease in both CCSP and *CCSP* mRNA in lung homogenates was seen, from as early as 6 hpi. The decreased levels of protein persisted for at least the first 5 days pi, but were restored to pre-infection levels by day 14 pi (Hayashida et al., 2000). The decrease in protein preceded the decrease in mRNA, suggesting that the reduction in protein was mediated by the viral infection. Reduction of CCSP due to Clara cell loss was discounted, as other Clara cell proteins were unaffected, and there was no histological evidence for necrosis or other forms of cell loss (Hayashida et al., 2000).

In the MHV-68 infected wood mice, the most remarkable changes in the expression of CCSP were seen in the bronchiolar epithelium (when analysed by quantification of immunohistological staining). This is perhaps not surprising, as the peribronchiolar tissue is the most frequent site of infection by MHV-68; the respiratory epithelium in the upper respiratory tract is anatomically remote from the inflammatory response. Additionally, this is the site of the greatest number of CCSP expressing Clara cells. In the bronchioles

of both M3.MR and M3.stop infected wood mice there were significant decreases in both the intensity of staining and the percentage area of tissue stained at 7 dpi (Figure 3-8), with an increase at 14 dpi (Figure 3-10), compared to mock-infected controls at each timepoint. Other significant changes were also seen in the trachea at 7 dpi, which also exhibited decreases in both intensity of staining and percentage area stained in response to infection (Figure 3-8). This is consistent with the findings of Hayashida et al. (2000), in that there is a decrease in the acute stages of bacterial infection followed by an increase at a later timepoint. A proposed mechanism for the decrease following acute infection with *Pseudomonas aeruginosa* has been suggested, in which TNFα induces a decrease in CCSP via decreased regulation of the CCSP promoter (Harrod and Jaramillo, 2002). At 14 dpi there remains an inflammatory response in the lungs of MHV-68 infected wood mice, but there is a decrease in interstitial infiltrates and granulomatous infiltrates, compared to 7 dpi, and inflammatory infiltrates in the lung continue to decrease beyond day 14 pi (Hughes et al., 2010). Thus, the increase in CCSP is associated with the time period in which the inflammatory response starts to subside. This increase in CCSP and its association with decreased inflammation is consistent with the viral infection of $CCSP^{-/-}$ mice, which exhibited an increased inflammatory response, compared to the wild type mice (Harrod et al., 1998; Wang et al., 2003). These findings are consistent with the proposition that CCSP plays an anti-inflammatory role in the lung (Harrod et al., 1998; Wang et al., 2003).

In addition to a decrease in CCSP protein, Hayashida et al. (2000) also documented a decrease in *CCSP* mRNA in response to infection with *P. aeruginosa*, at early timepoints (6 hours – 5 days). In LPS-induced injury there was also a decrease in *CCSP* mRNA in the acute response (the first 24 hours), associated with an increase in inflammatory cell numbers in the BAL fluid (Arsalane et al., 2000) or pro-inflammatory cytokines (Snyder et al., 2010). In the MHV-68 infected wood mice in this study, quantitative RT-PCR showed no significant differences in mRNA copy numbers between infected and mock-infected wood mice. This suggests that either any decrease similar to those described by other authors had already occurred prior to this

timepoint, or that this was not a feature in MHV-68 infection. However, the decrease in protein levels seen at this timepoint suggests that a prior reduction in mRNA was likely to have been the case. The *in situ* hybridisation for *CCSP* mRNA at day 7 pi (Figure 3-5) shows that some cells had a higher signal for *CCSP* than that seen in many of the mock-infected mice (Figure 3-4). However, there was a marked variation in the strength of signal seen within the bronchiolar epithelium of infected mice; this has not been quantified to obtain an overall signal strength and so is difficult to interpret. There appeared to be a tendency for reduced signal for *CCSP* in bronchioles with marked peribronchiolar infiltrates (Figure 3-5). At 14 dpi, there was an increase in *CCSP* in infected wood mice, as shown by RT-PCR, however, due to the wide range of values obtained, these results were not statistically significant (Figure 3-1). However, *in situ* hybridisation at 14 dpi showed many more epithelial cells positive for *CCSP* in the bronchioles, than at 7 dpi (Figure 3-5c,d).

The examination of the morphology of Clara cells in the respiratory tract of wood mice by TEM showed that there was a decrease in the number of Clara cells in M3.MR infected mice at 14 dpi, compared to mock-infected wood mice (Figure 3-23). Due to the small sample size, however, this result should be interpreted with caution, but is of interest, due to the paradoxical increase in intensity of staining and percentage area of tissue stained at this timepoint in M3.MR infected wood mice, compared to mock-infected wood mice. Additionally, in M3.MR infected wood mice, all three of the morphological types of Clara cell described by Pack et al. (1981) were present. In mock-infected mice, the Common type was the predominant cell type, with low numbers of type II Clara cells present in the bronchi (Figure 3-24). The increase in the vesiculated type of Clara cell is of interest as Pack et al. (1981) postulated that this cell type was an intermediary in the transition between a Clara cell and a mucous cell. Evans et al. (2004) also showed that Clara cells have the potential to become mucus secreting, while retaining the molecular and functional characteristics of Clara cells. Despite mucous metaplasia not being a recognised consequence of MHV-68 infection, in light of the different Clara cell types identified ultrastructurally, an attempt to quantify goblet type cells was made. This was performed using Alcian blue and period-acid Schiff (AB-

PAS) stains combined with immunohistology for CCSP and immunohistology with an antibody to Muc5ac, the most common mucin in the lung. As AB-PAS is not specific for mucin, the staining of other polysaccharides in numerous cells occurred to some extent and therefore accurate quantification of mucus positive cells was difficult. Unfortunately, the Muc5ac antibody led to significant non-specific staining in the wood mouse tissue, which also made accurate quantification difficult. This remains an area is of interest, however, and will be pursued further.

The investigation of the expression of CCSP in the respiratory epithelium in response to MHV-68 infection has provided interesting results. To investigate whether these changes were uniquely induced by MHV-68, or were a non-specific response to viral infection in the lung, other respiratory viral infections were examined. Infection of BALB/c mice with paramyxoviruses appeared to show a correlation between the strength of immunohistological staining for CCSP and the severity of the inflammatory response (Figure 3-46 to Figure 3-50). In all mice, including the mock-infected controls, there was an initial increase in staining for CCSP at 1 dpi (Figure 3-49a). However, as this was also present in the control mice, this may be due to a local irritation effect due to the installation of PBS, or may be an artefact, similar to the vacuolisation of the epithelial cytoplasm, which was also seen in H&E stained sections (Figure 3-45a and Figure 3-46a), and is most likely due to infusion of formalin. A similar effect was also present in mice which received allantoic fluid (control animals for the influenza virus experiment) at the earliest timepoint (12 hpi; Figure 3-57a).

In the mice infected with either strain of HRSV, the inflammatory response was mild to moderate, with evidence of resolution of inflammation by 7 dpi. In these mice there were limited alterations in the expression of CCSP in the bronchioles, with the exception of scattered strongly stained cells in the HRSV-BT2a infected mice at day 7 pi (Figure 3-50). However, the intensity of staining in these tissues has not been quantitatively analysed, which may indicate differences not apparent by subjective inspection. Wang et al. (2003) reported that the lack of CCSP led to increased inflammation in HRSV infected mice,

which was abrogated by the administration of recombinant CCSP to $CCSP^{-/-}$ mice. The difference in inflammation was greatest at 7 dpi between the $CCSP^{-/-}$ mice and the wild type mice, at which timepoint the inflammatory response was subsiding in the work described here. Therefore, it would be of interest to quantify the CCSP expression at these timepoints and also at later timepoints, to see if any changes in CCSP expression correlate with the magnitude of the inflammatory response.

In contrast, the SeV infected mice exhibited a more pronounced inflammatory response, which continued to increase in severity up to and including day 7 pi (Figure 3-47). Particularly noticeable in the SeV infected mice was the decrease in the strength of staining for CCSP seen in the bronchiolar epithelium at days 5 and 7 pi, when the inflammatory response was greatest. The decrease in the CCSP was most marked in bronchioles which exhibited peribronchiolar inflammation, despite the respiratory mucosa remaining intact (Figure 3-50c,d). However, the staining in these mice has not been quantified, and so these observations are subjective. This decrease in CCSP is consistent with the finding in both the MHV-68 infected wood mice at a similar timepoint and with the findings of other authors, which demonstrated a decrease in CCSP in the lung at earlier stages following infection of mice with microorganisms (Hayashida et al., 2000).

A similar correlation between the intensity and extent of staining for CCSP and the magnitude of the inflammatory response was present in the influenza virus infected mice. Comparatively, of the strains examined, the greatest inflammatory response was observed in the HPAI H5N1 infected mice and the least in LPAI H5N1 infected mice. H1N1 strains led to an intermediate response (Figure 3-57 and Figure 3-58). Lung tissue from these experiments was sampled during the first 72 hpi, and there was little difference in the distribution of staining for CCSP at the early timepoints, aside from the increases seen in both infected and control animals seen at 12 hpi, mentioned above. At later timepoints (48 and 72 hpi), in bronchioles associated with peribronchiolar inflammation, there was a decrease in the intensity of staining for CCSP, seen in mice infected with Ca H1N1, NC H1N1 and HPAI H5N1

(Figure 3-58). This decrease was not apparent in LPAI H5N1 infected mice. Similar to the paramyxovirus infected mice, these assessments are subjective and staining for CCSP has not been quantified, which may further clarify this pattern. However, these results do suggest a decrease in CCSP at early timepoints after infection, which is associated with the inflammatory response to infection. Examination of similar tissues at later timepoints would be interesting, to investigate the pattern of CCSP expression during the resolution of inflammation.

Regulation of CCSP expression *in vivo* has been shown to be influenced by IFNγ (Magdaleno et al., 1997). Intra-tracheal instillation of IFNγ led to a seven-fold increase in CCSP and an upregulation of *CCSP* mRNA. Investigations using *in vitro* systems suggest that this upregulation was dose dependent and instigated via HNF3β and the Jak/STAT1 pathway (Magdaleno et al., 1997; Yao et al., 1998a). Interestingly, production of IFNγ by stimulated peripheral blood mononuclear cells and lymphocytes, has been shown to be inhibited by the presence of CCSP, *in vitro* (Dierynck et al., 1995). This feedback mechanism has been suggested to be important in the regulation of inflammatory responses in the lung (Mukherjee et al., 1999). IFNγR$^{-/-}$ mice have been used to investigate the role of IFNγ in the response to viral infection. Previously, MHV-68 infection of IFNγR$^{-/-}$ mice has been shown to result in productive infection in the lung, with no difference in the viral titre or viral clearance compared to wild type mice (Dutia et al., 1997). Infection of IFNγR$^{-/-}$ mice with MHV-68 in the current study led to a more severe inflammatory response than that present in the wild type mice, both at 8 and 12 dpi (Figure 3-34 to Figure 3-37). In the IFNγR$^{-/-}$ mice, the inflammation was more widespread, and at 12 dpi consisted of macrophage dominated infiltrates in addition to the lymphoplasmacellular infiltrates seen in both wild type and knockout mice. Immunohistology for CCSP was quantitatively analysed and revealed that there was a significant decrease in the intensity of staining for CCSP in the bronchiolar epithelium in the IFNγR$^{-/-}$ mice, compared to the wild type mice, at all timepoints (Figure 3-39). Within the proximal respiratory tract, intensity of staining for CCSP was also reduced in the knockout mice, but these differences were not significant. Interestingly, the percentage area

stained in the bronchiolar epithelium was very similar between the wild type and the knockout mice, suggesting that the Clara cells retained the production of CCSP in the absence of IFNγ, but at reduced levels (Figure 3-39). This decrease in the intensity of CCSP in the mice lacking the ability to respond to IFNγ, suggests that IFNγ plays a role in the expression of CCSP, consistent with the findings of Magdaleno et al. (1997). However, as this decrease is also present in the uninfected IFNγR$^{-/-}$ mice, this also occurs in the absence of an inflammatory response. Moreover, the lack of IFNγ signalling led to a decrease in CCSP, compared to that seen in the wild type mice, but expression of the protein is not completely abrogated. If the extent of the inflammatory response influences the expression of CCSP, which has been observed in the other experiments in this work, the greater extent of the inflammation in the IFNγR$^{-/-}$ mice may also have a role in determining the level of CCSP expression in these mice. This is emphasised when the data is compared for either wild type or knockout mice over the time course of infection (Figure 3-40). This shows that in both groups of mice, there is a decrease in both the intensity of staining, and initially, in the percentage area of tissue stained. Interestingly, the percentage area of tissue stained for CCSP shows a significant increase in the bronchioles of both wild type and knockout mice between 8 and 12 dpi. It is possible that this is the first sign of a later increase in CCSP, similar to that seen in the MHV-68 infected wood mice, and described by Hayashida et al. (2000) in *P. aeruginosa* infected mice at later timepoints. However, in the work by Hayashida et al., this increase was associated with complete resolution of the inflammatory response, whereas in the MHV-68 infection of wood mice and the 129 wild type and IFNγR$^{-/-}$ mice there remains a significant inflammatory response. Examination of later timepoints in this model would be worthwhile. The stimulus for this increase in CCSP is not clear, but coincides with the decline in viral titre in the lung in both models (Dutia et al., 1997; Hughes et al., 2010). Therefore, either the decline in viral titre, or changes associated with this decline, for example in cytokines, chemokines or other inflammatory mediators, may be implicated.

The initial impetus for this work was the finding of Hughes (2006) that wood mice infected with MHV-68 virus lacking the *M3* gene resulted in lower levels

of CCSP, than mice infected with the wild type MHV-68, at 14 dpi. Quantitative analysis of immunohistology for CCSP has shown that, in the bronchioles both the intensity of staining and the percentage area of tissue stained were significantly reduced in M3.stop infected mice, compared to M3.MR at 14 dpi (Figure 3-10). In addition, at 7 dpi, the intensity of staining was also reduced in M3.stop infected wood mice, although there was no significant difference in the percentage area stained (Figure 3-8). This suggests that the presence of the M3 protein resulted in an elevation of the expression of CCSP (Hughes, 2006). However, the overall response in CCSP expression in comparison to mock-infected wood mice was similar in both M3.MR and M3.stop infection, i.e. CCSP was significantly lower in infected wood mice compared to mock-infected wood mice at 7 dpi, and increased at 14 dpi. M3 has been found to be expressed at both timepoints, but was significantly higher than other MHV-68 genes (M1, M2 and M4) at 14 dpi and *M3* mRNA is expressed predominantly within lymphocytes in perivascular and peribronchiolar infiltrates, as well as in granulomatous infiltrates and iBALT (Hughes, 2006). As M3 is a secreted protein, it is possible that the protein itself may have a direct effect on Clara cells and the expression of CCSP. However, as *M3* transcripts are located within inflammatory cells, and MHV-68 does not infect the bronchiolar epithelium, this appears to be unlikely. In addition, this does not explain why there would be an initial decrease in CCSP in the lungs of infected wood mice at 7 dpi (compared to mock-infected wood mice). In the lung of wood mice, infection with M3.stop was found to result in lower viral titres at 14 dpi, possibly as a result of the increased numbers of T cells associated with the absence of M3 (Hughes, 2006). This may be implicated in the lower levels of CCSP present in M3.stop, compared to M3.MR infected wood mice; however, comparative data for viral titres at day 7 were not available. These variations in inflammatory response and viral titre between M3.MR and M3.stop infection at 14 dpi did not influence the levels of IFNγ in the wood mice (Hughes, 2006). Therefore, the influence of IFNγ on CCSP discussed previously is unlikely to be a significant factor in the differences seen with the presence or absence of M3. Previously it has been suggested that one of the immunomodulatory roles of CCSP may be in the regulation of BALT, due to the increase in *IgA* mRNA positive lymphocytes in $CCSP^{-/-}$ mice, which was considered to be consistent

with the diffuse localisation of BALT (Watson et al., 2001). However, this is not consistent with the finding that wild type MHV-68 (M3.MR) infection is associated with the induction of BALT, which is generally uncommon in mice, and is absent in M3.stop infected wood mice (Hughes, 2006), as M3.MR infection results in higher CCSP expression. The function of M3 as a chemokine binding protein results in decreased levels of several T cell chemokines and subsequently, an altered composition of the inflammatory cell response in the lung (Hughes, 2006). Therefore it is possible that either the increased number of B lymphocytes, or the relatively higher levels of the associated chemokines (BLC and SDF-1α), led to the increased expression of CCSP. Alternatively, the decreased levels of numerous chemokines bound by M3 (e.g. MIP-1α, MIP-1β, MIP-2, MIP-3α, MIP-3β, MIG, RANTES, KC) in wild type MHV-68 infection are associated with the increased levels of CCSP. As it has been shown that CCSP is associated with decreased inflammation in viral infection (Harrod et al., 1998; Wang et al., 2003), and increases as the inflammatory response resolves (Hayashida et al., 2000), an association with altered chemokine signalling is possible. Virally infected $CCSP^{-/-}$ mice exhibited an increase in MIP-1α and MIP-2 (Harrod et al., 1998; Wang et al., 2003), two of the chemokines also increased in M3.stop infected mice (Hughes, 2006). This suggests that MHV-68 M3 and CCSP may therefore act in a similar manner, which is advantageous in manipulating the host response in favour of the establishment of viral infection. However, it is not possible to say at this stage whether the increase in CCSP is the cause of the decrease in inflammation, or is stimulated by the decrease in mechanisms associated with inflammation.

In vitro infection of 293T cells (which had been transfected with a vector containing either *CCSP*, *SPLUNC1*, *SPLUNC1* Cys mutant or *AGR3* genes) showed that only *CCSP* transfected cells had an effect on the rate of infection with MHV-68. In these cells, the rate of infection was significantly lower than in cells which were transfected with an empty vector. In contrast, the addition of CCSP to encephalomyocarditis virus infected monocytes *in vitro* was associated with reduced IFNγ-mediated anti-viral activity (Dierynck et al.,

1995). However, as it was not possible to confirm that the transfected cells were expressing CCSP, this finding requires further investigation.

In summary, CCSP expression is altered following infection with the respiratory viruses investigated in this study. At earlier timepoints, a reduction of expression occurs, most notably within the bronchiolar epithelium. This reduction has an association with the presence of pronounced inflammatory infiltrates. At later timepoints in MHV-68 infection, there is an increase in CCSP expression in the bronchioles. This increase may be associated with the resolution of the inflammatory response. MHV-68 M3 protein and IFNγ are both associated with increases in CCSP expression at all stages of infection.

4.4 Influence of viral infection on the expression of SPLUNC1

The palate lung and nasal epithelium clones (PLUNC) family of proteins are expressed in the epithelium of the oral, nasopharyngeal and respiratory epithelium (Bingle et al., 2004). Their predicted structural similarity to BPI and LBP led to the suggestion that these proteins would have an anti-inflammatory role (Bingle and Craven, 2004). Within this family of proteins, SPLUNC1 is a "short" PLUNC, meaning it displays homology with the N-terminal domain of BPI only (Bingle and Craven, 2003). Essential for the binding function between BPI and LPS are two conserved cysteine residues (Larsen et al., 2005), which are also conserved in *Apodemus sylvaticus* (Section 4.2.2).

Investigation of SPLUNC1 in naturally occurring disease has found that this protein is variably both increased and decreased in different conditions. Chronic exposure to epoxy resin in chemical workers, cigarette smoking and seasonal allergic rhinitis are all associated with a decrease in SPLUNC1 in nasal or BAL fluid (Ghafouri et al., 2002; Ghafouri et al., 2003; Ghafouri et al., 2006; Lindahl et al., 2001). In contrast, increases in SPLUNC1 in the small airways have been reported in patients with cystic fibrosis and progressive cases of idiopathic pulmonary fibrosis (Bingle et al., 2007; Boon et al., 2009). In COPD patients, SPLUNC1 was found to be increased in sputum samples (Di et al., 2003). *In vitro* investigation of the potential effect of SPLUNC1 in viral

infection, using EBV transformed B cells, showed that SPLUNC1 was associated with decreased survival of these cells in culture (Zhou et al., 2008).

Immunohistology for SPLUNC1 in the lungs of wood mice infected with MHV-68 showed that the infection altered the expression of this protein. At 7 dpi, the bronchioles exhibited a significant decrease in both the intensity of staining and the percentage area stained, following infection with either M3.MR or M3.stop (Figure 3-15). This may be expected as this is the location closest to the site of infection, and the consequential inflammatory response. However, the bronchioles show the least significant expression of SPLUNC1 in the respiratory tract. Elsewhere in the respiratory tract, the trachea and the bronchi showed no significant differences between mock-infected and infected wood mice (Figure 3-15). At 14 dpi the response was very different. In response to infection with M3.MR there was a significant increase in the intensity of staining at all levels of the respiratory tract, and significant increases in the percentage area of tissue stained in the bronchi and the bronchioles (Figure 3-16). This is interesting, as the effect of infection extends beyond the site of the inflammatory response, suggesting that it is unlikely that this is a direct effect of the presence of the virus, which is predominantly found within the inflammatory cell infiltrates in the lung. Therefore, the increase in SPLUNC1 in the upper respiratory tract is most likely due to an indirect response to the viral infection. This pattern of expression of SPLUNC1, namely a decrease at 7 dpi, followed by an increase at 14 dpi, is similar to that observed in this study for CCSP. *Mycoplasma pneumoniae* infection in mice has been associated with an increase in *SPLUNC1* mRNA in the peracute stage (4 hpi), but with no discernable difference at 72 hpi (Chu et al., 2007). In the current study, comparable early timepoints have not been studied, but it is possible that the decrease in *SPLUNC1* expression between 4 and 72 hpi continues, resulting in an overall decrease at 7 dpi, compared to mock-infected mice. In *Mycoplasma pneumoniae* infection, the ablation of SPLUNC1 using intra-tracheally instilled antibodies to the protein, or infection of SPLUNC1$^{-/-}$ mice, resulted in increased inflammatory responses at early timepoints (1 dpi), ascertained by increased neutrophils in BAL fluid (Chu et al., 2007; Gally et al., 2010a). This suggests that SPLUNC1 has an anti-inflammatory effect, which is

supported by the finding that in transgenic mice which overexpressed SPLUNC1, *Mycoplasma pneumoniae* infection resulted in reduced pro-inflammatory cytokines (KC and IL-6) in BAL fluid at 1 dpi (Gally et al., 2010a). These data support the assertion that SPLUNC1 has an anti-inflammatory effect in the lung, therefore a mechanism may occur to downregulate the expression of this protein in the acute and subacute stages of infection, to permit a meaningful inflammatory response to clear the infectious agent (Curran et al., 2009). This hypothesis is consistent with the observed changes in MHV-68 infected wood mice. Alternatively, SPLUNC1 can be interpreted as being critical in the elimination of the infectious agent, as ablation of SPLUNC1 also led to increased numbers of *Mycoplasma pneumoniae*, and overexpression of SPLUNC1 to a decrease in the numbers of bacteria, in the same experiments (Chu et al., 2007; Gally et al., 2010a).

Due to the observed alterations in the quantity of SPLUNC1 in response to infection with MHV-68, corresponding alterations in *SPLUNC1* mRNA would also be expected. Assessment of mRNA copy number by quantitative RT-PCR resulted in large variation within the groups and no significant differences were found (Figure 3-2). This may be due to variation between individual mice, or variation between tissue samples in the quantity of bronchiolar and/or bronchial epithelium. Analysis of the location of *SPLUNC1* transcription by *in situ* hybridisation revealed that bronchiolar epithelial cells were very rarely positive for *SPLUNC1.* There was little difference in signal between the bronchioles of mock-infected, M3.MR or M3.stop infected wood mice (Figure 3-11 and Figure 3-12). This was an unexpected result, as an increase in SPLUNC1 within bronchiolar epithelium at 14 dpi was thought most likely to be due to upregulation of transcription of *SPLUNC1* in this location at this timepoint. To further clarify this, combined immunohistology for SPLUNC1 and *in situ* hybridisation for *SPLUNC1* was performed on the same section of lung (Figure 3-17). This showed that in the bronchus and the proximal bronchioles, both *SPLUNC1* mRNA and SPLUNC1 protein were present simultaneously. However, in the distal bronchioles, despite the presence of SPLUNC1 in both the respiratory epithelium and within the lumen, no evidence of transcription of SPLUNC1 was present. This suggests that either *SPLUNC1* transcription had

occurred previously and the protein had been stored intracellularly, or transcription and translation of the protein had occurred elsewhere. However, as the ciliated epithelium functions to transport mucus, cellular debris and other material from distal airways up and out of the respiratory tract, movement of a secreted protein from the proximal to the distal airway seems unlikely. Bronchiolar expression of SPLUNC1 is uncommon in other species. The presence of SPLUNC1 in the lumen of human small airways has been shown to occur in the absence of epithelial staining (Campos et al., 2004). However, these authors did not discuss the origin of the protein within bronchiolar lumen. SPLUNC1 was found not to be expressed in the small airways (defined as those without cartilage or submucosal glands and therefore analogous to bronchioles in this study) of "normal" human lung, or in the lung of patients with bacterial pneumonia (Bingle et al., 2007). However, in cystic fibrosis, the hyperplastic bronchiolar epithelium exhibits SPLUNC1 towards the apical surface of cells, along the luminal surface and within the lumen, admixed with mucus and inflammatory cells. However, confirmation of *SPLUNC1* transcription at this location was not reported (Bingle et al., 2007).

In response to infection with paramyxoviruses, the expression of SPLUNC1 within bronchioles was largely unaltered. Strong staining for the protein was present within the trachea and bronchi and within the proximal bronchiole adjacent to the bronchial-bronchiolar junction, described as the "transitionary zone". Distal to this region, very few cells were positive for SPLUNC1 either in mock-infected or infected mice (Figure 3-51). The transitionary zone was the site of differences present in the extent of staining for SPLUNC1 following infection with Influenza A viruses. Expression of SPLUNC1 appears to extend further distally within the bronchiolar epithelium following infection with NC H1N1 at 48 and 72 hpi (Figure 3-60). Conversely, in HPAI H5N1 infected mice at 72 hpi showed decreased staining in this location (Figure 3-59b). This may correlate with the differences in the severity of the inflammatory response between these two infections; HPAI H5N1 infected mice exhibited a more pronounced inflammatory response, with greater evidence of necrosis and perivascular oedema at 72 hpi, in contrast to the NC H1N1 infected mice at 72 hpi, which exhibited mild multifocal necrosis and neutrophil-dominated

infiltrates that had not progressed in severity since the previous timepoint (48 hpi). To evaluate this further, timepoints beyond 72 hpi should be examined. It is possible that increased SPLUNC1 expression may occur during the resolution of inflammation, at later timepoints, as seen in the MHV-68 infection of wood mice. In other models of disease, SPLUNC1 has been shown to be reduced in BAL fluid in mice in acute inflammation induced either by Th1 or Th2 cells (Curran et al., 2009) or LPS (Britto et al., 2010). It is also possible that alteration of SPLUNC1 expression occurred in the upper respiratory tract, however, due to the intensity of staining, this is difficult to assess subjectively and therefore, performing quantitative analysis of these results may be informative.

Regulation of SPLUNC1 expression by IFNγ has been previously suggested following work which showed that SPLUNC1 levels in BAL fluid were elevated in naive IFNγR$^{-/-}$ mice (Curran et al., 2009). In addition, failure of IFNγR$^{-/-}$ mice to exhibit alterations in SPLUNC1 in response to ovalbumin induced inflammation (Britto et al., 2010) and Th1 and Th2 cell induced inflammation, lead to the hypothesis that IFNγ inhibits SPLUNC1 to promote an effective immune response (Curran et al., 2009). However, the findings of Curran et al. (2009) that SPLUNC1 was elevated in naive IFNγR$^{-/-}$ mice is in contrast to the results obtained by quantitative analysis of immunohistological staining in this study (Figure 3-42). Both the intensity of staining and the percentage area of tissue stained were very similar in the IFNγR$^{-/-}$ and wild type mice in the trachea and bronchioles at day 0 (uninfected). Unfortunately, there was a lack of bronchial tissue in the sections analysed in these mice, so it is possible, as this is a site of significant SPLUNC1 expression, that there may be a difference between wild type and IFNγR$^{-/-}$ mice in this location.

Following infection with MHV-68, there were alterations in the expression of SPLUNC1 between wild type and IFNγR$^{-/-}$ mice. At 8 dpi there were significant differences in both the intensity of staining and percentage area of tissue stained between wild type and IFNγR$^{-/-}$ mice in the bronchus (Figure 3-42). However, the decrease in SPLUNC1 in the IFNγR$^{-/-}$ mice is in contradiction to Curran et al. (2009) and also, is contrary to the data for day 12 dpi. It should

be noted that the data for the wild type mice in this case consists of measurements from a single mouse. Therefore a larger data set should be obtained to clarify this result. At 12 dpi there was an overall pattern consistent with higher levels of SPLUNC1 in IFNγR$^{-/-}$ mice than wild type mice, suggesting that IFNγ may inhibit SPLUNC1. Intensity of staining for SPLUNC1 was significantly higher in IFNγR$^{-/-}$ mice in the trachea and the bronchioles; in the bronchi of the IFNγR$^{-/-}$ mice the increase in intensity of staining was not significant, however there was a significant increase in the percentage area of tissue stained (Figure 3-42).

In the wild type mice, infection led to decreases (although not significant) in SPLUNC1 in the trachea and the bronchi, consistent with the hypothesis of Curran et al. (2009) that SPLUNC1 regulates inflammation in the healthy lung but is reduced via IFNγ following infection to promote an effective immune response. Unfortunately, these data sets are not complete, with timepoints missing in both groups. In the IFNγR$^{-/-}$ mice, the trachea showed a significant decrease in percentage area stained between 0 and 12 dpi, however the bronchi exhibited a large significant increase in both percentage area stained and intensity of staining between 8 and 12 dpi. However, as there is no data for uninfected bronchi, it is unclear whether this represents a decrease and a recovery of SPLUNC1 secretion, or an overall increase. Furthermore, at 12 dpi there remains a significant inflammatory response in the lungs of these mice and examining the SPLUNC1 levels at later timepoints to investigate whether there is an increase in expression of the protein alongside the resolution of inflammation, similar to that observed within the wood mice, would be of great interest.

It is interesting to note that, despite the changes in the bronchioles of both IFNγR$^{-/-}$ and wild type mice being statistically significant, the changes are small and the levels are very low. This is possibly comparable to the level of expression observed in the BALB/c mice infected with SeV, HRSV and the various Influenza A virus strains. Additionally, the changes are increases in response to infection, which is in contrast to the overall picture and the findings of others (Britto et al., 2010; Curran et al., 2009). The levels are, however, low

compared to the bronchi and trachea and unlikely to affect the overall pattern of expression of SPLUNC1 in the lung if assessment was performed by a method which did not distinguish between anatomical areas, for example by analysis of BAL fluid.

MHV-68 M3 protein has previously been shown by microarray analysis to increase transcription of *SPLUNC1*. A higher level of mRNA was detected in M3.MR infected wood mice, compared to M3.stop infected wood mice at 14 dpi, although this difference was not significant (Hughes, 2006). At the similar timepoint in this study, no significant differences were present in SPLUNC1 expression as quantified by analysis of immunohistological staining, between M3.MR and M3.stop infected wood mice within the different anatomical locations (Figure 3-16). In addition, although significant differences were seen in the intensity of staining in the trachea and the bronchioles between M3.MR and M3.stop infection at 7 dpi, the intensity was higher in the M3.stop infected, not the M3.MR infected wood mice (Figure 3-15). This is unlikely to be associated with a response to IFNγ, as levels of this cytokine were similar between M3.MR and M3.stop infected wood mice (Hughes, 2006). Therefore, the results of the current study do not support a role for the M3 protein in the expression of SPLUNC1.

In summary, MHV-68 infection in wood mice provides evidence to support the hypothesis of Curran et al (2009) that SPLUNC1 expression is decreased in acute inflammation to promote an effective immune response. In this model, SPLUNC1 expression is decreased in infected mice compared to mock-infected wood mice at 7 dpi, but increases by 14 dpi, most notably in the bronchioles. This is potentially associated with resolution of inflammation. No role for the MHV-68 M3 protein was found in the expression of SPLUNC1 in the airways of infected wood mice. In respiratory virus infections other than MHV-68, at the early timepoints studied, SPLUNC1 expression in the bronchioles is very low. However, there is evidence of reduced SPLUNC1 expression with an increase in inflammatory response. IFNγ may have a role in the suppression of SPLUNC1 in infected mice; however, further work is required to complete this data set.

4.5 Conclusions

Clara cell secretory protein and short palate lung and nasal epithelium clone 1 are two proteins which are expressed in the respiratory epithelium of the lung (Bingle et al., 2004; Broeckaert et al., 2000; Reynolds et al., 2002). Investigation of the function of both proteins has produced evidence which suggests that both may have anti-inflammatory roles in response to infection with bacterial and viral pathogens (Britto et al., 2010; Curran et al., 2009; Gally et al., 2010b; Gally et al., 2010a; Harrod et al., 1998; Harrod and Jaramillo, 2002; Hayashida et al., 2000; Liu et al., 2010a; Wang et al., 2003). The genes which encode these two proteins were amongst those identified as differentially expressed in MHV-68 infection of *Apodemus sylvaticus* (wood mouse), depending on the presence or absence of the virally encoded chemokine binding protein, M3 (Hughes, 2006). *CCSP*, *SPLUNC1* and *AGR3* were found to be expressed at higher levels in wood mice infected with the wild type MHV-68 (M3.MR) than those infected with a mutant MHV-68 which did not express M3 (M3.stop). Further investigation of these results has been the focus of the current study.

Anterior gradient homologue 3 (*AGR3*) is thought to be homologous in humans to another gene, anterior gradient 2 (*AGR2*). AGR2 is associated with the post-translational modification of mucins, prior to secretion, in the small intestine and the lung (Park et al., 2007; Park et al., 2009; Zhao et al., 2010). Both genes were found to be transcribed in non-ciliated cells of the respiratory mucosa at all levels of the respiratory tract, and the submucosal glands of the upper respiratory tract of *Apodemus sylvaticus*. Overall, *AGR2* was expressed at higher levels than *AGR3*. The cellular location of gene expression was consistent with the association of these genes with secretory cells. *AGR3* was found to be upregulated in response to wild type MHV-68 infection, whereas *AGR2* expression was decreased. This suggests that these two genes differ in regulation, despite being described as homologues in humans. AGR2 has been associated with differentiation of Clara cells to goblet cells, so a reduction in expression would suggest that MHV-68 infection in *Apodemus sylvaticus* does not induce goblet cell hyperplasia (Chen et al., 2009; Park et al., 2007). This is in contrast to the increased number of vesiculated Clara cells observed

ultrastructurally in MHV-68 infected wood mice (Figure 3-24). Therefore, the increase in *AGR3* may be implicated in this morphological change, if these two genes are homologous. The sample sizes for these experiments were small, however, and further work needs to be done to confirm these initial data and investigate potential relationships between AGR3 and goblet cell hyperplasia.

The distribution and morphology of Clara cells was found to be similar in *Apodemus sylvaticus* to that described for *Mus musculus* (Pack et al., 1981). Sequencing of the gene in *Apodemus sylvaticus* revealed that *CCSP* in this species has high homology with other rodent species. In response to infection with wild type MHV-68, there was a decrease of expression of the protein in the bronchiolar epithelium at 7 dpi, followed by an increase at 14 dpi. This was a similar pattern to that seen in the infection of laboratory mice with *Pseudomonas aeruginosa* (Hayashida et al., 2000). Hayashida et al. (2000) reported that CCSP expression initially decreased, but was restored to pre-infection levels by 14 dpi, which coincided with the resolution of the inflammatory response. In other studies, lack of CCSP (in $CCSP^{-/-}$ mice) has resulted in greater inflammatory responses following infection with viral and bacterial agents and intra-tracheal administration of recombinant CCSP led to abrogation of this increased response (Harrod et al., 1998; Hayashida et al., 2000; Wang et al., 2003). This suggests that CCSP expression is reduced during the inflammatory response, but increases in CCSP levels have a role in the resolution of inflammation. At 14 dpi there remains an inflammatory response in the lungs of MHV-68 wood mice. However, the pattern of inflammation has altered from the acute response seen at 7 dpi. This suggests that in MHV-68 infection of wood mice, CCSP may have a role in the resolution of inflammation following the acute inflammatory response.

Investigation of other respiratory viral infections in *Mus musculus* (Human respiratory syncytial virus, Sendai virus and Influenza A virus) revealed a decrease in CCSP expression in the bronchiolar epithelium when infection resulted in a significant inflammatory response. This was most notable in mice infected with Sendai virus and HPAI H5N1. The timepoints studied did not

allow for investigation as to whether CCSP levels later increased with resolution of inflammation in these experiments.

Interferon γ has been suggested to have a regulatory role in the expression of CCSP, as administration of IFNγ led to an increase in CCSP (Magdaleno et al., 1997). In the current study, infection of IFNγR$^{-/-}$ mice with MHV-68 was associated with decreased CCSP levels, compared to those in wild type mice. However, this decrease in CCSP was present in both infected and uninfected mice. Therefore, this suggests that although lack of IFNγ signalling results in a decrease in CCSP expression, this effect is less significant than the overall response to the viral infection. In addition, the reduced CCSP expression in the IFNγR$^{-/-}$ mice could be associated with the increased inflammatory response observed in these mice following infection, in a similar trend to that observed in mice infected with other viral agents.

The MHV-68 M3 protein binds a range of chemokines, which *in vivo* results in reduced levels of a number of T cell chemokines in MHV-68 infected wood mice at 14 dpi (Hughes, 2006). This has been suggested to be the underlying mechanism which results in differing inflammatory infiltrates in the lungs of wood mice infected with wild type MHV-68 (M3.MR) and MHV-68 M3.stop (Hughes, 2006). The lack of functional M3 protein was also associated with decreased expression of *CCSP* (Hughes, 2006). Investigation of the effect of M3 on the expression of CCSP in the current study concurred with the findings of Hughes (2006). In the bronchiolar epithelium of wood mice infected with M3.stop, the expression of CCSP was significantly reduced compared to those infected with M3.MR. The overall pattern of CCSP expression in response to infection was similar; the M3.stop infected wood mice also showed a decrease in expression of CCSP at 7 dpi, compared to mock-infected wood mice, and an increase at 14 dpi. However, at both timepoints, lack of M3 resulted in a reduction in the expression of CCSP in the bronchioles. M3 binds a large range of chemokines (e.g. MIP-1α, MIP-1β, MIP-2, MIP-3α, MIP-3β, MIG, RANTES, KC (Hughes, 2006)) and results in a reduction of T cells in the inflammatory infiltrate and an increase in B cells. Lack of CCSP in viral infection is associated with an increase in chemokines (MIP-1α, MIP-2 (Harrod

et al., 1998)). Therefore, it is possible that the decrease in the expression of CCSP in M3.stop infected mice is related to the increased level of these chemokines. Furthermore, the trend of decreased CCSP in the presence of increased inflammatory infiltrates in several of the experiments in this work suggested that a chemokine, or another inflammatory mediator, functions to down regulate the expression of CCSP. A decrease in this mediator with the resolution of inflammation, or the clearance of the infectious agent which initiated the inflammatory response, may then result in the restoration of CCSP levels. CCSP then may later have a role in the resolution of inflammation, as has been shown in work by other authors (Wang et al., 2003).

SPLUNC1 is a member of the palate lung and nasal epithelium clones (PLUNC) family of proteins, which have a predicted spatial similarity with LPS binding protein and bactericidal/permeability increasing protein, leading to the hypothesis that they have an anti-inflammatory role in the lung (Bingle and Gorr, 2004). Sequence analysis of the protein in *Apodemus sylvaticus* showed that the gene has high homology with those expressed in other rodents, including the presence of a repeat in exon 2, also found in *Mus musculus* (Bingle et al., 2004). The expression of SPLUNC1 in the respiratory tract of *Apodemus sylvaticus* was similar to that described for other species with the exception of the bronchiolar epithelium (Bingle et al., 2005; Bingle et al., 2007; LeClair et al., 2001; Weston et al., 1999). SPLUNC1 is strongly expressed in the upper respiratory tract in the respiratory mucosa and the submucosal glands. In both humans and laboratory mice, SPLUNC1 is rarely present within the bronchiolar epithelium. Expression of SPLUNC1 has been reported in hyperplastic bronchiolar epithelium in cystic fibrosis patients (Bingle et al., 2007) and in patients with progressive idiopathic pulmonary fibrosis (Boon et al., 2009). Staining for SPLUNC1 within the mucus in the bronchiolar lumen of COPD patients has also been described (Di et al., 2003).

Investigation of SPLUNC1 expression in the lung of laboratory mice and the effect of the absence of the protein in SPLUNC1$^{-/-}$ mice has led to the hypothesis that a mechanism to downregulate the expression of this protein occurs in the acute and subacute stages of infection, to permit a meaningful

inflammatory response to clear infectious agents (Curran et al., 2009). This hypothesis is supported by the findings in the current study, in which MHV-68 infected wood mice exhibited an initial decrease in SPLUNC1 expression in the bronchioles at 7 dpi and an increase at all levels of the respiratory tract at 14 dpi, compared to mock-infected controls. This was a similar response to that seen by other authors in infection with *Mycoplasma pneumoniae*, which was associated with a decrease in the acute stages of infection (Chu et al., 2007). The alteration of SPLUNC1 expression in the bronchiolar epithelium was anatomically closest to the inflammatory response in the MHV-68 infected wood mice, and therefore may be expected. However, a parallel increase in the expression of *SPLUNC1* in these cells was not detected, at either 14 dpi or earlier timepoints. The presence of the protein in these cells cannot be explained with the results obtained in this study. As previously mentioned, SPLUNC1 has been seen in this location in human patients with cystic fibrosis, but whether the bronchiolar cells expressed the gene was not investigated in this work (Bingle et al., 2007). SPUNC1 has also been detected in mucus within the bronchiolar lumen of humans, in the absence of protein in the bronchiolar epithelium; however, the source of this protein was not discussed (Campos et al., 2004).

Investigation of the effect of other respiratory viruses on the expression of SPLUNC1 was also performed. In mock-infected BALB/c mice, SPLUNC1 expression was strong within the trachea and bronchi, but largely absent from the bronchiolar epithelium. Following infection with Influenza A viruses, there was an increase in the expression of SPLUNC1 in the proximal bronchioles in infection with one strain (NC H1N1) and a decrease in another (HPAI H5N1). A correlation between the severity of the inflammatory response and the expression of SPLUNC1 was seen, with reduced SPLUNC1 in HPAI H5N1 infection, in which the inflammatory response was greater than that observed in other strains of Influenza A viruses. This suggests that an increase in inflammatory infiltrates and the associated increase in inflammatory mediators decrease the expression of SPLUNC1. The results are consistent with the hypothesis of Curran et al (2009).

Regulation of SPLUNC1 in response to infection has been suggested to be related to IFNγ, as mice lacking the IFNγ receptor ($IFN\gamma R^{-/-}$ mice) have been shown to lack the decrease of SPLUNC1 in response to either Th1 and Th2 induced inflammation, or ovalbumin induced inflammation (Britto et al., 2010; Curran et al., 2009). Infection of $IFN\gamma R^{-/-}$ mice with MHV-68 revealed that, at 12 dpi, SPLUNC1 was increased in the absence of IFNγ signalling. These data support the findings and hypothesis of Curran et al. (2009), which suggest that IFNγ has a role in the regulation of SPLUNC1.

Previously, the virally encoded chemokine binding protein, M3, has been found to effect the expression of SPLUNC1 in MHV-68 infection (Hughes, 2006). However, this is not consistent with the findings of the current study. The pattern of expression of SPLUNC1 showed no significant difference between M3.MR infected and M3.stop infected mice. This would suggest that the mechanism which induces the alteration of expression of SPLUNC1 in response to an infectious agent is unlikely to involve the chemokines which are bound by M3.

The results of investigation into the alterations of SPLUNC1 and CCSP in response to infection with respiratory viruses in this study suggest that both of these proteins have a role in the control of inflammation in the lung. Both proteins are constitutively expressed in the respiratory mucosa, which has a fundamental role in the innate immune response and protection of the lung against infectious agents. In the acute stages of infection, reduction in the expression of both proteins occurs, which appears to correlate with the extent of the inflammatory response. This is consistent with the hypotheses of other authors, that this occurs to allow a meaningful inflammatory response to eliminate the instigating cause of the inflammation (Curran et al., 2009). The subsequent increase in expression at later stages of infection are consistent with CCSP and SPLUNC1 having an anti-inflammatory role in the resolution of inflammation (Harrod et al., 1998; Reynolds et al., 2007; Wang et al., 2003). In view of this potential anti-inflammatory role, understanding the mechanisms which control the expression of these proteins is critical in the future management of both acute and chronic inflammatory lung disease.

To further investigate the role of these proteins in the host response to viral infection in the lung, in addition to the recommendations already made to extend the work outlined in this study, utilisation of transgenic mice which do not transcribe the genes of interest could be used. Experimental viral infection of $CCSP^{-/-}$ mice has been reported using HRSV and Adenovirus, but this work although quantitative, did not examine the location of the inflammatory response (Harrod et al., 1998; Wang et al., 2003). Furthermore, investigation of the viral agents in this study which exhibit different cellular tropisms within the lung, and comparison with the response in wild type mice could be informative as to the mechanisms of CCSP regulation and function. The investigation of viral infection in $SPLUNC1^{-/-}$ mice has not yet been reported in the literature. In view of the results demonstrating the variation in SPLUNC1 expression in response to viral infection in this study, use of a transgenic mouse model to further elucidate the role of this protein should be performed.

References

Aberger, F., Weidinger, G., Grunz, H. and Richter, K. (1998) Anterior specification of embryonic ectoderm: the role of the Xenopus cement gland-specific gene XAG-2. *Mech Dev* **72**, 115-130.

Ackermann, M. (2006) Pathogenesis of gammaherpesvirus infections. *Vet Microbiol* **113**, 211-222.

Adam, P.J., Boyd, R., Tyson, K.L., Fletcher, G.C., Stamps, A., Hudson, L., Poyser, H.R., Redpath, N., Griffiths, M., Steers, G., Harris, A.L., Patel, S., Berry, J., Loader, J.A., Townsend, R.R., Daviet, L., Legrain, P., Parekh, R. and Terrett, J.A. (2003) Comprehensive proteomic analysis of breast cancer cell membranes reveals unique proteins with potential roles in clinical cancer. *J Biol Chem* **278**, 6482-6489.

Alcami, A. (2003) Viral mimicry of cytokines, chemokines and their receptors. *Nat Rev Immunol* **3**, 36-50.

Alexander, J.M., Nelson, C.A., van Berkel, V., Lau, E.K., Studts, J.M., Brett, T.J., Speck, S.H., Handel, T.M., Virgin, H.W. and Fremont, D.H. (2002) Structural basis of chemokine sequestration by a herpesvirus decoy receptor. *Cell* **111**, 343-356.

Altschul, S., Madden, T., Schaffer, A., Zhang, J., Zhang, Z., Miller, W. and Lipman, D. (1997) Gapped BLAST and PSI-BLAST: a new generation of protein database search programs. *Nucl Acids Res* **25**, 3389-3402.

Altschul, S.F., Gish, W., Miller, W., Myers, E.W. and Lipman, D.J. (1990) Basic local alignment search tool. *J Mol Biol* **215**, 403-410.

Anderson, I.E., Buxton, D., Campbell, I., Russell, G., Davis, W.C., Hamilton, M.J. and Haig, D.M. (2007) Immunohistochemical study of experimental malignant catarrhal fever in rabbits. *J Comp Pathol* **136**, 156-166.

Arsalane, K., Broeckaert, F., Knoops, B., Wiedig, M., Toubeau, G. and Bernard, A. (2000) Clara cell specific protein (CC16) expression after acute lung inflammation induced by intratracheal lipopolysaccharide administration. *Am J Respir Cell Mol Biol* **161**, 1624-1630.

Bach, E.A., Aguet, M. and Schreiber, R.D. (1997) The IFN gamma receptor: a paradigm for cytokine receptor signaling. *Annu Rev Immunol* **15**, 563-591.

Ballard, P.L., Lee, J.W., Fang, X., Chapin, C.J., Allen, L., Segal, M.R., Fischer, H., Illick, B., Gonzales, L.W., Kolla, V. and Matthay, M.A. (2010) Regulated gene expression in cultured type II cells of adult human lung. *Am J Physiol Lung Cell Mol Physiol*, ajplung.00427.02009.

Barnard, B.J., Bengis, R.G., Griessel, M.D. and de Vos, V. (1989) Excretion of alcelaphine herpesvirus-1 by captive and free-living wildebeest (Connochaetes taurinus). *Onderstepoort J Vet Res* **56**, 131-134.

Barnes, F.A., Bingle, L. and Bingle, C.D. (2008) Pulmonary genomics, proteomics, and PLUNCs. *Am J Respir Cell Mol Biol* **38**, 377-379.

Bartlett, J.A., Hicks, B.J., Schlomann, J.M., Ramachandran, S., Nauseef, W.M. and McCray, P.B., Jr. (2008) PLUNC is a secreted product of neutrophil granules. *J Leukoc Biol* **83**, 1201-1206.

Becker, S.D., Bennett, M., Stewart, J.P. and Hurst, J.L. (2007) Serological survey of virus infection among wild house mice (Mus domesticus) in the UK. *Lab Anim* **41**, 229-238.

Bell, S.A., Balasuriya, U.B., Gardner, I.A., Barry, P.A., Wilson, W.D., Ferraro, G.L. and MacLachlan, N.J. (2006) Temporal detection of equine herpesvirus infections of a cohort of mares and their foals. *Vet Microbiol* **116**, 249-257.

Benlloch, S., Galbis-Caravajal, J.M., Alenda, C., Peiro, F.M., Sanchez-Ronco, M., Rodriguez-Paniagua, J.M., Baschwitz, B., Rojas, E. and Massuti, B. (2009) Expression of molecular markers in mediastinal nodes from resected stage I non-small-cell lung cancer (NSCLC): prognostic impact and potential role as markers of occult micrometastases. *Ann Oncol* **20**, 91-97.

Bingle, C. and Craven, C. (2002) PLUNC: a novel family of candidate host defence proteins expressed in the upper airways and nasopharynx. *Hum Mol Genet* **11**, 937 - 943.

Bingle, C.D. and Bingle, L. (2000) Characterisation of the human plunc gene, a gene product with an upper airways and nasopharyngeal restricted expression pattern. *Biochim Biophys Acta* **1493**, 363-367.

Bingle, C.D., Chiang, S., Veldhuizen, E.J., Haggsman, H.P., Bingle, L. and Craven, C.J. (2009) Evolutionary history of PLUNCs: the putative pulmonary mucosal host defence proteins, SPLUNC1 and LPLUNC1 are present only in the therian lineage. *Am J Resp Crit Care Med* **179**, A2816.

Bingle, C.D. and Craven, C.J. (2003) Comparative analysis of the PLUNC (palate, lung and nasal epithelium clone) protein families. *Biochem Soc Trans* **31**, 806-809.

Bingle, C.D. and Craven, C.J. (2004) Meet the relatives: a family of BPI- and LBP-related proteins. *Trends Immunol* **25**, 53-55.

Bingle, C.D. and Gorr, S.U. (2004) Host defense in oral and airway epithelia: chromosome 20 contributes a new protein family. *Int J Biochem Cell Biol* **36**, 2144-2152.

Bingle, C.D., Hackett, B.P., Moxley, M., Longmore, W. and Gitlin, J.D. (1995) Role of hepatocyte nuclear factor-3 alpha and hepatocyte nuclear factor-3 beta in Clara cell secretory protein gene expression in the bronchiolar epithelium. *Biochem J* **308**, 197-202.

Bingle, C.D., LeClair, E.E., Havard, S., Bingle, L., Gillingham, P. and Craven, C.J. (2004) Phylogenetic and evolutionary analysis of the PLUNC gene family. *Protein Sci* **13**, 422-430.

Bingle, L., Barnes, F., Cross, S., Rassl, D., Wallace, W., Campos, M. and Bingle, C. (2007) Differential epithelial expression of the putative innate immune molecule SPLUNC1 in Cystic Fibrosis. *Resp Res* **8**, 79.

Bingle, L., Cross, S.S., High, A.S., Wallace, W.A., Devine, D.A., Havard, S., Campos, M.A. and Bingle, C.D. (2005) SPLUNC1 (PLUNC) is expressed in glandular tissues of the respiratory tract and in lung tumours with a glandular phenotype. *J Pathol* **205**, 491-497.

Biron, C.A. and Sen, G.C. (2007) Innate responses to viral infections, In: Knipe, D.M., Howley, P.M. (Eds.) Field's Virology. Wolters Kluwer/Lippincott Williams and Wilkins, Philadelphia, pp. 249-276.

Blasdell, K., McCracken, C., Morris, A., Nash, A.A., Begon, M., Bennett, M. and Stewart, J.P. (2003) The wood mouse is a natural host for Murid herpesvirus 4. *J Gen Virol* **84**, 111-113.

Blaskovic, D., Stancekova, M., Svobodova, J. and Mistrikova, J. (1980) Isolation of five strains of herpesviruses from two species of free living small rodents. *Acta Virol* **24**, 468.

Boers, J.E., Ambergen, A.W. and Thunnissen, F.B. (1999) Number and proliferation of Clara cells in normal human airway epithelium. *Am J Respir Crit Care Med* **159**, 1585-1591.

Bojan, F., Kinsella, A.R. and Fox, M. (1983) Effect of tumor promoter 12-O-tetradecanoylphorbol-13-acetate on recovery of methotrexate-, N-(phosphonacetyl)-L-aspartate-, and cadmium-resistant colony-forming mouse and hamster cells. *Cancer Res* **43**, 5217-5221.

Boon, K., Bailey, N.W., Yang, J., Steel, M.P., Groshong, S., Kervitsky, D., Brown, K.K., Schwarz, M.I. and Schwartz, D.A. (2009) Molecular phenotypes distinguish patients with relatively stable from progressive idiopathic pulmonary fibrosis (IPF). *PLoS ONE* **4**, e5134.

Borchers, K., Wolfinger, U., Goltz, M., Broll, H. and Ludwig, H. (1997) Distribution and relevance of Equine Herpesvirus type 2 (EHV-2) infections. *Arch Virol* **142**, 917-928.

Bowden, R.J., Simas, J.P., Davis, A.J. and Efstathiou, S. (1997) Murine gammaherpesvirus 68 encodes tRNA-like sequences which are expressed during latency. *J Gen Virol* **78**, 1675-1687.

Boycott, R., Klenk, H.D. and Ohuchi, M. (1994) Cell tropism of influenza virus mediated by hemagglutinin activation at the stage of virus entry. *Virology* **203**, 313-319.

Breuer, R., Zajicek, G., Christensen, T.G., Lucey, E.C. and Snider, G.L. (1990) Cell kinetics of normal adult hamster bronchial epithelium in the steady state. *Am J Respir Cell Mol Biol* **2**, 51-58.

Bridgeman, A., Stevenson, P.G., Simas, J.P. and Efstathiou, S. (2001) A secreted chemokine binding protein encoded by murine gammaherpesvirus-68 is necessary for the establishment of a normal latent load. *J Exp Med* **194**, 301-312.

Britto, C.J., Curran, D., Liu, Q. and Cohn, L.E. (2010) Microbial and inflammatory signals promote airway inflammation by inhibiting the epithelial protein PLUNC. *Am J Respir Crit Care Med* **181**, A1389-.

Broeckaert, B. (2000) Clara cell secretory protein (CC16): characteristics and perspectives as lung peripheral biomarker. *Clin Exp Allergy* **30**, 469-475.

Broeckaert, F., Clippe, A., Knoops, B., Hermans, C. and Bernard, A. (2000) Clara cell secretory protein (CC16): features as a peripheral lung biomarker. *Ann N Y Acad Sci* **923**, 68-77.

Brown, C. (1998) In situ hybridization with riboprobes: an overview for veterinary pathologists. *Vet Pathol* **35**, 159-167.

Brownstein, D.G. (2007) Sendai virus and Pneumonia virus of mice (PVM), In: Fox, J.G., Davisson, M.T., Quimby, F.W., Barthold, S.W., Newcomer, C.E., Smith, A.L. (Eds.) The Mouse in Biomedical Research. Academic Press/Elsevier, Amsterdam, pp. 281-309.

Brownstein, D.G., Smith, A.L. and Johnson, E.A. (1981) Sendai virus infection in genetically resistant and susceptible mice. *Am J Pathol* **105**, 156-163.

Campos, M.A., Abreu, A.R., Nlend, M.C., Cobas, M.A., Conner, G.E. and Whitney, P.L. (2004) Purification and characterization of PLUNC from human tracheobronchial secretions. *Am J Respir Cell Mol Biol* **30**, 184-192.

Cardin, R.D., Brooks, J.W., Sarawar, S.R. and Doherty, P.C. (1996) Progressive loss of CD8+ T cell-mediated control of a gamma-herpesvirus in the absence of CD4+ T cells. *J Exp Med* **184**, 863-871.

Centers for Disease Control and Prevention, C.D.C. (2009) Outbreak of swine-origin Influenza A (H1N1) virus infection - Mexico, March-April 2009. *MMWR Morb Mortal Wkly Rep* **58**, 467-470.

Chang, Y., Cesarman, E., Pessin, M.S., Lee, F., Culpepper, J., Knowles, D.M. and Moore, P.S. (1994) Identification of herpesvirus-like DNA sequences in AIDS-associated Kaposi's sarcoma. *Science* **266**, 1865-1869.

Chen, G., Korfhagen, T.R., Xu, Y., Kitzmiller, J., Wert, S.E., Maeda, Y., Gregorieff, A., Clevers, H. and Whitsett, J.A. (2009) SPDEF is required for mouse pulmonary goblet cell differentiation and regulates a network of genes associated with mucus production. *J Clin Invest* **119**, 2914-2924.

Cheng, M., Chen, Y., Yu, X., Tian, Z. and Wei, H. (2008) Diagnostic utility of LunX mRNA in peripheral blood and pleural fluid in patients with primary non-small cell lung cancer. *BMC Cancer* **8**, 156.

Christensen, J.P., Cardin, R.D., Branum, K.C. and Doherty, P.C. (1999) CD4(+) T cell-mediated control of a gamma-herpesvirus in B cell-deficient mice is mediated by IFN-gamma. *Proc Natl Acad Sci U S A* **96**, 5135-5140.

Chu, H.W., Thaikoottathil, J., Rino, J.G., Zhang, G., Wu, Q., Moss, T., Refaeli, Y., Bowler, R., Wenzel, S.E., Chen, Z., Zdunek, J., Breed, R., Young, R., Allaire, E. and Martin, R.J. (2007) Function and regulation of SPLUNC1 protein in Mycoplasma infection and allergic inflammation. *J Immunol* **179**, 3995-4002.

Clambey, E.T., Virgin, H.W. and Speck, S.H. (2000) Disruption of the Murine gammaherpesvirus 68 M1 open reading frame leads to enhanced reactivation from latency. *J Virol* **74**, 1973-1984.

Cliffe, A.R., Nash, A.A. and Dutia, B.M. (2009) Selective uptake of small RNA molecules in the virion of Murine gammaherpesvirus 68. *J Virol* **83**, 2321-2326.

Cohen, A., Wolf, D.G., Guttman-Yassky, E. and Sarid, R. (2005) Kaposi's sarcoma-associated herpesvirus: clinical, diagnostic, and epidemiological aspects. *Crit Rev Clin Lab Sci* **42**, 101-153.

Collins, P.L. and Crowe, J.E., Jr. (2007) Respiratory Syncytial Virus and Metapneumovirus, In: Knipe, D.M., Howley, P.M. (Eds.) Field's Virology. Wolters Kluwer/Lippincott Williams and Wilkins, Philadelphia, pp. 1601-1646.

Cook, D.N., Beck, M.A., Coffman, T.M., Kirby, S.L., Sheridan, J.F., Pragnell, I.B. and Smithies, O. (1995) Requirement of MIP-1 alpha for an inflammatory response to viral infection. *Science* **269**, 1583-1585.

Cowan, M.J., Huang, X., Yao, X.L. and Shelhamer, J.H. (2000) Tumor necrosis factor alpha stimulation of human Clara cell secretory protein production by human airway epithelial cells. *Ann N Y Acad Sci* **923**, 193-201.

Craig, M.I., Barrandeguy, M.E. and Fernandez, F.M. (2005) Equine herpesvirus 2 (EHV-2) infection in thoroughbred horses in Argentina. *BMC Vet Res* **1**, 9.

Culley, F.J., Pennycook, A.M., Tregoning, J.S., Dodd, J.S., Walzl, G., Wells, T.N., Hussell, T. and Openshaw, P.J. (2006) Role of CCL5 (RANTES) in viral lung disease. *J Virol* **80**, 8151-8157.

Curran, D.R. and Cohn, L. (2010) Advances in mucous cell metaplasia: a plug for mucus as a therapeutic focus in chronic airway disease. *Am J Respir Cell Mol Biol* **42**, 268-275.

Curran, D.R., Patham, B., Lui, Q. and Cohn, L. (2009) The novel protein, PLUNC, has anti-inflammatory properties in the respiratory tract. In: American Thoracic Society, San Diego, p. A2535.

Dalton, D., Pitts-Meek, S., Keshav, S., Figari, I., Bradley, A. and Stewart, T. (1993) Multiple defects of immune cell function in mice with disrupted interferon-gamma genes. *Science* **259**, 1739-1742.

Davis, C.W. and Dickey, B.F. (2008) Regulated airway goblet cell mucin secretion. *Annu Rev Physiol* **70**, 487-512.

Davison, A.J. (2002) Evolution of the herpesviruses. *Vet Microbiol* **86**, 69-88.

Davison, A.J., Eberle, R., Ehlers, B., Hayward, G.S., McGeoch, D.J., Minson, A.C., Pellett, P.E., Roizman, B., Studdert, M.J. and Thiry, E. (2009) The order Herpesvirales. *Arch Virol* **154**, 171-177.

Davison, A.J., Eberle, R., Hayward, G.S., McGeoch, D.J., Minson, A.C., Pellett, P.E., Roizman, B., Studdert, M.J. and Thiry, E. (2005) Family Herpesviridae, In: Fauquet, C.M., Mayo, M.A., Maniloff, J., Desselberger, U., Ball, L.A. (Eds.) Virus Taxonomy Eighth Report of the International Committee on Taxonomy of Viruses. Elsevier Academic Press, San Diego, pp. 193-212.

de Lima, B.D., May, J.S., Marques, S., Simas, J.P. and Stevenson, P.G. (2005) Murine gammaherpesvirus 68 bcl-2 homologue contributes to latency establishment in vivo. *J Gen Virol* **86**, 31-40.

Di, Y.P., Harper, R., Zhao, Y., Pahlavan, N., Finkbeiner, W. and Wu, R. (2003) Molecular cloning and characterization of spurt, a human novel gene that is retinoic acid-inducible and encodes a secretory protein specific in upper respiratory tracts. *J Biol Chem* **278**, 1165-1173.

Dierynck, I., Bernard, A., Roels, H. and De Ley, M. (1995) Potent inhibition of both human interferon-gamma production and biologic activity by the Clara cell protein CC16. *Am J Respir Cell Mol Biol* **12**, 205-210.

Domachowske, J.B., Bonville, C.A. and Rosenberg, H.F. (2004) Animal models for studying Respiratory Syncytial virus infection and its long term effects on lung function. *Pediatr Infect Dis J* **23(11)**, S228-S234.

Dunowska, M., Wilks, C.R., Studdert, M.J. and Meers, J. (2002) Equine respiratory viruses in foals in New Zealand. *New Zeal Vet J* **50**, 140-147.

Dutia, B.M., Clarke, C.J., Allen, D.J. and Nash, A.A. (1997) Pathological changes in the spleens of gamma interferon receptor-deficient mice infected with murine gammaherpesvirus: a role for CD8 T cells. *J Virol* **71**, 4278-4283.

Dutia, B.M., Roy, D.J., Ebrahimi, B., Gangadharan, B., Efstathiou, S., Stewart, J.P. and Nash, A.A. (2004) Identification of a region of the virus genome involved in murine gammaherpesvirus 68-induced splenic pathology. *J Gen Virol* **85**, 1393-1400.

Dutia, B.M., Stewart, J.P., Clayton, R.A.E., Dyson, H. and Nash, A.A. (1999) Kinetic and phenotypic changes in murine lymphocytes infected with murine gammaherpesvirus-68 in vitro. *J Gen Virol* **80**, 2729-2736.

Ebrahimi, B., Dutia, B.M., Brownstein, D.G. and Nash, A.A. (2001) Murine gammaherpesvirus-68 infection causes multi-organ fibrosis and alters leukocyte trafficking in interferon-gamma receptor knockout mice. *Am J Pathol* **158**, 2117-2125.

Ebrahimi, B., Dutia, B.M., Roberts, K.L., Garcia-Ramirez, J.J., Dickinson, P., Stewart, J.P., Ghazal, P., Roy, D.J. and Nash, A.A. (2003) Transcriptome profile of Murine gammaherpesvirus-68 lytic infection. *J Gen Virol* **84**, 99-109.

Eccles, R. (2005) Understanding the symptoms of the common cold and influenza. *Lancet Infect Dis* **5**, 718-725.

Efstathiou, S., Ho, Y.M., Hall, S., Styles, C.J., Scott, S.D. and Gompels, U.A. (1990a) Murine herpesvirus 68 is genetically related to the gammaherpesviruses Epstein-Barr virus and herpesvirus saimiri. *J Gen Virol* **71**, 1365-1372.

Efstathiou, S., Ho, Y.M. and Minson, A.C. (1990b) Cloning and molecular characterization of the murine herpesvirus 68 genome. *J Gen Virol* **71**, 1355-1364.

Ehlers, B., Dural, G., Yasmum, N., Lembo, T., de Thoisy, B., Ryser-Degiorgis, M.P., Ulrich, R.G. and McGeoch, D.J. (2008) Novel mammalian herpesviruses and lineages within the gammaherpesvirinae: cospeciation and interspecies transfer. *J Virol* **82**, 3509-3516.

Ehlers, B., Kuchler, J., Yasmum, N., Dural, G., Voigt, S., Schmidt-Chanasit, J., Jakel, T., Matuschka, F.R., Richter, D., Essbauer, S., Hughes, D.J., Summers, C., Bennett, M., Stewart, J.P. and Ulrich, R.G. (2007) Identification of novel rodent herpesviruses, including the first gammaherpesvirus of Mus musculus. *J Virol* **81**, 8091-8100.

Ehtisham, S., Sunil-Chandra, N.P. and Nash, A.A. (1993) Pathogenesis of murine gammaherpesvirus infection in mice deficient in CD4 and CD8 T cells. *J Virol* **67**, 5247-5252.

Epstein, M.A. (2001) Historical background. *Philos Trans R Soc Lond B Biol Sci* **356**, 413-420.

Evans, A.G., Moorman, N.J., Willer, D.O. and Speck, S.H. (2006) The M4 gene of gammaHV68 encodes a secreted glycoprotein and is required for the efficient establishment of splenic latency. *Virology* **344**, 520-531.

Evans, A.G., Moser, J.M., Krug, L.T., Pozharskaya, V., Mora, A.L. and Speck, S.H. (2008) A gammaherpesvirus-secreted activator of Vβ4+ CD8+ T cells regulates chronic infection and immunopathology. *J Exp Med* **205**, 669-684.

Evans, C.M., Williams, O.W., Tuvim, M.J., Nigam, R., Mixides, G.P., Blackburn, M.R., DeMayo, F.J., Burns, A.R., Smith, C., Reynolds, S.D., Stripp, B.R. and Dickey, B.F. (2004) Mucin is produced by clara cells in the proximal airways of antigen-challenged mice. *Am J Respir Cell Mol Biol* **31**, 382-394.

Everard, M.L., Swarbrick, A., Wrightham, M., McIntyre, J., Dunkley, C., James, P.D., Sewell, H.F. and Milner, A.D. (1994) Analysis of cells obtained by bronchial lavage of infants with respiratory syncytial virus infection. *Arch Dis Child* **71**, 428-432.

Faísca, P. and Desmecht, D. (2007) Sendai virus, the mouse parainfluenza type 1: A longstanding pathogen that remains up-to-date. *Res Vet Sci* **82**, 115-125.

Fickenscher, H. and Fleckenstein, B. (2001) Herpesvirus saimiri. *Philos Trans R Soc Lond B Biol Sci* **356**, 545-567.

Flano, E., Husain, S.M., Sample, J.T., Woodland, D.L. and Blackman, M.A. (2000) Latent murine gamma-herpesvirus infection is established in activated B cells, dendritic cells, and macrophages. *J Immunol* **165**, 1074-1081.

Flano, E., Kim, I.J., Moore, J., Woodland, D.L. and Blackman, M.A. (2003) Differential gamma-herpesvirus distribution in distinct anatomical locations and cell subsets during persistent infection in mice. *J Immunol* **170**, 3828-3834.

Fletcher, G.C., Patel, S., Tyson, K., Adam, P.J., Schenker, M., Loader, J.A., Daviet, L., Legrain, P., Parekh, R., Harris, A.L. and Terrett, J.A. (2003) hAG-2 and hAG-3, human homologues of genes involved in differentiation, are associated with oestrogen receptor-positive breast tumours and interact with metastasis gene C4.4a and dystroglycan. *Br J Cancer* **88**, 579-585.

Follettie, M.T., Ellis, D.K., Donaldson, D.D., Hill, A.A., Diesl, V., DeClercq, C., Sypek, J.P., Dorner, A.J. and Wills-Karp, M. (2006) Gene expression analysis in a murine model of allergic asthma reveals overlapping disease and therapy dependent pathways in the lung. *Pharmacogenomics J* **6**, 141-152.

Fortier, G., van Erck, E., Pronost, S., Lekeux, P. and Thiry, E. (2009) Equine gammaherpesviruses: Pathogenesis, epidemiology and diagnosis. *Vet J*, In Press.

Fritzsche, F.R., Dahl, E., Pahl, S., Burkhardt, M., Luo, J., Mayordomo, E., Gansukh, T., Dankof, A., Knuechel, R., Denkert, C., Winzer, K.J., Dietel, M. and Kristiansen, G. (2006) Prognostic relevance of AGR2 expression in breast cancer. *Clin Cancer Res* **12**, 1728-1734.

Gakhar, L., Bartlett, J.A., Penterman, J., Mizrachi, D., Singh, P.K., Mallampalli, R.K., Ramaswamy, S. and McCray, P.B., Jr. (2010) PLUNC is a novel airway surfactant protein with anti-biofilm activity. *PLoS ONE* **5**, e9098.

Gally, F., Di, P., Smith, S., Minor, M.N., Case, S., Liu, Y., Christian, E., Martin, R.J. and Chu, H.W. (2010a) SPLUNC1 is necessary and sufficient to confer in vivo host defense against Mycoplasma pneumoniae infection. *Am J Respir Crit Care Med* **181**, A1388.

Gally, F., Minor, M., Smith, S., Case, S., Martin, R.J. and Chu, H.W. (2010b) Differing effects of airway epithelial SPLUNC1 deficiency on mucin and TLR2 expression following Mycoplasma infection. *Am J Respir Crit Care Med* **181**, A2486.

Ganem, D. (2006) KSHV infection and the pathogenesis of Kaposi's Sarcoma. *Annu Rev Pathol-Mech* **1**, 273-296.

Ganem, D. (2007) Kaposi's Sarcoma-associated herpesvirus, In: Knipe, D.M., Howley, P.M. (Eds.) Field's Virology. Wolters Kluwer/Lippincott Williams and Wilkins, Philadelphia, pp. 2847-2888.

Gangadharan, B., Dutia, B.M., Rhind, S.M. and Nash, A.A. (2009) Murid herpesvirus-4 induces chronic inflammation of intrahepatic bile ducts in mice deficient in gamma-interferon signalling. *Hepatol Res* **39**, 187-194.

Gangadharan, B., Hoeve, M.A., Allen, J.E., Ebrahimi, B., Rhind, S.M., Dutia, B.M. and Nash, A.A. (2008) Murine gammaherpesvirus-induced fibrosis is associated with the development of alternatively activated macrophages. *J Leukoc Biol* **84**, 50-58.

Garcia-Caballero, A., Rasmussen, J.E., Gaillard, E., Watson, M.J., Olsen, J.C., Donaldson, S.H., Stutts, M.J. and Tarran, R. (2009) SPLUNC1 regulates airway surface liquid volume by protecting ENaC from proteolytic cleavage. *Proc Natl Acad Sci U S A* **106**, 11412-11417.

Gasteiger, E., Gattiker, A., Hoogland, C., Ivanyi, I., Appel, R.D. and Bairoch, A. (2003) ExPASy: The proteomics server for in-depth protein knowledge and analysis. *Nucleic Acids Res* **31**, 3784-3788.

Geere, H.M., Ligertwood, Y., Templeton, K.M., Bennet, I., Gangadharan, B., Rhind, S.M., Nash, A.A. and Dutia, B.M. (2006) The M4 gene of murine gammaherpesvirus 68 modulates latent infection. *J Gen Virol* **87**, 803-807.

Ghafouri, B., Irander, K., Lindbom, J., Tagesson, C. and Lindahl, M. (2006) Comparative proteomics of nasal fluid in seasonal allergic rhinitis. *J Proteome Res* **5**, 330 - 338.

Ghafouri, B., Kihlstrom, E., Stahlbom, B., Tagesson, C. and Lindahl, M. (2003) PLUNC (palate, lung and nasal epithelial clone) proteins in human nasal lavage fluid. *Biochem Soc Trans* **31**, 810-814.

Ghafouri, B., Stahlbom, B., Tagesson, C. and Lindahl, M. (2002) Newly identified proteins in human nasal lavage fluid from non-smokers and smokers using two-dimensional gel electrophoresis and peptide mass fingerprinting. *Proteomics* **2**, 112-120.

Glezen, P. and Denny, F.W. (1973) Epidemiology of acute lower respiratory disease in children. *N Engl J Med* **288**, 498-505.

Goodbourn, S., Didcock, L. and Randall, R.E. (2000) Interferons: cell signalling, immune modulation, antiviral response and virus countermeasures. *J Gen Virol* **81**, 2341-2364.

Goodwin, M.M., Canny, S., Steed, A. and Virgin, H.W. (2010) Murine gammaherpesvirus 68 has evolved gamma interferon and Stat1-

repressible promoters for the lytic switch gene 50. *J Virol* **84**, 3711-3717.

Graham, B.S., Bunton, L.A., Wright, P.F. and Karzon, D.T. (1991) Role of T lymphocyte subsets in the pathogenesis of primary infection and rechallenge with respiratory syncytial virus in mice. *J Clin Invest* **88**, 1026-1033.

Graham, B.S., Rutigliano, J.A. and Johnson, T.R. (2002) Respiratory Syncytial virus immunobiology and pathogenesis. *Virology* **297**, 1-7.

Graham, F.L., Smiley, J., Russell, W.C. and Nairn, R. (1977) Characteristics of a Human Cell Line Transformed by DNA from Human Adenovirus Type 5. *J Gen Virol* **36**, 59-72.

Greenwood, A.G. and Sanchez, S. (2002) Serological evidence of murine pathogens in wild grey squirrels (Sciurus carolinensis) in North Wales. *Vet Rec* **150**, 543-546.

Gupta, R.P. and Hook, G.E.R. (1988) In vitro translation of rabbit lung Clara cell secretory protein mRNA. *Biochemical and Biophysical Research Communications* **153**, 470-478.

Harrod, K.S. and Jaramillo, R.J. (2002) Pseudomonas aeruginosa and tumor necrosis factor-alpha attenuate Clara cell secretory protein promoter function. *Am J Respir Cell Mol Biol* **26**, 216-223.

Harrod, K.S., Mounday, A.D., Stripp, B.R. and Whitsett, J.A. (1998) Clara cell secretory protein decreases lung inflammation after acute virus infection. *Am J Physiol* **275**, L924-930.

Hayashida, S., Harrod, K.S. and Whitsett, J.A. (2000) Regulation and function of CCSP during pulmonary Pseudomonas aeruginosa infection in vivo. *Am J Physiol Lung Cell Mol Physiol* **279**, L452-459.

He, Y., Zhou, G., Zhai, Y., Dong, X., Lv, L., He, F. and Yao, K. (2005) Association of PLUNC gene polymorphisms with susceptibility to nasopharyngeal carcinoma in a Chinese population. *J Med Genet* **42**, 172-176.

Hong, K.U., Reynolds, S.D., Giangreco, A., Hurley, C.M. and Stripp, B.R. (2001) Clara cell secretory protein-expressing cells of the airway neuroepithelial body microenvironment include a label-retaining subset and are critical for epithelial renewal after progenitor cell depletion. *Am J Respir Cell Mol Biol* **24**, 671-681.

Huang, S., Hendriks, W., Althage, A., Hemmi, S., Bluethmann, H., Kamijo, R., Vilcek, J., Zinkernagel, R. and Aguet, M. (1993a) Immune response in mice that lack the interferon-gamma receptor. *Science* **259**, 1742-1745.

Huang, S., Hendriks, W., Althage, A., Hemmi, S., Bluethmann, H., Kamijo, R., Vilcek, J., Zinkernagel, R.M. and Aguet, M. (1993b) Immune response in mice that lack the interferon-gamma receptor. *Science* **259**, 1742-1745.

Hughes, D.J. (2006) Pathogenesis of Murid herpesvirus 4 in its natural host, Apodemus sylvaticus. PhD thesis. University of Liverpool.

Hughes, D.J., Kipar, A., Milligan, S.G., Cunningham, C., Sanders, M., Quail, M.A., Rajandream, M.-A., Efstathiou, S., Bowden, R.J., Chastel, C., Bennett, M., Sample, J.T., Barrell, B., Davison, A.J. and Stewart, J.P. (2009) Characterization of a novel wood mouse virus related to murid herpesvirus 4. *J Gen Virol*, vir.0.017327-017320.

Hughes, D.J., Kipar, A., Sample, J.T. and Stewart, J.P. (2010) Pathogenesis of a model gammaherpesvirus in a natural host. *J Virol* **84**, 3949-3961.

Husain, S.M., Usherwood, E.J., Dyson, H., Coleclough, C., Coppola, M.A., Woodland, D.L., Blackman, M.A., Stewart, J.P. and Sample, J.T. (1999) Murine gammaherpesvirus M2 gene is latency-associated and its protein a target for CD8(+) T lymphocytes. *Proc Natl Acad Sci U S A* **96**, 7508-7513.

Hussell, T., Baldwin, C.J., O'Garra, A. and Openshaw, P.J. (1997) CD8+ T cells control Th2-driven pathology during pulmonary respiratory syncytial virus infection. *Eur J Immunol* **27**, 3341-3349.

Hussell, T. and Openshaw, P.J. (1998) Intracellular IFN-gamma expression in natural killer cells precedes lung CD8+ T cell recruitment during respiratory syncytial virus infection. *J Gen Virol* **79**, 2593-2601.

ICTVdb-Management (2006) The Universal Virus Database. In http://www.ncbi.nlm.nih.gov/ICTVdb/ICTVdB/, Büchen-Osmond, C., ed. (New York, Columbia University).

Itoh, T., Iwai, H. and Ueda, K. (1991) Comparative lung pathology of inbred strain of mice resistant and susceptible to Sendai virus infection. *J Vet Med Sci* **53**, 275-279.

Iwao, K., Watanabe, T., Fujiwara, Y., Takami, K., Kodama, K., Higashiyama, M., Yokouchi, H., Ozaki, K., Monden, M. and Tanigami, A. (2001) Isolation of a novel human lung-specific gene, LUNX, a potential molecular marker for detection of micrometastasis in non-small-cell lung cancer. *Int J Cancer* **91**, 433-437.

Jacoby, M.A., Virgin, H.W. and Speck, S.H. (2002) Disruption of the M2 gene of murine gammaherpesvirus 68 alters splenic latency following intranasal, but not intraperitoneal, inoculation. *J Virol* **76**, 1790-1801.

Jakab, G.J. (1975) Suppression of pulmonary antibacterial activity following Sendai virus infection in mice: dependence on virus dose. *Arch Virol* **48**, 385-390.

Jenner, R.G., Maillard, K., Cattini, N., Weiss, R.A., Boshoff, C., Wooster, R. and Kellam, P. (2003) Kaposi's sarcoma-associated herpesvirus-infected primary effusion lymphoma has a plasma cell gene expression profile. *Proc Natl Acad Sci U S A* **100**, 10399-10404.

Jensen, K.K., Chen, S.C., Hipkin, R.W., Wiekowski, M.T., Schwarz, M.A., Chou, C.C., Simas, J.P., Alcami, A. and Lira, S.A. (2003) Disruption of CCL21-induced chemotaxis in vitro and in vivo by M3, a chemokine-binding protein encoded by murine gammaherpesvirus 68. *J Virol* **77**, 624-630.

Johnston, C.J., Mango, G.W., Finkelstein, J.N. and Stripp, B.R. (1997) Altered pulmonary response to hyperoxia in Clara cell secretory protein deficient mice. *Am J Respir Cell Mol Biol* **17**, 147-155.

Jorens, P.G., Sibille, Y., Goulding, N.J., van Overveld, F.J., Herman, A.G., Bossaert, L., De Backer, W.A., Lauwerys, R., Flower, R.J. and Bernard, A. (1995) Potential role of Clara cell protein, an endogenous phospholipase A2 inhibitor, in acute lung injury. *Eur Respir J* **8**, 1647-1653.

Katavolos, P., Ackerley, C.A., Viel, L., Clark, M.E., Wen, X. and Bienzle, D. (2009) Clara cell secretory protein is reduced in equine recurrent airway obstruction. *Vet Pathol* **46**, 604-613.

Kershaw, O., von Oppen, T., Glitz, F., Deegen, E., Ludwig, H. and Borchers, K. (2001) Detection of equine herpesvirus type 2 (EHV-2) in horses with keratoconjunctivitis. *Virus Res* **80**, 93-99.

Kido, H., Yokogoshi, Y., Sakai, K., Tashiro, M., Kishino, Y., Fukutomi, A. and Katunuma, N. (1992) Isolation and characterization of a novel trypsin-like protease found in rat bronchiolar epithelial Clara cells. A possible activator of the viral fusion glycoprotein. *J Biol Chem* **267**, 13573-13579.

Kim, C.H., Kim, K., Jik Kim, H., Kook Kim, J., Lee, J.G. and Yoon, J.H. (2006) Expression and regulation of PLUNC in human nasal epithelium. *Acta Otolaryngol* **126**, 1073-1078.

Kipar, A., Kremendahl, J., Jackson, M.L. and Reinacher, M. (2001) Comparative examination of cats with feline leukemia virus-associated enteritis and other relevant forms of feline enteritis. *Vet Pathol* **38**, 359-371.

Komiya, T., Tanigawa, Y. and Hirohashi, S. (1999) Cloning of the gene gob-4, which is expressed in intestinal goblet cells in mice. *Biochim Biophys Acta* **1444**, 434-438.

Korteweg, C. and Gu, J. (2008) Pathology, molecular biology, and pathogenesis of avian influenza A (H5N1) infection in humans. *Am J Pathol* **172**, 1155-1170.

Kuiken, T. and Taubenberger, J.K. (2008) Pathology of human influenza revisited. *Vaccine* **26**, D59-D66.

Kuperman, D.A., Lewis, C.C., Woodruff, P.G., Rodriguez, M.W., Yang, Y.H., Dolganov, G.M., Fahy, J.V. and Erle, D.J. (2005) Dissecting asthma using focused transgenic modeling and functional genomics. *J Allergy Clin Immunol* **116**, 305-311.

Kutok, J.L. and Wang, E. (2006) Spectrum of Epstein-Barr Virus-associated diseases. *Annu Rev Pathol-Mech* **1**, 375-404.

Lamb, R.A. and Parks, G.D. (2007) *Paramyxoviridae*: The viruses and their replication., In: Knipe, D.M., Howley, P.M. (Eds.) Field's Virology. Wolters Kluwer/Lippincott Williams and Wilkins, Philadelphia, pp. 1449-1496.

Lande, J.D., Dalheimer, S.L., Mueller, D.L., Hertz, M.I. and King, R.A. (2005) Gene expression profiling in murine obliterative airway disease. *Am J Transplant* **5**, 2170-2184.

Larkin, M.A., Blackshields, G., Brown, N.P., Chenna, R., McGettigan, P.A., McWilliam, H., Valentin, F., Wallace, I.M., Wilm, A., Lopez, R., Thompson, J.D., Gibson, T.J. and Higgins, D.G. (2007) Clustal W and Clustal X version 2.0. *Bioinformatics* **23**, 2947-2948.

Larsen, K., Madsen, L.B. and Bendixen, C. (2005) Porcine SPLUNC1: molecular cloning, characterization and expression analysis. *Biochim Biophys Acta* **1727**, 220-226.

LeClair, E.E., Nguyen, L., Bingle, L., MacGowan, A., Singleton, V., Ward, S.J. and Bingle, C.D. (2001) Genomic organization of the mouse plunc gene and expression in the developing airways and thymus. *Biochem Biophys Res Commun* **284**, 792-797.

LeClair, E.E., Nomellini, V., Bahena, M., Singleton, V., Bingle, L., Craven, C.J. and Bingle, C.D. (2004) Cloning and expression of a mouse member of the PLUNC protein family exclusively expressed in tongue epithelium. *Genomics* **83**, 658-666.

Lee, K.S., Cool, C.D. and van Dyk, L.F. (2009) Murine gammaherpesvirus 68 infection of gamma interferon-deficient mice on a BALB/c background

results in acute lethal pneumonia that is dependent on specific viral genes. *J Virol* **83**, 11397-11401.

Liang, X., Collins, C.M., Mendel, J.B., Iwakoshi, N.N. and Speck, S.H. (2009) Gammaherpesvirus-driven plasma cell differentiation regulates virus reactivation from latently infected B lymphocytes. *PLoS Pathog* **5**, e1000677.

Liang, X., Shin, Y.C., Means, R.E. and Jung, J.U. (2004) Inhibition of interferon-mediated antiviral activity by murine gammaherpesvirus 68 latency-associated M2 protein. *J Virol* **78**, 12416-12427.

Lindahl, M., Stahlbom, B. and Tagesson, C. (2001) Identification of a new potential airway irritation marker, palate lung nasal epithelial clone protein, in human nasal lavage fluid with two-dimensional electrophoresis and matrix-assisted laser desorption/ionization-time of flight. *Electrophoresis* **22**, 1795-1800.

Liu, D., Rudland, P.S., Sibson, D.R., Platt-Higgins, A. and Barraclough, R. (2005) Human homologue of cement gland protein, a novel metastasis inducer associated with breast carcinomas. *Cancer Res* **65**, 3796-3805.

Liu, Q., Curran, D., Britto, C.J., Patham, B. and Cohn, L.E. (2010a) PLUNC is an immunoregulatory protein that controls eosinophilia in allergic airway inflammation. *Am J Respir Crit Care Med* **181**, A5595.

Liu, Y., Latoche, J., Pilewski, J.M. and Di, Y.P.P. (2010b) Differential expression of SPLUNC1 and LPLUNC1 in lungs of healthy human subjects and COPD patients. *Am J Respir Crit Care Med* **181**, A2915.

Lohr, C.V., DeBess, E.E., Baker, R.J., Hiett, S.L., Hoffman, K.A., Murdoch, V.J., Fischer, K.A., Mulrooney, D.M., Selman, R.L. and Hammill-Black, W.M. (2010) Pathology and viral antigen distribution of lethal pneumonia in domestic cats due to pandemic (H1N1) 2009 Influenza A virus. *Vet Pathol* **47**, 378-386.

Lu, X., Tumpey, T.M., Morken, T., Zaki, S.R., Cox, N.J. and Katz, J.M. (1999) A mouse model for the evaluation of pathogenesis and immunity to Influenza A (H5N1) viruses isolated from humans. *J Virol* **73**, 5903-5911.

Lukacs, N.W., Moore, M.L., Rudd, B.D., Berlin, A.A., Collins, R.D., Olson, S.J., Ho, S.B. and Peebles, R.S., Jr (2006) Differential immune responses and pulmonary pathophysiology are induced by two different strains of Respiratory Syncytial virus. *Am J Pathol* **169**, 977-986.

Macias, H., Pasapera, A.M., Pérez-Solis, M.A., Ulloa-Aguirre, A. and Gutiérrez-Sagal, R. (2004) cDNA sequence, 5'-flanking region, and promoter activity of the Neotomodon alstoni alstoni Clara cell secretory protein gene. *Archives of Biochemistry and Biophysics* **427**, 170-179.

Macrae, A.I., Dutia, B.M., Milligan, S., Brownstein, D.G., Allen, D.J., Mistrikova, J., Davison, A.J., Nash, A.A. and Stewart, J.P. (2001) Analysis of a novel strain of murine gammaherpesvirus reveals a genomic locus important for acute pathogenesis. *J Virol* **75**, 5315-5327.

Macrae, A.I., Usherwood, E.J., Husain, S.M., Flano, E., Kim, I.J., Woodland, D.L., Nash, A.A., Blackman, M.A., Sample, J.T. and Stewart, J.P. (2003) Murid herpesvirus 4 strain 68 M2 protein is a B-cell-associated antigen important for latency but not lymphocytosis. *J Virol* **77**, 9700-9709.

Madureira, P.A., Matos, P., Soeiro, I., Dixon, L.K., Simas, J.P. and Lam, E.W. (2005) Murine gamma-herpesvirus 68 latency protein M2 binds to Vav signaling proteins and inhibits B-cell receptor-induced cell cycle arrest and apoptosis in WEHI-231 B cells. *J Biol Chem* **280**, 37310-37318.

Magdaleno, S.M., Wang, G., Jackson, K.J., Ray, M.K., Welty, S., Costa, R.H. and DeMayo, F.J. (1997) Interferon-gamma regulation of Clara cell gene expression: in vivo and in vitro. *Am J Physiol* **272**, L1142-1151.

Malmgaard, L. (2004) Induction and regulation of IFNs during viral infections. *J Interf Cytok Res* **24**, 439-454.

Martin, A.P., Canasto-Chibuque, C., Shang, L., Rollins, B.J. and Lira, S.A. (2006) The chemokine decoy receptor M3 blocks CC chemokine ligand 2 and CXC chemokine ligand 13 function in vivo. *J Immunol* **177**, 7296-7302.

Massaro, G.D., Singh, G., Mason, R., Plopper, C.G., Malkinson, A.M. and Gail, D.B. (1994) Biology of the Clara cell. *Am J Physiol* **266**, L101-106.

Mauad, T., Hajjar, L.A., Callegari, G.D., da Silva, L.F.F., Schout, D., Galas, F.R.B.G., Alves, V.A.F., Malheiros, D.M.A.C., Auler, J.O.C., Jr., Ferreira, A.F., Borsato, M.R.L., Bezerra, S.M., Gutierrez, P.S., Caldini, E.T.E.G., Pasqualucci, C.A., Dolhnikoff, M. and Saldiva, P.H.N. (2010) Lung pathology in fatal novel human Influenza A (H1N1) infection. *Am J Respir Crit Care Med* **181**, 72-79.

McAdam, A.J. and Sharpe, A.H. (2005) Infectious Diseases, In: Kumar, V., Abbas, A.K., Fausto, N. (Eds.) Robbins and Cotran Pathologic Basis of Disease. Elsevier Saunders, Philadelphia, pp. 343-414.

McGeoch, D.J., Cook, S., Dolan, A., Jamieson, F.E. and Telford, E.A. (1995) Molecular phylogeny and evolutionary timescale for the family of mammalian herpesviruses. *J Mol Biol* **247**, 443-458.

McGeoch, D.J., Gatherer, D. and Dolan, A. (2005) On phylogenetic relationships among major lineages of the Gammaherpesvirinae. *J Gen Virol* **86**, 307-316.

Melendez, L.V., Daniel, M.D., Hunt, R.D. and Garcia, F.G. (1968) An apparently new herpesvirus from primary kidney cultures of the squirrel monkey (Saimiri sciureus). *Lab Anim Care* **18**, 374-381.

Miele, L., Cordella-Miele, E. and Mukherjee, A.B. (1987) Uteroglobin: structure, molecular biology, and new perspectives on its function as a phospholipase A2 inhibitor. *Endocr Rev* **8**, 474-490.

Miller, A.L., Bowlin, T.L. and Lukacs, N.W. (2004) Respiratory syncytial virus-induced chemokine production: linking viral replication to chemokine production in vitro and in vivo. *J Infect Dis* **189**, 1419-1430.

Miller, A.L., Strieter, R.M., Gruber, A.D., Ho, S.B. and Lukacs, N.W. (2003) CXCR2 regulates Respiratory Syncytial virus-induced airway hyperreactivity and mucus overproduction. *J Immunol* **170**, 3348-3356.

Mitas, M., Hoover, L., Silvestri, G., Reed, C., Green, M., Turrisi, A.T., Sherman, C., Mikhitarian, K., Cole, D.J., Block, M.I. and Gillanders, W.E. (2003) Lunx is a superior molecular marker for detection of non-small cell lung cancer in peripheral blood [corrected]. *J Mol Diagn* **5**, 237-242.

Moore, M.L., Chi, M.H., Luongo, C., Lukacs, N.W., Polosukhin, V.V., Huckabee, M.M., Newcomb, D.C., Buchholz, U.J., Crowe, J.E., Jr., Goleniewska, K., Williams, J.V., Collins, P.L. and Peebles, R.S., Jr. (2009) A chimeric A2 strain of Respiratory Syncytial virus (RSV) with the fusion protein of RSV strain line 19 exhibits enhanced viral load, mucus, and airway dysfunction. *J Virol* **83**, 4185-4194.

Mora, A.L., Torres-Gonzalez, E., Rojas, M., Xu, J., Ritzenthaler, J., Speck, S.H., Roman, J., Brigham, K. and Stecenko, A. (2007) Control of virus reactivation arrests pulmonary herpesvirus-induced fibrosis in IFN-gamma receptor-deficient mice. *Am J Respir Crit Care Med* **175**, 1139-1150.

Mora, A.L., Woods, C.R., Garcia, A., Xu, J., Rojas, M., Speck, S.H., Roman, J., Brigham, K.L. and Stecenko, A.A. (2005) Lung infection with gamma-herpesvirus induces progressive pulmonary fibrosis in Th2-biased mice. *Am J Physiol Lung Cell Mol Physiol* **289**, L711-721.

Mukherjee, A.B., Kundu, G.C., Mantile-Selvaggi, G., Yuan, C.J., Mandal, A.K., Chattopadhyay, S., Zheng, F., Pattabiraman, N. and Zhang, Z. (1999) Uteroglobin: a novel cytokine? *Cell Mol Life Sci* **55**, 771-787.

Muller, U., Steinhoff, U., Reis, L.F., Hemmi, S., Pavlovic, J., Zinkernagel, R.M. and Aguet, M. (1994) Functional role of type I and type II interferons in antiviral defense. *Science* **264**, 1918-1921.

Mundt, E., Gay, L., Jones, L., Saavedra, G., Tompkins, S.M. and Tripp, R.A. (2009) Replication and pathogenesis associated with H5N1, H5N2, and H5N3 low-pathogenic avian influenza virus infection in chickens and ducks. *Arch Virol* **154**, 1241-1248.

Murphy, B.R., Prince, G.A., Lawrence, L.A., Croen, K.D. and Collins, P.L. (1990) Detection of respiratory syncytial virus (RSV) infected cells by in situ hybridization in the lungs of cotton rats immunized with formalin-inactivated virus or purified RSV F and G glycoprotein subunit vaccine and challenged with RSV. *Virus Res* **16**, 153-162.

Nash, A.A., Dutia, B.M., Stewart, J.P. and Davison, A.J. (2001) Natural history of murine gamma-herpesvirus infection. *Philos Trans R Soc Lond B Biol Sci* **356**, 569-579.

Nash, A.A., Usherwood, E.J. and Stewart, J.P. (1996) Immunological features of murine gammaherpesvirus infection. *Semin Virol* **7**, 125-130.

Neilson, K.A. and Yunis, E.J. (1990) Demonstration of respiratory syncytial virus in an autopsy series. *Pediatr Pathol* **10**, 491-502.

Nishimura, H., Itamura, S., Iwasaki, T., Kurata, T. and Tashiro, M. (2000) Characterization of human influenza A (H5N1) virus infection in mice: neuro-, pneumo- and adipotropic infection. *J Gen Virol* **81**, 2503-2510.

Nordengrahn, A., Merza, M., Ros, C., Lindholmc, A., Palfl, V., Hannant, D. and Belak, S. (2002) Prevalence of equine herpesvirus types 2 and 5 in horse populations by using type-specific PCR assays. *Vet Res* **33**, 251-259.

Nordengrahn, A., Rusvai, M., Merza, M., Ekström, J., Morein, B. and Belák, S. (1996) Equine herpesvirus type 2 (EHV-2) as a predisposing factor for Rhodococcus equi pneumonia in foals: prevention of the bifactorial disease with EHV-2 immunostimulating complexes. *Vet Microbiol* **51**, 55-68.

Pack, R.J., Al-Ugaily, L.H. and Morris, G. (1981) The cells of the tracheobronchial epithelium of the mouse: a quantitative light and electron microscope study. *J Anat* **132**, 71-84.

Pack, R.J., Al-Ugaily, L.H., Morris, G. and Widdicombe, J.G. (1980) The distribution and structure of cells in the tracheal epithelium of the mouse. *Cell Tissue Res* **208**, 65-84.

Park, K.-S., Korfhagen, T.R., Bruno, M.D., Kitzmiller, J.A., Wan, H., Wert, S.E., Khurana Hershey, G.K., Chen, G. and Whitsett, J.A. (2007) SPDEF regulates goblet cell hyperplasia in the airway epithelium. *J Clin Invest* **117**, 978-988.

Park, S.W., Zhen, G., Verhaeghe, C., Nakagami, Y., Nguyenvu, L.T., Barczak, A.J., Killeen, N. and Erle, D.J. (2009) The protein disulfide isomerase AGR2 is essential for production of intestinal mucus. *Proc Natl Acad Sci U S A* **106**, 6950-6955.

Parry, C.M., Simas, J.P., Smith, V.P., Stewart, C.A., Minson, A.C., Efstathiou, S. and Alcami, A. (2000) A broad spectrum secreted chemokine binding protein encoded by a herpesvirus. *J Exp Med* **191**, 573-578.

Peebles, R.S., Jr. and Graham, B.S. (2005) Pathogenesis of Respiratory Syncytial virus infection in the murine model. *Proc Am Thorac Soc* **2**, 110-115.

Pellett, P.E. and Roizman, B. (2007) The Family Herpesviridae: A Brief Introduction, In: Knipe, D.M., Howley, P.M. (Eds.) Field's Virology. Wolters Kluwer Health/Lippincott Williams and Wilkins, Philadelphia, pp. 2479-2499.

Percy, D.H., Auger, D.C. and Croy, B.A. (1994) Signs and lesions of experimental Sendai virus infection in two genetically distinct strains of SCID/beige mice. *Vet Pathol* **31**, 67-73.

Percy, D.H. and Barthold, S.W. (2007) Mouse, In: Pathology of laboratory rodents and rabbits. Blackwell, Oxford, pp. 3-124.

Persson, S., Rosenquist, M., Knoblach, B., Khosravi-Far, R., Sommarin, M. and Michalak, M. (2005) Diversity of the protein disulfide isomerase family: identification of breast tumor induced Hag2 and Hag3 as novel members of the protein family. *Mol Phylogenet Evol* **36**, 734-740.

Pfeffer, S., Sewer, A., Lagos-Quintana, M., Sheridan, R., Sander, C., Grasser, F.A., van Dyk, L.F., Ho, C.K., Shuman, S., Chien, M., Russo, J.J., Ju, J., Randall, G., Lindenbach, B.D., Rice, C.M., Simon, V., Ho, D.D., Zavolan, M. and Tuschl, T. (2005) Identification of microRNAs of the herpesvirus family. *Nat Methods* **2**, 269-276.

Pilette, C., Godding, V., Kiss, R., Delos, M., Verbeken, E., Decaestecker, C., De Paepe, K., Vaerman, J.P., Decramer, M. and Sibille, Y. (2001) Reduced epithelial expression of secretory component in small airways correlates with airflow obstruction in chronic obstructive pulmonary disease. *Am J Respir Crit Care Med* **163**, 185-194.

Plopper, C.G., Hyde, D.M. and Buckpitt, A.R. (1997) Clara Cells, In: Crystal, R.G., West, J.B., Weibel, E.R., Barnes, P.J. (Eds.) The Lung: Scientific Foundations. Lippincott-Raven, Philadelphia, pp. 517-533.

Plowright, W., Ferris, R.D. and Scott, G.R. (1960) Blue wildebeest and the aetiological agent of bovine malignant catarrhal fever. *Nature* **188**, 1167-1169.

Power, U.F., Huss, T., Michaud, V., Plotnicky-Gilquin, H., Bonnefoy, J.-Y. and Nguyen, T.N. (2001) Differential histopathology and chemokine gene expression in lung tissues following Respiratory Syncytial virus (RSV) challenge of formalin-inactivated RSV- or BBG2Na-immunized mice. *J Virol* **75**, 12421-12430.

Ramsay, P.L., Luo, Z., Magdaleno, S.M., Whitbourne, S.K., Cao, X., Park, M.S., Welty, S.E., Yu-Lee, L.Y. and DeMayo, F.J. (2003) Transcriptional regulation of CCSP by interferon-gamma in vitro and in vivo. *Am J Physiol Lung Cell Mol Physiol* **284**, L108-118.

Randall, R.E. and Goodbourn, S. (2008) Interferons and viruses: an interplay between induction, signalling, antiviral responses and virus countermeasures. *J Gen Virol* **89**, 1-47.

Ray, M.K., Wang, G., Barrish, J., Finegold, M.J. and DeMayo, F.J. (1996) Immunohistochemical localization of mouse Clara cell 10-KD protein using antibodies raised against the recombinant protein. *J Histochem Cytochem* **44**, 919-927.

Reynolds, S.D., Reynolds, P.R., Pryhuber, G.S., Finder, J.D. and Stripp, B.R. (2002) Secretoglobins SCGB3A1 and SCGB3A2 define secretory cell subsets in mouse and human airways. *Am J Respir Cell Mol Biol* **166**, 1498-1509.

Reynolds, S.D., Reynolds, P.R., Snyder, J.C., Whyte, F., Paavola, K.J. and Stripp, B.R. (2007) CCSP regulates cross talk between secretory cells and both ciliated cells and macrophages of the conducting airway. *Am J Physiol Lung Cell Mol Physiol* **293**, L114-123.

Rickinson, A.B. and Kieff, E. (2007) Epstein-Barr Virus, In: Knipe, D.M., Howley, P.M. (Eds.) Field's Virology. Wolters Kluwer/Lippincott Williams and Wilkins, Philadelphia, pp. 2655-2700.

Rizvi, S., Slater, J., Wolfinger, U., Borchers, K., Field, H. and Slade, A. (1997) Detection and distribution of equine herpesvirus 2 DNA in the central and peripheral nervous systems of ponies. *J Gen Virol* **78**, 1115-1118.

Robin, M., Dong, P., Hermans, C., Bernard, A., Bersten, A.D. and Doyle, I.R. (2002) Serum levels of CC16, SP-A and SP-B reflect tobacco-smoke exposure in asymptomatic subjects. *Eur Respir J* **20**, 1152-1161.

Roizman, B., Carmichael, L.E., Deinhardt, F., de-The, G., Nahmias, A.J., Plowright, W., Rapp, F., Sheldrick, P., Takahashi, M. and Wolf, K. (1981) Herpesviridae. Definition, provisional nomenclature, and taxonomy. The Herpesvirus Study Group, the International Committee on Taxonomy of Viruses. *Intervirology* **16**, 201-217.

Roizman, B., Desrosiers, R.C., Fleckenstein, B., Lopez, C., Minson, A.C. and Studdert, M.J. (1992) The family Herpesviridae: an update. The

Herpesvirus Study Group of the International Committee on Taxonomy of Viruses. *Arch Virol* **123**, 425-449.

Rollins, B.M., Garcia-Caballero, A., Stutts, M.J. and Tarran, R. (2010) SPLUNC1 expression reduces surface levels of the epithelial sodium channel (ENaC) in Xenopus laevis oocytes. *Channels (Austin)* **4**.

Ross, A., Dailey, L., Brighton, L. and Devlin, R. (2007) Transcriptional profiling of mucociliary differentiation in human airway epithelial cells. *Am J Respir Cell Mol Biol* **37**, 169 - 185.

Roxo-Rosa, M., da Costa, G., Luider, T., Scholte, B., Coelho, A., Amaral, M. and Penque, D. (2006) Proteomic analysis of nasal cells from cystic fibrosis patients and non-cystic fibrosis control individuals: search for novel biomarkers of cystic fibrosis lung disease. *Proteomics* **6**, 2314 - 2325.

Roy, D.J., Ebrahimi, B.C., Dutia, B.M., Nash, A.A. and Stewart, J.P. (2000) Murine gammaherpesvirus M11 gene product inhibits apoptosis and is expressed during virus persistence. *Arch Virol* **145**, 2411-2420.

Russell, G.C., Stewart, J.P. and Haig, D.M. (2009) Malignant catarrhal fever: a review. *Vet J* **179**, 324-335.

Ryerse, J.S., Hoffmann, J.W., Mahmoud, S., Nagel, B.A. and deMello, D.E. (2001) Immunolocalization of CC10 in Clara cells in mouse and human lung. *Histochem Cell Biol* **115**, 325-332.

Sarawar, S.R., Cardin, R.D., Brooks, J.W., Mehrpooya, M., Hamilton-Easton, A.M., Mo, X.Y. and Doherty, P.C. (1997) Gamma interferon is not essential for recovery from acute infection with murine gammaherpesvirus 68. *J Virol* **71**, 3916-3921.

Sarawar, S.R., Cardin, R.D., Brooks, J.W., Mehrpooya, M., Tripp, R.A. and Doherty, P.C. (1996) Cytokine production in the immune response to murine gammaherpesvirus 68. *J Virol* **70**, 3264-3268.

Schroder, K., Hertzog, P.J., Ravasi, T. and Hume, D.A. (2004) Interferon-gamma: an overview of signals, mechanisms and functions. *J Leukoc Biol* **75**, 163-189.

Shannon-Lowe, C.D., Neuhierl, B., Baldwin, G., Rickinson, A.B. and Delecluse, H.J. (2006) Resting B cells as a transfer vehicle for Epstein-Barr virus infection of epithelial cells. *Proc Natl Acad Sci U S A* **103**, 7065-7070.

Shinya, K., Ebina, M., Yamada, S., Ono, M., Kasai, N. and Kawaoka, Y. (2006) Avian flu: influenza virus receptors in the human airway. *Nature* **440**, 435-436.

Shope, R.E. (1935) The infection of mice with influenza virus. *J Exp Med* **62**, 561-572.

Siegel, A.M., Herskowitz, J.H. and Speck, S.H. (2008) The MHV68 M2 protein drives IL-10 dependent B cell proliferation and differentiation. *PLoS Pathogens* **4**, e1000039.

Simas, J.P., Bowden, R.J., Paige, V. and Efstathiou, S. (1998) Four tRNA-like sequences and a serpin homologue encoded by murine gammaherpesvirus 68 are dispensable for lytic replication in vitro and latency in vivo. *J Gen Virol* **79**, 149-153.

Simas, J.P., Marques, S., Bridgeman, A., Efstathiou, S. and Adler, H. (2004) The M2 gene product of murine gammaherpesvirus 68 is required for efficient colonization of splenic follicles but is not necessary for expansion of latently infected germinal centre B cells. *J Gen Virol* **85**, 2789-2797.

Simas, J.P., Swann, D., Bowden, R. and Efstathiou, S. (1999) Analysis of murine gammaherpesvirus-68 transcription during lytic and latent infection. *J Gen Virol* **80**, 75-82.

Singh, G. and Katyal, S.L. (1997) Clara cells and Clara cell 10 kD protein (CC10). *Am J Respir Cell Mol Biol* **17**, 141-143.

Singh, G. and Katyal, S.L. (2000) Clara cell proteins. *Ann N Y Acad Sci* **923**, 43-58.

Slater, J. (2007) Equine herpesviruses, In: Sellon, D.C., Long, M.T. (Eds.) Equine Infectious Diseases. Saunders Elsevier, St. Louis, Missouri, pp. 134-152.

Snyder, J.C., Reynolds, S.D., Hollingsworth, J.W., Li, Z., Kaminski, N. and Stripp, B.R. (2010) Clara cells attenuate the inflammatory response through regulation of macrophage behavior. *Am J Respir Cell Mol Biol* **42**, 161-171.

Spackman, E., Swayne, D.E., Suarez, D.L., Senne, D.A., Pedersen, J.C., Killian, M.L., Pasick, J., Handel, K., Pillai, S.P., Lee, C.W., Stallknecht, D., Slemons, R., Ip, H.S. and Deliberto, T. (2007) Characterization of low-pathogenicity H5N1 avian influenza viruses from North America. *J Virol* **81**, 11612-11619.

Steed, A., Buch, T., Waisman, A. and Virgin, H.W. (2007) Gamma interferon blocks gammaherpesvirus reactivation from latency in a cell type-specific manner. *J Virol* **81**, 6134-6140.

Steed, A.L., Barton, E.S., Tibbetts, S.A., Popkin, D.L., Lutzke, M.L., Rochford, R. and Virgin, H.W. (2006) Gamma interferon blocks gammaherpesvirus reactivation from latency. *J Virol* **80**, 192-200.

Stewart, J.P., Hughes, D.J., Roaden, L. and Ebrahimi, B. (2005) Murid herpesvirus 4 as a model for gammaherpesvirus pathogenesis. In: SGM sympoium 64: Molecular pathogenesis of virus infections., pp. 319-339.

Stewart, J.P., Janjua, N.J., Pepper, S.D., Bennion, G., Mackett, M., Allen, T., Nash, A.A. and Arrand, J.R. (1996) Identification and characterization of murine gammaherpesvirus 68 gp150: a virion membrane glycoprotein. *J Virol* **70**, 3528-3535.

Stewart, J.P., Silvia, O.J., Atkin, I.M., Hughes, D.J., Ebrahimi, B. and Adler, H. (2004) In vivo function of a gammaherpesvirus virion glycoprotein: influence on B-cell infection and mononucleosis. *J Virol* **78**, 10449-10459.

Stewart, J.P., Usherwood, E.J., Ross, A., Dyson, H. and Nash, T. (1998) Lung epithelial cells are a major site of murine gammaherpesvirus persistence. *J Exp Med* **187**, 1941-1951.

Stricker, T.P. and Kumar, V. (2010) Neoplasia, In: Kumar, V., Abbas, A., Fausto, N., Aster, J.C. (Eds.) Robbins and Cotran Pathologic Basis of Disease. Saunders Elsevier, Philadelphia.

Stripp, B.R., Huffman, J.A. and Bohinski, R.J. (1994) Structure and regulation of the murine Clara cell secretory protein gene. *Genomics* **20**, 27-35.

Stripp, B.R., Lund, J., Mango, G.W., Doyen, K.C., Johnston, C., Hultenby, K., Nord, M. and Whitsett, J.A. (1996) Clara cell secretory protein: a determinant of PCB bioaccumulation in mammals. *Am J Physiol Lung Cell Mol Physiol* **271**, L656-664.

Stripp, B.R., Maxson, K., Mera, R. and Singh, G. (1995) Plasticity of airway cell proliferation and gene expression after acute naphthalene injury. *Am J Physiol* **269**, L791-799.

Stripp, B.R. and Reynolds, S.D. (2008) Maintenance and repair of the bronchiolar epithelium. *Proc Am Thorac Soc* **5**, 328-333.

Stripp, B.R., Reynolds, S.D., Boe, I.M., Lund, J., Power, J.H., Coppens, J.T., Wong, V., Reynolds, P.R. and Plopper, C.G. (2002) Clara cell secretory protein deficiency alters clara cell secretory apparatus and the protein composition of airway lining fluid. *Am J Respir Cell Mol Biol* **27**, 170-178.

Sung, Y.K., Moon, C., Yoo, J.Y., Moon, C., Pearse, D., Pevsner, J. and Ronnett, G.V. (2002) Plunc, a member of the secretory gland protein family, is up-regulated in nasal respiratory epithelium after olfactory bulbectomy. *J Biol Chem* **277**, 12762-12769.

Sunil-Chandra, N.P., Arno, J., Fazakerley, J. and Nash, A.A. (1994) Lymphoproliferative disease in mice infected with murine gammaherpesvirus 68. *Am J Pathol* **145**, 818-826.

Sunil-Chandra, N.P., Efstathiou, S., Arno, J. and Nash, A.A. (1992a) Virological and pathological features of mice infected with murine gamma-herpesvirus 68. *J Gen Virol* **73**, 2347-2356.

Sunil-Chandra, N.P., Efstathiou, S. and Nash, A.A. (1992b) Murine gammaherpesvirus 68 establishes a latent infection in mouse B lymphocytes in vivo. *J Gen Virol* **73**, 3275-3279.

Tashiro, M., Yokogoshi, Y., Tobita, K., Seto, J.T., Rott, R. and Kido, H. (1992) Tryptase Clara, an activating protease for Sendai virus in rat lungs, is involved in pneumopathogenicity. *J Virol* **66**, 7211-7216.

Taubenberger, J.K. (2006) The origin and virulence of the 1918 "Spanish" influenza virus. *Proc Am Philos Soc* **150**, 86-112.

Taubenberger, J.K. and Morens, D.M. (2008) The pathology of Influenza virus infections. *Annu Rev Pathol-Mech* **3**, 499-522.

Telfer, S., Bennett, M., Carslake, D., Helyar, S. and Begon, M. (2007) The dynamics of Murid gammaherpesvirus 4 within wild, sympatric populations of bank voles and wood mice. *J Wildl Dis* **43**, 32-39.

Thorley-Lawson, D.A. and Allday, M.J. (2008) The curious case of the tumour virus: 50 years of Burkitt's lymphoma. *Nat Rev Micro* **6**, 913-924.

Torfason, E.G., Thorsteinsdottir, L., Torsteinsdottir, S. and Svansson, V. (2008) Study of equid herpesviruses 2 and 5 in Iceland with a type-specific polymerase chain reaction. *Res Vet Sci* **85**, 605-611.

Townsley, A.C., Dutia, B.M. and Nash, A.A. (2004) The M4 gene of Murine gammaherpesvirus modulates productive and latent infection in vivo. *J Virol* **78**, 758-767.

Tripp, R.A., Hamilton-Easton, A.M., Cardin, R.D., Nguyen, P., Behm, F.G., Woodland, D.L., Doherty, P.C. and Blackman, M.A. (1997) Pathogenesis of an infectious mononucleosis-like disease induced by a murine gamma-herpesvirus: role for a viral superantigen? *J Exp Med* **185**, 1641-1650.

Tripp, R.A. and Tompkins, S.M. (2009) Animal models for evaluation of influenza vaccines. *Curr Top Microbiol Immunol* **333**, 397-412.

Tumpey, T.M., Basler, C.F., Aguilar, P.V., Zeng, H., Solorzano, A., Swayne, D.E., Cox, N.J., Katz, J.M., Taubenberger, J.K., Palese, P. and Garcia-Sastre, A. (2005) Characterization of the reconstructed 1918 Spanish Influenza pandemic virus. *Science* **310**, 77-80.

Turner, P.C. and Moyer, R.W. (2002) Poxvirus immune modulators: functional insights from animal models. *Virus Res* **88**, 35-53.

Usherwood, E.J., Ross, A.J., Allen, D.J. and Nash, A.A. (1996a) Murine gammaherpesvirus-induced splenomegaly: a critical role for CD4 T cells. *J Gen Virol* **77** 627-630.

Usherwood, E.J., Roy, D.J., Ward, K., Surman, S.L., Dutia, B.M., Blackman, M.A., Stewart, J.P. and Woodland, D.L. (2000) Control of gammaherpesvirus latency by latent antigen-specific CD8(+) T cells. *J Exp Med* **192**, 943-952.

Usherwood, E.J., Stewart, J.P., Robertson, K., Allen, D.J. and Nash, A.A. (1996b) Absence of splenic latency in murine gammaherpesvirus 68-infected B cell-deficient mice. *J Gen Virol* **77**, 2819-2825.

van Berkel, V., Barrett, J., Tiffany, H.L., Fremont, D.H., Murphy, P.M., McFadden, G., Speck, S.H. and Virgin, H.W. (2000) Identification of a gammaherpesvirus selective chemokine binding protein that inhibits chemokine action. *J Virol* **74**, 6741-6747.

van Berkel, V., Levine, B., Kapadia, S.B., Goldman, J.E., Speck, S.H. and Virgin, H.W. (2002) Critical role for a high-affinity chemokine-binding protein in gamma-herpesvirus-induced lethal meningitis. *J Clin Invest* **109**, 905-914.

van Berkel, V., Preiter, K., Virgin, H.W. and Speck, S.H. (1999) Identification and initial characterization of the murine gammaherpesvirus 68 gene M3, encoding an abundantly secreted protein. *J Virol* **73**, 4524-4529.

van Dyk, L.F., Hess, J.L., Katz, J.D., Jacoby, M., Speck, S.H. and Virgin, H.W. (1999) The murine gammaherpesvirus 68 v-cyclin gene is an oncogene that promotes cell cycle progression in primary lymphocytes. *J Virol* **73**, 5110-5122.

van Dyk, L.F., Virgin, H.W. and Speck, S.H. (2000) The murine gammaherpesvirus 68 v-cyclin is a critical regulator of reactivation from latency. *J Virol* **74**, 7451-7461.

van Riel, D., Munster, V.J., de Wit, E., Rimmelzwaan, G.F., Fouchier, R.A., Osterhaus, A.D. and Kuiken, T. (2007) Human and avian influenza viruses target different cells in the lower respiratory tract of humans and other mammals. *Am J Pathol* **171**, 1215-1223.

Vargas, P.A., Speight, P.M., Bingle, C.D., Barrett, A.W. and Bingle, L. (2008) Expression of PLUNC family members in benign and malignant salivary gland tumours. *Oral Dis* **14**, 613-619.

Virgin, H.W., Latreille, P., Wamsley, P., Hallsworth, K., Weck, K.E., Dal Canto, A.J. and Speck, S.H. (1997) Complete sequence and genomic analysis of murine gammaherpesvirus 68. *J Virol* **71**, 5894-5904.

Virgin, H.W., Presti, R.M., Li, X.Y., Liu, C. and Speck, S.H. (1999) Three distinct regions of the murine gammaherpesvirus 68 genome are transcriptionally active in latently infected mice. *J Virol* **73**, 2321-2332.

Virgin, H.W. and Speck, S.H. (1999) Unraveling immunity to gamma-herpesviruses: a new model for understanding the role of immunity in chronic virus infection. *Curr Opin Immunol* **11**, 371-379.

Wakeling, M.N., Roy, D.J., Nash, A.A. and Stewart, J.P. (2001) Characterization of the murine gammaherpesvirus 68 ORF74 product: a novel oncogenic G protein-coupled receptor. *J Gen Virol* **82**, 1187-1197.

Walsh, J.J., Dietlein, L.F., Low, F.N., Burch, G.E. and Mogabgab, W.J. (1961) Bronchotracheal response in human influenza. Type A, Asian strain, as studied by light and electron microscopic examination of bronchoscopic biopsies. *Arch Intern Med* **108**, 376-388.

Wang, G.H., Garvey, T.L. and Cohen, J.I. (1999) The murine gammaherpesvirus-68 M11 protein inhibits Fas- and TNF-induced apoptosis. *J Gen Virol* **80**, 2737-2740.

Wang, S.Z., Rosenberger, C.L., Bao, Y.X., Stark, J.M. and Harrod, K.S. (2003) Clara cell secretory protein modulates lung inflammatory and immune responses to respiratory syncytial virus infection. *J Immunol* **171**, 1051-1060.

Wang, S.Z., Rosenberger, C.L., Espindola, T.M., Barrett, E.G., Tesfaigzi, Y., Bice, D.E. and Harrod, K.S. (2001) CCSP modulates airway dysfunction and host responses in an Ova-challenged mouse model. *Am J Physiol Lung Cell Mol Physiol* **281**, L1303-1311.

Wang, S.Z., Xu, H., Wraith, A., Bowden, J.J., Alpers, J.H. and Forsyth, K.D. (1998) Neutrophils induce damage to respiratory epithelial cells infected with respiratory syncytial virus. *Eur Respir J* **12**, 612-618.

Watson, T.M., Reynolds, S.D., Mango, G.W., Boe, I.M., Lund, J. and Stripp, B.R. (2001) Altered lung gene expression in CCSP-null mice suggests immunoregulatory roles for Clara cells. *Am J Physiol Lung Cell Mol Physiol* **281**, L1523-1530.

Webb, L.M., Clark-Lewis, I. and Alcami, A. (2003) The gammaherpesvirus chemokine binding protein binds to the N terminus of CXCL8. *J Virol* **77**, 8588-8592.

Webster, R.G., Bean, W.J., Gorman, O.T., Chambers, T.M. and Kawaoka, Y. (1992) Evolution and ecology of influenza A viruses. *Microbiol Rev* **56**, 152-179.

Weck, K.E., Barkon, M.L., Yoo, L.I., Speck, S.H. and Virgin, H.W. (1996) Mature B cells are required for acute splenic infection, but not for establishment of latency, by murine gammaherpesvirus 68. *J Virol* **70**, 6775-6780.

Weck, K.E., Kim, S.S., Virgin, H.W. and Speck, S.H. (1999a) B cells regulate murine gammaherpesvirus 68 latency. *J Virol* **73**, 4651-4661.

Weck, K.E., Kim, S.S., Virgin, H.W. and Speck, S.H. (1999b) Macrophages are the major reservoir of latent murine gammaherpesvirus 68 in peritoneal cells. *J Virol* **73**, 3273-3283.

Weinberg, J.B., Lutzke, M.L., Alfinito, R. and Rochford, R. (2004) Mouse strain differences in the chemokine response to acute lung infection with a murine gammaherpesvirus. *Viral Immunol* **17**, 69-77.

Weinberg, J.B., Lutzke, M.L., Efstathiou, S., Kunkel, S.L. and Rochford, R. (2002) Elevated chemokine responses are maintained in lungs after clearance of viral infection. *J Virol* **76**, 10518-10523.

Weston, W.M., LeClair, E.E., Trzyna, W., McHugh, K.M., Nugent, P., Lafferty, C.M., Ma, L., Tuan, R.S. and Greene, R.M. (1999) Differential display identification of plunc, a novel gene expressed in embryonic palate, nasal epithelium, and adult lung. *J Biol Chem* **274**, 13698-13703.

Whitaker, K.A., Wessels, M.E., Campbell, I. and Russell, G.C. (2007) Outbreak of wildebeest-associated malignant catarrhal fever in Ankole cattle. *Vet Rec* **161**, 692-695.

Willer, D.O. and Speck, S.H. (2003) Long-term latent murine Gammaherpesvirus 68 infection is preferentially found within the surface immunoglobulin D-negative subset of splenic B cells in vivo. *J Virol* **77**, 8310-8321.

Williams, K.J., Maes, R., Del Piero, F., Lim, A., Wise, A., Bolin, D.C., Caswell, J., Jackson, C., Robinson, N.E., Derksen, F., Scott, M.A., Uhal, B.D., Li, X., Youssef, S.A. and Bolin, S.R. (2007) Equine multinodular pulmonary fibrosis: a newly recognized herpesvirus-associated fibrotic lung disease. *Vet Pathol* **44**, 849-862.

Winn, W.C. and Walker, D.H. (1994) Viral Infections, In: Dail, D.H., Hammar, S.P. (Eds.) Pulmonary Pathology. Springer-Verlag, New York, pp. 429-463.

Wright, P.F., Neumann, G. and Kawaoka, Y. (2007) Orthomyxoviruses, In: Knipe, D.M., Howley, P.M. (Eds.) Field's Virology. Wolters Kluwer/Lippincott Williams and Wilkins, Philadelphia, pp. 1691-1740.

Yao, X.L., Ikezono, T., Cowan, M., Logun, C., Angus, C.W. and Shelhamer, J.H. (1998a) Interferon-gamma stimulates human Clara cell secretory protein production by human airway epithelial cells. *Am J Physiol Lung Cell Mol Physiol* **274**, L864-869.

Yao, X.L., Levine, S.J., Cowan, M.J., Logun, C. and Shelhamer, J.H. (1998b) Tumor necrosis factor-alpha stimulates human Clara cell secretory protein production by human airway epithelial cells. *Am J Respir Cell Mol Biol* **19**, 629-635.

Yeh, T.H., Lee, S.Y. and Hsu, W.C. (2010) Expression of SPLUNC1 protein in nasal polyp epithelial cells in air-liquid interface culture treated with IL-13. *Am J Rhinol Allergy* **24**, 17-20.

Zhang, B., Nie, X., Xiao, B., Xiang, J., Shen, S., Gong, J., Zhou, M., Zhu, S., Zhou, J., Qian, J., Lu, H., He, X., Li, X., Hu, G. and Li, G. (2003) Identification of tissue-specific genes in nasopharyngeal epithelial tissue and differentially expressed genes in nasopharyngeal carcinoma by suppression subtractive hybridization and cDNA microarray. *Gene Chromosome Canc* **38**, 80-90.

Zhang, J.S., Gong, A., Cheville, J.C., Smith, D.I. and Young, C.Y. (2005) AGR2, an androgen-inducible secretory protein overexpressed in prostate cancer. *Gene Chromosome Canc* **43**, 249-259.

Zhang, L., Deng, T., Li, X., Liu, H., Zhou, H., Ma, J., Wu, M., Zhou, M., Shen, S., Li, X., Niu, Z., Zhang, W., Shi, L., Xiang, B., Lu, J., Wang, L., Li, D., Tang, H. and Li, G. (2010) microRNA-141 is involved in a nasopharyngeal carcinoma related genes network. *Carcinogenesis*, bgp335.

Zhang, Y., Luxon, B.A., Casola, A., Garofalo, R.P., Jamaluddin, M. and Brasier, A.R. (2001) Expression of respiratory syncytial virus-induced chemokine gene networks in lower airway epithelial cells revealed by cDNA microarrays. *J Virol* **75**, 9044-9058.

Zhao, F., Edwards, R., Dizon, D., Afrasiabi, K., Mastroianni, J.R., Geyfman, M., Ouellette, A.J., Andersen, B. and Lipkin, S.M. (2010) Disruption of Paneth and goblet cell homeostasis and increased endoplasmic reticulum stress in Agr2-/- mice. *Dev Biol* **338**, 270-279.

Zhou, H.D., Li, X.L., Li, G.Y., Zhou, M., Liu, H.Y., Yang, Y.X., Deng, T., Ma, J. and Sheng, S.R. (2008) Effect of SPLUNC1 protein on the Pseudomonas aeruginosa and Epstein-Barr virus. *Mol Cell Biochem* **309**, 191-197.